MEDITERRANEAN ACTION PLAN
MED POL

UNITED NATIONS ENVIRONMENT PROGRAMME

WORLD METEOROLOGICAL ORGANIZATION

AIRBORNE POLLUTION OF THE MEDITERRANEAN SEA
REPORT AND PROCEEDINGS OF THE SECOND WMO/UNEP WORKSHOP

MAP Technical Reports Series No. 64

UNEP
Athens, 1992

Note: The designations employed and the presentation of the material in this document do not imply the expression of any opinion whatsoever on the part of UNEP or WMO concerning the legal status of any State, Territory, city or area, or of its authorities, or concerning the delimitation of their frontiers or boundaries. The views expressed in this volume are those of the authors and do not necessarily represent the views of UNEP or WMO.

For bibliographic purposes this volume may be cited as:

UNEP/WMO: Airborne Pollution of the Mediterranean Sea. Report and Proceedings of the Second WMO/UNEP Workshop. MAP Technical Reports Series No.64, UNEP, Athens, 1992.

This volume is the sixty-fourth issue of the Mediterranean Action Plan Technical Report Series.

This series contains selected reports resulting from the various activities performed within the framework of the components of the Mediterranean Action Plan: Pollution Monitoring and Research Programme (MED POL), Blue Plan, Priority Actions Programme, Specially Protected Areas and Regional Marine Pollution Emergency Response Centre for the Mediterranean Sea.

GENERAL INTRODUCTION

The United Nations Environment Programme (UNEP) convened an Intergovernmental Meeting on the Protection of the Mediterranean (Barcelona), 28 January - 4 February 1975), which was attended by representatives of 16 States bordering on the Mediterranean Sea. The meeting discussed the various measures necessary for the prevention and control of pollution of the Mediterranean Sea, and concluded by adopting an Action Plan consisting of three substantive components:

- Integrated planning of the development and management of the resources of the Mediterranean Basin (management component);

- Co-ordinated programme for research, monitoring and exchange of information and assessment of the state of pollution and of protection measures (assessment component);

- Framework convention and related protocols with their technical annexes for the protection of the Mediterranean environment (legal component).

All components of the Action Plan are interdependent and provide a framework for comprehensive action to promote both the protection and the continued development of the Mediterranean ecoregion. No component is an end in itself. The Action Plan is intended to assist the Mediterranean Governments in formulating their national policies related to the continuous development and protection of the Mediterranean area and to improve their ability to identify various options for alternative patterns of development and to make choices and appropriate allocations of resources.

MED POL - Phase I (1976-1980)

The Co-ordinated Mediterranean Research and Monitoring Programme (MED POL) was approved as the assessment (scientific/technical component of the Action Plan.

The general objectives of its pilot phase (MED POL - Phase I), which evolved through a series of expert and intergovernmental meetings, were:

- to formulate and carry out a co-ordinated pollution monitoring and research programme taking into account the goals of the Mediterranean Action Plan and the capabilities of the Mediterranean research centres to participate in it;

- to assist national research centres in developing their capabilities to participate in the programme;

- to analyse the sources, amounts, levels, pathways, trends and effects of pollutants relevant to the Mediterranean Sea;

- to provide the scientific/technical information needed by the Governments of the Mediterranean States and the EEC for the negotiation and implementation of the Convention for the Protection of the Mediterranean Sea against Pollution and its related protocols;

- to build up consistent time-series of data on the sources, pathways, levels and effects of pollutants in the Mediterranean Sea and thus to contribute to the scientific knowledge of the Mediterranean Sea.

MED POL - Phase I was implemented in the period from 1975 to 1980. The large number of national research centres designated by their Governments to participate in MED POL (83 research centres) from 15 Mediterranean States and the EEC),the diversity of the programme and its geographic coverage, the impressive number of Mediterranean scientists and technicians (about 200) and the number of co-operating agencies and supporting organizations involved in it, qualifies MED POL as certainly one of the largest and most complex co-operative scientific programmes with a specific and well-defined aim ever undertaken in the Mediterranean Basin.

MED POL - Phase II (1981-1990)

The Intergovernmental Review Meeting of Mediterranean Coastal States and First Meeting of the Contracting Parties to the Convention for the Protection of the Mediterranean Sea against Pollution, and its related protocols (Geneva, 5-10 February 1989), having examined the status of MED POL - Phase I, recommended that during the 1979/80 biennium a Long-term pollution monitoring and research programme should be formulated.

Based on the recommendations made at various expert and intergovernmental meetings, a draft Long-term (1981-1990) Programme for pollution monitoring and Research in the Mediterranean (MED POL-Phase II) was formulated by the Secretariat of the Barcelona Convention (UNEP), in co- operation with the United Nations Agencies which were responsible for the technical implementation of MED POL-Phase I, and it was formally approved by the Second Meeting of the Contracting Parties of the Mediterranean Sea against pollution and its related protocols and Intergovernmental Review Meeting of Mediterranean Coastal States of the Action Plan held in Cannes, 2-7 March 1981.

The general long-term objectives of MED POL-Phase II were to further the goals of the Barcelona Convention by assisting the Parties to prevent, abate and combat pollution of the Mediterranean Sea area and to protect and enhance the marine environment of the area. The specific objectives were designed to provide, on a continuous basis, the Parties to the Barcelona Convention and its related protocols with:

- information required for the implementation of the Convention and the protocols;

- indicators and evaluation of the effectiveness of the pollution prevention measures taken under the Convention and the protocols;

- scientific information which may lead to eventual revisions and amendments of the relevant provisions of the Convention and the protocols and for the formulation of additional protocols;

- information which could be used in formulating environmentally sound national, bilateral and multilateral management decisions essential for the continuous socio- economic development of the Mediterranean region on a sustainable basis;

- periodic assessment of the state of pollution of the Mediterranean Sea.

The monitoring of, and research on, pollutants affecting the Mediterranean marine environment reflects primarily the immediate and long-term requirements of the Barcelona Convention and its protocols, but also takes into account factors needed for the understanding of the relationship between the socio-economic development of the region and the pollution of the Mediterranean Sea.

As in MED POL-Phase I, the overall co-ordination and guidance for MED POL-Phase II is provided by UNEP as the secretariat of the Mediterranean Action Plan (MAP). Co- operating specialized United Nations Agencies (FAO, UNESCO, WHO, WMO, IAEA, IOC) are responsible for the technical implementation and day-to-day co-ordination of the work of national centres participating in monitoring and research.

The first eight volumes of the MAP Technical Reports Series present the collection of final reports of the principal Investigators who participated in the relevant pilot projects (MED POL I - MED POL VIII). The ninth volume of the MAP Technical Reports Series is the final report on the implementation of MED POL-Phase I, prepared, primarily, on the basis of individual final reports of the principal investigators with the co-operation of relevant United Nations Agencies (FAO, UNESCO, WHO, WMO, IAEA, IOC).

From the tenth volume onwards, the MAP Technical Report Series contains final reports on research projects, assessment documents, and other reports on activities performed within the framework of MED POL-Phase II, as well as documentation originating from other components of the Mediterranean Action Plan.

This sixty-fourth volume of the MAP Technical Reports Series contains the report and proceedings of the second WMO/UNEP Workshop on Airborne Pollution of the Mediterranean Sea (Monaco, 8-12 April 1991).

AIRBORNE POLLUTION OF THE MEDITERRANEAN SEA

Report and Proceedings of the Second WMO/UNEP Workshop

Monaco, 8-12 April 1991

Sponsored by WMO and UNEP

TABLE OF CONTENTS

TABLE OF CONTENTS (Continued...)

ABSTRACT

The second WMO/UNEP Workshop on Airborne Pollution of the Mediterranean Sea was convened from 8 to 12 April 1991, in Monaco, to discuss the results of the monitoring and research activities implemented in the Mediterranean countries since 1988 within the Monitoring of the Transport of Pollutants to the Mediterranean Sea through the Atmosphere (one of the monitoring components of MED POL), and the MED POL Research Activity "L" on pollutant-transfer processes at air-sea interface coordinated by the World Meteorological Organization (WMO).

The workshop recommended that the airborne pollution research, monitoring and modelling programme adopted at the first workshop on Airborne Pollution of the Mediterranean Sea (Belgrade, November 1987) (see MAP Technical Reports Series No. 31) should be continued as fully as possible, and made recommendations on the further development of the programme. In particular, it was recommended that the same attention should be given to the research and monitoring of atmospheric transport and deposition of nutrients (nitrogen and phosphoran compounds) as to that of heavy metals which was recommended earlier. The report of the workshop and recommendations are presented as Part I of the present publication. Scientific papers presented at the workshop are included in Part II. Most of the papers are based on the results of research projects completed within the framework of the MED POL Research Activity L.

FOREWORD

On the basis of available measurement data and model calculations, it has now become evident that a significant part of pollutants entering the Mediterranean Sea is transported from land-based sources via the atmosphere. For soluble forms of Pb, Cd and Zn, as well as for synthetic organics, the atmospheric inputs exceed their riverine inputs. Trajectory modelling of air flows shows that Cd, for example, could be transported to the Mediterranean from long-distance sources in Europe and that, of the total European emissions of heavy metals, 4-20% is deposited over the Northwestern Mediterranean. The atmospheric deposition of nitrogen and phosphorous compounds, which may cause eutrophication, is also approximately equal to their riverine fluxes and the great amount of desert dust, transported by the atmosphere from the African continent and deposited into the sea, can affect biogeochemical processes in the seawater. Moreover, air pollution in some Mediterranean cities and industrial areas endanger both human health and the marine environment in coastal zones. In general, the levels of atmospheric pollution over the Mediterranean are comparable to those over other European seas and are much higher than pollution over the open oceans.

The MED POL Airborne Pollution Monitoring and Modelling Programme was adopted at the first workshop on this subject which was held in Belgrade, Yugoslavia, from 10 to 13 November 1987 (see MAP Technical Report Series No.31). In addition, more than fifteen national research projects related to the study of atmospheric transport and deposition of pollutants into the Mediterranean were supported as a part of MED POL. The World Meteorological Organization has been the coordinating agency for these activities which are also a contribution to the WMO Global Atmosphere Watch (GAW) system.

The second workshop on Airborne Pollution of the Mediterranean Sea, held in Monaco from 8 to 12 April 1991, provided a forum for scientists from 11 Mediterranean countries to exchange their experience, to discuss the results and to prepare recommendations for the further development of the research, monitoring and modelling activities aimed at assessing pollution of the Mediterranean sea through the atmosphere.

PART I

REPORT OF THE SECOND WMO/UNEP WORKSHOP ON AIRBORNE POLLUTION OF THE MEDITERRANEAN SEA

(Monaco, 8-12 April 1991)

Background

The study, monitoring and the assessment of pollution of the Mediterranean Sea through the atmosphere is one of the four major components of the Long-term Programme for Pollution Monitoring and Research in the Mediterranean Sea (MED POL) launched by the United Nations Environment Programme (UNEP) in 1981 with the World Meteorological Organization being responsible for coordination activities on airborne pollution.

The MED POL airborne pollution monitoring and modelling programme was prepared at the First WMO/UNEP Workshop on Airborne Pollution of the Mediterranean Sea held in Belgrade, Yugoslavia in November 1987. The report of the workshop was published as the Mediterranean Action Plan (MAP) Technical Report Series No. 31. In may 1988, the Scientific and Technical Committee for MED POL agreed that the programme should be initiated within the framework of national MED POL monitoring programmes in as many countries as possible. Since that time airborne pollution monitoring has been started in many Mediterranean countries and a number of relevant research projects have been completed.

Important quantitative estimates of pollution of the Mediterranean Sea through the atmosphere was made in 1989 by the IMO/FAO/UNESCO/WMO/WHO/IAEA/UN/UNEP Joint Group of Experts on the Scientific Aspects of Marine Pollution (GESAMP) in its study on the Atmospheric Input of Trace Species to the World Ocean (GESAMP Report and Studies No.38).

In view of the above-mentioned developments, it was proposed that the Second Workshop on Airborne Pollution of the Mediterranean Sea be held in 1991 to consider and discuss the results of research and monitoring conducted in the countries and to prepare recommendations for future research, monitoring and modelling activities, bilateral and multi-lateral cooperation, data collection and exchange, quality assurance and training.

The workshop was organized and convened by WMO with financial support provided by the Coordinating Unit for MAP (MED Unit). The premises for the workshop were kindly provided by the Musee Oceanographique of Monaco and the International Laboratory of Marine Radioactivity (ILMR) of IAEA rendered assistance in providing some meeting facilities. The workshop took place from 8 to 12 April 1991. It was attended by 21 participants from 11 Mediterranean countries. Representatives from WMO, IAEA, and ICSEM were also present. A list of participants is given in Annex.

1. OPENING OF THE WORKSHOP

1.1 The workshop was opened by Mr. A. Soudine, Senior Scientific Officer, WMO who welcomed the participants on behalf of WMO and the MED Unit and thanked the representatives of the Musee Oceanographique and ILMR for their kind assistance in organizing the workshop. Mr. A. Soudine reminded the meeting about the important results of the first workshop held in 1987 where the MED POL airborne pollution monitoring and modelling programme was developed and briefly outlined the major developments which occurred since 1987. The most encouraging sign is that measurements of pollutant contents in air and in precipitation are under way now in more countries than three years ago. Significant achievements have also been made in the improvement of atmospheric transport models. It was noted that, in the Mediterranean region, there is a number of stations of the WMO Background Air Pollution Monitoring Network (BAPMoN) which is at present a part of the WMO Global Atmosphere Watch (GAW) system established in 1989 and oriented at monitoring and assessing the changes in atmospheric composition both on global and regional scales. Close cooperation and inter-

connection between GAW and relevant MED POL activities will be of benefit to both programmes in the region. Mr. A. Soudine underlined that the workshop should provide a forum for Mediterranean scientists studying the airborne pollution of the sea to exchange results and experience and, on that basis, to elaborate clear guidelines and recommendations for improving and extending the monitoring and modelling and to outline the urgent research needs.

1.2 On behalf of the Musee Oceanographique, the workshop participants were greeted by Commandant P. Roy who noted the important role which has been played by the Museum in promoting research and public awareness in the marine environment protection.

1.3 Mr. J-P. Villeneuve, the representative of the IAEA International Laboratory of Marine Radioactivity also welcomed the participants and invited them to visit ILMR. This invitation was accepted with great appreciation and the visit took place in the afternoon of 8 April 1991.

1.4 Mr. A. Soudine requested the workshop participants to present short information on their national current and future activities aimed at studying, monitoring and modelling the atmospheric transport and deposition of pollutants into the Mediterranean Sea area. Information was presented by participants from Egypt, France, Greece, Israel, Italy, Monaco, Morocco, Spain, Tunisia, Turkey and Yugoslavia.

2. NOMINATING OF OFFICERS AND ORGANIZATION OF WORK

2.1 The meeting agreed that the scientific papers would be discussed at plenary sessions and draft recommendations for the future work would be prepared at meetings of the two working groups to deal with measurement and monitoring needs and with meteorological aspects and modelling.

2.2 To guide the work of the plenary sessions and the working groups, the meeting nominated Mr. T. Cvitas as chairman of Messrs. G. Bergametti and Y. Mahrer as vice-chairmen of the working groups respectively on measurements and modelling.

3. PRESENTATION OF PAPERS

3.1 A total of 19 papers were presented and discussed at the five plenary sessions of the workshop. Full texts of the fifteen papers and two abstracts are presented in Part II of this publication. In addition the following papers were presented and discussed: a proposal for a European research programme on atmospheric input and its impact on Mediterranean seawater and sediments (AIMS) presented by Dr. F. Dulac, France and draft guidelines on collection and presentation of emission data for heavy metals prepared and presented by Dr. E. Auli, Spain.

3.2 Almost all papers presented at the workshop were based on the results of national research projects completed in 1990-1991 within the framework of the MED POL Research Activity L on pollutant-transfer processes at air-sea interface including atmospheric transport and deposition of pollutants.

4. SUMMARY OF THE DISCUSSIONS AND RECOMMENDATIONS

4.1 Monitoring

1. The workshop recognized that the recommendations for the monitoring programme made at the Belgrade workshop in November 1987 have contributed to the establishment of new sampling stations in the region, to the extension of measurement programmes and to the improvement of data quality. Thus, for their major part, these recommendations remain valid and only a few amendments and additional recommendations are needed in view of the latest research results.

2. The high volume sampling technique for monitoring of airborne species associated with the particulate matter proved to be the best one in providing reliable data. However, it was reiterated that when possible, the sampling period should be less than one week in order to facilitate interpretation of measurement results with air mass trajectories and other meteorological parameters. In the same way, it was pointed out that, when the sampling time is reduced, the cellulose filters such as Whatman 41 should be used to obtain sufficiently lower and constant blanks especially for heavy metals.

3. Recent research results showed that there is a strong seasonal pattern in the atmospheric transport and deposition of many pollutants into the Mediterranean Sea area. Moreover, sometimes high pollution episodes of the natural or anthropogenic origin produce large inputs of airborne species into the sea during very short time periods. The workshop recommended that an intensive and long-term monitoring be organized at 1-2 selected stations to study such events with sufficient time resolution. Taking into account the difficulty of such a study, two or more research teams from various countries should be encouraged to cooperate. The study of high pollution episodes connected with major anthropogenic sources was also discussed under the modelling component of the programme.

4. The workshop recognized the importance of the atmospheric input of nutrient species into the Mediterranean Sea. The studies carried out in the western part of the sea have revealed that, on an annual basis, the atmospheric input of nitrogen species is of the same order of magnitude as the riverine input. This could be more important in the eastern basin where the deep waters do not supply nutrients to the euphotic zone and the riverine input is greatly reduced due to irrigation, etc. The workshop recommended that nutrients be added to the list of priority measurement parameters within the MED POL airborne pollution monitoring programme. In view of inherent difficulties in measuring the nutrient species (especially nitrogenous) in aerosols, the priority should be given to their determination in wet deposition.

5. The workshop noted that techniques had been developed to measure carbonaceous particles (C-soot) in air and in wet precipitation. C-soot is an unreactive and long-lived pollutant which could be a very useful tracer for monitoring and modelling atmospheric transport and deposition of carbonaceous material and other man-made pollutants. To evaluate the efficiency of these new techniques, it was recommended that a few aethalometers (C-soot measuring instruments) should be established at some selected stations and operated with the assistance of and in cooperation with French scientists.

6. It was recommended that detailed information about the active monitoring stations in the region should be collected including the station location and elevation, typical meteorological and air pollution characteristics, instrumentation used, length of record, type and timing of observations, description of site surroundings, etc. Drs. S. Guerzoni and L. Cruciani agreed to prepare a questionnaire which will be distributed by WMO.

4.2 Intercalibration and Quality Assurance

1. The workshop stressed the need for an intercalibration exercise to be held at one site with the exchange of fractions of a common high-volume reference sample to be prepared by one of the participants. It was agreed that for thorough preparation of the sampling equipment intercalibration Drs. G. Bergametti (France), S. Guerzoni (Italy), A. Nejjar (Morocco) and G. Tuncel (Turkey) would develop a plan and a draft programme which should be sent to the workshop participants by mid-1992 in order to perform the exercise in 1993 or in early 1994.

2. The WMO was requested to provide reference rain samples for intercomparison of analytical procedures to all the participating stations and laboratories as defined through the inquiry mentioned in 4.1.6.

3. The WMO was also requested to provide the stations and laboratories participating in the programme with the available reference methods descriptions, manuals and other guidance material.

4. It was agreed that Dr. S. Guerzoni (with the help of WMO) would collect information on the sampling equipment used in the Mediterranean countries, review their performance characteristics and prepare recommendations on their use and handling with the aim of ensuring the uniformity of measurements.

5. The workshop requested Drs. S. Guerzoni (Italy) and A. Soudine (WMO) to prepare an outline of a quality assurance programme for the MED POL airborne pollution monitoring programme and to discuss this matter with the workshop participants mentioned in 4.2.1, if possible in October 1992. The ICSEM meeting in Trieste might be used for this discussion.

4.3 Modelling

1. The workshop noted the progress and developments since 1987 in atmospheric pollution modelling which is a powerful tool for describing the regional and mesoscale transport diffusion and removal processes and for assessing the pollution of the Mediterranean Sea region through the atmosphere. The workshop reconfirmed the modelling-related recommendations of the Belgrade meeting and made proposals for additional studies.

2. The workshop considered the importance of high pollution episodes and proposed to organize an 18 month special study of these events with participation of all the Mediterranean countries. This study will consist of the following steps:

- Selection of specific case-studies on the basis of high pollutant concentrations recorded at existing monitoring stations and of concomitant synoptic conditions. The information about such natural or anthropogenic pollution episodes will be furnished by each participating country, and the analysis of this information and the selection

and classification of the cases will be made by Drs. G. Kallos (Greece) and U. Dayan (Israel);

- Collection of information about major point sources of pollution in each country (location, elevation, type of amount of fuel used, etc.) on the basis of a questionnaire to be prepared by Dr. Y. Mahrer (Israel). Later in 1992 and in 1993, the information about emissions of heavy metals should be also collected on the basis of agreed guidelines, a draft of which was prepared and presented by Dr. E. Auli (Spain).

- An *ad hoc* group of modellers consisting of Drs. G. Kallos (Greece), U. Dayan and Y. Mahrer (Israel), and S. Nickovic (Yugoslavia) will conduct model simulations for the selected episodes. The modelling will include long-range transport simulations as well as regional and mesoscale ones.

3. It was proposed that the assessment of the pollution of the Mediterranean Sea through the atmosphere by heavy metals and acidifying compounds be made in 1992-1993 by one of participating institutes.

4. The workshop noted that some individual scientists and research groups not belonging to the meteorological services meet with difficulties in obtaining meteorological information they need for their research. The WMO was requested to bring this to the attention of its Members in the region and to facilitate the obtainment of the meteorological information.

4.4 Research

1. In view of the results presented at the workshop, an evaluation of uncertainties linked with each type of sampling system (high and low volume samplers, mesh) was recommended (see also 4.2.4). This will include the determination of the range of mass size distribution collected by each type of the systems. A particular research effort was recommended for simultaneous determination of mass size distribution for suspended matter in air, rain and dry deposition samples.

2. In view of the importance of nutrient depositions and difficulties in their measurements, research efforts are needed to improve the measurement techniques.

3. The workshop recognized that the photo-oxidant pollution is an important problem in many regions of the Mediterranean and that the changing oxidazing capacity of the atmosphere may affect the atmospheric transport and transformation of many important pollutants and thus recommended that concerted ozone measurements be made at 4-5 locations, especially during May-September. The group of Dr L. Klasinc from Zagreb offered to provide the instrumentation and expertise for such a campaign.

4. The information about seasonal precipitation fields over the Mediterranean including rain frequencies and rates, is not sufficient. The research in this field can benefit from using radar and microwave satellite data.

4.5 Training

1. The workshop welcomed the proposal of WMO and the Coordinating Unit for the Mediterranean Action Plan to hold a training course in Malta at the end of 1992 or at the beginning of 1993 and recommended that some scientists involved in the programme be invited as lecturers.

2. It was also recommended that the WMO training courses on background air pollution measurements held every year in English or in French should be used for training as fully as possible.

3. The workshop recommended that an international training seminar be organized with the focus on biogeochemical processes in the Mediterranean Sea and their alteration by anthropogenic activities and pollution including pollution through the atmosphere. Dr. J. Morelli (France) was requested to explore the possibility to organize such a seminar.

4. Noting the urgent need for emission data and the preparation of the guidelines for assessing air pollutant emissions, especially for heavy metals (see 4.6) the workshop recommended that a training seminar on this matter be organized as soon as possible.

4.6 Emission Inventories

The workshop stressed the urgent need for emission data especially for such pollutants as heavy metals and welcomed that the guidelines for collecting such data are being prepared by Dr. E. Auli (Spain). It was recommended that this work be completed and the Mediterranean countries be invited to start collecting the data as soon as possible.

4.7 Data Reporting

The workshop confirmed that monitoring data from background stations be reported by using the existing WMO formats as it was recommended by the Belgrade workshop. Noting that the MED POL data are collected at present at the Coordinating Unit for the Mediterranean Action Plan, it was recommended that the airborne pollution data be sent to this Unit from which they would be also available to the WMO Global Atmosphere Watch data centres.

4.8 Coordination

The workshop recommended that the Expert Group on Airborne Pollution of the Mediterranean Sea be established in 1992 to start coordinating and guiding all the research, monitoring and modelling activities in this field and to provide relevant recommendations to the governments. It was also recommended that the next workshop on airborne pollution of the Mediterranean Sea be held in 1994.

5. ADOPTION OF THE REPORT AND CLOSURE OF THE WORKSHOP

A draft report of the workshop was adopted at the final plenary session and the WMO representative was requested to finalize it.

The workshop was closed at 12.00 on 12 April 1991.

ANNEX

LIST OF PARTICIPANTS

1. MS MARTA ALARCON

Centre d'Estudis Avancats de Blanes
Cami de Santa Barbara
17300 Blanes, Girona
Spain

Tel: (34) 72 336101/02/03
Fax: (34) 72 337806
Telex: 56372 CEABL-E

2. MR ENRIC AULI

Servei Sanitat Ambiental
Departament de Sanitat i Seguretat Social
Generalitat de Catalunya
Calabria 169
Barcelona 08015
Spain

Tel: (34) 3 2267000 (ext. 295)
Fax: (34) 3 2268936

3. MR GILLES BERGAMETTI

LPCA
VA 1406
Université Paris 7
2 place Jussieu
F-75251 Paris Cédex 05
France

Tel: (33) 1 44 27 57 45
Fax: (33) 1 44 27 57 09

4. MR HEDI BOUSNINA

Institut National de la Météorologie
BP 156
2035 Tunis Carthage
Tunisia

Tel: (21) 61 782 400
Fax: (21) 61 784 608

5. MR FREDERIC BRIAND

Commission Internationale pour l'Exploration
Scientifique de la Mer Mediterranée
16 Boulevard de Suisse
MC-98030 Monaco Cedex

Tel: (33) 93 30 38 79
Fax: (33) 93 30 24 74

5. MR LUCIANO CRUCIANI

Italian Meteorological Service
Piazzale degli Archivi 34
I-00144 Rome
Italy

Tel: (396) 49865261
Fax: (396) 49865423

6. MR TOMISLAV CVITAŠ

Fraunhofer Institute (IFU)
Kreuzeckbahnstrasse 19
D-8100 Garmisch-Partenkirchen
Federal Republic of Germany

7. MR URI DAYAN

Applied Physics and Mathematical Department
Soreq Nuclear Research Centre
Yavne 70600
Israel

Tel: (97) 28 43 45 83
Fax: (97) 28 43 73 64

8. MR FRANÇOIS DULAC

Centre des Faibles Radio Activités
CNRS-CEA
F-91198 Gif-sur-Yvette
France

Tel: (33) 1 69 82 35 24
Fax: (33) 1 69 82 35 68

9. DR STEFANO GUERZONI

Istituto per la Geologia
Marina CNR
Via Zamboni No. 65
40127 Bologna
Italy

Tel: (39) 51 244004
Fax: (39) 51 243117

10. MR GEORGE KALLOS

University of Athens
Department of Applied Physics
Ippokratous 33
Athens 10680
Greece

Tel: (30) 1 7233690
Fax: (30) 1 3233846

11. MR LEO KLASINC

Ruder Boskovic Institute
P.O. Box 1016
Zagreb
Croatia

Tel: (38) 41 424 690
Fax: (38) 41 425 497

12. MR YITZHAK MAHRER

Department of Soil and Water Sciences
Hebrew University of Jerusalem
P.O. Box 12
Rehovot 76100
Israel

Tel: (97) 28 481 386
Fax: (97) 28 462 181

13. MR CLAUDE MARMENTEAU

Office Monégasque de l'Environnement
16, Bd. de Suisse
MC-98000 Monaco

Tel: (33) 93 30 78 03

14. MR CHRISTOPHE MIGON

Université de Corte
Grosseti
B.P. 52
F-20230 Corte
France

Tel: (33) 95 45 00 48
Fax: (33) 95 46 03 21

15. MR JACQUES MORELLI

Institut de Biogéochimie Marine
Ecole Normale Supérieure
1 rue Maurice Arnoux
F-91120 Montrouge
France

Tel: (33) 1 46 57 12 86 (Ext. 611)
Fax: (33) 1 46 57 04 97
Telex: 202601 ENULM F

16. MR AHMED NEJJAR

Ecole Mohammadia d'Ingénieurs
B.P. 765
Rabat
Morocco

Fax: (21) 27 77 8853
Telex: 32939 M

17. MR SLOBODAN NIÈKOVIÆ

Federal Hydrometeorological Institute
Bircaninova 6
P.O. Box 604
11001 Belgrade
Yugoslavia

Tel: (38) 11 646 555
Fax: (38) 11 646 369

18. MR CEMAL SAYDAM

Middle East Technical University
Institute of Marine Sciences
P.O. Box 28
33731 Erdemli
Turkey

Tel: (90) 7586 1406
Fax: (90) 7586 1327

19. MR ALEXANDER SOUDINE

World Meteorological Organization
Environment Division
P.O. Box 2300
CH-1211 Geneva 2
Switzerland

Tel: (41) 22 730 84 20 /730 81 11
Fax: (41) 22 734 23 26

20. MR GURDAL TUNCEL

Middle East Technical University
Department of Environmental Engineering
06531 Ankara
Turkey

Tel: (90) 4 223 7100
Fax: (90) 4 223 6946

21. MR ANDRÉ VEGLIA

Office Monégasque de l'Environnement
16, Bd. de Suisse
MC-98000 Monaco

Tel: (33) 93 30 78 03

22. MR JEAN-PIERRE VILLENEUVE

IAEA
Aigue Marine
24 Avenue de Fontvieille
MC-98000 Monaco

Tel: (33) 93 25 12 92
Telex: 479378 MC

23. MR HUSSEIN ZOHDY

13 Gisr El-Swis
Manshiat El-Bakry
Cairo
Egypt

Tel: (20) 2 256 2652
Fax: (20) 2 342 0768

PART II

SCIENTIFIC PAPERS

THE ATMOSPHERIC INPUT OF LEAD INTO THE NORTHWESTERN MEDITERRANEAN SEA

By

EMMANOUELA REMOUDAKI[(1)], GILLES BERGAMETTI[(1)] and PATRICK BUAT-MÉNARD[(2)]

[(1)] Laboratoire de Physico-Chimie de l'Atmosphère, UA CNRS 1404, Université Paris 7, 2 place Jussieu, 75251 Paris Cedex 05, France.
[(2)] Centre des Faibles Radioactivités, Laboratoire Mixte CNRS-CEA, 91198 Gif-sur-Yvette, France.

A B S T R A C T

Beginning in 1985, daily 24-hour aerosol samples were collected on 0.4-µm pore size filters at a coastal location in northwestern Corsica. Total atmospheric deposition (wet + dry) were sampled between February 1985 and October 1987 with a collection period of about 15 days. As indicated by three-dimensional air mass trajectories, lead aerosol particles collected at this site are primarily derived from European continental source regions. The variability of lead aerosol concentrations on both daily and seasonal time scales is primarily due to the scavenging of lead aerosol particles by rain rather than to changes in source regions. Our results suggest that the ratio between the total atmospheric deposition of Pb and the corresponding mean daily precipitation (mdp) rate is not constant. This ratio reaches a maximum during the Mediterranean summer. We attribute this difference to wet scavenging processes which wash a more loaded atmosphere during the dry season than during the wet season. The precipitation frequency (F_p) is a major factor influencing seasonal variability of the total atmospheric deposition of lead over the western Mediterranean. An intermediate value of F_p allows sufficient reloading of the atmosphere with long-range transported Pb aerosol particles as well as efficient scavenging by precipitation events.

1. INTRODUCTION

During the last decade, it has become increasingly evident that the atmosphere is the major pathway for pollutant lead input to the world's ocean (Boyle *et al.*, 1986). This anthropogenic input outweighs natural inputs by orders of magnitude (Arimoto *et al.*, 1985; Patterson and Settle, 1987). Indeed, it has been shown that surface water maxima observed from measured concentration profiles of lead in the North Pacific (Schaule and Patterson, 1981, Flegal and Patterson, 1983) and North Atlantic (Schaule and Patterson, 1981, 1982) are the fingerprints of the atmospheric input of lead.

In a regional sea, such as the Mediterranean, the effects of the atmospheric input of lead aerosols are even more pronounced. Data obtained in western Mediterranean waters indicate an average Pb concentration of 60 ng l^{-1} in surface waters and an average

---

N.B. This contribution is a shortened version of the paper published by the same authors in J.G.R. 96, 1991.

concentration of 30 ng l^{-1} in deep waters (Laumond *et al.*, 1984). These values are much higher than those observed in the Atlantic Ocean (Settle and Patterson, 1982) and in the Pacific Ocean (Flegal and Patterson, 1983). Observations of surface maxima confirm the atmospheric origin of Pb. Previous works have suggested that this atmospheric lead is primarily derived from European emissions (Arnold *et al.*, 1982; Dulac *et al.*, 1987; Maring *et al.*, 1987); 60% of these emissions derive from vehicle exhaust due to gasoline alkyllead additives (Pacyna, 1984).

Data from various cruises in the Mediterranean Sea indicate an atmospheric Pb concentration range from 1.6 to 144 ng m^3 (Dulac *et al.*, 1987). Results from these cruises also show that the atmospheric Pb concentrations are highly variable on a daily time scale. This is due to changes in continental source strengths, airflow and precipitation patterns. Unfortunately, such data cannot provide a quantitative assessment of the atmospheric input to this basin, mainly because of the short duration of these campaigns.

In this paper, we have addressed this problem through a continuous sampling of total Pb atmospheric deposition at a coastal site of Corsica Island. From simultaneous measurements of lead contained in aerosol samples and data from air mass trajectory analyses and precipitation patterns, we have attempted to evaluate the major factors which control the deposition of lead to this marine area.

2. SAMPLING AND ANALYSIS

2.1 Aerosol Sampling

Aerosol samples were collected at Capo Cavallo (42E31 N, 8E40 E), on the northwestern coast of Corsica Island, between February 1985 and October 1987 (Bergametti *et al.*, 1989). We present here only results covering the period from February 1985 to April 1986. The aerosol samples were collected at the top of a 10-m high meteorological tower. Bulk filtration samples were performed on 0.4-µm porosity Nucleopore filters. Sampling duration was 24 hours with a nominal airflow of 1 $m3h^{-1}$. Blank filters were subjected to all the manipulations made on the filters, except air filtration.

2.2 Total Deposition Sampling

During the same period and at the same site, total (wet + dry) atmospheric deposition was sampled continuously within a period of about 15 days. We used a hemispherical polycarbonate collector having a collection surface area of 0.1 m^2. The collector had been used to sample atmospheric deposition of radioactive aerosols (Lambert, 1963). Results of this study have shown that this collector simulates satisfactorily the radioactive fallout onto the various surfaces. The sampling procedure is detailed in Remoudaki *et al.*, 1991a.

During the whole sampling period, the amount of precipitation (in mm) corresponding to each event was measured using a standard rain gauge operated by the French National Meteorological Station located at the sampling site. This allowed us to calculate the volume of precipitation (in litres) which should correspond to each sample (CPV in litres).

During a short campaign at the sampling site in April 1986, we collected total deposition samples, using an ultraclean single-use collector at the top of the 10-m high meteorological tower (TDTL : total deposition at the tower level) simultaneously, with our collector placed at ground level (TDGL : total deposition at ground level). The results show a satisfactory reproducibility of the total deposition measurements for various elements

between the two collection systems. Such a comparison suggests the reliability of our collection system installed permanently at the sampling site.

2.3 Analysis

All manipulations and analyses of samples were performed in the clean room of the laboratory. Laboratory material brought into contact with samples was precleaned according to the procedure described above for the sampling bottles.

For the aerosol samples, we present here only the concentrations of Pb determined by flameless atomic absorption spectrometry. Results concerning the concentrations of other elements have been presented in previous papers (Bergametti, 1987, Bergametti *et al.*, 1989, Remoudaki et al, 1991a and b). For atomic absorption analysis, each sample is placed, for about 1 week, in a teflon bomb with 4 ml of HNO3 Normatom Prolabo and 1 ml of HClO4 Normatom Prolabo at a temperature of 60EC. The liquid residue (about 1 ml) is then adjusted to 5 ml with Milli-Q water. Working standards were prepared in a similar solution to allow matrix matching with samples. The analysis was performed by using a Perkin Elmer model 400 unit with HGA 500 graphite furnace. Mean relative errors have been estimated to be 10%.

Total atmospheric deposition samples were filtered on Nucleopore filters (0.4 µm pore size) to separate the particulate from the dissolved fraction. The analysis of the dissolved fraction has been performed directly without any preconcentration, by flame atomic absorption spectrometry (Perkin Elmer 300) for Na and flameless atomic absorption spectroscopy for Pb (using the above unit). Experimental evidence showed that Pb is 100% soluble in our acidified samples (pH about 1). For complementary information, see Remoudaki *et al.*, 1991a).

3. RESULTS AND DISCUSSION

3.1 Temporal Variability of Lead Aerosol Concentrations

The yearly geometric mean aerosol concentration of lead at Capo Cavallo for the study period is 15.9 ng m^3. Lead aerosol concentrations are highly variable on a time scale of 1 day (Fig.1). Such a high variability confirms the observations of Dulac *et al.*, 1987.

Our data also indicate a seasonal pattern for particulate lead concentrations in the western Mediterranean atmosphere: during the dry period (May-October) the geometric mean concentration is about 24 ng m^3 while during the wet period (October-May) the geometric mean concentration is only 11.8 ng m^3. This seasonal pattern is also observed for other elements of continental origin (natural and man made) (Bergametti *et al.*, 1989) and is inversely related to that of precipitation. At first glance, our data suggest that precipitation is a major factor influencing the variability of the measured aerosol lead concentrations. Indeed, it appears from Fig.1 that precipitation events are systematically followed by abrupt decreases of the aerosol lead concentration. To properly assess this influence, however, we have to consider simultaneously the variability induced by changes in source regions and air flow patterns.

Influence of the source regions. For each sample, we have computed three-dimensional 4-day backward air mass trajectories (Imbard, 1983; Bergametti *et al.*, 1989). Briefly, the calculation assumes that the instantaneous movement of the air mass is equal to the wind vector at the center of the air mass. This wind vector is computed, every 5 minutes, by linear, spatial, and temporal interpolation (Imbard, 1983) from the three-dimensional wind field analyzed at the European Center for Medium Term Meteorological Forecasts, in Reading, England. Moreover, along these trajectories, the model reports the forecasted precipitations greater than 0.1 mm h^{-1}. Our trajectories were calculated for the midpoint of each sampling period and finished at the 925 hPa barometric level.

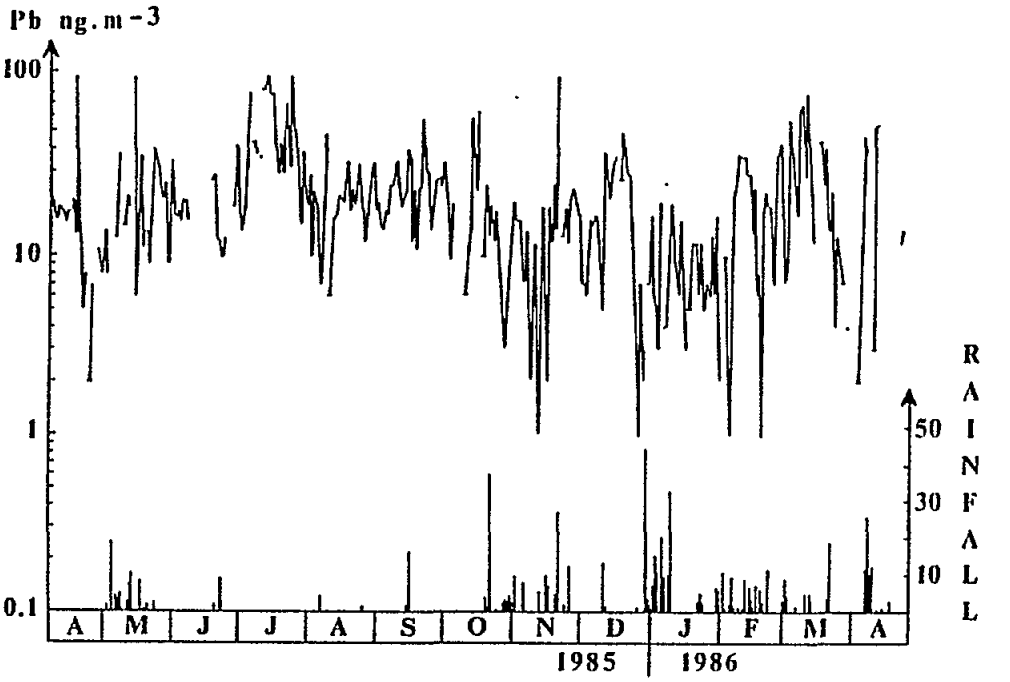

Fig.1 Daily atmospheric concentrations (in ng m^{-3}) of Pb at Capo Cavallo for the period February 1985 to April 1986. The daily amount of local precipitation is reported at the bottom of the figure.

To classify the samples with respect to the origin of the air masses, we made no "*a priori*" hypotheses concerning the various source regions of lead for the western Mediterranean atmosphere. We divided a wind rose into 16 sectors of 22°5, and each sample was classified in the 22°5 sector corresponding to the position of the air masses 2 days before their arrival over the sampling site. However, some trajectories were too short and, consequently, it was difficult to assign a precise source region. Thus we defined a seventeenth sector for these particular trajectories.

As previously mentioned, local precipitation may strongly change atmospheric lead concentrations on a short time scale and thus affect the "fingerprints" of the source regions. Thus we have not considered the samples collected when local precipitation occurred. Further, because the mean reloading time of the local atmosphere with continental aerosols following a local rain has been estimated to be about 2 days (Bergametti *et al.*, 1989), the

samples for which a local precipitation occurred 2 days or less before sampling were also excluded.

For each sector, we calculated the geometric mean aerosol concentration and we grouped together adjacent sectors when the mean concentrations were found to be similar. The results of these calculations are illustrated in Fig.2 . The highest concentrations are associated with transport cases from the north-northeast (27 ng m^3) and west (21.9 ng m^3). In contrast, the south sector, corresponding to air masses coming from North African countries, exhibits the lowest concentrations of lead (7.4 ng m^3). This may be due to the low industrial activity and vehicular traffic in these countries.

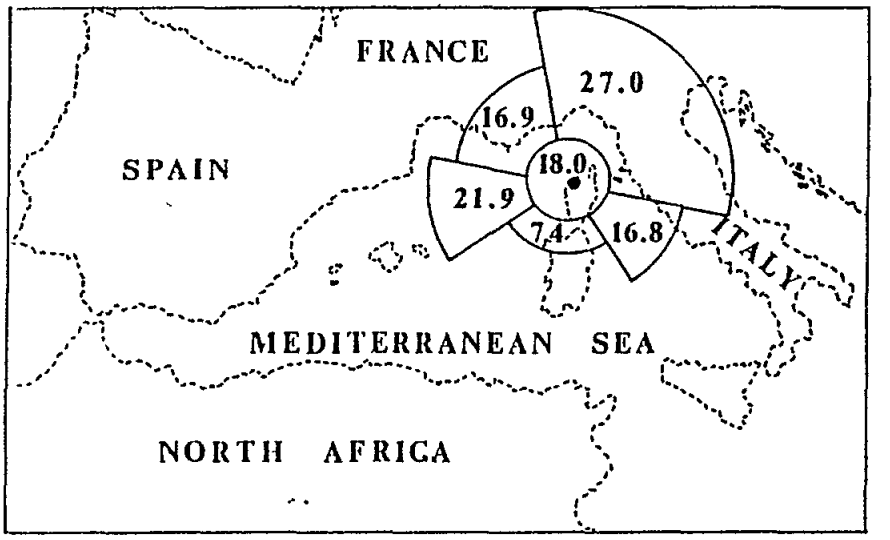

Fig.2 Classification of Pb concentrations (in ng m^{-3}) according to the origin of the air masses arriving at the sampling site (the small circle corresponds to short trajectories).

Northwest and southeast sectors and the sector corresponding to the shortest trajectories are associated with intermediate concentrations of lead (16.1, 16.8, and 18 ng m^3 respectively).

Such a classification does not, however, provide any direct quantitative information on the emission rates of lead in the various source regions. Indeed, it will be shown that such an assessment requires the separation of air masses washed during their transport from those transported during "dry" conditions.

Influence of rain occurring during transport. To estimate the influence of rains, we have used the precipitation events forecast by the trajectory model. Only two sectors (for which the number of samples was sufficient, i.e., the northwest and the northeast) were selected. The samples were separated into three groups: (1) samples for which a precipitation event occurred during the last day of transport, (2) samples for which a

precipitation event occurred 2 days before the arrival of the air mass over the sampling site, and (3) samples with no precipitation event during the last 2 days of transport.

The results presented in Fig.3 show a strong influence of the occurrence of precipitation during air mass transport on the aerosol concentrations of lead. For the northwest sector, mean Pb concentrations in air masses washed during the last 24 hours before their arrival at Corsica (7.2 ng m^3, group 1) are 4 times lower than those corresponding to dry transport cases (28.5 ng m^3, group 3). The second group (rain in the 1-2 days interval) exhibits intermediate Pb concentrations.

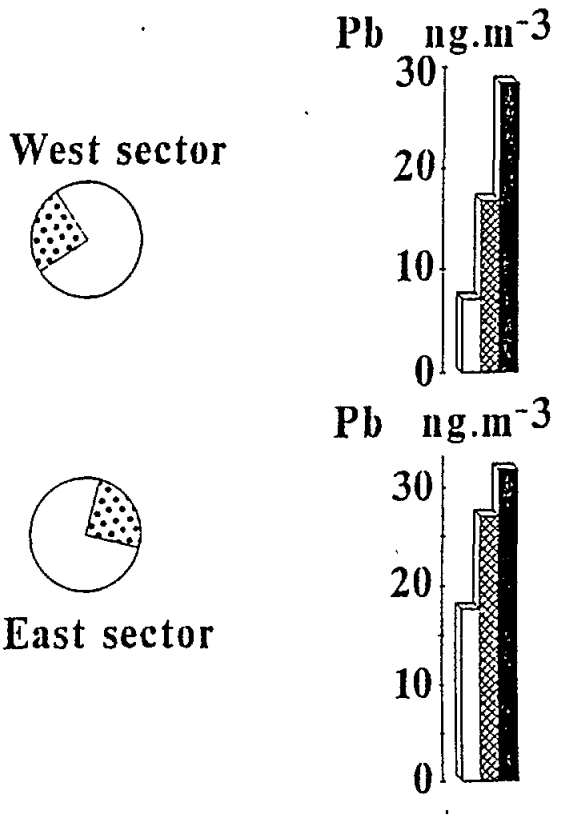

Fig.3 Influence of precipitations occurring during the transport of the aerosol particles on the concentrations of lead (in ng m^{-3}) at Capo Cavallo.

Similar results are obtained for the northeast sector with only a factor of 2 between the two extreme cases (17.7 ng m^3, group 1, and 31.9 ng m^3, group 3). There is only a small difference between samples corresponding to groups (2) and (3).

The different pictures obtained for northwest and northeast sectors can be explained when considering the distances separating Corsica from the Mediterranean coastlines. For the Northeast sector the distance between Corsica and the Mediterranean coast corresponds generally to 1 day of transport. In this case, air masses, washed 2 days before arriving in Corsica, can be reloaded by the emissions of industrial and urban areas located on the Italian and French Rivieras. For air masses originating from the northwest, 2 days of transport are

generally necessary for travel from the French or Spanish coasts to Corsica. In this case, the air masses cannot be reloaded during their travel over the sea.

For the northwest sector, the mean Pb concentrations range between 7.2 ng m^3 (group 1) and 28.5 ng m^3 (group 3). This range is similar to that observed from the classification in the various sectors (Fig.2). Moreover, if we consider now the non-washed air masses (group 3, Fig.3), the difference in lead concentrations is not significant between the northwest and the northeast sector.

It can therefore be concluded that precipitation occurring during transport is the major factor controlling the variability of lead concentrations in the Western Mediterranean atmosphere.

3.2 Atmospheric Lead Deposition into the Western Mediterranean

Temporal variability of atmospheric lead deposition. Fifty-seven total deposition samples (wet + dry) were collected between February 1985 and October 1987. The measured deposition of lead for each sample and the corresponding mean daily precipitation rate (mdp) are reported in Fig.4. The temporal variability of these two parameters is quite similar. The highest Pb fluxes appear almost systematically when the mdp exhibits a high value. In contrast, the lowest Pb fluxes correspond to periods with no or little precipitation. This suggests that the high Pb fluxes result primarily from wet deposition. This is in agreement with what is generally observed in the marine atmosphere (Galloway *et al.*, 1982).

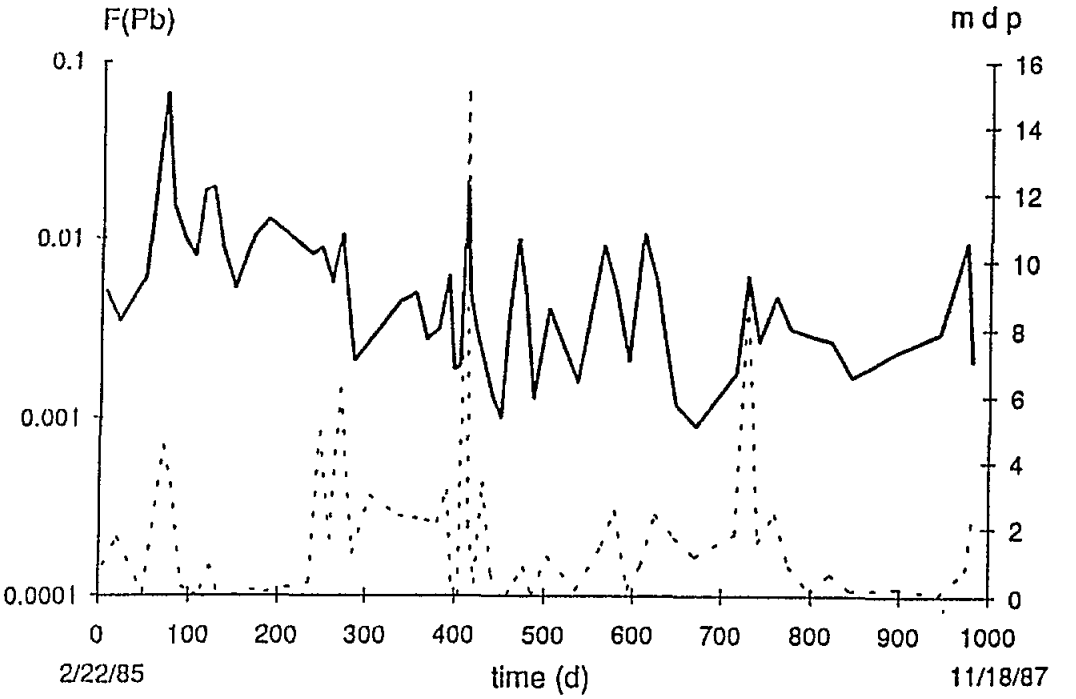

Fig.4 Solid line: temporal variability of lead deposition *F*(Pb) (in µg cm^{-2} d^{-1} for each sample). Dotted line: mean daily precipitation mdp (in mm d^{-1}) corresponding to each sample.

Relationship between atmospheric lead deposition and local precipitation. As indicated in Fig.5, it is apparent that the ratio between the lead flux and the corresponding mdp is not constant. This ratio is higher during spring and summer. This clearly suggests that atmospheric lead fluxes to marine areas cannot be estimated by algorithms linearly relating the Pb flux to the mdp. This can be explained by the combined influence of two factors: the scavenging of the aerosol particles by wet and/or dry deposition, and the concentration of the element in the air column over the sampling site.

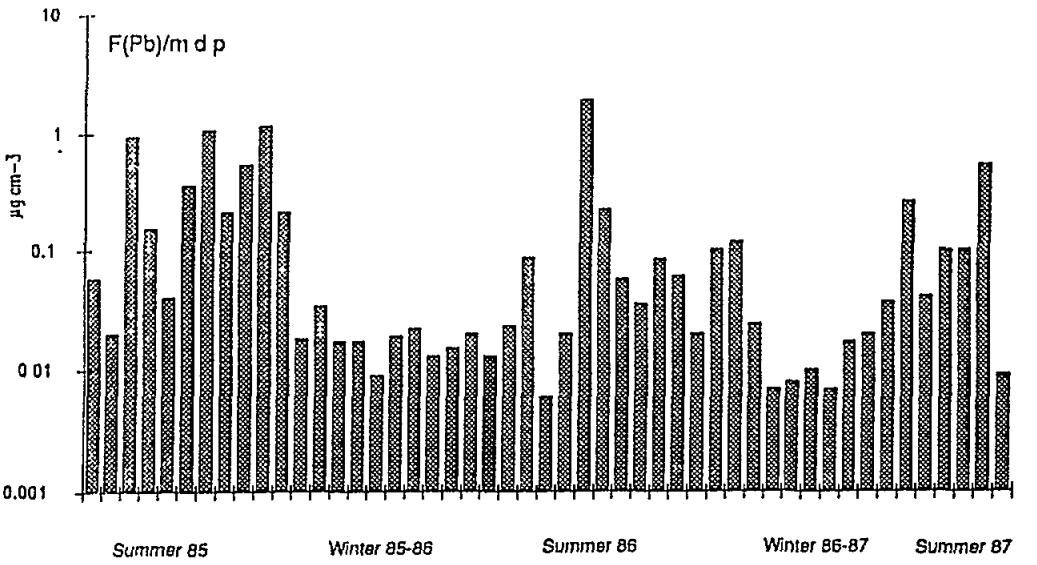

Fig.5 Ratios between the atmospheric lead deposition F(Pb) (in µg cm^{-2} d^{-1}) and the corresponding mean daily precipitation rate (in cm d^{-1}) for each sample.

Influence of dry deposition. The low values of mdp, during the dry season, could mean that dry deposition contributes significantly to the total deposition of Pb. To test this assumption, we calculated apparent dry deposition velocities using measured dry flux data and arithmetic mean aerosol concentrations corresponding to the duration of each sample.

The mean value of the dry deposition velocity of Pb is 1.8 cm s^{-1}. This value is in agreement with those measured using surrogate surfaces at other coastal or island sites (0.6 to 0.8 cm s^{-1}) (Cambray *et al.*, 1975). However, the measured value of Pb dry deposition velocity in this work is surprisingly high compared to values found using a modeling approach. Dulac *et al.* (1989) calculated a value of 0.05 cm s^{-1} based on observed mass-size distribution of lead and the dry deposition model of Slinn and Slinn (1980). The use of a surrogate surface to measure dry deposition rates causes significant uncertainty arising from the properties of such a surface. However, it is difficult to quantify this uncertainty by comparing our measured dry deposition velocity with those calculated by a modeling approach. This difficulty is mainly due to the uncertainties existing in dry deposition modeling. Sievering (1984) has suggested that the uncertainty in modelling dry deposition of small particles (D close to 1 µm) to natural water surfaces is about an order of magnitude.

A possible explanation is that factors, such as the occurrence of fog, may be responsible for the high value of the observed mean dry deposition velocity. Indeed, fog

episodes have been reported at our sampling site during periods with no precipitation. Hence the "dry" scavenging of aerosol particles during such periods is likely to include the effect of Pb scavenging by fog droplets.

Using our data, total (wet + dry) deposition velocities have been calculated for the samples, presenting a mean daily precipitation rate lower than 1 mm d^{-1}. The total deposition velocities ranged from 4 to 16 cm s^{-1}. This clearly suggests that dry deposition accounts for a minor fraction of the total Pb deposition flux even when precipitation events are scarce. Consequently, the relative fraction of dry deposition in our samples does not explain the large variation of the ratio F_{Pb}/mdp.

3.3 Relationship between atmospheric deposition of lead and the occurrence of rainy days

In Fig.6a we have reported the Pb fluxes after application of a moving mean method to our data, with a time span of about 60 days. In the same figure, we have reported the occurrence of rainy days using the same method. These results suggest that the major factor which controls the temporal variability of lead deposition is related to the ability of Pb to be transported from the source regions to the sampling area. This hypothesis is strongly supported by the comparison between the Pb and Na fluxes (Fig.6b). Indeed, Na is primarily present as locally produced sea-salt aerosol. Na deposition is therefore independent of transport processes. We observe that sodium deposition becomes important during the "rainy" season and is at a minimum during the "dry" season. Such behavior can be attributed to a very fast reloading of the local atmosphere, following a rain event, with locally produced sea-salt aerosol. The deposition of Na is enhanced during the rainy season because of the more frequent scavenging of the atmosphere by precipitation. In contrast, sea-salt aerosol particles are less frequently scavenged by precipitation events during the dry season (Fig.6b).

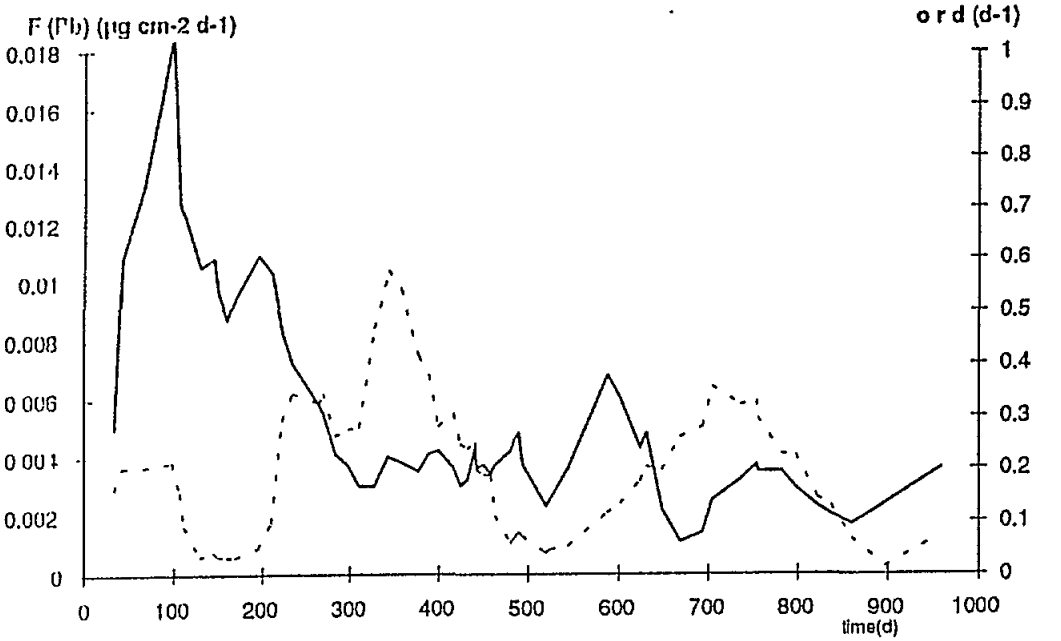

Fig.6a Solid line: lead deposition F(Pb) (in µg cm^{-2} d^{-1}) after application of a moving mean method with a time span of 60 days. Dotted line: occurrence of the rainy days (ord. in d^{-1}) from local precipitation data, after application of the moving mean method with the above time span. The occurrence of the rainy days (in d^{-1}) is defined as the number of the rainy days during a sample divided by the duration of the sample in days.

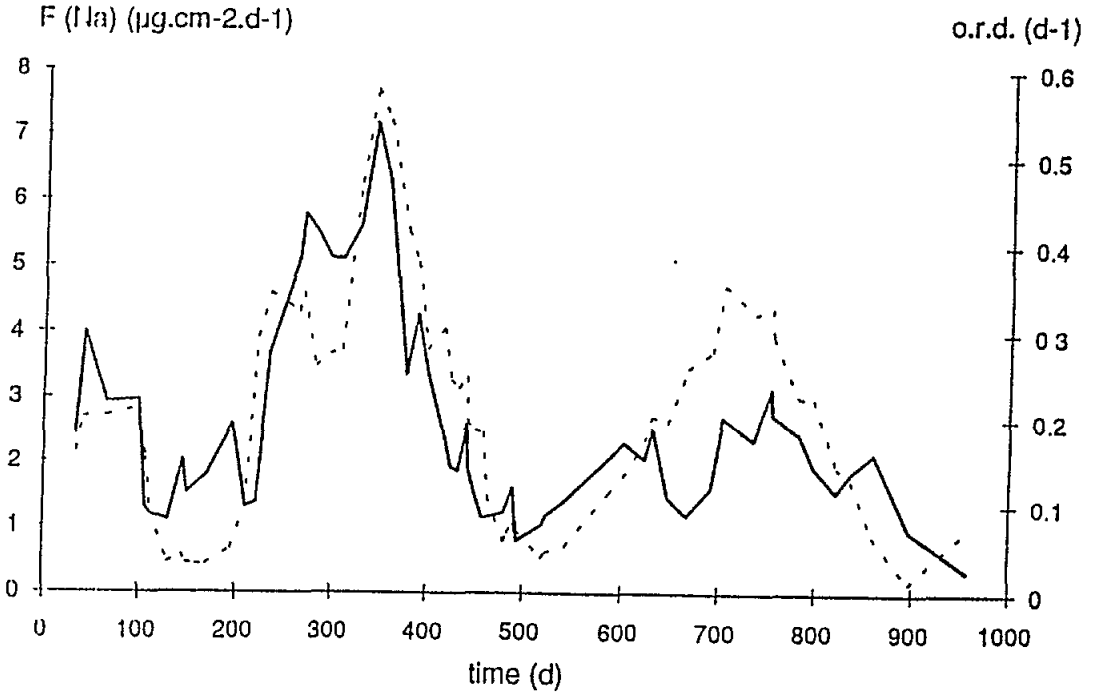

Fig.6b Solid line: sodium deposition F(Na) (in µg cm^{-2} d^{-1}) after application of a moving mean method with the above time span. Dotted line: the same as in Fig.6a.

On the other hand, total Pb deposition is highest during the dry season and lowest during the rainy season (Fig.6a). In addition, the variations of lead deposition are anti-correlated with those of the occurrence of the rainy days. The low Pb deposition values during the Mediterranean "winter" can be ascribed to the fact that the atmosphere being scavenged by rain is characterized by a relatively low Pb aerosol content.

Influence of local precipitation frequency on the seasonal variability of Pb deposition. As discussed previously, the existence of low atmospheric Pb concentrations during the rainy season can be explained by two closely connected arguments. Firstly, since lead concentrations result from transport from continental sources, the aerosol particles containing lead are frequently washed out by precipitation events before their arrival over the sampling site. Secondly, during the rainy season, there is not sufficient time between two rain events to reload the atmosphere of the receptor site with Pb aerosol particles.

Thus it is expected that the time needed for sufficient reloading of the receptor atmosphere is longer than the time interval between two rain events during the Mediterranean winter. To test this assumption, we have used data on precipitation forecast by the air mass trajectory model used in this work. The occurrence of precipitation events, during the transport of the air masses, was found relatively well correlated with the occurrence of local precipitation at Capo Cavallo. Local precipitation data for the whole sampling period were therefore used to estimate the effect of the local removal of lead aerosol particles by wet deposition and the scavenging of atmospheric lead during transport from the source regions to the sampling site.

If we now consider the temporal variation of total Pb deposition (Plate 1), we observe that the highest Pb fluxes correspond systematically to sampling periods characterized by the absence of rain during at least the first 4 days of sampling and the occurrence of precipitation

events at the end of the sampling period (i.e., samples 9, 10, 13, 28, 43, 54). High Pb fluxes are also observed if rain occurred during a sampling period preceded by a "dry" period of 4 days at least (i.e., samples 5, 31, 41, 46, 52). The lowest Pb deposition values correspond to sampling periods with no precipitation (8, 11, 12, 29, 30, 36, 40) and/or to sampling periods preceded by precipitation events (i.e., samples 3, 6, 19, 21, 26, 42, 45).

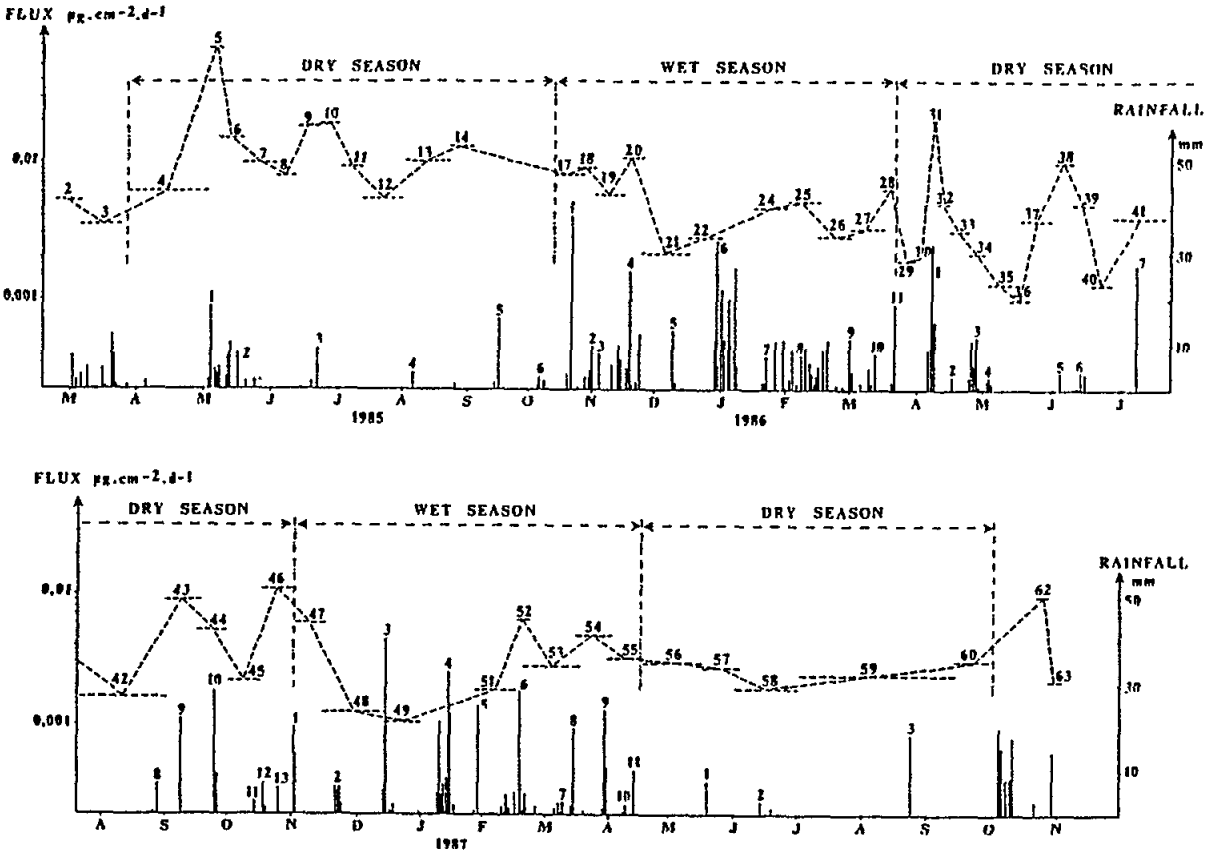

Plate 1 Lead deposition *F*(Pb) (in µg cm^{-2} d^{-1}) for each sample. The daily amount of precipitation is reported at the bottom of the figure. The curve is divided into dry and wet seasons. The groups of precipitation events, corresponding to each season, are also reported.

These observations suggest that the high values of Pb fluxes result from wet deposition, primarily when precipitation events occur after a long dry period.

As shown in Fig.1, we divided the sampling period into dry and wet seasons. For both seasons, we defined the frequency of the precipitation periods F_p as the number of groups of precipitation events divided by the duration of the corresponding period in days. The groups of precipitation events are separated from each other by a period of 4 "dry" days at least.

Pb and Na deposition fluxes, as well as the frequency of the precipitation periods F_p corresponding to each season, are reported in Table 1. These results allow us to conclude that the frequency of the precipitation periods influences the following factors.

Table 1

Seasonal Pb and Na Deposition and the Corresponding Frequency of Precipitation

Date Begin	Date End	Season	Sample	*F*p d^{-1}	*F*Pb $\mu g\ cm^{-2}d^{-1}$	*F*Na $\mu g\ cm^{-2}d^{-1}$
Mar. 25, 1985	Oct. 11, 1986	dry	4-14	0.30	0.0118	2.3
Oct. 11, 1985	Mar. 22, 1986	wet	17-28	0.74	0.0025	5.2
Mar. 22, 1986	Nov. 01, 1986	dry	29-46	0.58	0.0042	1.7
Nov. 01, 1986	Apr. 16, 1987	wet	47-55	0.79	0.0028	2.2
Apr. 16, 1987	Oct. 02, 1987	dry	56-60	0.08	0.0024	1.1

The degree of loading of the receptor atmosphere with Pb aerosol particles: High values of F_p imply that there is not sufficient time to reload the atmosphere with aerosol particles of continental origin. Thus the Pb deposition presents low values during both rainy seasons (1985-1986, 1986-1987). On the other hand, during the summer of 1986, the atmosphere was frequently scavenged by rains. This period therefore cannot be classified as a "normal" dry season. The value of the total Pb deposition during the summer of 1986 is lower than that observed during the summer of 1985, but higher than that observed during both rainy seasons (Table 1).

The relative importance of wet and dry deposition of lead: A low value of F_p implies that dry deposition may become significant. For example, the value of the Pb flux during the summer of 1987 can be ascribed to the lack of precipitation. Indeed, as previously discussed, dry deposition processes are less efficient in removing Pb aerosol particles than precipitation scavenging. Consequently, in such a case, even if the local atmosphere has a high lead content, the corresponding Pb deposition flux is low.

These two influences of F_p on the seasonal variability of Pb fluxes seem to be operating simultaneously during the summer of 1985. An intermediate value of F_p allows sufficient reloading of the local atmosphere with Pb aerosol particles as well as efficient scavenging by precipitation events. In this case, the Pb deposition flux is the highest observed.

4. CONCLUDING REMARKS

We have shown that the variability of aerosol lead concentrations on both daily and seasonal time scales is primarily due to the scavenging of lead aerosol particles by rain rather than to changes in source regions.

On a daily time scale, local precipitation events are responsible for the sharpest decreases of atmospheric lead concentrations.

On a seasonal time scale, rains occurring during transport, as well as locally, generate a seasonal cycle for lead concentrations in the western Mediterranean atmosphere with high atmospheric concentrations during the dry season, and low concentrations during the wet season.

Our results suggest that the ratio between the Pb flux and the corresponding mdp is not constant. This ratio reaches a maximum during the Mediterranean summer. We attribute this difference to the fact that the local atmosphere is more heavily loaded with lead during the "dry" season.

Consequently, the seasonal variability of Pb deposition is more pronounced when the frequency of precipitation events occurring during the dry season, exhibiting an intermediate value. There is probably a lower and an upper limit for this intermediate value of F_p. Above this upper limit, the seasonal variability of Pb fluxes becomes less pronounced, as was the case during the summer of 1986. In contrast, below the lower limit (i.e., summer 1987), the Pb fluxes may become less important than those corresponding to the rainy season.

Our measurements also show that, during rainy periods, Pb is not transported efficiently to the open sea. This implies that, during the rainy period, Pb atmospheric deposition measured at Capo Cavallo is probably much lower than that occurring at the same time on the continental shoreline, where the Pb deposition flux is probably better correlated with the occurrence of rainy days. Hence the open sea is probably more affected by atmospheric Pb input during the dry season, while the continental coastal regions are probably more affected during the wet season. We can therefore expect both a spatial and a temporal pattern of Pb deposition to the western Mediterranean. This raises some doubts about the validity of extrapolating lead deposition fluxes from a single sampling site to the entire basin.

The annual flux of lead for the first year of measurements (from March 25, 1985 to March 22, 1986), was 3.1 µg cm^{-2} yr^{-1}, while for the second year (from March 22, 1986 to April 16, 1987) this flux was only 1.5 µg cm^{-2} y^{-1}. Therefore a significant inter-annual variability is also observed at our sampling site. This results primarily from the different Pb deposition fluxes recorded during the two dry seasons.

Finally, we stress that the impact of the atmospheric input on Pb concentrations in the surface waters of this area is more pronounced during summer and fall, as is also observed for phosphorus (Bergametti et al;, in press). This is because of the high Pb deposition flux during this period of the year and the existence of a well-developed surface mixed layer in the Mediterranean waters (about 50 m in depth) which favours the buildup of atmospherically derived lead inputs.

5. ACKNOWLEDGMENTS

We wish to thank the staff of the signal station of Capo Cavallo for logistical support during the field experiments in Corsica. We also thank the French Marine Nationale for free access to the signal station and the French Direction de la Météorologie Nationale for use of the meteorological tower at Capo Cavallo. We are grateful to R. Losno, B. Chatenet, L. Gomes, A. Dutot and F. Dulac for assistance in sampling and analysis and for helpful discussion. We are particularly grateful to D. Martin, B. Strauss, and J. M. Gros, who computed the air mass trajectories. This work was supported in part by the Ministère de l'Environnement, the Programme Flux Océanique of INSU CNRS (DYFAMED), by UNEP/WMO (MEDPOL), and by a doctoral fellowship (sectoral grant B/87000259, E. R) of the Environmental Research Programme of the European Economic Communities.

6. REFERENCES

Arimoto, R., R.A. Duce, B.J. Ray and C.K. Unni (1985). Atmospheric trace elements at Enewetac Atoll, 2, Transport to the ocean by wet and dry deposition, *J. Geophys. Res*., 90:2391-2408.

Arnold, M., A. Seghaier, D. Martin, P. Buat-Ménard, and R. Chesselet (1982). Géochimie de l' aérosol marin au-dessus de la Méditerranée Occidentale. Paper presented at the VI journées d'études sur les pollutions marines en Méditerranée, Monaco.

Bergametti, G. (1987). Apports de matière par voie atmosphérique à la Mediterranée Occidentale: Aspects géochimiques et météorologiques, Thesis, Univ. Paris 7.

Bergametti, G., A.L. Dutot, P. Buat-Ménard, R. Losno, and E. Remoudaki (1989). Seasonal variability of the elemental composition of atmospheric aerosol particles over the northwestern Mediterranean. *Tellus*, 41B:353-361.

Bergametti, G., E. Remoudaki, R. Losno, E. Steiner, B. Chatenet and P. Buat-Ménard. Source, transport and deposition of atmospheric phosphorus over the Western Mediterranean. *J. Atmos. Chem*. (in press).

Boyle, E. A., S.D. Chapnick, G.T. Shen, and M.P. Bacon (1986). Temporal variability of lead in the western north Atlantic. *J. Geophys. Res*., 91:8573-8593.

Cambray, R.S., D.F. Jefferies, and G. Topping (1975). An estimate of the input of atmospheric trace elements into the North Sea and the Clyde Sea (72-73), U.K. At. Energy Autho., *Publ. AERE-R7733*, London, 30pp.

Dulac, F., P. Buat-Ménard, M. Arnold, and U. Ezat (1987). Atmospheric input of trace metals to the western Mediterranean Sea, 1, Factors controlling the variability of atmospheric concentrations. *J. Geophys. Res*., 92:8437-8453.

Dulac, F., P. Buat-Ménard, U. Ezat, S. Melki, and G. Bergametti (1989). Atmospheric trace metals to the western Mediterranean Sea: Uncertainties in modelling dry deposition from cascade impactor data. *Tellus*, 41B:362-378.

Feinberg, M. (1984). Reflexion prospective sur quelques concepts de la chimie analytique et sur sa demarche expérimentale, Thesis, Univ. Pierre et Marie Curie, Paris.

Flegal, A.R., and C.C. Patterson (1983). Vertical concentration profiles of Pb in the central Pacific at 15 N and 20 S, *Earth Planet. Sci. Lett.*, 64:19-32.

Galloway, J.N., J.D. Thornton, S.A. Norton, H.L. Vol chok, and R.A. MacLean (1982). Trace metals in atmospheric deposition: A review and assessment. *Atmos. Environ*., 16:1677-1700.

Hewitt, C.N., and R.M. Harrison (1987). Atmospheric concentrations and chemistry of alkyllead compounds and environmental alkylation of lead. *Environ. Sci. Technol*., 21:260-266.

Imbard, M. (1983). Trajectoires: transport à longue distance, *Note CETI*, Météorol. Natl., Paris.

Lambert, G. (1963). Etude du comportement des aerosols radioactifs artificiels, Applications à quelques problèmes de circulation atmosphérique, Thesis, Faculté des Sci. de l'Univ. de Paris.

Laumond, F., G. Copin-Montegut, P. Courau and E. Nicolas (1984). Cadmium, copper and lead in the western Mediterranean Sea. *Mar. Chem.*, 15:251-261.

Maring, H., D. Settle, P. Buat-Ménard, F. Dulac and C. Patterson (1987). Stable lead isotope tracers of air mass trajectories in the Mediterranean region. *Nature*, 330:154-156.

Pacyna, J. (1984). Estimation of the atmospheric emissions of trace elements from anthropogenic sources in Europe. *Atmos. Environ.*, 18:41-50.

Patterson, C.C. and D.M. Settle (1987). Review of data on eolian fluxes of industrial and natural lead to the lands and seas in remote regions on a global scale. *Mar. Chem*., 22:137-162.

Remoudaki, E., G. Bergametti and P. Buat-Ménard (1991a). Temporal variability of atmospheric lead concentrations and fluxes over the northwestern Mediterranean sea. *J. Geophys. Res*., 96:1043-1055.

Remoudaki, E., G. Bergametti and R. Losno (1991b). On the dynamic of the atmospheric input of copper and manganese into the western Mediterranean sea. *Atmos. Environ*., 25A:733-744.

Schaule, B.K. and C.C. Patterson (1981). Lead concentrations in the Northeast Pacific: Evidence for global anthropogenic perturbations. *Earth Planet. Sci. Lett*., 54:97-116.

Schaule, B.K. and C.C. Patterson (1982). Perturbations of the natural lead depth profile in the Sargasso Sea by industrial lead. In: *Trace Metals in Sea Water*, Plenum, New York.

Settle, D.M. and C.C. Patterson (1982). Magnitudes and sources of precipitation and dry deposition fluxes of industrial and natural leads to the North Pacific at Enewetak. *J. Geophys. Res*., 87:8857-8869.

Sievering, H. (1984). Small particle dry deposition on natural waters: How large the uncertainty? *Atmos. Environ*., 18:2271-2272.

Slinn, S.A. and W.G. Slinn (1980). Prediction for particle deposition on natural waters. *Atmos. Environ*., 14:1013-1016.

A NEW SAMPLING STATION AT THE COASTAL SITE OF CAPO CARBONARA (SARDINIA, CENTRAL MEDITERRANEAN): PRELIMINARY DATA AND TECHNICAL PROPOSALS

By

S. GUERZONI[(1)], G. CESARI[(2)], R. LENAZ[(1)] and L. CRUCIANI[(3)]

(1) Ist. Geologia Marina, CNR, via Zamboni n.65, 40127 Bologna, Italy.
(2) Ist. FISBAT, CNR, via Dè Castagnoli n. 1, 40126 Bologna, Italy.
(3) Servizio Meteorologico, Piazzale degli Archivi n.34, 00144 Roma, Italy.

A B S T R A C T

A new sampling station was implemented at a remote coastal station in the Southeast part of Sardinia Island, in the Central Mediterranean Sea. Before commencing routine sampling, some intercomparisons were done between Hi-(60 m^3/h) and Low-Vol (3 m^3/h) samplers using different filtering media (cellulose, Nucleopore and nylon). Single rain events were concurrently sampled using a wet and dry sampler. Some differences in the collection efficiency are discussed, in relation to low and high volume instruments, filter media and grain-size of the samples.

During the first six months (Oct.90 - March.91) more than 40 air samples and 20 precipitation events were collected. Preliminary data showed a mean value of total suspended particles (TSP) of 27 µg/m^3 (range 10-78), with the insoluble fraction usually 10-15% of the total particulate. Several samples with high SPM values (> 50 µg/m^3) resulted to be associated with South-Southeast winds, i.e. Saharan transport episodes, and were composed of more than 50% of mineral fraction.

1. INTRODUCTION

Measurements of the chemical composition of rainwater and suspended particles collected in parallel at a remote site in Sardinia were done, in order to investigate the concentration and fluxes of trace metals and the input of Saharan dust to the Mediterranean Sea. The sampling site (Fig.1) is 250 km north of the Sahara desert and more than 400 from Italy (Northeaast) and France (Northwest). The principal winds are from the West and East-Southeast, and the location is far from local sources of pollutants (ENEL-SMAM, 1983).

Before starting the daily sampling, some intercomparisons were made between Hi- (60 m^3/h) and Low-Vol (3 m^3/h) samplers using different filtering media (cellulose, Nucleopore and nylon).

1.1. Technical details

Routine sampling was done with a Hi-Vol Sierra Andersen sampler, using a 5 µm nominal porosity nylon filter (8'x11'). The sampling duration was 24 to 72 hours. The filters were washed in acidified DDW, dried overnight and weighted before sampling. After collection, the filters were left overnight in the same dry-box and re-weighted. This insured that all samples were brought to the same degree of dryness before being weighted.

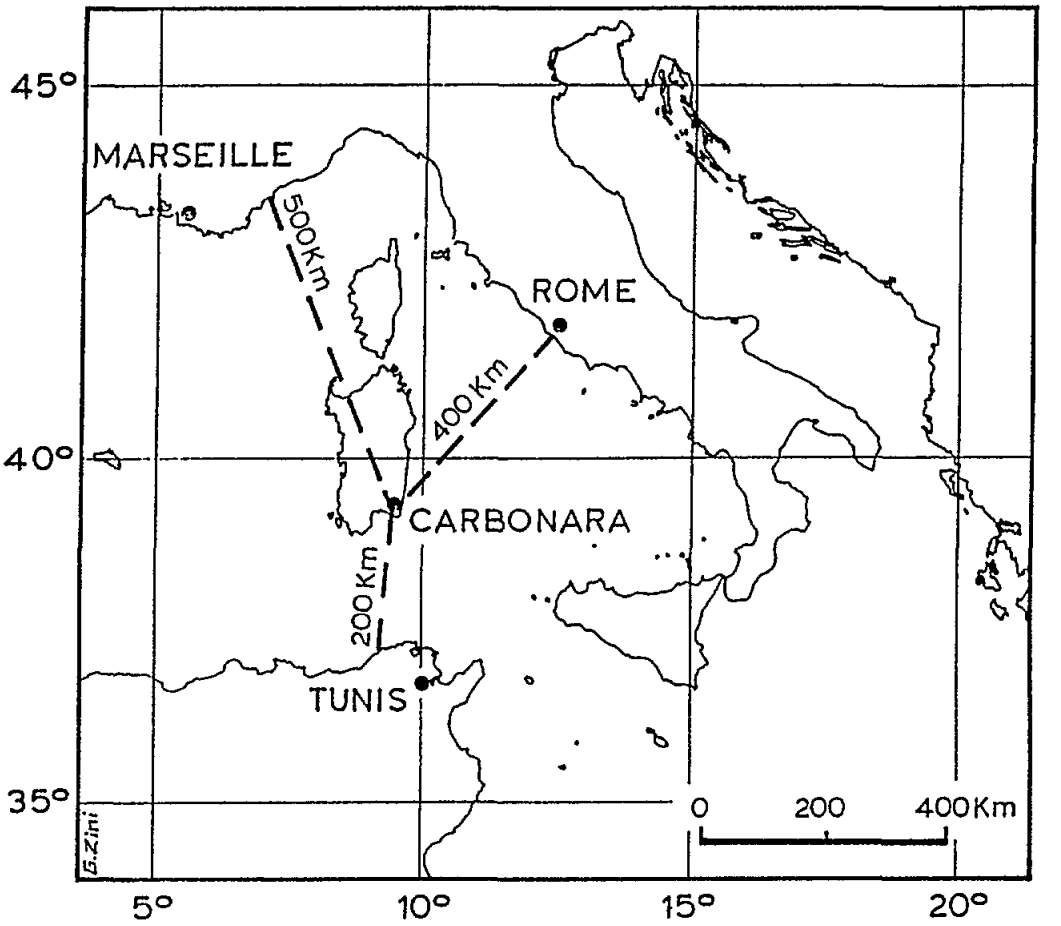

Fig.1 Location of the sampling station

Single rain events were concurrently sampled using a wet and dry sampler, and the specimen was filtered and subdivided into two phase fractions, dissolved and particulate.

The same occurred in the Hi-Vol filters: they were put in a Milli-Q DD water bath for 20-30 minutes. After that, the sub-sample for mineralogical and grain-size analyses was made and all the solution centrifuged to recover the soluble parts to be analyzed. The particles at the bottom of the centrifuge tube were transferred to crucibles, dried at 60°C and weighted.

On both the Hi-Vol soluble and mineral fractions major geochemical (Fe,Si,Al,Ca,Mn) and some trace metal (Cd,Pb,Cr) analyses were carried out. In addition, on the dry fraction grain-size, mineralogical and SEM determinations were carried out. Analytical methods are described in detail elsewhere (Guerzoni *et al.*, 1987; Correggiari *et al.*, 1989). Meteorological data during sampling were provided by the Italian Meteorological Service.

2. RESULTS

2.1 Intercomparisons

All relevant data related to the intercomparisons are shown in Figs.2 and 3 and listed in Table 1.

The first intercomparison was made using different sampling equipment: one low/vol (3 m^3/h) sampler with "total" filters (Teflon 0.2 µm porosity) and one Hi/Vol (60 m^3/h) with filters of nylon monofilament fabrics. Fig.2 reports the recovery data for the sampling equipment: the values are in quite good agreement, with slightly higher values of TSP in the Hi-Vol sampler, probably due to better efficiency in collecting the coarse particles.

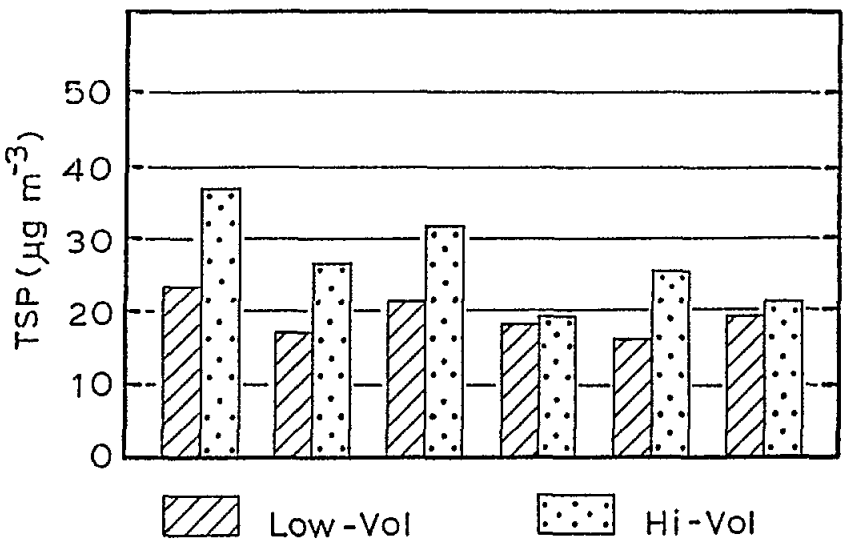

Fig.2 TSP recovery (µg/m^3) of two different samplers: left, Low-Vol (3m^3/h) with "total" teflon filter (0.2 µm); right, Hi-Vol (60 m^3/h), with nylon monofilament (5 µm).

The second intercomparison was performed between nylon and Waghtman 41 filters, using the same Hi/Vol sampler. Table 1 presents the recovery data on different filter media, together with grain-size values and information on rain events during the sampling period. The total recovery was less than 30 mg of particles for most of the samples, and the total suspended particles (TSP) values ranged from 17 to 61 µg/m^3. The total Waghtman 41 filtering system was slightly more efficient (avg. TSP = 50 µg m^{-3}) than that of the nylon (avg. TSP = 35 µg m^{-3}). The lower recovery of the nylon filters was also due to the sampling period in the proximity of rain events.

On nylon filters we did recover the particles for subsequent grain-size analyses. The methodology for grain-size analyses was experimental (the frequency histograms are shown in Fig.3), since we used the coulter counter, usually devoted to suspended sediment analysis. The data of the five studied samples showed very interesting results, with a good discriminating power of the analytical method. The data showed two different groups: (a) samples 1 and 2, with the mode of 10-20 µm, and North-Northwest winds during

sampling; (b) samples 4, 6 and 8 with mixed winds during sampling. In the second group the grain-size is bimodal, 2-5/10-15 μm, with some differences in the samples which were also affected by rain events during collection (Nos.4 and 6).

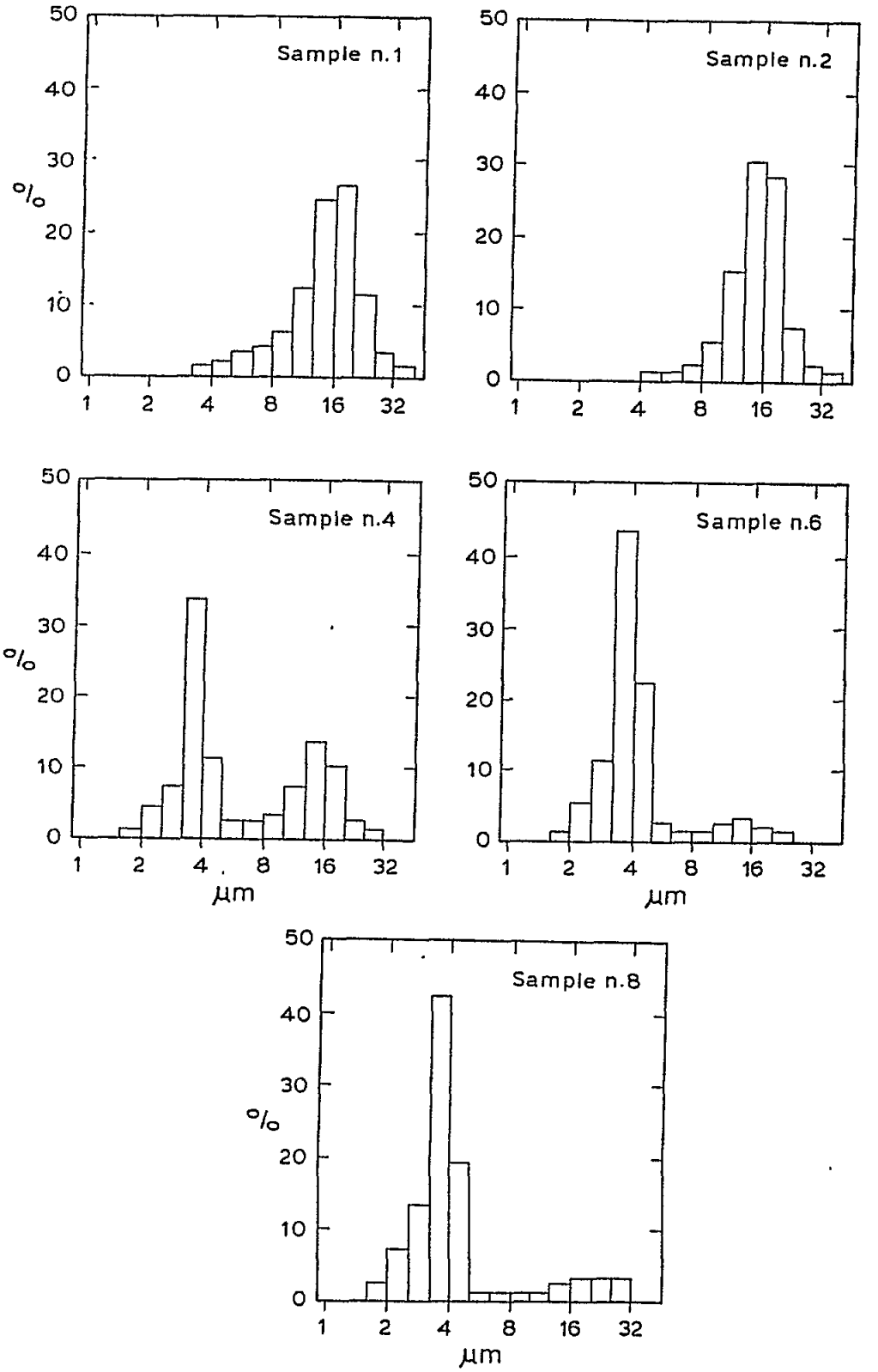

Fig.3 Grain-size histograms of the samples used for the intercomparison.

Table 1

Filter media intercomparison for Hi/Vol aerosol samples : relevant data

Sample No.	TSP g/m^3	Prevailing winds	Grain-size mode (µm)	Filter media
01	17	N-NW	10-20	Nylon 5 µM
02	40	N-NW	10-20	Nylon 5 µm
03	42	N-NW	---	Waghtman 41
04	17	S-SE	2-4/10-15	Nylon 5 µm
05	61	E-SE	---	Waghtman 41
06	49	MIX/S	2-4/10	Nylon 5 µm
07	56	MIX	---	Waghtman 41
08	37	N	2-4/10-20	Nylon µm
09	31	N	---	Waghtman 41

2.2 Hi-Vol samples

From October 1990 to March 1991, we collected more than 40 air samples. The mean value of total suspended particulate (TSP) is 27 µg/m^3 (range 10-78) and the insoluble fraction, i.e. mineral suspended particulate (MSP) is 10-15% of the total particulate, with some variation in the composition according to air mass provenance. In particular (see Table 2), most of the time the TSP values are - on average - 18 µg/m^3, whilst during the southern wind episodes the mass loading increases up to 70-90 µg/m^3. Accordingly, the mineral (insoluble) fraction is 2-4 µg/m^3 (i.e. 10-20%) for non-southern winds and 20-50 µg/m^3 (30-60%) during southern events. These figures are slightly higher than other TSP data published from Chester *et al.*, 1984 and Dulac *et al.*, 1989.

Table 2

Average total suspended particles (TSP) and mineral suspended particles (MSP) content of the Hi-Vol samples collected during the period Oct.90-Mar.91 at Capo Carbonara

Wind direction	TSP µg/m^3	MSP µg/m^3	MSP/TSP %
Southern	50	30	60
Others	18	3-4	20

Several episodes with very high TSP values (> 50 µg/m^3) and more than 50% of insoluble fraction resulted to be associated with East-Southeast winds, i.e. Saharan transport. One of these events with the highest TSP value (> 70µg/m^3) is presented here: it occurred in October 1990 and Fig.4 shows the associated meteosat photograph and the meteorological synoptic situation at 500mb.

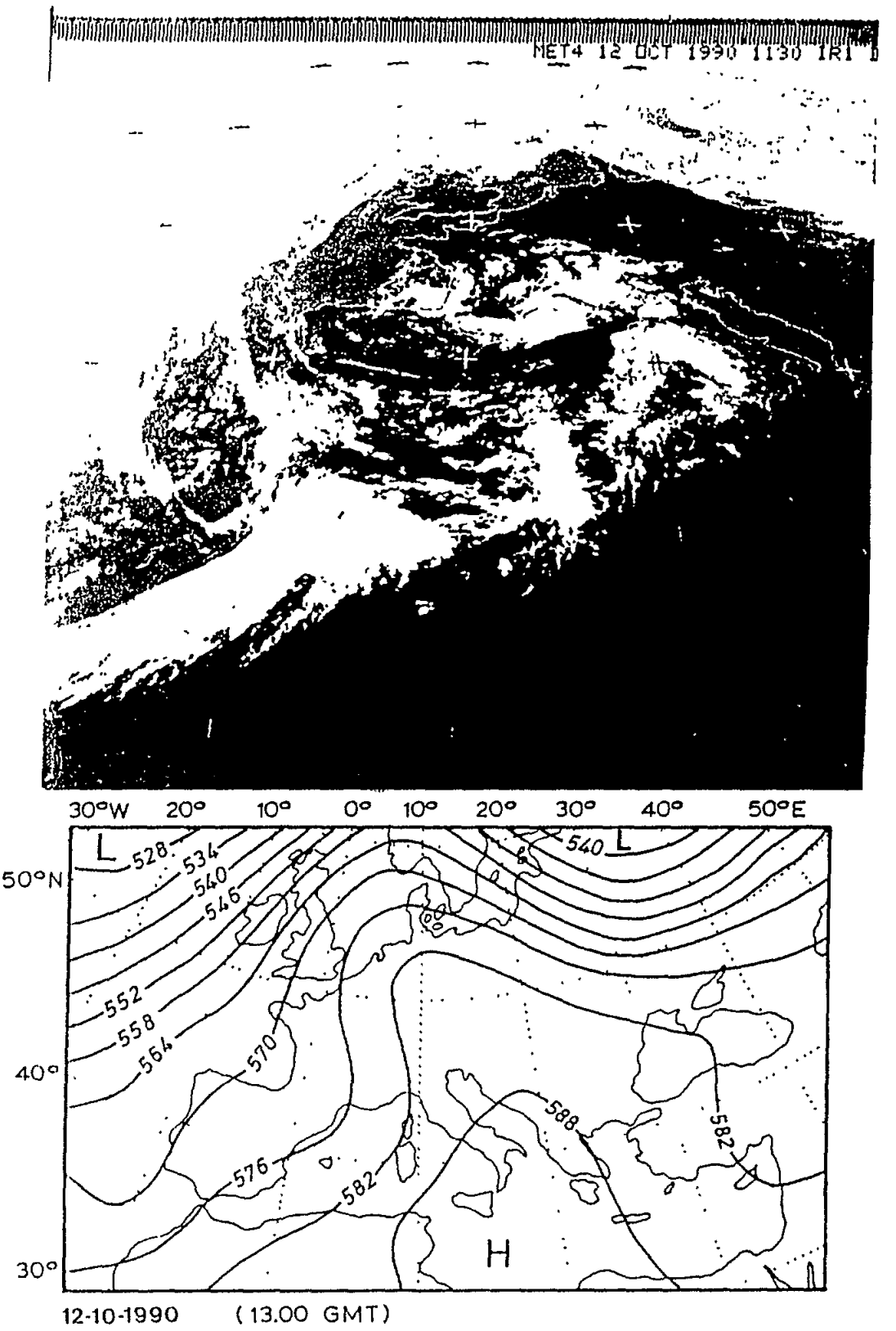

Fig.4 IR Meteosat photo (above) and synoptic meteorological situation at 500 mb (below) of the southern transport episode on October 12th, 1990.

During the first six months of continuous sampling the number of days with this high load (avg MSP 30 µg/m^3) were between 25 and 30: we can therefore calculate the total flux of Saharan dust to the area. If we assume a deposition velocity of 1 cm/sec (and probably twice as much for mineral dust) the flux resulted in 2.6 g/cm^2/day, whilst the mean flux for the rest of the period is 0.2 µg/cm^2/day.

Since approximately 15% (27 days out of 180) of the trajectories came from the south to the sampling site, the total mineral flux during the first six months was 100 g/cm^2, 70% of which is due to Saharan inputs.

2.3 Precipitation data

Rain analyses from Carbonara are not presented here, and we will discuss data from a nearby station, at the boundaries of the wood at Pixinamanna, in an area of about 5 km^2 at the foot (150 m above sea level) of the mountains, a few kilometres from the South coast of Sardinia (period: Oct 87- Oct 88, from Caboi *et al.*, 1990).

Table 3 shows some relevant data of the rainwater collected in Southern Sardinia, with distinct characteristics according to meteorological conditions. When Northwest perturbances occurred, the average pH was 4.7 (Ca=15 eq/l); southern Trades transported Saharan dust that neutralized the rainwater (avg pH=6.6) with its large calcite content (Ca=252 µeq/l).

Table 3

General characteristics and element concentrations in rain collected near Cagliari (period: Oct.87-Oct.88, from Caboi *et al*., 1989)

Wind	No. of Events	mm of rain	pH (st. dev)	Ca^{++} µeq/l	Pb	ZN
					- - ppb - -	
NW	(20)	150	4.7 (0.4)	15	12	11
S	(09)	84	6.6 (0.9)	252	2	9
mix	(13)	120	6.2 (0.9)	174	2	7

The influence of more distant source regions was examined by separating the precipitation events by wind direction. The events with mixed and/or low winds had the highest SO_4^{-2} to NO_3^- ratios. NO_3^- showed no directional dependence.

3. CONCLUSIONS

Some discrepancies between TSP data published by other authors and our own suggest that in the future comparisons among different sampling instrumentation, filter media and TSP measurements should be done. In particular, attention should be devoted to determine the collection efficiency of the different instruments (total amounts, grain-size selection, etc.).

Additional studies on mesoscale modelling for the area would be useful, in particular to assess the annual atmospheric inputs (in weight), natural and polluted, to the Mediterranean Sea.

It will probably be very important to distinguish the part of the aerosol and precipitation input that affects marine waters from the insoluble part that contributes to sedimentation processes.

A comparative study of the ionic composition of rainwater and atmospheric aerosol collected recently is underway. In the near future we also intend to study the implications of the washout ratios for the mechanism of acidification of rainwater and deposition of trace metals.

4. ACKNOWLEDGMENTS

We thank G. Zini for the drawings. This work was partially supported by WMO SSA No. 16.566/A/CNS. This is IGM-CNR scientific contribution no. 834.

5. REFERENCES

Caboi R., A. Cristini, F. Faru, R. Pinna and A. Piu (1990). Distinzione delle componenti marina e continentale nelle precipitazioni piovose dell'area forestale di Pixina Manna (Sardegna sud-occidentale). *Acqua-Aria*, 8:665-671.

Chester R., E.J. Sharples and G.S. Sanders (1984). Saharan dust incursion over the Thyrrenian Sea. *Atmospheric Environment*, 18:929-935.

Correggiari A., S. Guerzoni, R. Lenaz, G. Quarantotto and G. Rampazzo (1989). Dust deposition in the central Mediterranean (Thyrrenian and Adriatic Seas): relationships with marine sediments and riverine input. *Terra Nova*, 1(6):549-558.

Dulac F., P. Buat-Ménard, U. Ezat, S. Melki and G. Bergametti (1989). Atmospheric input of trace metals to the western Mediterranean: uncertainities in modelling dry deposition from cascade impactor data. *Tellus*, 41B:362- 378.

ENEL-SMAM (1983). In: *Caratteristiche diffusive dei bassi strati dell'atmosfera: Sardegna*, Vol 16, pp.300.

Guerzoni S., G. Rovatti, E. Molinaroli and G. Rampazzo (1987). Total and "selective" extraction methods for trace metals in marine sediments reference samples. *Chemistry and Ecology*, 3:39-48.

SIX YEARS (1985-1990) OF SUSPENDED PARTICULATE MATTER (SPM) AND PRECIPITATION DATA AT MESSINA STATION, ITALY : RELATIONSHIPS BETWEEN DUST TRANSPORT AND RAIN CHEMISTRY

By

L. CRUCIANI[1], L. FALASCONI,[2] S. GUERZONI,[3] G. QUARANTOTTI[3] and G. RAMPAZZO[4]

(1) Servizio Meteorologico, Piazzale degli Archivi 34, 00144 Roma, Italy.
(2) R.S.M.A, Via Braccianese Km 18, 00062 Vigna di Valle, Italy.
(3) Istituto per la Geologia Marina - CNR, Via Zamboni 65, 40127 Bologna, Italy.
(4) Dipartimento di Scienze Ambientali, Università di Venezia, Dorsoduro 2137, 30123 Venezia, Italy.

A B S T R A C T

Precipitation and aerosol samples have been collected weekly at Messina station since 1985. Ionic composition and pH of rain samples have been analyzed according to the WMO-BAPMoN procedures. Suspended particulate matter (SPM) content and the abundance of some metals (major and minor elements) were determined on the Hi-Vol air samples.

The arithmetic mean and the standard deviation for mass loading are 59 and 26 $\mu g/m^3$ respectively. The mean pH value decreases from 5.1 to 4.7 during the second half of the sampling period (1988-1890). Seasonal variability of SPM values higher than 100 $\mu g/m^3$ was studied and compared with pH values and Ca^{2+} content in rain.

An attempt to present some relationships amongst dust transport, meteorological conditions, rain and particulate chemistry is also discussed.

1. INTRODUCTION

Since 1985 the Italian Meteorological Service has been operating a sampling station at Messina (Lat. N 38N12'; Long. E 15N33'), at first only involved in the MED POL programme and later, from 1988, also in the BAPMoN programme. The station is located on a low hill facing the harbour, at a height of 50 meters above sea level. Taking into account the anthropogenic emissions related with the harbour activities, we can consider the station as an "impact station".

At this station, suspended particulate matter (SPM) and weekly rain samples have been collected since 1985 (Ciattaglia and Cruciani, 1989). Whilst rain samples were analyzed according to standard methods, no attempt was made until now to characterize major and minor elements collected on filters, and the only information obtained to date were related to the SPM weight. The careful storage of the filters and the co-operation between the Italian Meteorological Service and the Marine Geology Institute (Guerzoni *et al.*, 1987; Correggiari *et al.*, 1989) have allowed the analysis of some exposed filters, in order to obtain information on the concentration and origin of heavy metals.

This paper describes the results obtained during six years of sampling, in order to create a clearer understanding of the relationships between Saharan dust transport (Chester *et al.*, 1984), rain chemistry and anthropogenic activities related to the Messina area.

2. SAMPLING AND MATERIALS

2.1 Precipitations

Rain samples are collected weekly by a wet/dry rain collector, type MTX-ARS 1000. The sampling starts on monday at 09.00 GMT and stops on the following monday at 08.59 GMT. The sample collected is removed, treated with toluene and properly stored (in the dark and at 4NC) to prevent biological activity and to minimize solubilization of soil-derived ions. At the end of the sampling period the rain sample is shaken and, when possible, a subsample of 500 ml is sent to the chemical laboratory located at the R.S.M.A., Vigna di Valle, where all data related to environmental programmes are collected, processed and stored.

2.2 Suspended particulate matter

Suspended particulate matter (SPM) is collected using a Hi-Vol sampler, type STROHLEIN HVS 150, filtering air on a SM 13400 Glass fiber Prefilter. The sampling duration is 24 hours, subdivided into two periods of 12 hours each, with an interval of 15 minutes between them. Filter conditioning operations, which are very important in order to obtain acceptable data, are as follows:

(a) "blank" filter desiccation for 24 h;
(b) dried filter weighting and exposure for the 24 h sampling, according to the described protocols;
(c) "exposed" filter desiccation for 24 h;
(d) filter re-weighting and storage.

3. ANALYTICAL TECHNIQUES

3.1 Precipitations

Chemical and physical analyses are carried out according to the methodologies of the BAPMoN programme and using the instrumentation described in the following Table 1.

3.2 Suspended particulate matter (SPM)

On the assumption that the SPM distribution is homogeneous on the whole filter, we can use a portion of it to perform chemical analysis, thereby preserving a substantial part of the filter for retrospective surveys of new parameters. For this reason we used only 1/4 of the total exposed filter and of the filter used as a blank during the analysis. The filters were placed into teflon test-tubes to which HF 50% aqua regia and ultrapure double distilled water (DDW) was added. The test-tubes were then put into a microwave oven and the following two digestion cycles were applied to obtain the solutions indicated:

	1E step	2'	35% of the power (500 W)
1E cycle	2E step	5'	60% " " "
	3E step	2'	30% " " "
	1E step	5'	35% of the power (500 W)
2E cycle	2E step	10'	70% " " "
	3E step	2'	30% " " "

Table 1

Measurements carried out on precipitation samples

Programme	Station	Sampling	Parameter to be determined (1)	Instrumentation used at Vigna di Valle Laboratory
BAPMoN AND RIDEP	M. Cimone (2) Verona Viterio S. Maria di Leuca Messina (2) Trapani	W E E K L Y	pH, Ac/Alc	PHILIPS PW 9422 pHmeter
			Conductivity	PHILIPS PW 9527 conductivimeter
			NO_3^- - N SO_4^{2-} - S Cl^-	DIONEX 4000i Ionic chromatograph equipped with autosampler
			NH_4^+ - N	PYE UNICAM SP8 - 150 spectrophotometer UV/VIS
MED POL	Messina	Weekly	Na^+, K^+, Ca^{2+}, Mg^{2+}	PYE UNICAM SP2900 AAS, equipped with PU 9090 (data graphic system), PU 9095 (video furnace programmer), SP9 (furnace power supply) and autosampler
RIDEP (3)	Vigna di Valle	Weekly		

(1) They are the same in all programmes;
(2) At these stations also SPM (Suspended Particulate Matter) is monitored;
(3) RIDEP is the Italian National Programme related to Acidic Deposition.

After cooling the container, we added H_3BO_3 to eliminate the interferences due to fluorides. However, as there were some insoluble glass-fiber particles, we filtered the solution with Waghtman 42 filter paper. Calibration standards, to perform a quantitative analysis, were prepared using blanks added with an internal standard. Cd and Pb have been

analyzed by flameless electrothermal atomization, while for Febyatomic absorption spectrometry was used.

4. DISCUSSION

4.1 Suspended particulate matter

The whole gravimetric data set and the frequency tabulation for SPM values are shown in Fig.1 and listed in Table 2.

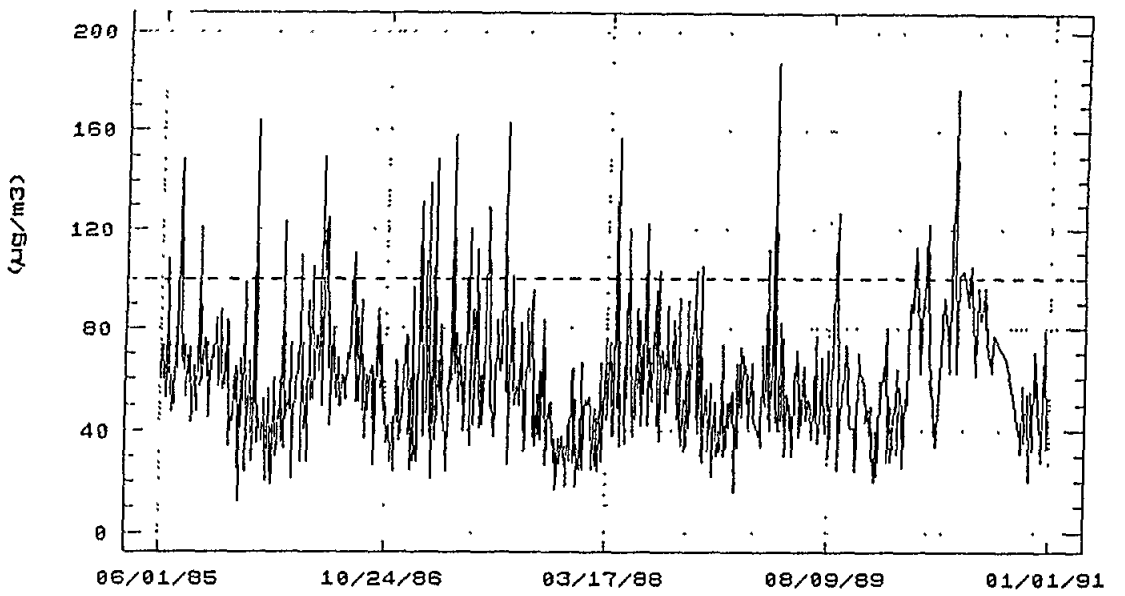

Fig.1 Plot of SPM weight vs sampling date from 1985 to 1990

As can be seen, some values are more than twice the average. Even if the anthropogenic influence of the harbour activities is taken into account, we think that some of the samples are surely influenced by Saharan dust transport, as will be discussed later.

The whole sampling period was divided into two sub-periods, 1985-1987 and 1988-1990, because of a change from monthly to weekly rain sampling that occurred at the beginning of 1988. From Figs. 2 and 3 and from Tables 3, 4 and 5, we can see that:

(1) Most of the episodes with SPM values higher than 100 $\mu g/m^3$ occurred during the sampling period 1985-1987;

(2) The number of episodes with values of SPM > 120 $\mu g/m^3$ during the sampling period 1985-1987 are twice as much as those recorded during the period 1988-1990;

(3) More than 40% of the episodes with high values of SPM occurred during spring (see Table 5).

Table 2

Frequency tabulation of SPM values (µg/m^3) at Messina
(June 1985 - December 1990; 67 months)

Class	(a)	(b)	(c)	(d)	(e)
1	0	20	10	9	02
2	20	40	30	125	21
3	40	60	50	211	36
4	60	80	70	150	26
5	80	100	90	48	08
6	100	120	110	22	04
7	120	140	130	11	02
8	140	160	150	5	01
9	160	180	170	3	01
10	180	200	190	1	00
Mean = 59.1		Std. dev. = 25.9		Median = 55	

(a) lower limit; (b) upper limit; (c) midpoint; (d) number of episodes;
(e) relative frequency in %

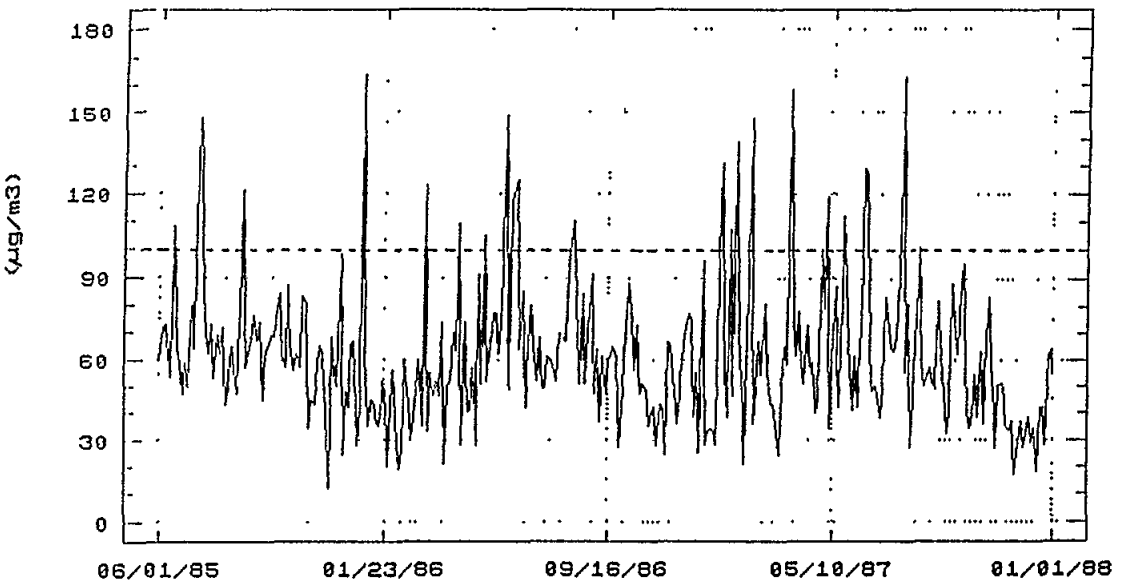

Fig.2 Plot of SPM weight vs sampling date from 1985 to 1987

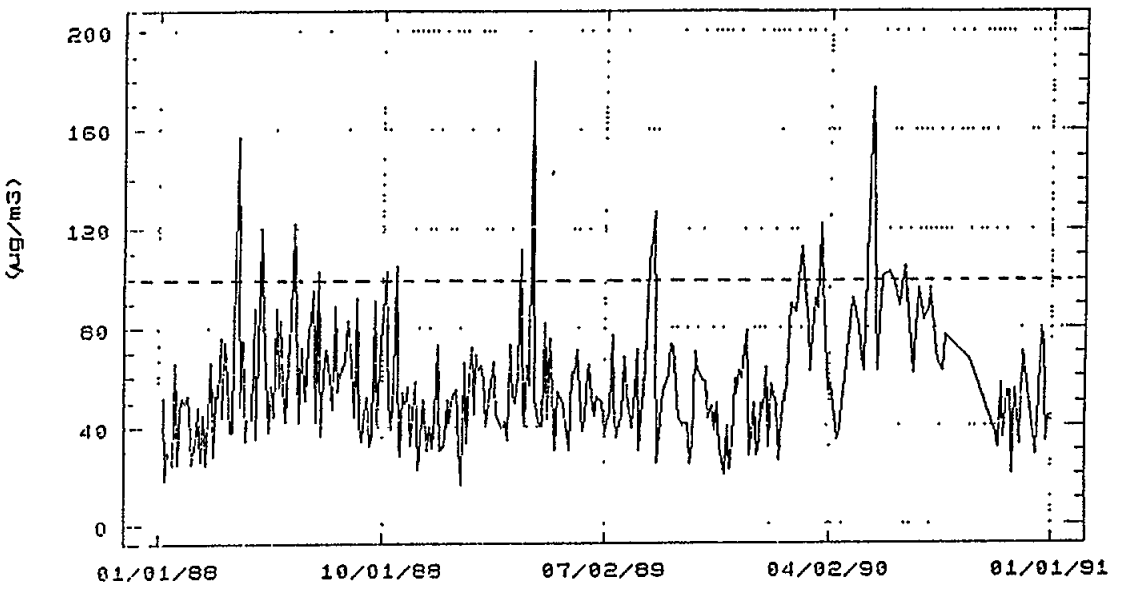

Fig.3 Plot of SPM weight vs sampling date from 1988 to 1990

Table 3

Frequency tabulation of SPM values (µg/m^3) at Messina
(June 1985 - December 1987; 31 months)

Class	(a)	(b)	(c)	(d)	(e)
1	0	20	10	5	02
2	20	40	30	59	19
3	40	60	50	101	33
4	60	80	70	90	30
5	80	100	90	24	08
6	100	120	110	10	03
7	120	140	130	8	03
8	140	160	150	4	01
9	160	180	170	2	01
10	180	200	190	0	00
Mean = 60.7		Std. dev. = 26.6		Median = 57	

(a) lower limit; (b) upper limit; (c) midpoint; (d) number of episodes;
(e) relative frequency in %

Table 4

Frequency tabulation of SPM values (µg/m^3) at Messina
(January 1988 - December 1990; 36 months)

Class	(a)	(b)	(c)	(d)	(e)
1	0	20	10	4	01
2	20	40	30	66	23
3	40	60	50	110	39
4	60	80	70	60	21
5	80	100	90	24	09
6	100	120	110	12	04
7	120	140	130	3	01
8	140	160	150	1	00
9	160	180	170	1	00
10	180	200	190	1	00
Mean = 57.48		Std. dev. = 25.0		Median = 53	

(a) lower limit; (b) upper limit; (c) midpoint; (d) number of episodes;
(e) relative frequency in %

Table 5

Number of episodes with SPM values higher than 100 and 120 µg/m^3 related to the sampling year and according to seasons classified as follows:

Winter: Jan-Feb-Mar Spring: Apr-May-Jun
Summer: Jul-Aug-Sep Autumn: Oct-Nov-Dec

Season / Year	Winter	Spring	Summer	Autumn	Total Yearly	Susp. Partic. Matter (SPM)
1985	/// ///	/// ///	4 3	1 1	5 4	> 100 µg/m^3 > 120 µg/m^3
1986	1 1	5 2	1 0	0 0	7 3	> 100 µg/m^3 > 120 µg/m^3
1987	5 4	4 2	3 1	0 0	12 7	> 100 µg/m^3 > 120 µg/m^3
1988	0 0	4 3	1 0	2 0	7 3	> 100 µg/m^3 > 120 µg/m^3
1989	1 0	1 1	2 1	0 0	4 2	> 100 µg/m^3 > 120 µg/m^3
1990	2 1	4 1	1 0	0 0	7 2	> 100 µg/m^3 > 120 µg/m^3
Total Season	9 6	18 9	12 5	3 1	42 21	> 100 µg/m^3 > 120 µg/m^3

4.2 **pH**

We treated pH data in the same way we did for SPM data, i.e. dividing the sampling period in two parts and calculating the frequency distribution for each of them. From Tables 6, 7 and 8 and Figs. 4, 5, and 6 it can observed that:

(1) pH mean value of the period 1985-1990 is less than 5.0. This value is completely different from the mean values we recorded, even if for monthly samples, at two other coastal stations at the same latitude (~38N Lat N), Santa Maria di Leuca and Trapani, where the mean values of pH were 5.5 and 6.2 respectively (Ciattaglia and Cruciani, 1989), such a shift can be explained only by local anthropogenic sources;

(2) If we compare the pH mean value of the two sub-periods, we can see that in recent years (1988-90) the precipitation are more acidic than in the previous period, with mean pH values of 4.72 and 5.09 respectively. As for SPM data, also pH values have been divided in two sub-groups, i.e. pH > 6.0 and pH # 6.0, and their seasonal distribution is reported in Table 9, where we observe that:

(3) pH values > 6.0 are generally more frequent in summer;

(4) Weekly rain samples with pH values # 6.0 are distributed homogeneously during the different sampling years, while the episode with pH > 6.0 are much more frequent during the first period (1985-1987).

Table 6

Frequency tabulation of pH values at Messina for the whole period (1985-1990)

Class	(a)	(b)	(c)	(d)	(e)
1	3.0	3.5	3.25	1	.01
2	3.5	4.0	3.75	14	.08
3	4.0	4.5	4.25	65	.39
4	4.5	5.0	4.75	37	.22
5	5.0	5.5	5.25	12	.07
6	5.5	6.0	5.75	7	.04
7	6.0	6.5	6.25	10	.06
8	6.5	7.0	6.75	16	.10
9	7.0	7.5	7.25	3	.02
10	7.5	8.0	7.75	0	.00
Mean = 4.91		Std. dev. = 0.94		Median = 4.6	

(a) lower limit; (b) upper limit; (c) midpoint; (d) number of episodes;
(e) relative frequency in %

Table 7

Frequency tabulation of pH values at Messina : first sub-period
(1985-1987)

Class	(a)	(b)	(c)	(d)	(e)
1	3.0	3.5	3.25	0	.00
2	3.5	4.0	3.75	5	.06
3	4.0	4.5	4.25	29	.34
4	4.5	5.0	4.75	21	.24
5	5.0	5.5	5.25	7	.08
6	5.5	6.0	5.75	5	.06
7	6.0	6.5	6.25	6	.07
8	6.5	7.0	6.75	11	.13
9	7.0	7.5	7.25	2	.02
10	7.5	8.0	7.75	0	.00
Mean = 5.09		Std. dev. = 0.97		Median = 4.7	

(a) lower limit; (b) upper limit; (c) midpoint; (d) number of episodes;
(e) relative frequency in %

Table 8

Frequency tabulation of pH values at Messina : second sub-period
(1988-1990)

Class	(a)	(b)	(c)	(d)	(e)
1	3.0	3.5	3.25	1	.01
2	3.5	4.0	3.75	09	.11
3	4.0	4.5	4.25	36	.46
4	4.5	5.0	4.75	16	.20
5	5.0	5.5	5.25	5	.06
6	5.5	6.0	5.75	2	.03
7	6.0	6.5	6.25	4	.05
8	6.5	7.0	6.75	5	.06
9	7.0	7.5	7.25	1	.01
10	7.5	8.0	7.75	0	.00
Mean = 4.72		Std. dev. = 0.87		Median = 4.4	

(a) lower limit; (b) upper limit; (c) midpoint; (d) number of episodes;
(e) relative frequency in %

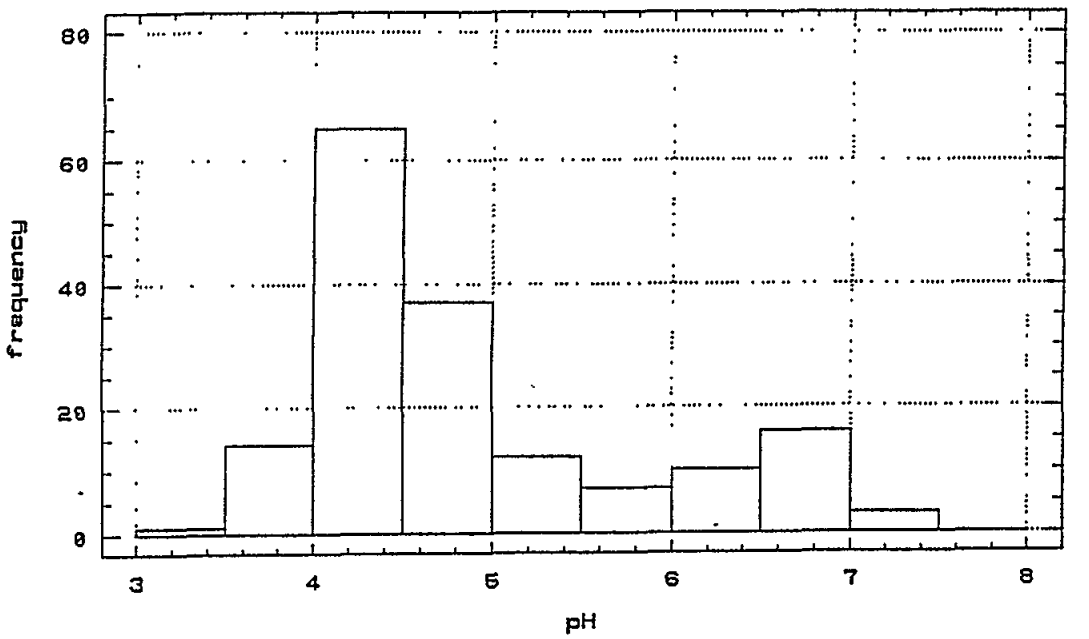

Fig.4 pH frequency histogram (1985 - 1990)

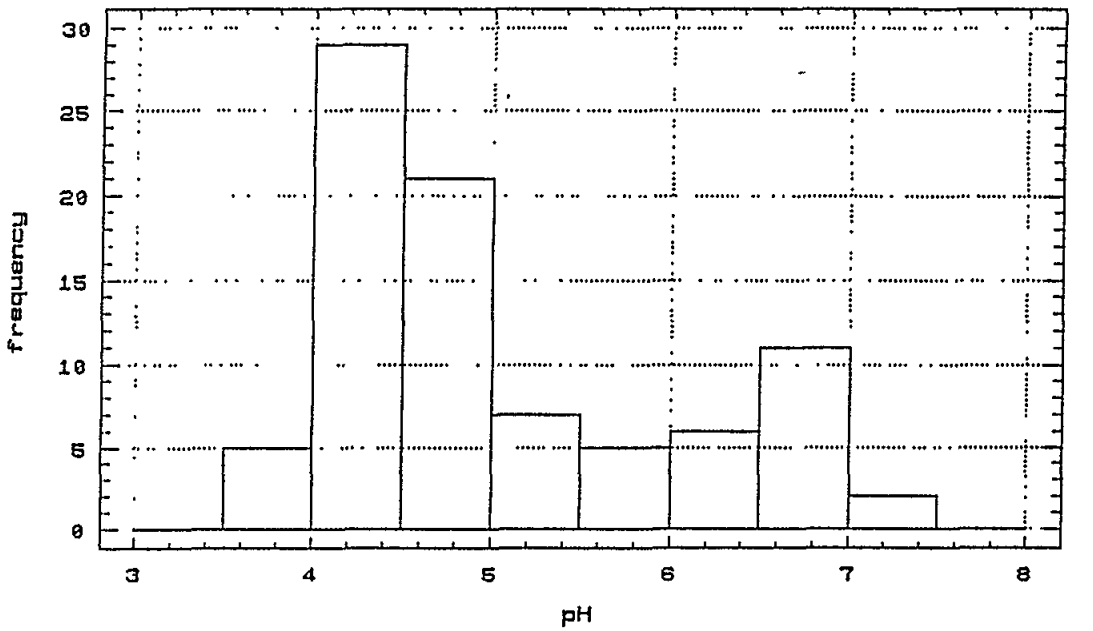

Fig.5 pH frequency histogram (1985 - 1987)

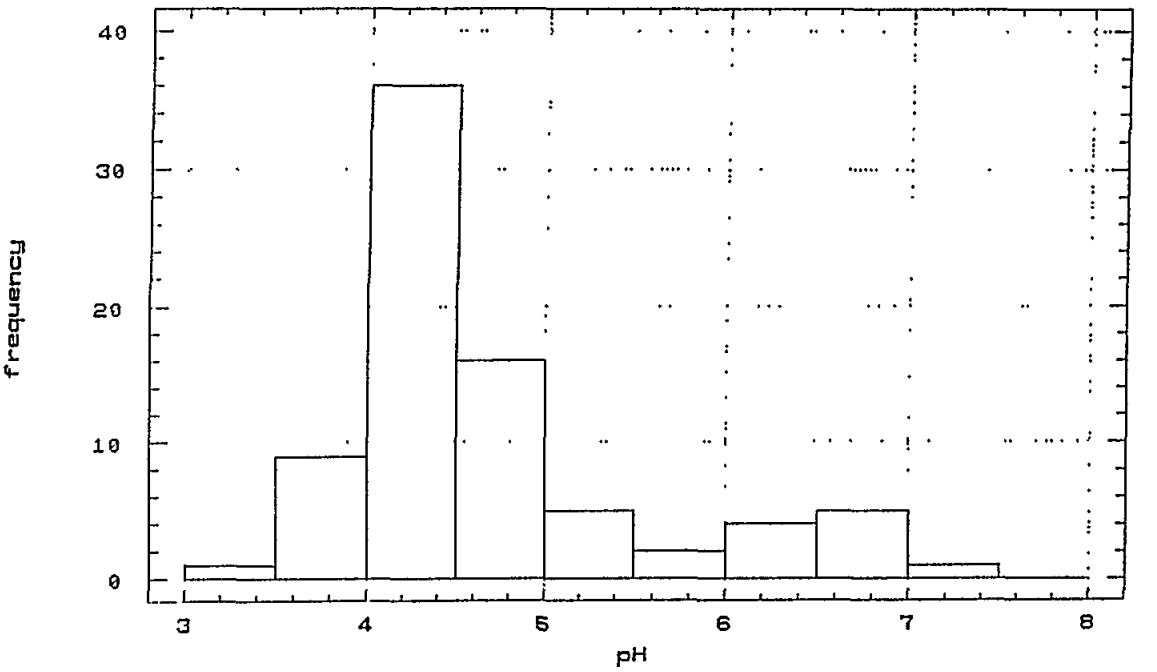

Fig.6 pH frequency histogram (1988 - 1990)

Table 9

Episodes with pH values higher than 6.0 and minus or equal to 6.0, related to the sampling year and according to previous seasons classification

Season / Year	Winter	Spring	Summer	Autumn	Total Yearly	Susp. Partic. Matter (SPM)
1985	///	///	4	2	6	> 6.0
	///	///	4	8	12	≤ 6.0
1986	2	2	3	0	7	> 6.0
	11	3	4	11	29	≤ 6.0
1987	4	0	1	1	6	> 6.0
	8	7	2	9	26	≤ 6.0
1988	0	3	1	0	4	> 6.0
	10	3	2	9	27	≤ 6.0
1989	2	0	2	0	4	> 6.0
	4	5	3	9	21	≤ 6.0
1990	0	1	0	1	2	> 6.0
	6	5	2	11	24	≤ 6.0
Total Season	8	6	11	4	29	> 6.0
	39	23	17	57	136	≤ 6.0

If we compare mean pH values for the two periods with mean Ca^{2+} concentrations, we see that when pH values are higher than 6.0 the concentrations of Ca^{2+} are higher than 6.0 mg/lt. On the contrary, if pH is # 6.0, Ca^{2+} drastically decreases to values less than 2.0 mg/lt (Table 10). This finding is very consistent with data from Caboi *et al.* (1990): these authors found, in precipitation collected in Sardinia Island, an average Ca^{2+} content of 1 mg/l with pH values of 4.7 and more than 10 mg/l of calcium with pH of 6.6. It is therefore likely that the parallel decrease of the number of episodes with SPM value above 100 $\mu g/m^3$ and more acidic pH value in rain at Messina station is partially due to the reduced neutralizing effect of Saharan carbonates (Loye-Pilot *et al.*, 1986; Glavas, 1988).

4.3 SPM chemical characterization

As we have seen, the Messina station is characterized by several episodes with SPM values higher than 100 $\mu g/m^3$. The best way to determine if these episodes were related to Saharan dust transport would be:

(1) to determine major and minor elements of the particulate matter collected on the filters;

(2) to compare particulate data with rain chemical data, if available;

(3) to verify the meteorological conditions during sampling and for a few days before.

Table 10

Mean values of pH and Ca^{2+}, for the two different sub-periods; number of episodes with pH values > or # 6.0 and related Ca^{2+} content (mg/l)

	1985-1987 (31 months)	1988-1990 (36 months)
pH	5.09	4.73
Ca^{2+}	2.76	1.74
pH > 6.0 *(number of episodes)*	19	10
Ca^{2+}	6.06	7.25
pH # 6.0 *(number of episodes)*	67	69
Ca^{2+}	1.78	0.90

To find episodes of direct transport from the south, we used the meteorological analysis at 850, 700 and 500 hPa and, in some cases, some black and white METEOSAT pictures taken in the IR and visible ranges. We examined the meteorological analysis, looking for air mass circulations suitable of direct transport, to verify the correspondence between SPM high values

and meteorological patterns. Among the large number of episodes with high values of SPM, nine significant episodes in different periods were selected. Two elements related to anthropogenic sources (Cd,Pb) and one of crustal origin (Fe) were analyzed.

In Table 11 the analytical results and some other relevant information are listed. Dust loadings (SPM) range from 104 to 184 (avg. 129) $\mu g/m^3$, Cd from 0.1 to 0.3 ng/m^3 and Pb values from 71 to 301 ng/m^3. Fe concentrations range from 800 to more than 4000 ng/m^3, with the maxima clearly related to the filter colour, with beige indicating prevailing dust transport.

Table 11

Chemical data of particles collected on Hi-Vol filters. Suspended particulate matter content (SPM) is listed in the first column

Sampling date	SPM ($\mu g/m^3$)	Cd	Pb	Fe	Filter colour
		---------- ng/m^3 ----------			
04/03-04/88	107	0.242	71.0	2639	Light beige
04/06-07/88	151	0.142	107.0	4302	Yellowish beige
10/18-19/88	104	0.289	111.0	2763	Grey
03/20-21/89	107	0.168	110.0	2460	Grey
04/04-05/89	184	0.194	301.0	3739	Beige grey
02/26-27/90	111	0.139	187.0	1086	Light grey
03/22-23/90	122	0.242	117.0	838	Black grey
05/24-25/90	175	0.172	173.0	2213	Grey
06/14-15/90	104	0.095	201.0	962	Yellowish grey

We have compared our data from a land-based site in Messina with some dust samples collected at sea to the North and South of the sampling point (Correggiari *et al.*,1989). Table 12 shows the mean values (in ng/m^3) of Cd, Pb and Fe and the enrichment factors (EF) calculated with reference to the average crustal values (Taylor, 1964). The same table lists also the average mass loadings, very high in the Messina samples, if compared to samples collected on board ship around Sicily .

Enrichment Factor values for Cd are practically the same in all samples, whilst high EF-Pb values are found at Messina station, if compared to the open sea. Values higher than 100 can be considered a clear sign of pollution (Guerzoni *et al.*, 1989). In fact, as we stated before, not all the episodes with high values of SPM are related only to a direct transport, but they could be linked with the harbour activity, which increased the SPM value, without any direct transport from Sahara. This consideration is also supported by the meteorological pattern of the studied episodes.

Table 12

Comparison of dust samples collected at Messina with other samples from different sites around Sicily (see Fig.7 for location of samples)

Site	Unit	Cd	Pb	Fe	SPM ($\mu g/m^3$)
Messina	(ng/m^3)	0.19	153.0	2334	129
	E.F.	28	280	1	---
North (●)	(ng/m^3)	0.07	16.3	910	20
	E.F.	29	92	1	---
South (■)	(ng/m^3)	0.35	19.6	2261	56
	E.F.	47	34	1	---

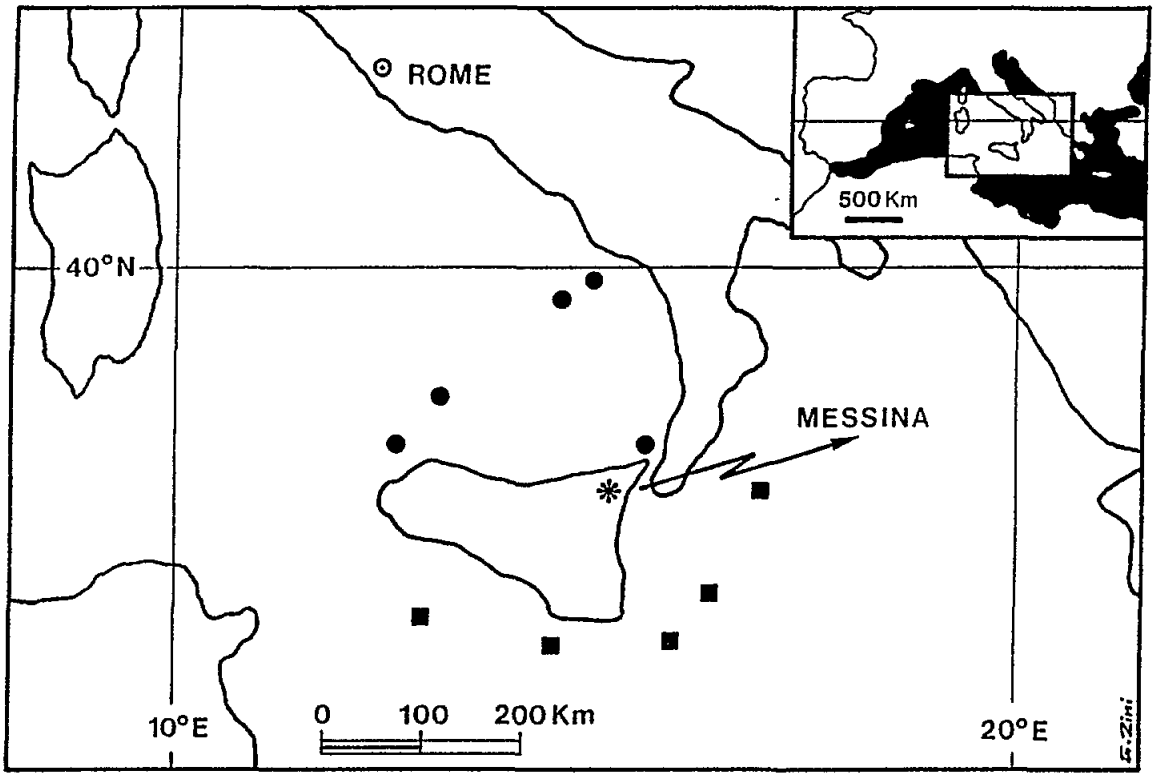

Fig.7 Location of the coastal station at Messina (*) and of the mesh-panels samples collected at sea, North (●) and South (■) of the land-based station.

5. CONCLUSIONS

From our previous considerations we can summarize as follows:

(1) For the period 1985-1987 there are much more episodes with high values of SPM than usual, and they are more frequent in the spring season;

(2) for the same period, the pH mean value is higher than the mean value of 1988-1990, and in summer we have more episodes with pH > 6.0;

(3) For the period 1988-1990 both mean pH values and episodes with SPM high values have a coincident decrease;

(4) The mean pH value at Messina is lower than at the other two coastal stations operated by the Italian Meteorological Service for the BAPMoN programme located at the same latitude (Trapani and S. Maria Leuca, ~38N Lat N);

(5) Rain episodes with pH > 6.0 normally have Ca^{2+} concentrations higher than 6.0 mg/lt;

(6) Major and minor element concentrations, obtained by chemical analysis of filters, and meteorological conditions, as shown by standard surface charts and satellite pictures, make it clear that not all episodes with high SPM values are related to Saharan dust transport.

We can therefore conclude that:

(a) Messina station is a suitable impact station to evaluate the input of pollutants into the Mediterranean Sea through meteorological processes;

(b) High SPM values are not always related to direct transport phenomena, but they can be associated with indirect transport or with anthropogenic activities;

(c) pH values in southern rain samples are influenced by the presence of high Ca^{2+} concentrations;

(d) It seems likely that the Messina Hi/Vol samples are a mixture of southern inputs - rich in carbonates and Fe - and of more polluted northern sources. On the other hand, a local input is probably due to the shipping activity in the harbour, which increases the total amount of dust enriched in Pb.

6. ACKNOWLEDGMENTS

We thank G. Zini for the drawings. This work was partially supported by WMO SSA no. 16.566/A/CNS. This is IGM-CNR scientific contribution no. 844.

7. REFERENCES

Caboi R., A. Cristini, F. Faru, R. Pinna and A. Piu (1990). Distinzione delle componenti marina e continentale nelle precipitazioni piovose dell'area forestale di Pixina Manna (Sardegna sud-occidentale). *Acqua-Aria*, 8:665-671.

Chester R., E.J. Sharples and G.S. Sanders (1984). Saharan dust incursion over the Tyrrhenian Sea. *Atmospheric Environment*, 18:929-935.

Ciattaglia I. and L. Cruciani (1989). Review of chemical data by the Italian Meteorological Service. *MAP Technical Report Series*, 31:101-123.

Correggiari A., S. Guerzoni, R. Lenaz, G. Quarantotto and G. Rampazzo (1989). Dust deposition in the central Mediterranean (Tyrrhenian and Adriatic Seas): relationships with marine sediments and riverine input. *Terra Nova*, 1(6):549-558.

Glavas S. (1988). A wet-only precipitation study in a mediterranean site, Patras, Greece. *Atmospheric Environment*, 22:1505-1507.

Guerzoni S., G. Rovatti, E. Molinaroli and G. Rampazzo (1987). Total and "selective" extraction methods for trace metals in marine sediments reference samples. *Chemistry and Ecology*, 3:39-48.

Guerzoni S., R. Lenaz, G. Quarantotto, G. Rampazzo, A. Correggiari and P. Bonelli (1989). Trace metal composition of airborne particles over the Mediterranean Sea. *Giornale di Geologia*, 51:117-130.

Loye-Pilot M.D., J.M. Martin and J. Morelli (1986). Influence of Saharan dust on the rain acidity and atmospheric input to the Mediterranean. *Nature*, 321:427-428.

Taylor S.R. (1964). Abundance of chemical elements in the continental crust: a new table. *Geochimica Cosmochimica Acta*, 28:1273-1285.

DETERMINATION OF SEASONAL VARIATIONS IN THE ATMOSPHERIC CONCENTRATIONS OF LEAD, CADMIUM AND POLYCYCLIC AROMATIC HYDROCARBONS IN MONACO

By

C. MARMENTEAU and A. VEGLIA

Office Monégasque de l'Environnnement
16, boulevard de Suisse
MC 98000 Monaco, Principality of Monaco

1. INTRODUCTION

According to a recommendation of the United Nations Environment Programme (UNEP, 1988), the Principality of Monaco has undertaken airborne pollution monitoring of its coastal waters.

As a first step, we surveyed the variations in the concentrations of heavy metals (lead and cadmium) in atmospheric particles over a period of three consecutive years. Samples of atmospheric dust were collected from February 1988 until December 1990. Polycyclic aromatic hydrocarbons (PAH) were also determined in these samples in order to get an indication of the origin of heavy metals in the atmosphere.

2. MATERIALS AND METHODS

Airborne particulate matter was collected on glass-fibre filter papers (porosity 0.2 µm) by means of high volume air samples (GMWS - 2310, General Metal Works Inc.). This apparatus was positioned on the roof of the Oceanographic Museum in Monaco. Air flow through the system was maintained at a constant rate by an electronic probe, which automatically corrected for filter loading. The duration of filtration was about 15 days for each sample, and large volumes of air (> 10,000 m^3) were pumped each time.

After sampling, filters were divided into two equal parts. One half of the filter was used for the analysis of heavy metals, and the other half for the determination of Aromatic hydrocarbons.

2.1 Determination of heavy metals

One half of the filter was put in an Erlenmeyer flask equipped with a glass column (height 20 cm, diameter 1 cm). Extraction of metals was performed using 30 ml of 65% nitric acid (analytical purity). After leaching overnight at room temperature, the flask contents were progressively heated for one week (until boiling), then 20 ml of 35% hydrogen peroxide were added to complete the extraction. After cooling, the contents of the flask were filtered on Whatman GF/C glass-fibre filter paper previously washed with concentrated nitric acid. Filtered solutions were diluted to 100 ml with high purity demineralized water and analyzed for cadmium and lead by means of a Zeeman atomic absorption spectrophotometer equipped with a graphite furnace (HITACHI Z-7000).

"Blank" filters were analyzed by the same method. Their lead and cadmium concentrations were found to be negligible by comparison with their concentrations in the "sample" filters.

2.2 Determination of total aromatic hydrocarbons

The other half of the filter was put in a Soxhlet extraction system. Aromatic hydrocarbons were extracted by 300 ml of n-hexane (quality for spectroscopy) for 24 hours. Extraction solutions were then analyzed by fluorometry with an Aminco-Bowman spectro-fluorometer (excitation wavelength 310 nm, emission wavelength 360 nm). The spectro-fluorometer was calibrated with a standard solution of chrysene in n-hexane (dissolution is facilitated by application of ultrasonic energy). Results are expressed as chrysene-equivalents.

3. RESULTS

Concentrations of lead, cadmium and PAH measured in 1988, 1989 and 1990 at the rate of two samples per month are given in Table 1.

Table 1

Cd, Pb and PAH in air-filter samples.

(MONACO, 1988-1989)

SAMPLING TIME			Cd (mg/m^3)	Pb (mg/m^3)	PAH (mg/m^3)
15-29	2	1988	1.07	142	***
1-15	3	1988	.60	93	39.3
1-15	4	1988	.40	67	16.4
1-15	5	1988	.35	62	10.7
1-15	6	1988	.54	61	10.4
15-30	6	1988	.61	53	8.4
15-30	9	1988	.53	172	30.6
1-15	10	1988	.84	141	***
15-31	10	1988	.33	68	26.2
1-15	11	1988	.91	159	73.0
15-30	11	1988	.75	103	96.2
1-15	12	1988	.67	141	84.2
1-15	1	1989	.68	87	86.6
15-31	1	1989	.91	118	102.8
1-15	2	1989	1.09	165	57.8
15-28	2	1989	.60	76	44.4
1-15	3	1989	.79	98	33.6
1-15	4	1989	.29	34	27.2
15-30	4	1989	.42	49	18.8
1-15	5	1989	1.29	120	17.8
15-31	5	1989	.32	32	13.2
1-15	6	1989	.54	56	17.8
15-30	6	1989	.52	57	10.0

Table 1 (Continued)

Cd, Pb and PAH in air-filter samples.

(MONACO, 1988-1989)

SAMPLING TIME			Cd (mg/m^3)	Pb (mg/m^3)	PAH (mg/m^3)
1-15	7	1989	.54	49	10.4
15-31	7	1989	.58	71	15.0
1-15	8	1989	.44	55	10.8
15-31	8	1989	.40	65	11.0
1-15	9	1989	.52	48	13.2
15-30	9	1989	.65	77	13.0
1-15	10	1989	.64	81	27.7
15-31	10	1989	.76	138	48.2
1-15	11	1989	.67	106	64.3
15-30	11	1989	.64	91	75.0
1-15	12	1989	.79	87	135.0
15-31	12	1989	.70	114	107.0

***** Not Determined**

(MONACO, 1990)

SAMPLING TIME			Cd (mg/m^3)	Pb (mg/m^3)	PAH (mg/m^3)
1-15	1	1990	.70	90	147.3
15-31	1	1990	1.45	106	97.2
1-15	2	1990	.73	72	76.8
15-28	2	1990	.86	82	56.2
1-15	3	1990	.65	53	46.1
15-31	3	1990	.60	64	32.1
1-15	4	1990	1.09	50	25.6
15-30	4	1990	.47	61	27.3
1-15	5	1990	.80	26	12.1
15-31	5	1990	.19	31	11.1
1-15	6	1990	.02	22	7.9
15-30	6	1990	.44	48	11.2
1-15	7	1990	.41	32	9.4
15-31	7	1990	.40	47	5.9
1-15	8	1990	.42	48	6.4
15-31	8	1990	.45	62	13.1
1-15	9	1990	.58	38	12.8
15-30	9	1990	.73	52	18.2
1-15	10	1990	.41	61	22.3
15-31	10	1990	.53	50	37.5
1-15	11	1990	1.08	69	65.0
15-30	11	1990	.72	71	78.8
1-15	12	1990	.74	66	90.0

The distribution of the values of the lead concentrations measured during this period of time is given in Fig.1. The most frequent value is between 60 and 70 ng m^{-3}. This value is well below the limit of 2,000 ng m^{-3} which corresponds to the European standard for the annual average concentration of lead in the atmosphere.

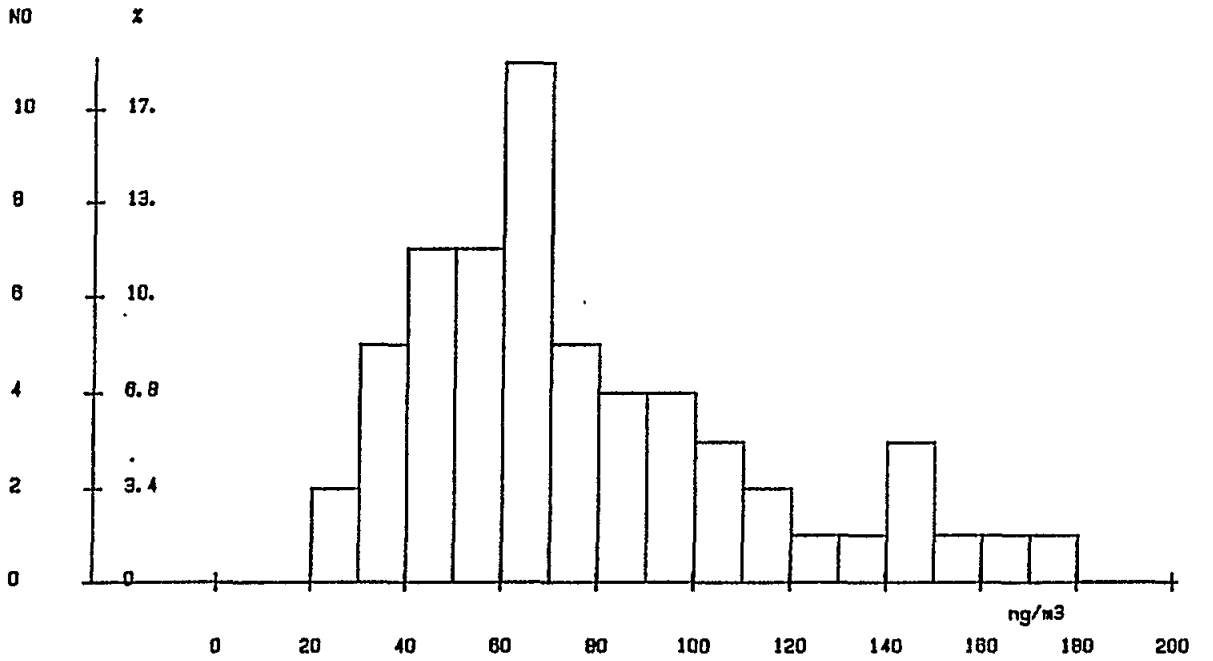

Fig.1 Lead in air-filter samples (1988-1989-1990)

The distribution of the cadmium concentrations is given in Fig.2. There is no defined modal value but one can deduce that the most frequent value lies between 0.4 and 0.8 ng m^{-3}.

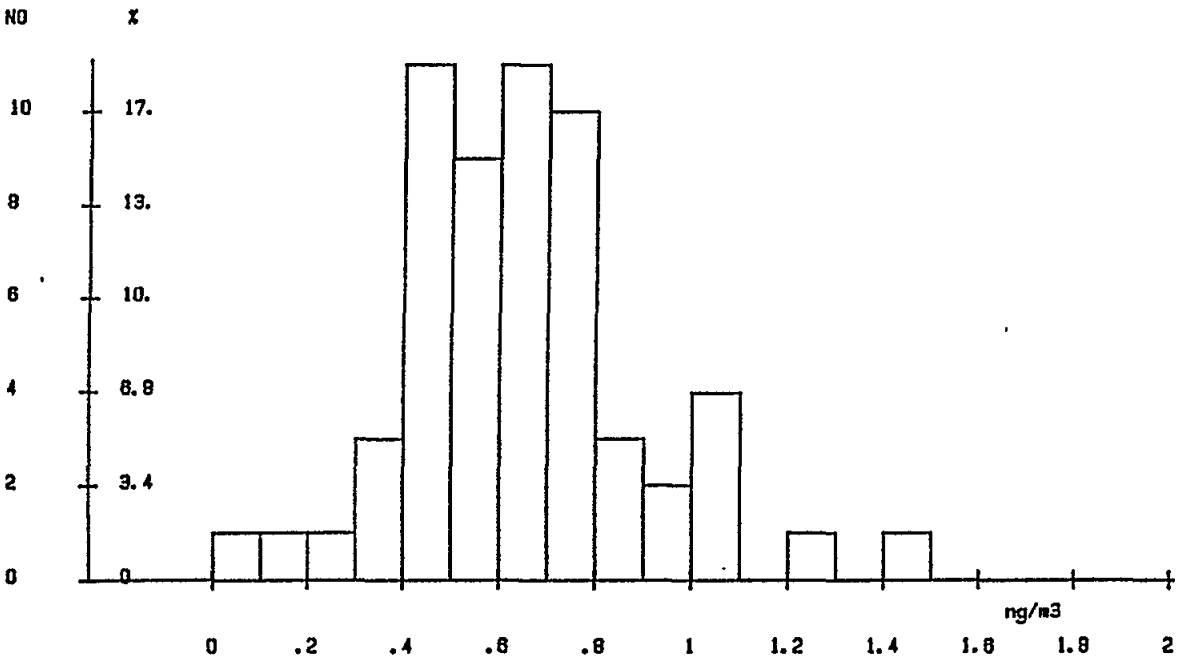

Fig.2 Cadmium in air-filter samples (1988-1989-1990)

The measured concentrations of these metals are of the same order of magnitude as those which were reported by other authors for coastal areas of the Mediterranean which do not lie in the vicinity of important pollution sources (Bergametti *et al.*, 1988; Ioannilli, 1988; Migon and Caccia, 1990; Thiessen *et al.*, 1988).

The distribution of the concentrations of the total aromatic hydrocarbons is given in Fig.3. 35% of the values lie between 10 and 20 ng m^{-3}. These values are of the same order of magnitude as those which were measured in the district of Los Angeles (Gordon, 1976).

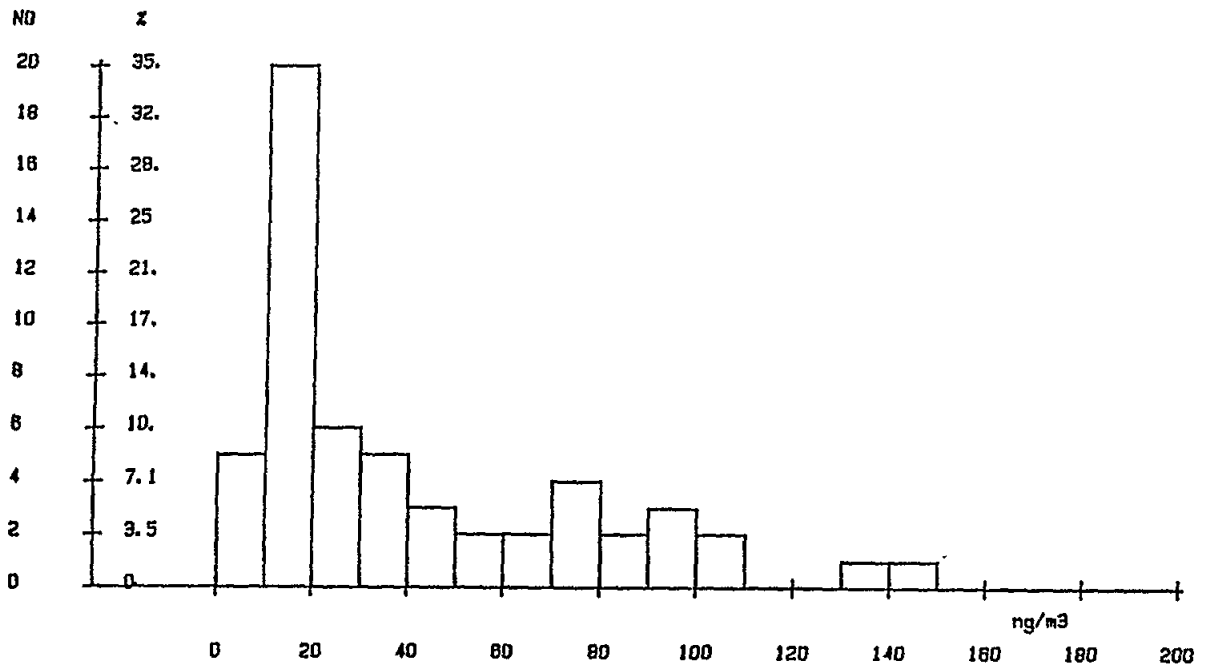

Fig.3 Total aromatic hydrocarbons in air-filter samples (1988-1989-1990)

Fig.4 shows the variations of the measured parameters during the period 1988-1990. Unfortunately, there is a lack of data for July and August 1988 which is due to failure of the air sampler at that time. Generally speaking, however, one can state that higher concentrations of lead, cadmium and PAH are observed in winter (mainly from November to January). This trend is more obvious for PAH than for metals.

Significant correlations are observed between the different parameters. Fig.5 shows the correlation between lead and cadmium ($r = 0.623$, $p < 0.001$). The highest correlation between coefficient ($r = 0.663$, $p < 0.001$) was obtained for the correlation lead-PAH (Fig.6), while a smaller correlation ($r = 0.568$, $p < 0.001$) was observed between cadmium and PAH (Fig.7). The curves corresponding to the best fitting by the method of least squares are not linear, however, and they correspond to functions of the kind : $y = ax^b$ or $y = ae^{bx}$ (Fig.5, 6 and 7).

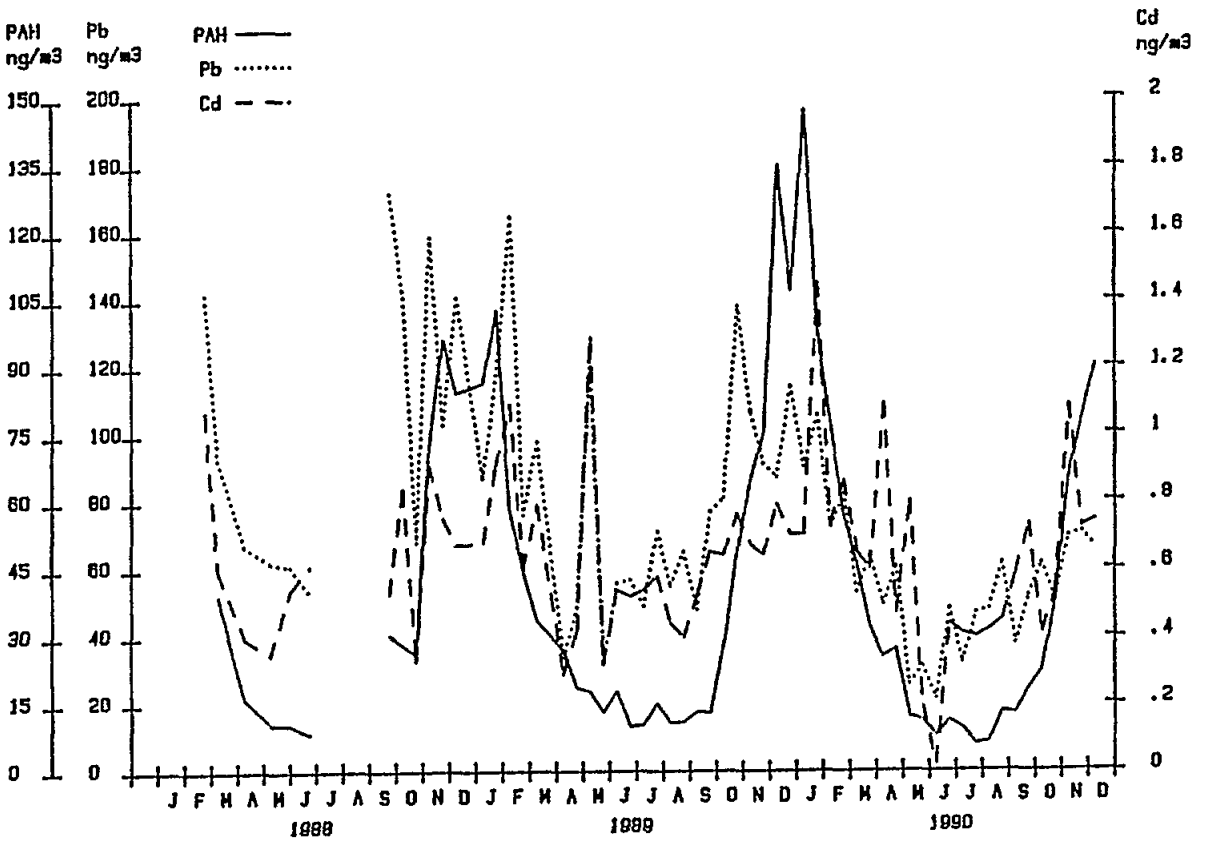

Fig.4 Seasonal variations of metals and aromatic hydrocarbons in the atmosphere (Monaco)

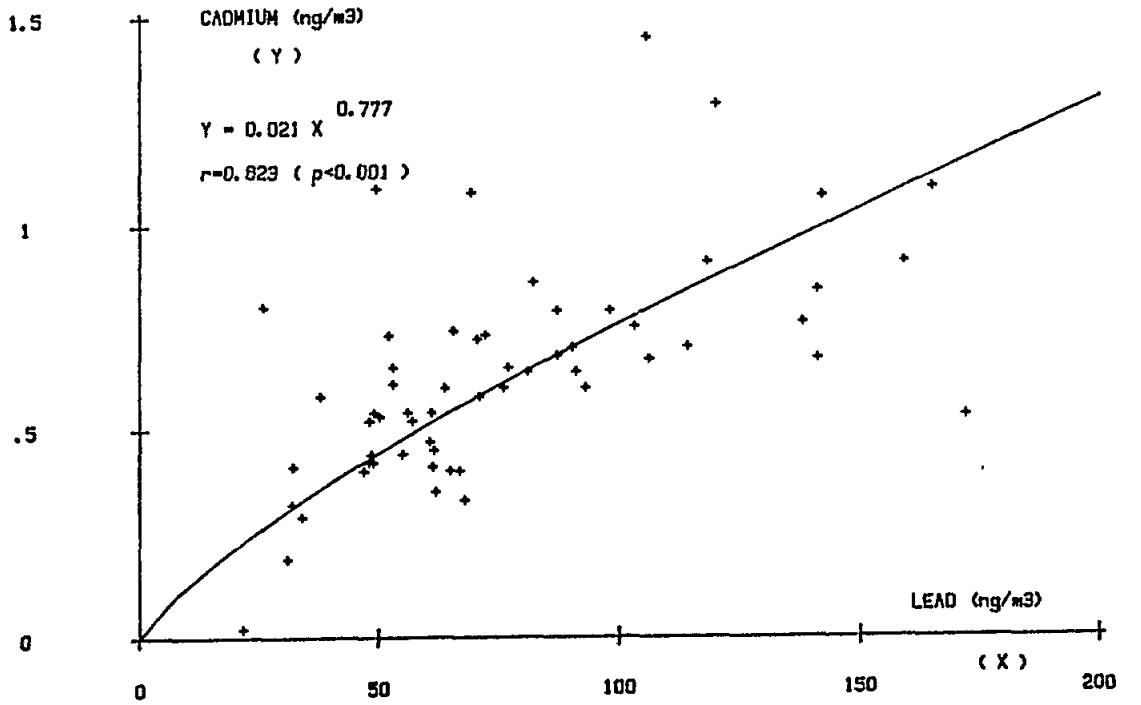

Fig.5 Lead and cadmium in the atmosphere (Monaco)

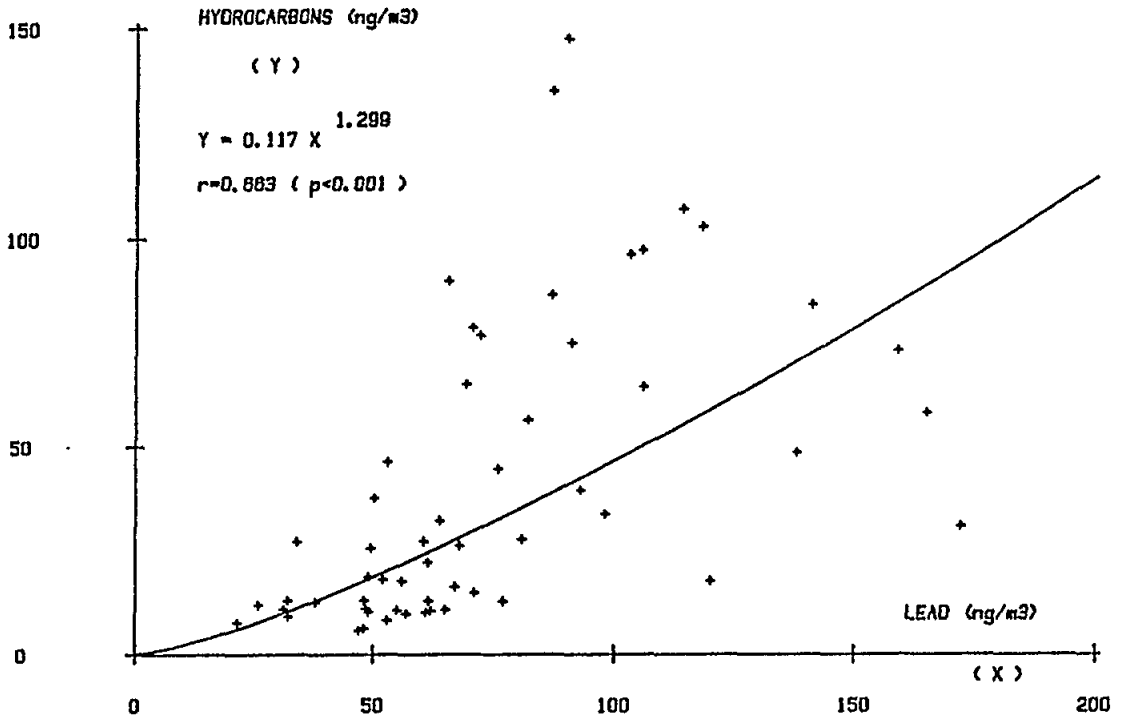

Fig.6 Lead and total aromatic hydrocarbons in the atmosphere (Monaco)

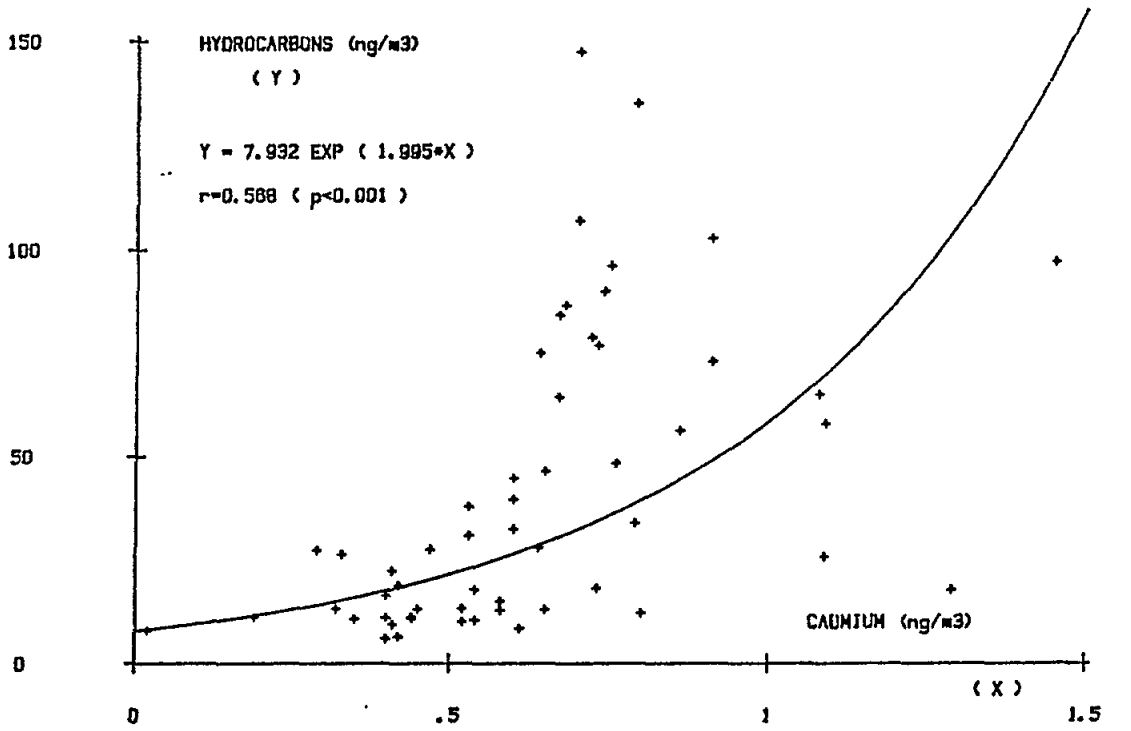

Fig.7 Cadmium and total aromatic hydrocarbons in the atmosphere (Monaco)

4. DISCUSSION

It has become more and more obvious during recent years that airborne pollution plays a major role in the transport and deposition of pollutants into the oceans. This is especially important in the case of the Mediterranean Sea, which is near the pollution sources of Northern Europe, and is exposed to deposition of Saharan dust through Aeolian transport (Martin *et al.*, 1989).

The good correlations that were observed between heavy metals and PAH suggest that, in the case of Monaco, metals in the atmosphere originate mostly from the combustion of fossil fuels. No correlation was however observed with the traffic intensity, which is higher in summer in this country. Indeed, the observed variations are probably due to a combination of several factors, such as the increase of the use of domestic fuels in winter, air mass transfer which depends on variations in wind direction, and anticyclonic conditions which, in recent years, prevailed in winter in the South of France. A similar increase of atmospheric concentrations in winter was observed in 1988 in the district Languedoc-Roussillon, not only for lead but also for other pollutants such as nitrogen oxides, sulphur dioxide, etc. (Ampadi, 1989). Anticyclonic conditions in winter correspond to reduced winds, absence of rain and thermally stable air columns. Pollutants which are emitted into the atmosphere may accumulate locally under such conditions and be dispersed only when the anticyclone breaks down, which is normally the case at the end of winter.

It is interesting to notice that the average atmospheric concentrations of lead decreased from 1988 to 1990, while cadmium and PAH were rather constant (Fig.8). The application of Wilcoxon's test shows that the decrease of lead is particularly significant between 1989 and 1990 ($T = 3.328$, $p < 0.001$) while the other parameters showed no significant variations according to this test (Hollander and Wolfe, 1973). This phenomenon is probably due to the reduction of the lead concentration in gasoline, and was also observed in other places in France (Agence pour la qualité de l'air, 1990).

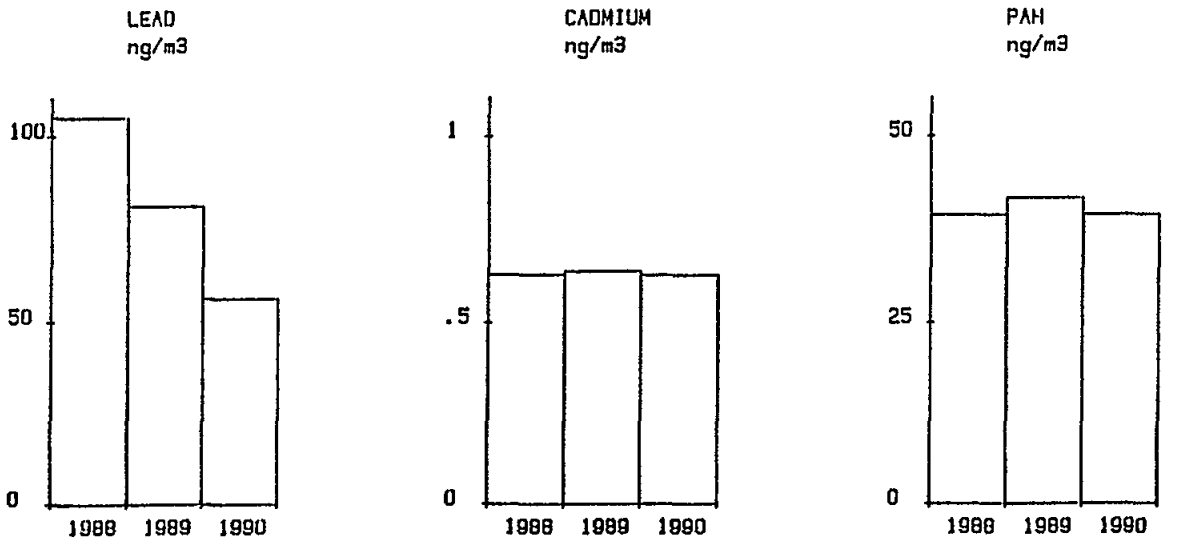

Fig.8 Variations of annual means of metals and total aromatic hydrocarbons in the atmosphere (Monaco)

The observed decrease in lead concentrations, which is not accompanied by a corresponding lowering of cadmium concentrations, results in a better correlation between these two metals if one considers only the years 1988-1989 ($r = 0.780$, $p < 0.001$) instead of the complete period of time 1988-1990 ($r = 0.623$, $p < 0.001$).

5. CONCLUSION

This monitoring of the air pollution for three consecutive years in Monaco revealed seasonal variations of the atmospheric concentrations of heavy metals and PAH in this coastal area of the Mediterranean Sea.

Further work is necessary, however, to confirm these seasonal variations and to define their origins as well as to determine the influence of the airborne transport of pollutants on the pollution of seawater around Monaco.

7. REFERENCES

Agence pour la qualité de l'Air (1990). Bulletin d'information No.9 (juin 1990).

Amapadi-LR (1989). Surveillance de la qualité de l'air en Languedoc-Roussillon. Rapport d'activité 1988 (juin 1989).

Bergametti, G., P. Buat-Ménard and D. Martin (1988). Trace metals in the Mediterranean atmosphere. EEC, Air pollution research report No.14, Field measurements and their interpretation, document EUR 11690, pp. 88-95.

Gordon, R.J. (1976). Distribution of airborne polycyclic aromatic hydrocarbons throughout Los Angeles. *Environ. Sci. Technol.*, 10:370-373.

Hollander, M. and D.A. Wolfe (1973). Nonparametric statistical methods. (Ed.) John Wiley and Sons, New York.

Ioannilli, E. (1988). Trace elements atmospheric concentration patterns in Brindisi-Lecce airshed (Italy). EEC, Air pollution research report No.14, Field measurements and their interpretation, document EUR 11690, pp. 72-82.

Martin, J.M., F. Elbaz-Poulichet, C. Guieu, M.D. Loye-Pilot and G. Han (1989). River versus atmospheric input of material to the Mediterranean Sea : an overview. *Mar. Chem.*, 28:159-182.

Migon, C. and J.L. Caccia (1990). Separation of anthropogenic and natural emissions of particulate heavy metals in the western Mediterranean atmosphere. *Atmos. Environ.*, 24A(2):399-405.

Thiessen, L.M., F. Claeys-Thoreau, S. Hallez, G. Verduyn and P. Bruaux (1988). Extended environmental study on heavy metals in Malta. EEC, Air interpretation, document EUR 11690, pp. 83-87.

UNEP (1989). Rapport de la prèmier réunion du Comité scientifique et technique. Document UNEP(OCA)MED WG.1/2 (27 mai 1988), p.4 para.16.

SAMPLING AND ANALYSIS OF AEROSOLS IN THE BLACK SEA ATMOSPHERE

By

G. HACISALIHOGLU[(1)], T.I. BALKAS[(1)], M. ARAMI[(1)], I. ÖLMEZ[(2)] and G. TUNCEL[(1)]

(1) Middle East Technical University, Environmental Engineering Department, Ankara, Turkey.
(2) Massachusetts Institute of Technology, Nuclear Reactor Laboratory, Cambridge, Massachusetts.

A B S T R A C T

During 1988, atmospheric particulate samples were collected over the Black Sea using cellulose filters. Chemical composition of atmospheric particles collected near sea level has been analyzed for 39 elements by non-destructive instrumental neutron activation analysis (INAA) and for $SO_4^=$ and $NO_3^=$ by ion chromatography. With few exceptions, elemental concentrations follow log-normal distribution. The Cl/Na ratio was smaller than the corresponding ratio in seawater, owing to evaporation of Cl from sea-salt particles as Hcl. This ratio is inversely related with non-sea-salt SO_4.

Concentrations of elements in the Black Sea atmosphere were found to be intermediate between continental rural sites where local aerosols and long range transported particles affects observed concentrations and a remote marine site where local sources, other than ocean, do not exist.

1. INTRODUCTION

Since many elements are emitted from their sources on particles and remain on them during their transport to remote regions, major and minor elemental composition of particles are excellent tracers to determine sources of particles in ambient aerosols (Kowalczyk, 1982; Hopke *et al.*, 1976; Thurston and Spengler, 1985; Dutkiewicz *et al.*, 1986).

Transport of elements and acid precursors across frontiers in Europe and their deposition to water systems is very important, due to the high level of industrialization and dense populations of the continent. Transport of trace elements from various source regions in Europe to Norway (Pacyna *et al.*, 1985; 1989) and to the Western Mediterranean (Dulac *et al.*, 1987) have been documented. Transport of atmospheric pollutants by neighbouring countries have been incorporated into the Mediterranean Action Plan (GESAMP, 1985).

The Black Sea is on the east coast of Europe and is surrounded by Turkey, Romania, Bulgaria and Russia. During winter, the Black Sea is under the influence of a low pressure system over Europe, and a high pressure system located over Siberia. During summer, the region is affected by the high pressure over North Africa and the Basra low (Coleri, 1989).

Two main tracks of depressions are particularly noted: (1) from the Mediterranean, moving in a north-eastward direction over the Sea of Marmara, (2) from Bulgaria and Romania, moving in an eastward and south-eastward direction. These systems generate a general easterly flow both during summer and winter (Coleri, 1989). These meteorological pictures suggest a strong influence of the European sources on the elemental composition of collected particles at the Black Sea.

2. MATERIALS AND METHODS

2.1 Sampling

Atmospheric aerosol samples were collected during the third leg of the Black Sea cruise of the research vessel R/V Knorr, between 3 and 16 June, and during the summer monitoring cruise of the Turkish research vessel R/V Bilim, between 26 August and 12 September 1988. A sampling system was located on the foredeck at approximately 10 m above sea level. Nineteen daily atmospheric particulate samples were collected during 2 cruises. The tracks of the sampling cruises are shown in Fig.1.

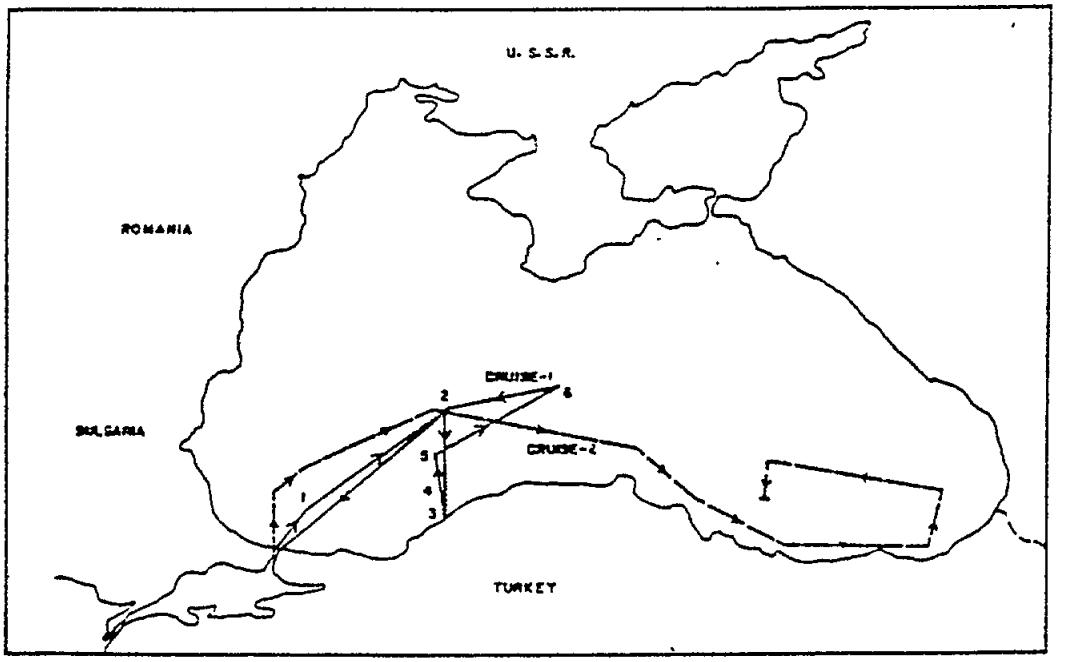

Fig.1 Tracks of sampling cruises

Particulate samples were collected on a double Whatman 41 (cellulose) filter by using a standard General Metal Works high-volume sampler, at a flow rate of about 45 $m^3 hr^{-1}$. The total volume of air passed through the filters during a 24-hour sampling period was determined using calibrated high volume dry-gas meters, which were checked against critical orifice plates before the cruises. Since trace element concentrations were expected to be very low in the Black Sea atmosphere, care was taken to minimize contamination during sampling. To avoid contamination of samples by emissions within the ship, including stack emissions and emissions from human activities, sampling was controlled by an "automatic wind sector controller". The high volume sampler, which was connected to the sector

controller was activated only when the wind was blowing from the sampling sector, which is an adjustable sampling angle that allows only air approaching from the front to be sampled. The sampler was automatically turned off when wind was blowing off this sector. Although there was no automated control on the wind speed, the pump was manually turned off when the wind speed was less than 2 knots. After collection, filters were heat sealed in acid-washed polyethylene bags.

The cleaning procedure for the plastic equipment, such as polyethylene bags, tweezers, etc., consisted of consecutive washes in 10% high purity nitric acid followed by several rinses with deionized water.

During sampling, all sample manipulations were done using teflon coated tweezers. Samples were never touched directly by hand, and powder-free disposable polygloves were used to prevent contamination of tweezers. All personnel involved with trace element sampling wore clean laboratory garb and particle-free polyethylene gloves, while mounting filter samplers on the sampling site or working with them in the laboratory. During the first cruise, samples and blanks were changed in a trace metal clean area available on the ship. However, during the second cruise, such a particle free area was not available and filters were changed on the foredeck. After collection, filters were stored at 4EC until analysis. Eventually, samples were reopened and prepared for analysis in a laminar flow clean hood.

2.2 Analytical techniques

Samples and blanks were analyzed by instrumental neutron activation analysis (INAA) for 39 elements. Samples were reopened at the Massachusetts Institute of Technology (M.I.T.) reactor laboratories in a laminar flow clean hood. Filters were cut into four quarters, each of which was separately weighted and recorded. One of the quarter filters was formed into a pellet using a high pressure press and a Ni die, for the INAA. The second quarter filter was saved in acid washed polyethylene bags for analysis of ions, such as $SO_4^{=}$, NO_3^{-} and NH_4^{+} by ion chromatography. The third quarter filter was saved for analysis of Pb and Ni by atomic absorption spectrometry, and the last quarter was stored in our archives.

All irradiations were carried out at the 5 MW M.I.T. reactor which has a thermal neutron flux of 8×10^{12} neutrons/cm^{-2}/sec^{-1}. For analysis, the INAA procedure developed by Germani *et al.* (1980) was used after some modifications. Briefly, pellets formed were first heat sealed in acid washed polyethylene bags and placed in pneumatic tube sample carriers which are called "rabbits", and irradiated for 5 minutes. Irradiated samples were counted twice with high resolution Ge(Li) and ultra-pure Ge detectors (typical resolution 2.0 keV at 1332 keV gamma-ray of ^{60}Co). The first gamma-ray spectrum was collected for 5 minutes for the determination of ^{27}Mg, ^{27}S, ^{51}Ti, ^{49}Ca, ^{52}V, ^{66}Cu and ^{28}Al. The samples were then allowed to decay for 10 minutes and a second gamma-ray spectrum was acquired from each sample by counting for 20 minutes. The second spectra were analyzed for ^{24}Na, ^{38}Cl, ^{42}K, ^{56}Mn, ^{69m}Zn, ^{116m}In, ^{128}I, ^{87m}Sr isotopes. Samples were then allowed to decay for several days and reirradiated at the same neutron flux for 4 hours to determine longer lived isotopes. Two additional spectra were taken after conclusion of the "long" irradiation and subsequent cooling. The first spectra were collected for 4 hours approximately three days after irradiation for isotopes ^{24}Na, ^{42}K, ^{68}Zn, ^{72}Ga, ^{76}As, ^{83}Br, ^{99}Mo, ^{115}Cd, ^{122}Sb, ^{140}La, ^{153}Sm, ^{175}Yb, ^{177}Lu, ^{187}W and ^{198}Au. For the second count long spectrum, samples were allowed to decay for 25-40 days and the spectrum was collected for 12 hours. Isotopes searched in this spectrum include, ^{46}Sc, ^{51}Cr, ^{59}Fe, ^{60}Co, ^{65}Zn, ^{75}Se, ^{95}Zr, ^{86}Rb, ^{110}Ag, ^{124}Sb, ^{131}Ba, ^{134}Cs, ^{141}Ce, ^{147}Nd, ^{152}Eu, ^{160}Tb, ^{169}Yb ^{177}Lu, ^{181}Hf, ^{182}Ta and ^{192}Ir. Although all isotopes were not detected in all samples, the procedure allowed us to determine average concentrations

of 35 elements in the Black Sea atmosphere. Concentrations of elements were determined by comparing activities of isotopes in samples with those in prepared mixed synthetic standards which were irradiated together with the samples. Synthetic standards were prepared from 1,000 ppm commercial atomic absorption stock solutions (Aldrich) with appropriate dilutions. Diluted solutions were mixed in a volumetric flash and a 10011 portion was pipetted onto a piece of Whatman-41 filter, which was then dried, formed into a pellet, and irradiated together with the samples. Flux variations along the "rabbits" were corrected using Co-flux monitors which are 5% Co in Al. The accuracy of the method used was checked by analyzing standard reference materials, i.e. fly ash (SRM 1633a) and coal (SRM 1632b), along with the samples. A second quarter of each filter was analyzed by ion chromatography for $SO_4^{=}$, NO_3^{-} and Cl^{-} ions. Sulphate and particulate nitrate on filters were dissolved in an ultrasonic bath for 30 minutes. Solutions were then analyzed for ions using a Varian Model 2010 High Performance Liquid Chromatograph (HPLC), interfaced to an Amstrad CPC6128 microcomputer.

3. RESULTS AND DISCUSSIONS

3.1 Filter blanks

Whatman filters are not particularly clean for trace elements. However, they are widely used in atmospheric sampling owing to their low pressure drop which allows sampling of large volumes of air, and also because they are easy to handle and are suitable for irradiating ion in INAA (Watts *et al.*, 1987). Double Whatman-41 filters were used for particulate sampling at the Black Sea, because of the known low efficiency of this type of filter media for submicron particles. The consensus in the literature is that the efficiency of Whatman-41 filter is greater than 80% over the radii range 0.01 to 2 mm for high volume sampling (Watts *et al.*, 1987).

Percentages of elements on bottom filters are given in Fig.2. Many elements were not detected on the second filter. Fig.2 shows that, approximately 50% of Cr, 43% of Au, 35% of I, 20% of Cl, 18% of Br and 22% of Nd were on bottom filters. For the rest of the elements, the average penetration of elements through top to bottom filters was less than 15%. A larger fraction of Br, Cl and I on bottom filters was probably due to adsorption of gaseous Br, Cl and I by cellulose filters.

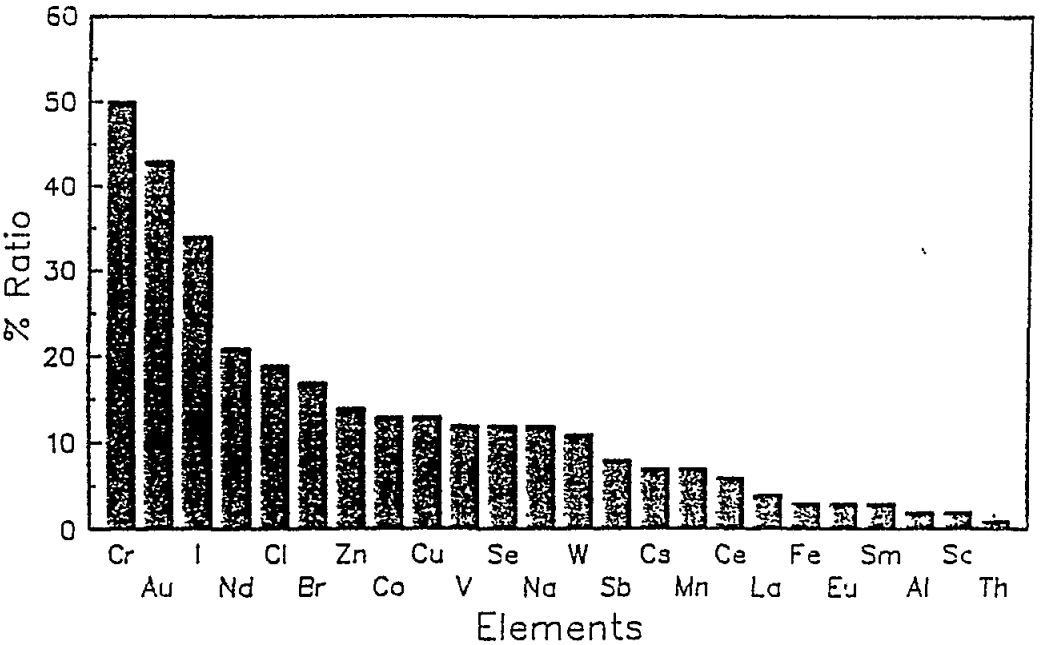

Fig.2 Percentages of elements on bottom filters

Similar adsorption of gas phase halogens by Whatman filters were observed in the remote atmosphere (Tuncel, 1984; Cunningham, 1979; Raemdonck *et al.*, 1986). Concentrations of other elements on bottom filters were comparable to, or higher than blank levels of these elements. High Cr concentrations observed on bottom filters may be due to contamination of bottom filters by the filter holder. Blank substraction of Cr on both filters is approximately 50% of the total observed mass on filters which may also contribute to the high penetration.

Blank filters were treated similarly with sample filters, except that air was pulled through blanks for only one minute. The blank/sample ratio for elements calculated and results show that; for top filters, blank substraction was significant only for Cr (40%), Mo (22%), W (40%), U (53%) and Au (25%). For the rest of the elements substracted blank values were less than 20% of the total observed masses of elements on filters. However, for bottom filters, blank substraction was higher than 50% for all elements. Since fractions of elements which passed through top filters were small, large blank substractions in bottom filters did not contribute significantly to uncertainties in final concentrations.

3.2 Detection limited

One of the most important advantages of instrumental neutron activation analysis over other multi-element techniques, is its high sensitivity to a large number of elements. The definition of the detection limit in instrumental neutron activation analysis is not straight-forward, and changes with the abundance of elements in a given sample. In Black Sea samples, twice the standard deviation of blank measurements were used as detection limits of elements (Galasyn *et al.*, 1987; Dzubay and Stevens, 1984). Detection limits of elements are shown in Table 1. Observed concentrations of elements in filters are generally one or two orders of magnitude higher than detection limits.

3.3 Frequency distribution of elements

The uncertainties shown in Table 2 are standard deviations which reflect the combined effect of experimental errors and real variations in concentrations. To understand relative magnitudes of these two contributors to standard deviations, propagated errors for each element were calculated using statistical uncertainty in counting, errors in volume and weighting. Results of calculations showed that propagated errors for most elements, including the ones with relatively poor counting statistics, are less than 15% of the corresponding average concentration. However, standard deviations can be close to 100%. Consequently, standard deviations of elemental averages are mostly due to real variations in concentrations.

Trace elements in the atmosphere show log-normal rather than gaussian distribution. Frequency histograms were prepared for each element, and assumed log-normal distribution curves were drawn. The goodness of the assumed log-normal distribution was tested with the "Kolmogorov" test using the "STATGRAPH" statistical package. The "Kolmogorov" test showed within 95% confidence limits that the majority of tested elements followed log-normal distribution. The frequency distribution histogram and assumed distribution curve for element V which shows typical log-normal behaviour is shown in Fig.3.

However, for some elements such as Mn and $SO_4^=$, the frequency distribution was bimodal. The Mn is a crustal element, and its concentration in remote atmosphere, free from anthropogenic contribution, can be accounted for by aluminasilicate particles (Tuncel *et al.*, 1989). However, in regions affected by pollution derived from aerosols, the ferromanganase

industry is an important source for atmospheric Mn (Pacyna *et al.*, 1984). Similarly, the main source of $SO_4^=$ in a polluted atmosphere is fossil fuel combustion, but oxidation of dimethyl sulphide (DMS) which is released from the sea also contributes to observed $SO_4^=$ concentrations on a regional scale. The contribution of the mixture of sources on ambient concentrations of Mn and SO_4 can explain the observed biomodal distributions.

Table 1

Detection limit of trace elements observed on Whatman-41 filters by INAA

Elements		Mean Concentrations[a]	Detection Limits[a]
Na		2000±2100	20
Al		460±250	6
Cl		2100±2000	60
Cr		6.3±3.1	1.51
Mn		16±9	0.55
Fe		400±220	1.82
Co		0.19±0.06	0.005
Zn		42±26	3.10
Br		22±20	0.22
Mo		0.14±0.20	0.02
Sb		0.52±0.30	0.003
I		25±15	0.23
Ba		4.5±2.8	0.50
Ce		0.61±0.35	0.006
Nd		2.6±2.0	0.003
Sm	(pg/m^3)	37±21	0.83
Eu	(pg/m^3)	11±6	0.08
Hf	(pg/m^3)	28±17	1.15
W	(pg/m^3)	66±20	15
Au	(pg/m^3)	5.0±2.5	0.65
Th	(pg/m^3)	90±75	1.00
U[b]	(pg/m^3)	12	11

[a] Concentrations are ng/m^3, unless otherwise indicated.
[b] Standard deviations are not given owing to small number of date.

3.4 Concentration of elements

Average concentrations and standard deviations of elements observed in the Black Sea atmosphere are shown in Table 2. Values shown in Table 2 include arithmetic and geometric means and associated standard deviations. The number of samples above blank values and propagated errors are also given in the table.

Concentrations of 40 elements were detected in aerosols collected over the Black Sea. For 25 elements, data were obtained in nearly all samples. For 15 elements, observed masses were comparable to blanks and for these elements ambient concentrations were determined in only a few samples.

Table 2

Arithmetic and Geometric Means and Standard Deviations of Atmospheric Concentrations observed at the Black Sea

Element		Arithmetic Means=s.d.[a]	Geometric Mean (=s.d.)[a]		Range	Number of Samples
SO_4		8.1±3.2	7.4	(1.8)	2.3-13	18
NO_3		3±0.9	2.8	(1.2)	1.3-4.6	18
Na		2000±2100	1300	(2.6)	174-9350	19
Al		460±250	400	(1.8)	102-1210	17
Cl		2100±2000	1200	(3.0)	160-7150	17
K		270±90	260	(1.4)	100-394	6
Ca		800±950	490	(2.7)	140-2900	6
Sc		0.10±0.08	0.08	(2.0)	0.02-0.15	19
Ti		60±15	58	(1.3)	33-83	6
V		2.4±1.0	2.2	(1.5)	1.0-5.1	18
Cr		6.3±3.1	5.4	(1.9)	1.8-30	15
Mn		16±9	14	(1.8)	4.5-37	17
Fe		400±220	340	(1.9)	56-950	19
Co		0.19±0.06	0.18	(1.4)	0.03-0.55	8
Cu		140±30	141	(1.2)	110-190	8
Zn		42±26	34	(2.0)	2.0-105	19
As		1.1±0.7	0.87	(1.9)	0.32-2.6	10
Se		0.76±0.27	0.57	(1.8)	0.08-1.06	19
Br		22±20	17	(2.1)	5.5-92	17
Rb		1.5±0.8	1.3	(1.8)	0.37-3.8	16
Sr		19±26	8.4	(3.6)	2.9-68	8
Mo		0.14±0.20	0.06	(5.2)	-	5
Sb		0.52±0.30	0.44	(2.0)	0.11-1.10	17
I		25±15	20	(2.1)	4-58	9
Cs		0.15±0.10	0.13	(1.8)	0.03-0.48	18
Ba		4.5±2.8	2.8	(1.9)	1.42-10.6	12
La		0.32±0.25	0.24	(2.4)	0.04-1.1	18
Ce		0.61±0.35	0.52	(1.8)	0.13-1.7	19
Nd		2.6±2.0	1.7	(2.9)	0.3-5.5	12
Sm	(pg/m^3)	37±21	28	(0.46)	3-60	14
Eu	(pg/m^3)	11±6	9.8	(0.27)	2-30	17
Gd	(pg/m^3)	37±29	25	(1.3)	5-13	16
Y[b]	(pg/m3)	26±21	15	(0.41)	4-30	5
Lu	(pg/m^3)	2.8±1.6	2.1	(2.1)	0.6-6.0	11
Hf	(pg/m^3)	28±17	23	(0.31)	4-80	17
Ta	(pg/m^3)	7.2±1.5	7.1	(1.3)	5-9	5
W	(pg/m^3)	66±20	61	(1.6)	24-82	5
Au	(pg/m^3)	5.0±2.5	4.1	(2.1)	0.9-9.0	11
Th	(pg/m^3)	90±75	71	(0.3)	15-380	19

[a] Concentrations are ng/m^3, unless otherwise indicated
[b] Standard deviations are not given owing to the small number of data

Standard deviations shown in Table 2 are comparable to observed concentrations for most of the elements. Such high standard deviations are not unusual for atmospheric trace element data, and does not indicate poor sampling or analysis. Large uncertainties are mostly due to large sample-to-sample variations in concentrations of elements which are real. Factors such as variation in sea-salt generation and different concentrations of particles associated with different air masses, contribute to the observed high standard deviation.

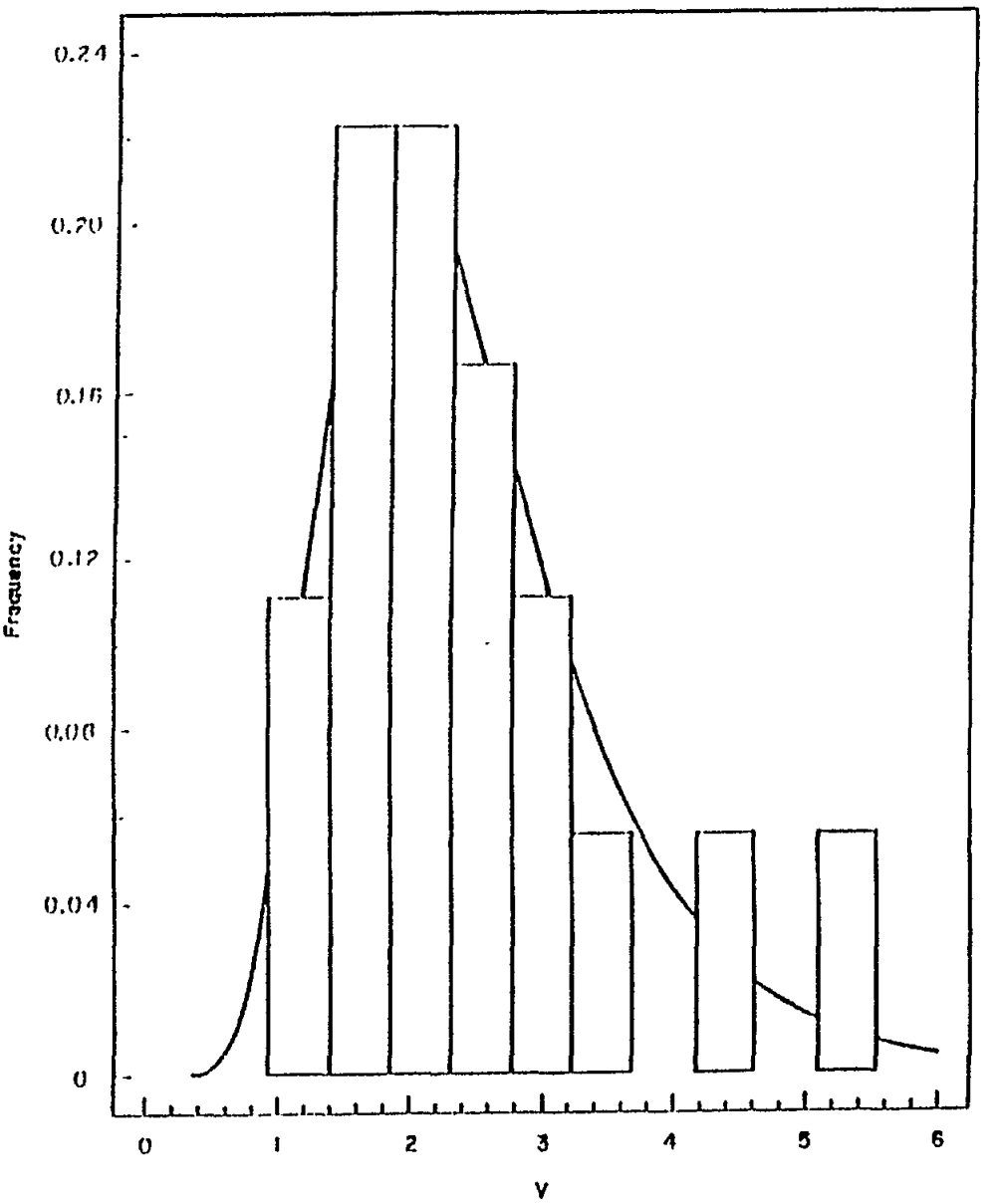

Fig.3 The frequency distribution of V

Observed concentrations of elements at the Black Sea are compared with data from urban, regional marine, rural and remote sites. Results of comparison of selected elements are shown in Table 3. Elemental concentrations in the Black Sea atmosphere are at least an order of magnitude smaller than concentrations in urban atmosphere, such as Katowice.

Table 3

Concentrations of selected elements measured in the Black Sea atmosphere and in other regions (ng/m^3)

ELEMENTS	KATOWICE[1*]	JUNGFRAUJOCH[2]		SOVIET GEORGIA[3*]	MEDITERRANEAN[4]		ENEWETAK[5]		THIS WORK	
Na	1120±550	22	(2.0)	30±37	1515	(2.20)	4400	(1.2)	1300	(2.6)
Mg	1860±1900	10	(2.6)	-	-		660	(1.3)	300	
Al	6700±2900	51	(2.8)	807±283	214	(2.47)	21	(4.3)	400	(1.8)
Cl	3200±2100	7.2	(3.1)	33±14	-		8300	(1.3)	1200	(3.0)
Sc	1.35±0.63	0.0077	(2.9)	-	-		0.005	(4.8)	0.08	(2.0)
V	20±8	0.29	(2.6)	-	-		0.082	(2.3)	2.25	(1.5)
Cr	46±36	0.36	(2.2)	-	-		0.091	(2.3)	5.45	(1.9)
Mn	700±1400	1.5	(3.0)	-	-		0.29	(4.0)	14.06	(1.8)
Co	5.5±3.5	0.045	(1.7)	-	-		0.008	(3.9)	0.18	(1.4)
Cu	1740±960	0.88	(1.9)	-	-		0.044	(2.7)	141	(1.2)
Zn	1760±2300	9.9	(2.2)	-	-		0.160	(2.1)	34	(2.0)
As	16±10	0.23	(2.0)	-	-		-		0.89	(1.9)
Se	15±19	0.042	(2.5)	-	-		0.130	(1.4)	0.57	(1.8)
Br	120±104	1.3	(1.8)	4.3±0.1	-		20	(1.3)	17	(2.1)
Sb	20±12	0.2		-	-		0.005	(2.3)	0.44	(2.0)
I	194±330	0.27	(1.4)	-	-		2.7	(2.0)	20	(2.1)

* Normal means and standard deviations
1 Data from (Tomza *et al.*, 1982)
2 Data from (Dams and Jonge, 1976)
3 Data from (Dzubay and Stevens, 1987)
4 Data from (Dulac *et al.*, 1987)
5 Data from Duce *et al.*, 1983)

For marine elements, such as Na, Cl and Mg, the Black Sea is a typical marine site. Concentrations of these elements in the Black Sea atmosphere are higher than in continental rural sites, and comparable to or lower than in other marine sampling locations. The lower Na, Cl and Mg concentrations in the Black Sea relative to Enewetak, are probably due to milder sea conditions during sampling, which took place in spring and summer.

Concentrations of elements associated with anthropogenic activities, such as V, Zn, Se, Sb, Mn, Mo, Cu, Cr and As, are of an order of magnitude higher in the Black Sea atmosphere than concentrations measured in remote marine areas. These elements have comparable concentrations in continental rural sites, such as Soviet Georgia.

At the Black Sea, concentrations of elements which are associated with aluminosilicate particles are much higher than corresponding concentrations measured at pristine sites, such as Enewetak, lower than concentrations measured in Soviet Georgia, and comparable to concentrations measured in the Mediterranean atmosphere.

In general, elemental concentrations at the Black Sea appear to be intermediate between continental rural sites where local aerosols and long-range transported particles effect observed concentrations, and a remote marine site where local sources other than ocean do not exist.

3.5 Sulphate and Nitrate

Determination of concentrations and sources of $SO_4^=$ is important because it is the main acid-rain precursor. Table 4 shows average sulphate and particulate nitrate concentrations measured in this work. Literature values are also shown in the same table for comparison. The sulphate concentrations measured in the Black Sea atmosphere are comparable with Central and Western European values, but much higher than SO^4 values reported for remote sites. The main source of sulphate in the remote marine atmosphere is the oxidation of dimethylsulphide (DMS) released from the ocean in gas phase, first to SO_2 then to SO_4 (Bates and Cline, 1985; Bates *et al.*, 1987). The measured SO_4 concentrations in the Black Sea are much higher than values reported for most productive regions of the world oceans and, consequently, anthropogenic sources dominate in sulphate observed in the Black Sea atmosphere.

Table 4

Concentrations of Sulphate and Nitrate particles in the Black Sea atmosphere and other places

	$SO_4^=$ ($\mu g/m^3$)	NO_3^- ($\mu g/m^3$)	Reference
Indian Ocean	0.5	0.15	Meszaros, 1978
Soviet Georgia	4.67	0.25	Dzubay and Stevens, 1984
Central Asia, USSR	16.3	-	Andreiev and Lavrinenko, 1968
Central Europe	5.4	-	Meszaros, 1978
Sweden	3.0	-	Meszaros, 1978
Western Europe	7.9-9.0	-	Meszaros, 1978
Black Sea	7.73	2.96	This study

Nitrate concentrations in the Black Sea atmosphere are also much higher than those reported for remote sites. The sources of particulate nitrate in remote atmosphere are stratospheric mixing and production by lightning (Legrand and Delmas, 1986). These sources obviously do not contribute too much to the observed concentrations of nitrate in the Black Sea atmosphere.

Fig.4 shows variations of total and non-sea-salt SO_4 (nss-SO_4) in the collected samples. More than 90% of the observed SO_4 concentrations cannot be accounted for by SO_4 associated with sea-salt. Since biogenic source also cannot account for nss-SO_4, the main source for nss-SO_4 in the Black Sea atmosphere should be long-range transported, pollution-derived aerosol. The anthropogenic source for nss-SO_4 was also suggested by the good correlation between nss-SO_4 and some of the pollution-derived elements such as V, Zn and Se. Fig.5 shows the regression between nss-$SO_4^=$ and Se as an example.

Variations in NO_3 concentrations are more difficult to interpret, because Whatman-41 filters are known to adsorb HNO_3 vapours in the atmosphere, and adsorption is not quantitative (Glasyn, 1987). However, good correlation between NO_3 and nss-SO_4 observed in the Black Sea [r = 0.67, P(17, 0.67) = 0.95] shows that the main source of NO_3 is also anthropogenic.

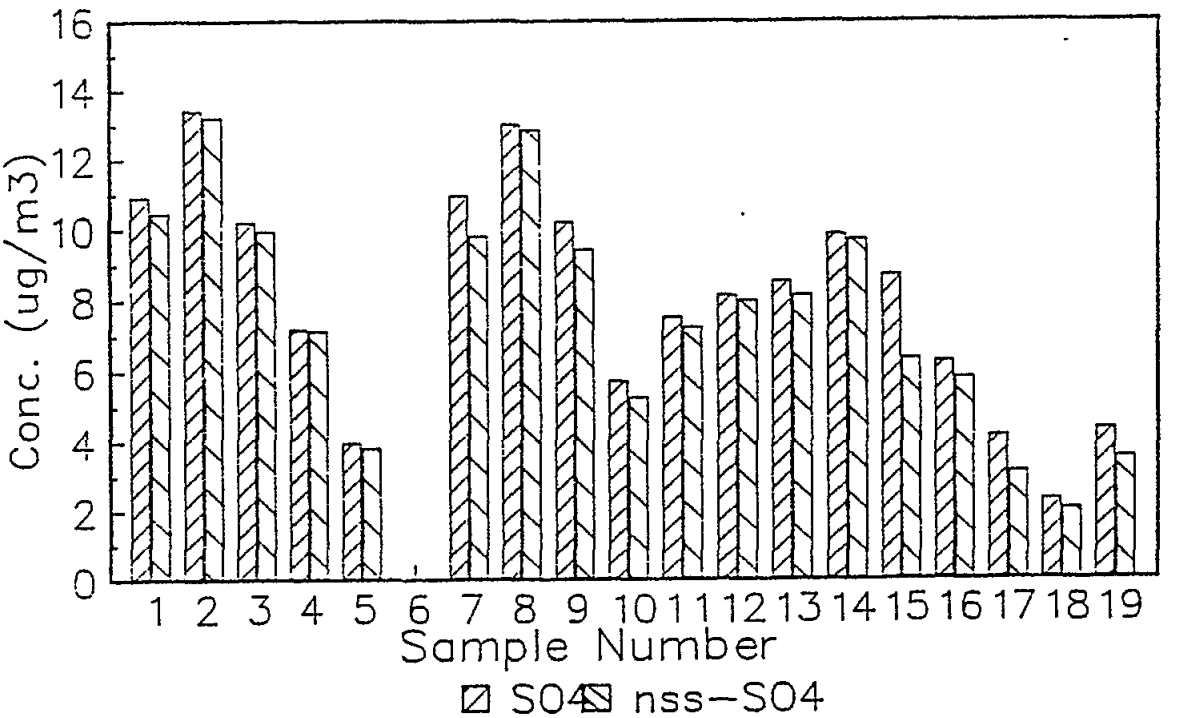

Fig.4 Variations of total and non-sea-salt SO_4

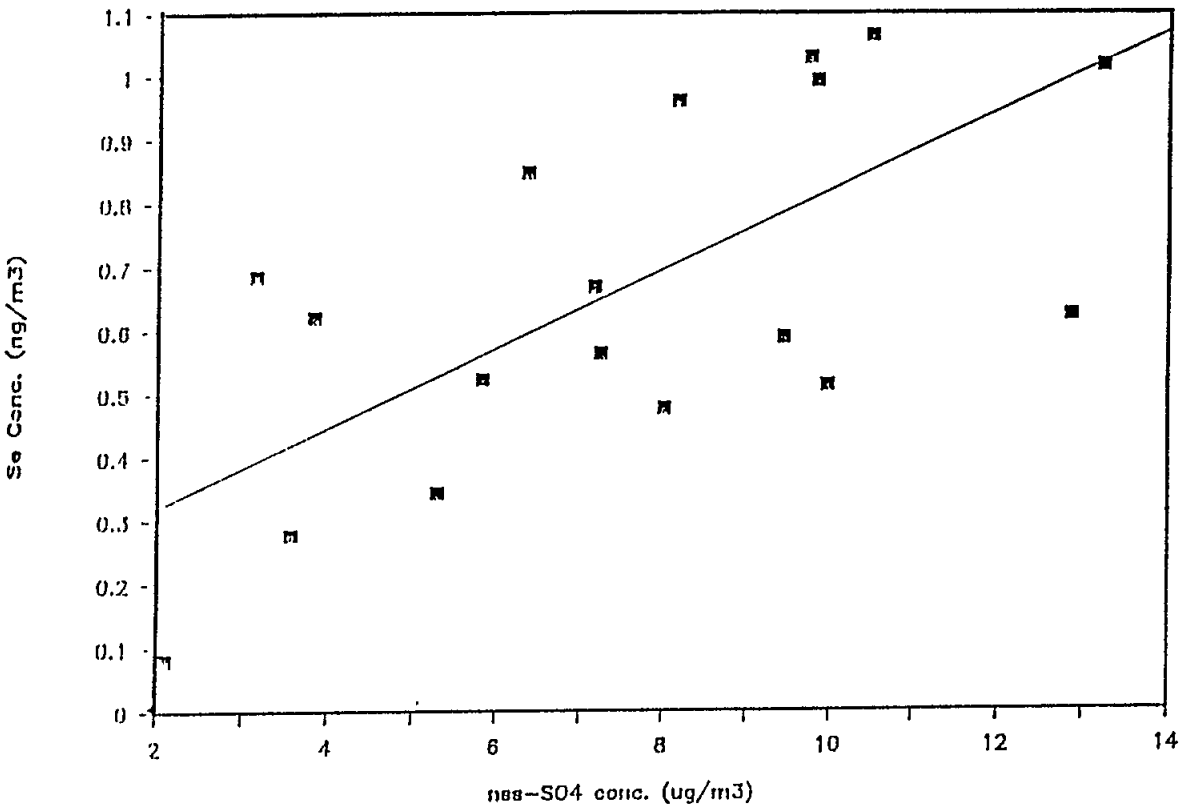

Fig.5 Regression between nss-SO_4 and Se concentrations

3.6 Crustal and marine contribution on elements

Atmospheric aluminosilicate particles and sea-salt can account for a significant fraction of certain elements in the Black Sea atmosphere. Marine and crustal contributions to the observed concentrations of elements were calculated.

The percentage crustal contribution on each element was calculated by using the crustal abundance pattern (Taylor, 1972) and Al as a reference element. Aluminium is frequently used as a reference element because (1) its most important source in atmospheric particles is crustal material, (2) it can be measured accurately with many analytical techniques. However, other elements which possess the same characteristics, such as Fe, can also be used. The percentage of marine contributions on each element was calculated by using Goldberg's (1963) seawater composition and non-crustal Na as the reference element. The non-crustal Na instead of total Na concentrations was used as a reference because crustal contribution on Na concentrations in the Black Sea atmosphere is significant. Results are shown in Table 5.

Table 5 shows that the Earth's crust and the Sea together account for large fractions of elements, Na, Mg, Al, Cl, K, Ca, Sc, Ti, Fe, Co, Br, Rb, Sr, Ba, La, Ce, Sm, Eu, Gd, Tb, Yb, Lu, Hf, Ta and Th. The unaccounted fractions of these elements are either due to differences in crustal dust and seawater compositions used, or due to the presence of other sources which affect the aerosol composition to a small extent. For example, emissions from steel

production can affect the Fe concentrations, emissions from refineries can affect concentrations of rare earth elements, and cement factories can contribute to Ca concentrations. However, the effect of these sources is small compared to crustal dust. The main source of Cl in the marine atmosphere is sea-salt, and observed Cl and Na values in the Black Sea atmosphere showed excellent correlation (r=0.95, P[16, 0.95]=0.99. However, the observed Cl/Na ratio was less than the corresponding ratio in seawater due to volatilization of Cl probably as Hcl from sea-salt particles with the presence of acid (mostly H_2SO_4) in the atmosphere. Fig.6 shows sample to sample variations of nss-SO_4 and Cl/Na ratio. High sulphate concentrations are always accompanied by low Cl concentrations. This also supports the loss of Cl from particles with reaction of H_2SO_4 in the atmosphere. The remaining elements cannot be accounted for by crustal and sea-salt particles and other sources must be sought.

Table 5

Crustal and marine contribution on the observed concentrations of elements

Element	Observed Concentration [(a)]	Marine %	Crustal %
Na	2000±2100	100	14±11
Mg	313±104	48±20	52±4
Al	460±254	--	100
Cl	2100±2100	210±62	0.09±0.09
K	275±87	14±7	36±10
Ca	805±948	16±13	62±16
Sc	0.10±0.08	0.01±0.01	147±45
Ti	60±15	--	65±26
V	2.4±1.0	0.02±0.02	33±13
Cr	6.3±3.1	--	14±15
Mn	16±9	--	35±12
Fe	400±220	--	88±23
Co	0.19±0.06	0.03±0.03	62±8
Cu	144±29	--	0.19±0.09
Zn	42±26	--	1.2±0.6
As	1.1±0.7	0.05±0.04	1.3±0.4
Se	0.65±0.27	0.15±0.15	0.53±0.35
Br	22±20	56±27	0.09±0.05
Rb	1.5±0.8	1.8±1.6	38±12
Sr	19±26	21±15	38±24
Mo	0.14±0.20	3.7±3.5	30±15
Cd	1.0	0.02	0.21
Sb	0.52±0.30	0.28±0.29	0.25±0.14
I	25±15	0.05±0.05	0.01
Cs	0.15±0.10	0.08±0.08	11±4
Ba	4.5±2.8	0.15±0.11	57±24
La	0.32±0.25	--	55±11
Ce	0.61±0.35	0.02±0.02	38±8
Nd	2.6±2.0	--	8±7
Sm	0.04±0.02	--	82±12
Eu	0.01±0.01	--	65±8
Gd	0.04±0.03	--	186±297
Tb	0.01±0.00	--	82±22
Yb	0.02±0.01	--	95±13
Lu	0.003±0.002	--	129±103
Hf	0.03±0.02	--	69±20
Ta	0.01±0.00	--	172±38
W	0.07±0.02	0.02±0.01	12±4
Au	0.005±0.002	0.02±0.02	0.77±0.78
Hg	0.38±0.19	--	0.11±0.04
Th	0.09±0.08	0.02±0.02	68±16
U	0.01±0.01	0.33±0.20	166±54

[(a)] Concentrations are ng/m^3

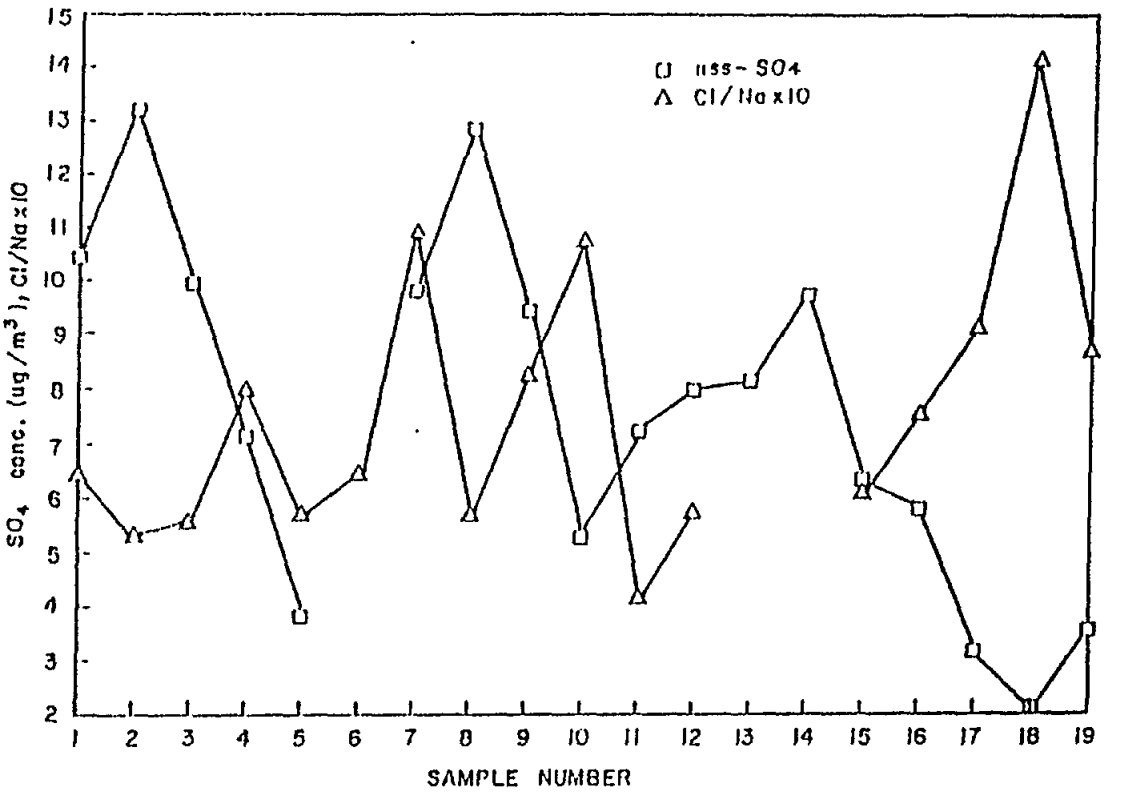

Fig.6 Temporal variations of nss-SO_4 and Cl/Na ratio

4. CONCLUSION

During the summer of 1988, nineteen aerosol samples were collected from the Black Sea atmosphere using double cellulose filters. The elemental composition of atmospheric particles collected near sea level have been determined by instrumental neutron activation analysis for 39 elements and by ion chromatography for $SO_4^=$ and NO_3^-ions.

Detection limits and blanks for most of the elements were not a limitation in measurements. However, relatively large blank substraction for Cr, Au and I contributed significantly to the observed uncertainties of these elements.

Concentrations of most elements and ions showed large sample-to-sample variations. These variations were found to be real, with insignificant contributions from sampling and analytical uncertainties.

With few exceptions, elements showed log-normal distribution. However, some anthropogenic elements, such as Mn and $SO_4^=$, showed frequency distribution due to contribution by mixed sources. Concentrations of elements in the Black Sea atmosphere were found to be intermediate between continental rural sites, where local aerosols and long range transported particles affects observed concentrations, and a remote marine site where local sources, other than ocean, do not exist. Crustal dust and sea-salt were natural sources contributing to the Black Sea aerosols. For the elements which are depleted in these natural sources, anthropogenic activities in surrounding regions were the dominant source.

The Cl/Na ratio was found to be smaller than the corresponding ratio in seawater, owing to evaporation of Cl from sea-salt particles as HCl. The main source for $SO_4^=$ ion, which is an important acid precursor, in the Black Sea atmosphere was anthropogenic. The biogenic release of DMS and its subsequent oxidation to SO_4 is not a significant source for Black Sea aerosols.

5. ACKNOWLEDGMENTS

We wish to thank M. Coleri for valuable discussions on the meteorology of the region. This work was supported in part by the Turkish Scientific and Technical Research Council Grant No. DEBCAG-48, NATO TU-WASTEWATERS and also US Department of Energy Grant No. DE-FG-2-80ER10770. However, any opinions, findings, conclusions or recommendations expressed herein are those of authors, and do not necessarily reflect the view of institutions.

6. REFERENCES

Andreiev, B.G. and R.F. Lavrinenko (1968). Some data on the chemical composition of atmospheric aerosols over Central Asia. *Meteorologia Gidrologia*, 4:63-69 (in Russian).

Bates, T.S. and J.D. Cline (1985). The Role of the Ocean in a Regional Sulfur Cycle. *J. Geophys.Res.*, 90:9168-9172.

Bates, T.S., J.D. Cline, R.H. Gammon and S.R.K. Hansen (1987). Regional and seasonal variations in the flux of oceanic dimethylsulfide to the atmosphere. *J. Geophys. Res.*, 92:2930-2938.

Coleri (1989). Personnel communication.

Cunningham, W.C. (1979). Ph.D. Thesis, University of Maryland, College Park.

Dams, R.J. and J. De Jonge (1976). Chemical composition of Swiss aerosols from the Jungfraujoch. *Atmos. Environ.*, 10:1079-1084.

Duce, R.A., R. Arimoto, B.J. Ray, C.K. Unni and P.J. Harder (1983). Atmospheric trace elements at Enewetak Atoll: 1. Concentrations, sources and temporal variability. *J. Geophys. Res.*, 88:5321-5342.

Dulac, F., P. Buat-Ménard, M. Arnold and U. Ezat (1987). Atmospheric input of trace metals to the Western Mediterranean Sea. 1. Factors controlling the variability of atmospheric concentrations. *J. Geophys. Res.*, 92:8437-8453.

Dutkiewicz, V.A., P.P. Parekh and L. Husain (1986). An evaluation of regional elemental signatures relevant to the Northeastern United States. *Atmos. Environ.*, 21:1033-1044.

Dzubay, T.G., R.K. Stevens and P.L. Haagenson (1984). Composition and origins of aerosol at a forested mountain in Soviet Georgia. *Environ. Sci. Technol.*, 18:873-883.

Galasyn, J.F., K.L. Tschudy and F.J. Huebert (1987). Seasonal and diurnal variability of nitric acid vapor and ionic aerosol species in the remote free troposphere. *J. Geophys. Res.*, 92:3105-3133.

Germani, M.S., I. Gokmen, A.C. Sigleo, G.S. Kowalczyk, I. Ölmez, A.M. Small, D.L. Anderson, M.P. Failey, M.C. Gulovali, C.E. Choquette, E.A. Lepel, G.E. Gordon and W.H. Zoller (1980). Concentrations of elements in the NBS Bituminous and Subbituminous Coal Standard Reference Materials. *Anal. Chem.*, 52:240.

GESAMP (IMO/FAO/UNESCO/WMO/IAEA/UN/UNEP Joint Group of Experts on the Scientific Aspects of Marine Pollution): Atmospheric transport of contaminants into the Mediterranean region, UNEP Regional Seas Reports and Studies No.68, UNEP, 1985.

Goldberg, E.D. (1963). The oceans as a chemical system. *The Sea*, Ed. by M.N. Hill, Vol.2, Ch.1, Interscience, NY.

Hopke, P.K., E.S. Gladney, G.E. Gordon, W.H. Zoller and A.G. Jones (1976). *Atmos. Environ.*, 10:1015-1025.

Kowalczyk, G.S., G.E. Gordon and S.W. Rheingrover (1982). Identification of atmospheric particulate sources in Washington D.C., using chemical element balances. *Environ. Sci. Technol.*, 16:79-90.

Legrand, M.R. and R.J. Delmas (1986). Relative contributions of tropospheric and stratospheric sources to nitrate in Antarctic snow. *Tellus*, 38B:236-249.

Meszaros, E. (1978). Concentration of sulfur compounds in remote continental and oceanic areas. *Atmos. Environ.*, 12:699-705.

Pacyna, J.M., A. Semb and J.E. Hanssen (1984). Emission and long-range transport of trace elements in Europe. *Tellus*, 36B:163-178.

Raemdonck, H., W. Maenhaut and M.O. Andrea (1986). Chemistry of marine aerosol over the tropical and equatorial Pacific. *J. Geophys. Res.*, 91:8623-8636.

Taylor, R. (1972). Abundance of chemical elements in the Continental Crust: A new table. *Geochim. Cosmochim. Acta.*, 28:1273.

Thurston, G.D. and J.D. Spengler (1985). *Atmos. Environ.*, 19:9-25.

Tomza, U., W. Maenhaut and J. Cafmeyer (1982). Trace elements in atmospheric aerosols at Katowice, Poland. In. *Trace substances in environmental health*, D.D. Hemphill (Ed.), 105-115.

Tuncel, G. (1984). Ph.D. Thesis, University of Maryland, College Park.

Tuncel, G., N.K. Aras, W.H. Zoller (1989). Temporal variations and sources of elements in the South Pole atmosphere: 1. Non-enriched and moderately enriched elements. *J. Geophys. Res.*, 94:13025-13039.

Watts, S.F., R. Yaaqub and T. Davies (1987). The use of Whatman 41 filter papers for high volume aerosol sampling. *Atmos. Environ.*, 21:2731-2736.

TRACE METALS CHARACTERIZATION OF PRECIPITATION AND AEROSOLS : PRELIMINARY RESULTS

By

A. NEJJAR and R. AZAMI

Atmospheric and marine pollution laboratory
EMI, BP 765, Rabat, Morocco

1. INTRODUCTION

The deposition of a number of heavy metals with ecotoxic significance contributes substantially to the burden of terrestrial and aquatic ecosystems and causes, in an increasing number of regions, severe damage on components of vegetation and aquatic organisms, particularly in waters such as oceanic systems. Withn the framework of our contribution to the monitoring of the transport of pollutants to the Mediterranean Sea through the atmosphere, a monitoring programme has been taking place for about two years. This study deals particularly with the input of heavy metals from the atmosphere into the Mediterranean Sea; dry and wet deposition has been considered.

The trace elements considered are those whose distribution in oceanic systems are influenced by atmospheric concentrations. These elements are associated with aerosol particles which are produced both naturally, and as a result of anthropogenic activities.

Using Atomic Absorption Spectrometry, the trace element (Zn, Cd, Pb and Cu) composition of aerosols and rain waters collected at two cities in Morocco was estimated, and dry and wet deposition fluxes calculated. The results are presented in this paper.

2. SAMPLES COLLECTED AND ANALYSIS

Aerosol samples were collected over a period of eighteen months (September 1989 to February 1991) at two sites, viz. Tangiers and Beni-Mellal.

Tangiers (Latitude 35E 43'N, Longitude 05E 54'W), is situated on the coast of the Mediterranean Sea, in Northern Morocco. Tangiers, which has approximately 300,000 inhabitants, is moderately industrialized. While a few industries are situated along the coast, several mid-size industries are spread throughout the city and in nearby areas. The sampling site (elevation 20,52 m) was located about 13 km northwest of the city centre at the meteorological station.

Beni-Mellal (Latitude 32E 22'N, Longitude 06E 24'W), a reference monitoring station about 500 km southwest of Tangiers in Central Morocco, is located at a remote (about 200 km) coastal rural site and is not directly influenced by identifiable local sources of air pollution. Sampling was done at the meteorological station (Altitude 468 m).

A first exploratory study was started in September 1989 in two sampling stations, both for aerosol and precipitations.

Besides the sampling, the common meteorological parameters (precipitation amount, wind speed and direction, air temperature, dew point, relative humidity and barometric pressure) were measured at the sampling sites. Airborne particles were collected on glass-fibre filters using high volume samplers, on at least a monthly basis; about 1,500 m^3 of air was drawn through the filters per day (twenty-one samples in Tangiers and eighteen in Beni-Mellal). Rainwater was collected on a weekly average basis in pre-acidified rain-collecting bottles (twelve samples in Tangier and seven in Beni-Mellal). The samples were analyzed using a AAS Sepetr AA20, equipped with a graphite furnace type GTA 96.

3. RESULTS AND DISCUSSIONS

The mean concentrations and the maximum to minimum concentration ratio of the studied trace elements (Zn, Cd, Pb and Cu) in the atmospheric aerosols are given for both sampling sites in Table 1, while the same parameters in precipitations are presented in Table 2.

Table 1

Mean concentrations (ng m^{-3}) of trace metals in aerosols

ELEMENT	TANGIERS		BENI-MELLAL	
	Mean	Ratio	Mean	Ratio
Zn	45	12	63	24
Cd	0.6	11	0.3	30
Pb	28	5	10	4
Cu	7.2	14	4.7	6

It can be seen from Table 1 that the element levels in air in both sites are found to be lower than those reported (Schneider, 1987; Nurnberg *et al.*, 1984) for urban and rural areas. This is probably due to the poorer collection efficiency of our filters for the fine particles, at least at the beginning of the sampling; therefore, the concentrations given in Table 1, as well as the estimated TSPM, are likely to be lower than the actual levels. This would, however, not materially affect the observed tendencies and patterns. The concentrations of Cu, Pb and Cd are higher for the urban area, while the levels of Zn are more important for the rural area. This higher Zn could be related to the soil rather than increased industrial emission (The TSPM levels were generally higher for Beni-Mellal as compared to Tangier).

The level concentrations of the same anthropogenic elements (zinc, lead and copper) in rainwaters are presented in Table 2; cadmium could not be detected.

If we consider the maximum to minimum concentration ratio, it was found to be between 3 and 32 at the urban area, while it was between 7 and 19 at the rural zone. The variations in all cases were generally larger for precipitations than for aerosols.

Table 2

Mean concentrations ($\mu g l^{-1}$) of trace metals in precipitations
(n.d. = not determined)

ELEMENT	TANGIERS		BENI-MELLAL	
	Mean	Ratio	Mean	Ratio
Zn	13	32	9	17
Cd	n.d.	-	n.d.	-
Pb	12	3	3	7
Cu	2.5	9	1	19

Deposition flux calculations

Using the reported data, dry (Fp) and wet (Fr) deposition flux calculations were done.

The dry deposition velocity which averaged 0.3 cm s^{-1} was, while a mean scavenging ratio (S) of 200 was assumed for the pollutant aerosols. The mean annual rainfall at Tangier and Beni-Mellal is 737.3 and 392.3 mm respectively.

Table 3 which summarizes the results, also gives total atmospheric deposition fluxes (F) of the elements.

Table 3

Dry, wet and total deposition fluxes ($mg m^{-2} yr^{-1}$) of trace metals
to Northern Morocco

ELEMENT	TANGIERS			BENI-MELLAL		
	Fp	Fr	F	Fp	Fr	F
Zn	4.26	5.51	9.8	5.95	4.1	10
Cd	0.057	0.073	0.13	0.028	0.02	0.05
Pb	1.134	3.43	4.6	0.945	0.65	1.05
Cu	0.68	0.88	1.6	0.445	0.31	0.76

The assumed values for the mean dry deposition velocity v_d and the scavenging ratio are literature values (GESAMP, 1989). On one hand they are adopted for remote open oceans and on the other hand the values for coastal and nearshore areas would probably be higher. We therefore made another calculation, taking into account these remarks, with 1 cm s^{-1} for dry deposition velocity and a scavenging ratio of 500 (Table 4).

Tables 3 and 4 provide an order of magnitude estimate of the elemental deposition. The observed results are generally lower than the literature values for the Northwestern Mediterranean (Bergametti, 1987).

Table 4

Dry, wet and total atmospheric deposition fluxes ($mgm^{-2}\ yr^{-1}$) calculations
(v_d = 1 cm s^{-1}, S = 500)

ELEMENT	TANGIERS			BENI-MELLAL		
	Fp	Fr	F	Fp	Fr	F
Zn	14.2	13.8	28	19.8	10.2	30
Cd	0.18	0.18	0.36	0.09	0.05	0.14
Pb	3.8	8.6	12.4	3.15	1.68	4.7
Cu	2.27	2.2	4.47	1.49	0.78	2.27

From the data it is seen that dry deposition fluxes are in most cases more important than wet deposition, particularly in the rural area, while most literature works for the input of trace metals are reporting the predominant significance of wet deposition. This is probably due to the relatively low amount of rain, and changes in airflow and precipitation patterns. From the tables, it is estimated that dry deposition represents 25-50% of the total deposition flux for the urban region, while it represents 50-70% for the rural zone.

4. CONCLUSION

The reported data regarding the level concentrations of the trace metal elements (Zn, Cd, Pb, Cu) represent a good preliminary description of the principal constituents in atmospheric aerosols and rainwaters, as accomplished in this exploratory study. Refinement should be possible as more data becomes available.

To determine the contribution of sea-salt, mineral and anthropogenic aerosols, indicator elements such as Na and Al will also be included in future work.

The partitioning of trace elements between soluble and insoluble form, and the particle-size dependence of solubility is also an important area for our future research. Consequently, future efforts will be focused on wet deposition, aerosol composition and particle-size distribution, in order to contribute and obtain a clearer perspective of all the problems involved in estimating trace metals contribution to the Mediterranean Sea from the atmosphere.

5. REFERENCES

Bergametti, G. (1987). *Apports de matière par voie atmosphérique à la Méditerranée Occidentale.* Ph.D. Thesis, University of Paris 7, France.

GESAMP (1989). The atmospheric input of trace species to the world ocean. *Rep. Stud. No.38*.

Nurnberg, H.W. *et al.* (1984). Studies on the deposition of acid and of ecotoxic heavy metals with precipitates from the atmosphere. Frenesius, *A. Anal. Chem*., 317:314-323.

Schneider, B. (1987). Source characterization for atmospheric trace metals of Kiel Bight. *Atmos. Environ.*, 6:1275-1283.

IMPACT OF THE ATMOSPHERIC DEPOSITION ON TRACE METAL LEVELS IN THE LIGURIAN SEA

By

CHRISTOPHE MIGON[1] and JACQUES MORELLI[2]

[1] CMCS, Université de Corte, Grossetti, BP 52, F 20250 Corte, France.
[2] Institut de Biogéochimie Marine, URA 386 CNRS, Ecole Normale Supérieure, 1 rue Maurice Arnoux, F 92120 Montrouge, France.

1. INTRODUCTION

The impact of heavy metals on marine fauna and their accumulation in the human foodchain has become an increasing problem, particularly in the Mediterranean Sea (Romeo *et al.*, 1985; Fowler, 1986; Romeo and Nicolas, 1986).

Although the atmosphere is the main route for the transport of these elements from land-based sources to the sea (Nriagu and Pacyna, 1988), atmospheric metal pollution is still underestimated. Therefore, the present work aims to assess the contribution of four metals well known for their toxicity: Pb and Cd, which have no biological role and whose traces can change the metabolic processes in phytoplankton (Fitzwater *et al.*, 1982), and Cu and Zn which are necessary for the growth of aquatic organisms.

The purpose of this paper is to evaluate the atmospheric inputs of Pb, Cd, Cu and Zn to the Ligurian Sea on the basis of a two-year sampling period, and to discuss the impact of such loadings on metal concentrations in seawater. Moreover, this study should provide new data for a global estimation of the problems of inorganic pollution in the Mediterranean Sea.

2. SAMPLING

A sampling station was set up at Cap Ferrat (43E41'10"N; 7E19'30"E), on the Southeastern coast of France (see Fig.1).

This site is sheltered from close continental sources, as discussed elsewhere (Migon, 1988; Migon and Caccia, 1990). Dry and wet inputs were continuously collected over a period of two years (1986 and 1987). Dry and total depositions, being very difficult to measure directly, aerosol samples were analyzed in order to determine dry fluxes, with the help of dry deposition velocities found in the literature.

The filtration apparatus (filter holder Sartorius SM 16510 and cellulose acetate membranes Sartorius SM 11106, porosity 0.45 µm, diameter 47 mm) was raised to the top of a six-metre mast and connected to pumps and counters. The flow rate of the pumps was about 1 m^3 per hour and the filtration was carried out over 4 to 8 hours. The particle size was not taken into account.

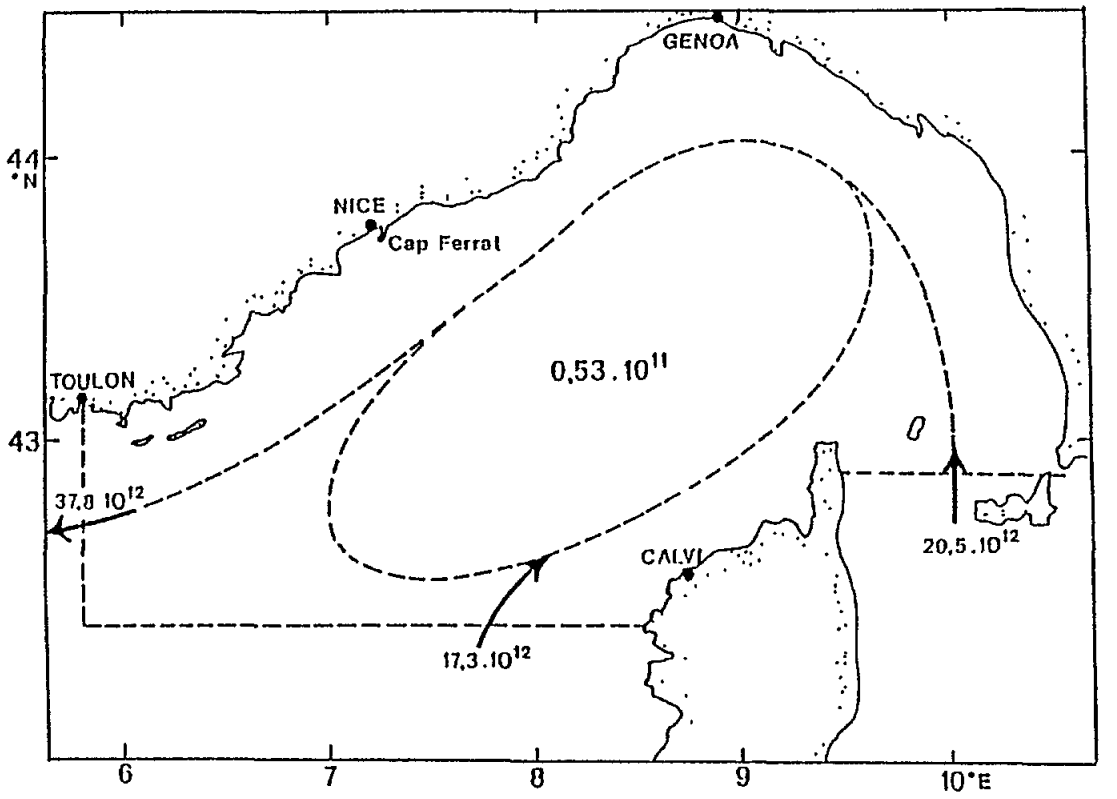

Fig.1 Surface area, expressed in m^2, and cyclonic circulation in the Ligurian Sea. The flows are expressed in m^3 per year.

Wet deposition was collected with a rain collector, used and described previously (Nurnberg *et al.*, 1984; Migon, 1988), which automatically opens when it rains. Rainwater was automatically filtered on Sartorius SM 11106 membranes previously cleaned with Suprapur HCl 1 to 2 N.

3. ANALYSIS

Aerosol concentration was measured by graphite furnace atomic absorption spectrophotometry (GFAAS). Parts of the membrane filters (3 mm in diameter) were cut out of the filters, and aliquots were directly introduced into the carbon-rod atomizer. The atomic absorption spectrophotometer was a Varian Techtron AA 1275 equipped with a CRA 90 atomizer. The detection limits were 50, 0.2, 13 and 25 pg for Pb, Cd, Cu and Zn respectively. Reproducibility was always >90% for Pb, Cd and Zn, and >95% for Cu.

Rainwater was analyzed by both GFAAS (Zn) and differential pulse anodic stripping voltammetry (DPASV) on a hanging mercury drop electrode (Pb, Cd and Cu). DPASV measurements were performed with an EG&G Princeton Applied Research (P.A.R.) 264 A polarographic analyzer in conjunction with a 303 A static mercury drop electrode. A medium mercury drop (1.6 mm^2) was used as a working electrode. The detection limits with DPASV was 0.1 $\mu g.l^{-1}$ for Pb and Cu and 0.02 $\mu g.l^{-1}$ for Cd. The blank values were at maximum equal to these detection limits and the reproducibility was always better than 95%. All the analyses were carried out on laminar airflow benches, in a 100% clean room.

4. EVALUATION OF THE TOTAL ATMOSPHERIC INPUT

The metal concentration ranges are recorded in Table 1, as well as mean values. Bulk data can be found elsewhere (MIGON, 1988). The metal concentrations in rainwater are geometric means, which better describe the distribution of the atmospheric concentrations (Bergametti, 1987). In the case of aerosol concentrations, the calculation of appropriated mean values has been described in detail in a previous paper (MIGON and CACCIA, 1990).

Atmospheric fluxes are given in Table 2. Wet fluxes were calculated for each rain event by multiplying the concentration with the amount of rainfall and then summarized within a year. Dry fluxes were calculated after the following relationship:

$$F(x) = C(x).\ V(x) \qquad \text{(Equation 1)}$$

where for an element x, F is the associated dry flux, C the concentration in the aerosol and V the dry deposition rate, found in the literature (Dulac *et al.*, 1989; Flament, 1985; Remoudaki, 1990). This flux is multiplied by the mean number of dry days in a year in order to calculate the annual dry deposition. Nevertheless, this method raises a problem: the dry deposition rates are questionable and the experimental values are very different to the theoretical ones (Dulac *et al.*, 1989).

Table 1

Toxic metal concentrations in the atmospheric aerosol, expressed in $ng.m^{-3}$, and in rainwater, expressed in $\mu g.l^{-1}$

	Concentration ranges in the aerosol ($ng.m^{-3}$)	Mean values ($ng.m^{-3}$)	Concentration ranges in the rainwater ($\mu g.l^{-1}$)	Mean values ($\mu g.l^{-1}$)
Pb	5.22-106.85	34.2	0.6-74.1	4.6
Cd	0.03-1.61	0.29	<d.l.-10.3	0.18
Cu	2.18-24.04	4.58	<d.l.-36.2	2.15
Zn	7.63-123.71	26.4	0.5-82.5	8.6

Assuming that the chemical composition of the aerosol at Cap Ferrat is similar to that of the open sea, a total atmospheric flux can be given (see Table 2).

It appears that the dry loadings are often as important as wet inputs. Except for Cd, where the dry contribution is only 2% of the total fluxes, the dry deposition should be responsible for 9- 83%, 27% and 33% of the total deposition for Pb, Cu and Zn respectively. The importance of the dry atmospheric Pb could be partly due to continuous gasoline combustion in southeastern Europe, taking into account that unleaded fuel was scarcely used in the Ligurian coasts during 1986 and 1987.

Considering the limits of the Ligurian Sea given in Fig.1, one can calculate the total annual atmospheric deposition over this marine area (see Table 2).

Table 2

Wet and dry atmospheric fluxes and total annual deposition on the Ligurian Sea. The fluxes are in $kg.km^{-2}.yr^{-1}$ and the total deposition in tons per year.

	Dry fluxes ($kg.km^{-2}.yr^{-1}$)	Wet fluxes ($kg.km^{-2}.yr^{-1}$)	Total fluxes ($kg.km^{-2}.yr^{-1}$)	Total annual atmospheric deposition ($T.yr^{-1}$)
Pb	0.3-15	3	3.3-18	175-950
Cd	$3.6.10^{3}$	1.34	$173.5.10^{3}$	9.2
Cu	0.5	0.170	1.85	98
Zn	3.0	6.03	9.0	480

5. IMPACT ON SEAWATER METAL CONCENTRATIONS

In this section, an attempt is being made to estimate the modification of trace metal levels in the Ligurian Sea due to atmospheric deposition.

Fig.1 shows a cyclonic circulation in the Ligurian Sea. According to Bethoux (1980), the surface flux (0-200m) of Atlantic waters ascending along the west coast of the Corsican Cape is $17.3.10^{12} m^3.yr^{-1}$. Off the Corsican Cape, the mixing of this flux with that coming from the Tyrrhenian Sea via the Corsican channel causes the Ligurian current whose flow F is $37.8.10^{12} m^3.yr^{-1}$. This flows in a northeast-southwest direction along the Riviera and goes out of the Ligurian Sea. Considering a surface area of $5.3.10^{10}$ m^2 for the Ligurian Sea, let us call V the volume which is the water layer 0 to 200 m of the Ligurian Sea. Without any vertical mixing nor biological activity, one can calculate that the residence time of the waters should be 102 days. This period represents the water residence time besides short winter episodes of deep water formation. The superficial waters can be considered as an homogeneous zone during the greater part of the year. Considering that A.I. is the yearly atmospheric input of trace metals, the mean increase of the seawater metal concentration during the residence in the Ligurian Sea (ÄC) can be calculated as:

$$\ÄC = A.I./F \qquad \text{(Equation 2)}$$

These ÄC values are to be compared with the typical concentrations given by Copin-Montegut *et al.*, (1986), Breder (1987), Nicolas and Courau (1988), Bethoux *et al.*, (1990) and Nicolas (unpublished data) for the Western Mediterranean basin (see Table 3).

The ÄC values represent a mean situation, but much higher values should be observed at a shorter scale of time and space, according to the flow more or less impulsive of the atmospheric deposition and its confinement into a water layer much lower than 200 m during all the period when the seasonal thermocline exists. Nevertheless, these mean values allow to forecast that the increase of the Pb levels in the waters transiting in the Ligurian Sea should be easily evidenced with *in situ* measurements, but this should be far more difficult for Cd and Cu.

Table 3

Mean increase of the seawater metal concentration during the residence in the Ligurian Sea (ÄC), compared with several values of concentration in this area (C). All the concentrations are expressed in $\mu g.m^{-3}$. The ÄC/C values are expressed in percent.

	ÄC	C[(1)]	ÄC / C	C[(2)]	ÄC / C	C[(3)]	ÄC / C	C[(4)]	ÄC / C	C[(5)]	ÄC / C
Pb	4.6-25.2	59	7.8-42.7	144	3.2-17.5	70	6.6-36	52	8.8-48.5	-	-
Cd	0.24	7.8	3.1	6	4	-	-	6.5	3.7	-	-
Cu	2.6	202	1.3	250	1	-	-	136	1.9	-	-
Zn	12.7	-	-	-	-	-	-	232	5.5	269	4.7

(1) Copin-Montegut *et al.*,
(2) Breder (1987)
(3) Nicolas and Courau (1988)
(4) Bethoux *et al.*, (1990)
(5) Nicolas (unpublished data)

6. CONCLUSION

Among other factors, the atmosphere plays a major role in the heavy metal supply in a relatively small surface area such as the Ligurian Sea. Hence a need to evaluate the atmospheric deposition, such assessment should be included in a total Mediterranean study at different coastal sampling sites.

Despite the fact that the dry deposition rates are very questionable, the impact of the atmospheric matter on the seawater metal concentrations (expressed by the Ä/C values) can be pointed out. It appears that in a mean situation, only Pb has a significant incidence on the seawater concentration levels. This could be explained by the close environment of the Ligurian Sea where Pb emissions are strong because of large urban areas but where industrial activities are not very important and so that emissions of Cd, Cu and Zn are lower.

7. REFERENCES

Bergametti, G. (1987). *Apports de matière par voie atmosphérique à la Méditerranée Occidentale: aspects géochimiques et météorologiques*, Ph.D Thesis, Université de Paris VII, pp.296.

Bethoux, J.P. (1980). Mean water fluxes across sections in the Mediterranean Sea, evaluated on the basis of water and salt budgets and of observed salinities. *Oceanol. Acta, 3*, 1:9-88.

Bethoux, J.P., P. Courau, E. Nicolas and D. Ruiz-Pino (1990). Trace metal pollution in the Mediterranean Sea. *Oceanologica Acta*, (in press).

Breder, R. (1987). Distribution of heavy metals in Ligurian and Tyrrhenian coastal waters, *Sci. Total Environ.*, 60:197-212.

Copin-Montegut, G., P. Courau and E. Nicolas (1986). Distribution and transfer of trace elements in the Western Mediterranean. *Mar. Chem.*, 18:189-195.

Dulac, F., P. Buat-Ménard, U. Ezat, S. Melki and G. Bergametti (1989). Atmospheric input of trace metals to the Western Mediterranean: uncertainties in modelling dry deposition from cascade impactor data. *Tellus*, 41B:362-378.

Fitzwater, S.E., G.A. Knauer and J.H. Martin (1982). Metal contamination and its effects on primary production measurements. *Limnol. Oceanogr.*, 27(3):544-551.

Flament, P. (1985). *Les métaux-traces associés aux aérosols atmosphériques: apports au milieu marin du littoral Nord-Pas-de-Calais*, Ph.D Thesis, Université des Sciences et Techniques de Lille, pp.169.

Fowler, S.W. (1986). Trace metal monitoring of pelagic organisms from the open Mediterranean Sea. *Environ. Monit. Assess.*, 7:59-78.

Migon, C. (1988). *Etude de l'apport atmosphérique en métaux-traces et sels nutritifs en milieu côtier méditerranéen; implications biogéochimiques*, Ph.D Thesis, Université de Nice, pp.217.

Migon, C., and J.L. Caccia (1990). Separation of anthropogenic and natural emissions of particulate heavy metals in the Western Mediterranean atmosphere. *Atmos, Environ., 24A*, 2:399-405.

Nicolas, E., and P. Courau (1988). Le plomb dans les eaux côtières du bassin méditerranéen nord-occidental, In: *Proc. of the XXXIE Congrès de la CIESM, Athens*, Vol. 31, Fasc. 2, CIESM, Monaco.

Nriagu, J.O., and J.M. Pacyna (1988). Quantitative assessment of worldwide contamination of air, water and soils by trace metals. *Nature*, 333:134-139.

Nurnberg, H.W., P. Valenta, V.D. Nguyen, M. Godde, and E. Urano De Carvalho (1984). Studies on the deposition of acid and ecotoxic heavy metals with precipitates from the atmosphere, *Fresenius Z. Anal. Chem.*, 317:314-323.

Remoudaki, E. (1990). *Etude des processus controlant la variabilité temporelle des flux atmosphériques de polluants et de poussières minérales en Méditerranée occidentale*, Ph.D Thesis, Université de Paris VII, pp.223.

Romeo, M., M. Gnassia-Barelli and E. Nicolas (1985). Concentrations en plomb du plancton de la Mer Ligure (Méditerranée Nord-Occidentale). *Chemosphere, 14*, 9:1423-1431.

Romeo, M. and E. Nicolas (1986). Cadmium, copper, lead and zinc in three species of planktonic crustaceans from the East coast of Corsica. *Mar. Chem.*, 18:359-367.

AN INITIAL ASSESSMENT OF AIRBORNE POLLUTION LOAD IN THE NORTHEASTERN MEDITERRANEAN FROM VARIOUS SOURCES

By

A.C. SAYDAM, N. KUBILAY and O. BASTURK

Middle East Technical University
Institute of Marine Sciences
Erdemli-Icel, Turkey

A B S T R A C T

A 20 metre high atmospheric collection tower has been constructed at the harbour jetty of IMS/METU at Erdemli, Turkey, for the collection of airborne particulate samples. The 1990 collections were performed by using mesh techniques. The preliminary results of airborne pollution monitoring in the northeastern Mediterranean has revealed that the region is mainly affected by crust-derived materials. The "European" background material or the fingerprints of anthropogenic inputs, can only be found during the winter season, in association with the northwesterly wind regimes. The atmospheric dust load is especially high during the dry seasons and up to 1 g of dust can be collected per day by using mesh techniques. The possible use of the remote sensing method has been looked into with the present remote sensing instrumental facilities of IMS/METU. It has been demonstrated that the transport of airborne dust outbreaks of known events can be traced and documented by the use of AVHRR satellite data.

Satellite IR and VIS pictures were also used to detect and follow up the recent fires in the Gulf. The transport and the wet deposition of black smoke was observed at the southeastern corner of the Levantine Basin. Analysis of rainwater showed that, during the burning and subsequent wind transport of the smoke, lightweight hydrocarbons were lost.

1. INTRODUCTION

Pollution of the marine atmosphere has received increasing attention over the past few years, and it is now apparent that large amounts of material can be transported to the oceans via the atmosphere. The effect of such atmospheric transport is expected to be of importance in the Mediterranean, which is a semi-enclosed sea. However, there are relatively little data available on atmospheric material transported to the eastern Mediterranean. Because it is surrounded by a number of aerosol catchment regions, the Mediterranean Sea is particularly attractive for the study of atmospheric processes. It is bordered to the north by countries having a variety of economies, ranging from industrial to semi-industrial to agricultural, and to the south by the North African desert belt. There is also volcanic activity in the region, and the Mediterranean is one of the most crowded seaways of the World Ocean. These various areas give rise to a variety of natural and pollutant particulates which combine to form the Mediterranean aerosol. Turkey may be regarded as an "intermediate" aerosol source, lying between the industrial and the true desert areas.

2. REVIEW OF REGIONAL CHARACTERISTICS

2.1 Atmospheric characteristics influencing the Mediterranean Sea

Variability in meteorological conditions is a distinguishing aspect of the Eastern Mediterranean. Many local wind systems are generated within the Mediterranean region as a result of its complex topography (Fig.1). This is due to the fact that the region is a pathway for cyclones during winter and spring. On average, 51 depressions moving towards the Levantine and the Aegean track in such a way that nearly 21 of them pass over the Levantine, the remaining 30 taking a northerly route over the Anatolian Peninsula (Fig.2) (Mediterranean Pilot, 1976; Karein, 1977; Ozsoy, 1981). Sufficiently strong sea-breeze systems modify the mid-latitude westerlies during summer and autumn. Additional space-time variability is introduced into the region because of the coastal topography. In this respect, the Eastern Mediterranean much resembles the western basin, where a series of complex atmospheric processes are generated because of the interactions of the air masses with local geographical features of the water-land boundary which, in particular, lead to the strong coupling of the various scales of motion of the atmosphere. The review by Reiter (1975) covers the atmospheric characteristics of the Mediterranean at large. An excellent review of the atmospheric setting of the Levantine is given by Ozsoy (1981). The following summarize the meteorological conditions that are relevant to the Eastern Mediterranean.

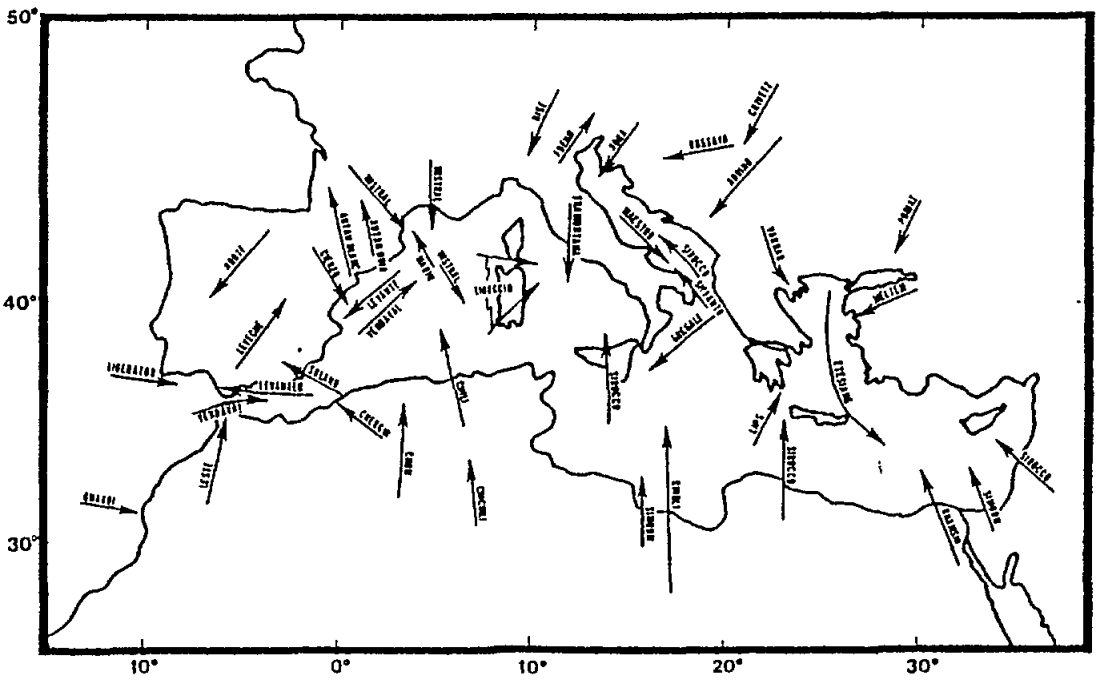

Fig.1 Major local wind systems in the Mediterranean region (Reiter, 1975)

In the northern Levantine a local northerly wind regime called Poyraz exists, which is similar to the Mistral of the northwestern Mediterranean and the Bora of the Adriatic Sea. During each Poyraz event, extremely dry air is brought to the coastal area. It is well known along the southern Turkish coast that, even in winter, the passing depressions are usually followed by bright skies and dry conditions which suddenly clear the dense clouds observed earlier. Especially after Pouraz events, the visibility is so much improved in the Akkuyu Silifke

area that the mountains of Cyprus are visible from a distance of 100 km or more. The wind speed of Poyraz can reach up to 36 m/s and the resulting mixing and evaporation lead to rapid cooling of the surface waters (Unljata, 1986).

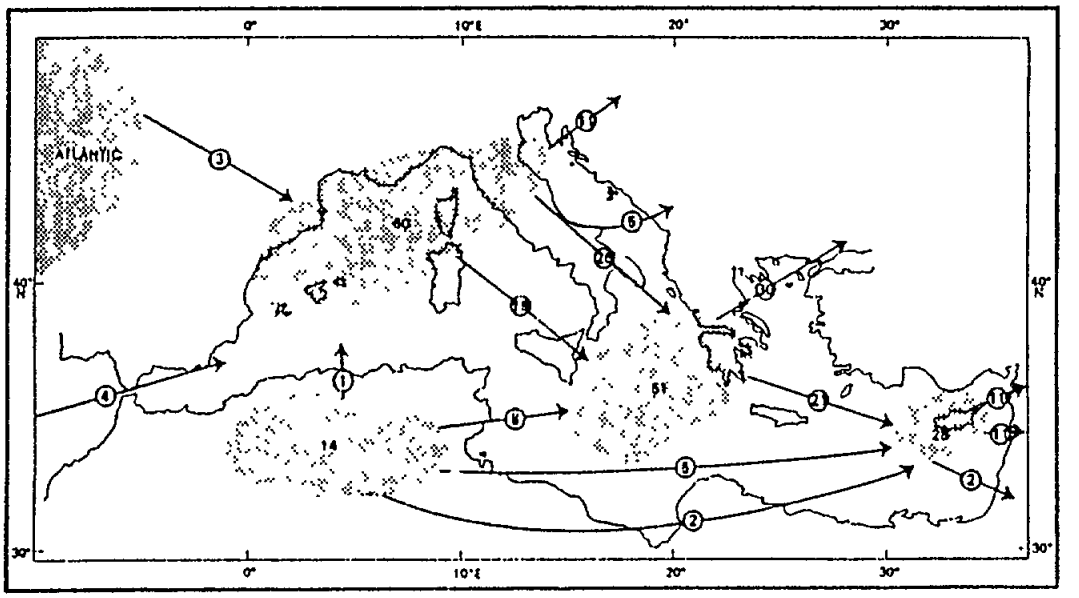

Fig.2 Tracks of Mediterranean depression. Numbers indicate average annual frequencies

During summer the sea-breeze becomes an important aspect of the meteorology of the Levantine Basin. This is especially true for the northern areas. Other regional winds of the Levantine Basin are the Sirocco and the Etesian, which affect the Aegean. The dry Sirocco winds emanate from the deserts of North Africa and the Arabian Peninsula. The Sirocco leads the cyclones developing in the western Levantine and the southern Aegean, and is most common during November-April. It is more intense in the southern Levantine areas. In the northern Levantine and the Aegean, it loses its strength and dryness.

The Etesian is the most frequently prevailing northerly wind system of the Aegean, lasting from June to October. Sufficiently strong sea-breeze systems also exist in the Aegean. With the vanishing of the Etesian system in late autumn, the Aegean comes under the influence of violent storms with cyclonic circulations.

2.2 Hydrography

The most distinctive characteristics of the Levantine Basin is its extreme variability. Recent studies, as reported by Ozsoy *et al.* (1989), confirmed the existence of persistent features. In the Levantine Basin there exist three different water bodies. These are Atlantic Water (AW), Levantine Intermediate Water (LIW) and Deep Water (DW).

! ***Atlantic water***

The presence of AW in the Levantine Basin in summer coincides with an increase in its inflow through the Straits of Gibraltar and Sicily (La Violette, 1987). In Levantine, during the summer season, the AW is overtopped by surface waters with a higher temperature and salinity, so that its fingerprint along the northeastern Levantine Basin is a subsurface salinity minimum of 38.5-39.0 ‰ (Fig.4).

! ***Levantine intermediate water***

LIW is a water mass that affects the entire Mediterranean Sea. The observed annual change at the depth of the AW/LIW interface at the Alboran Sea is 40 metres. The depth of LIW rises to a level of 300 m in November, which is the time period where minimum amounts of AW pour into the Mediterranean Sea. The maximum flow of AW is observed during March where the AW/LIW interface depth is observed at around 340 metres. The amount of AM entering the Mediterranean Sea is hydraulically controlled by the LIW leaving the Straits (Paul La Violette. Pers.comm., 1989).

The formation of LIW is influenced by the cold dry continental airflows. It is primarily formed along the northern borderline of the Levantine Basin, i.e. along the southern coast of Turkey. Its characteristic salinity is 39.1 ‰ and a temperature of 15.5EC at its formation region. The formation of LIW involved the generation of highly saline surface waters under the influence of the cold and dry northerly air masses during February and March, when the seawater temperature reaches a minimum and is typically greater than the air temperature. As a result, surface waters with larger density than the waters below are generated and sink until they reach a denser layer. In the meantime, with increasing inflow through the Strait of Sicily, the surface waters are replaced by AW (Unljata, 1986).

! ***Deep water***

When compared with the data collected in order to understand the physical oceanographic characteristics of the AW and the LIW, knowledge about the deep waters of the Basin is comparatively poor. The Adriatic and the South Aegean Sea have been suggested as source areas (Pollak, 1951). The deep waters of the Basin are characterized by a temperature of 13.6EC and a salinity of 38.7 ‰ with little variation below 1,500 m.

2.3 General circulation

The cyclonic Rhodes gyre is a well known persistent feature covering a large area centred upon the Rhodes Basin, which is of importance for this study due to a constant upwelling process within the gyre. The dissolved nutrients also show similar variability depending on the regional circulation described previously. In general, two different vertical structures can be identified, which are associated with the location of selected stations to be present either at cyclonic or anticyclonic gyres (Figs. 3 and 4).

The stations which are located at the cyclonic gyres as shown in Fig.3 have uniform densities below the thin surface-mixed layer. The temperature and salinity of the thin surface-mixed layer decrease from 14.5-15.0EC and 38.85-39.00 ppt salinity to their representative values of deep water masses of 13.6EC and 38.7 ppt, with no local increase in the salinity to indicate the LIW. The dissolved nutrient concentrations, however, remain at nearly zero level down to a depth of 100 metres.

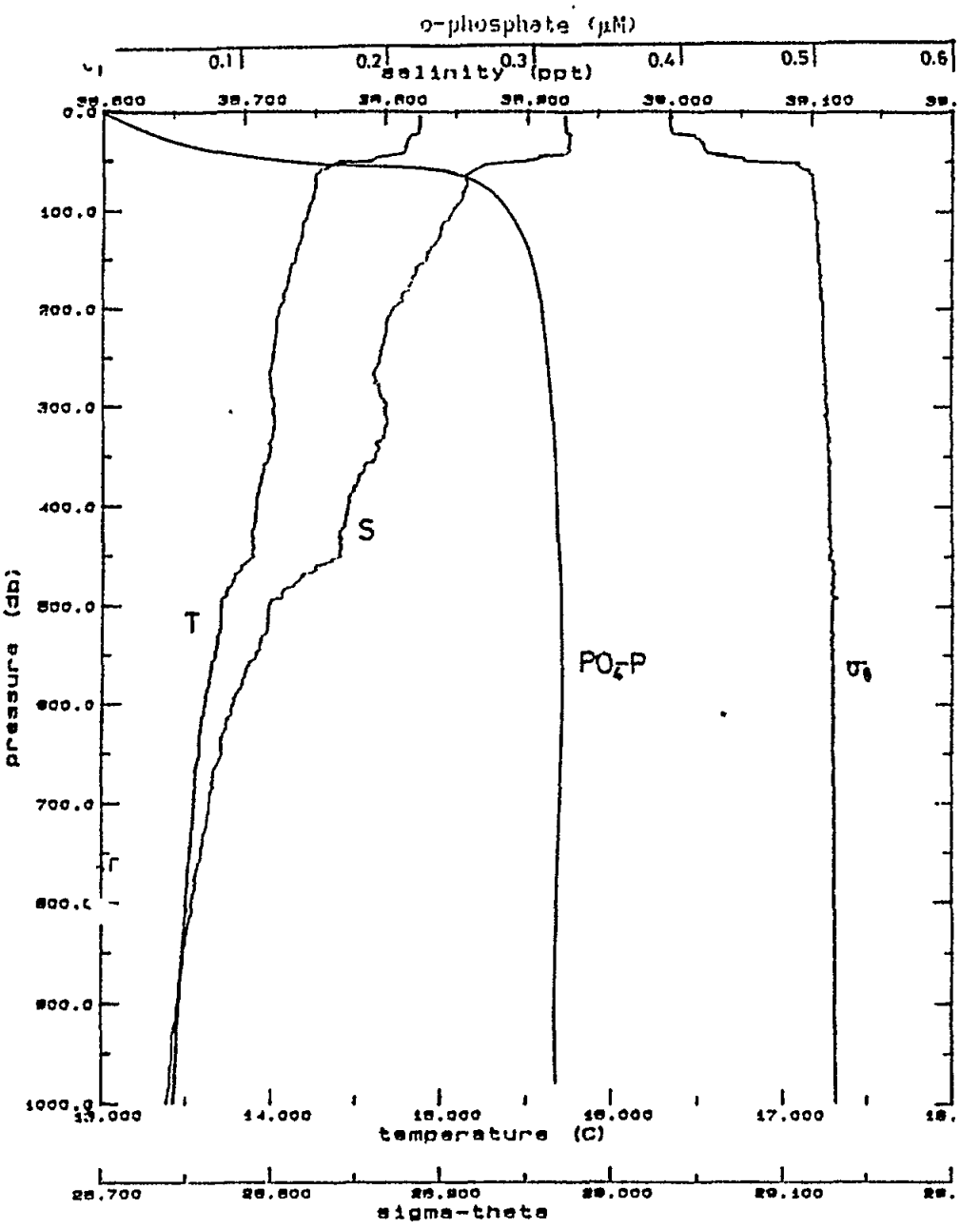

Fig.3 Vertical variation of temperature (T), Salinity (S), Sigma-theta (σ_θ), and o-PO_4 at station FOOK30 located in upwelling region - March, 1989

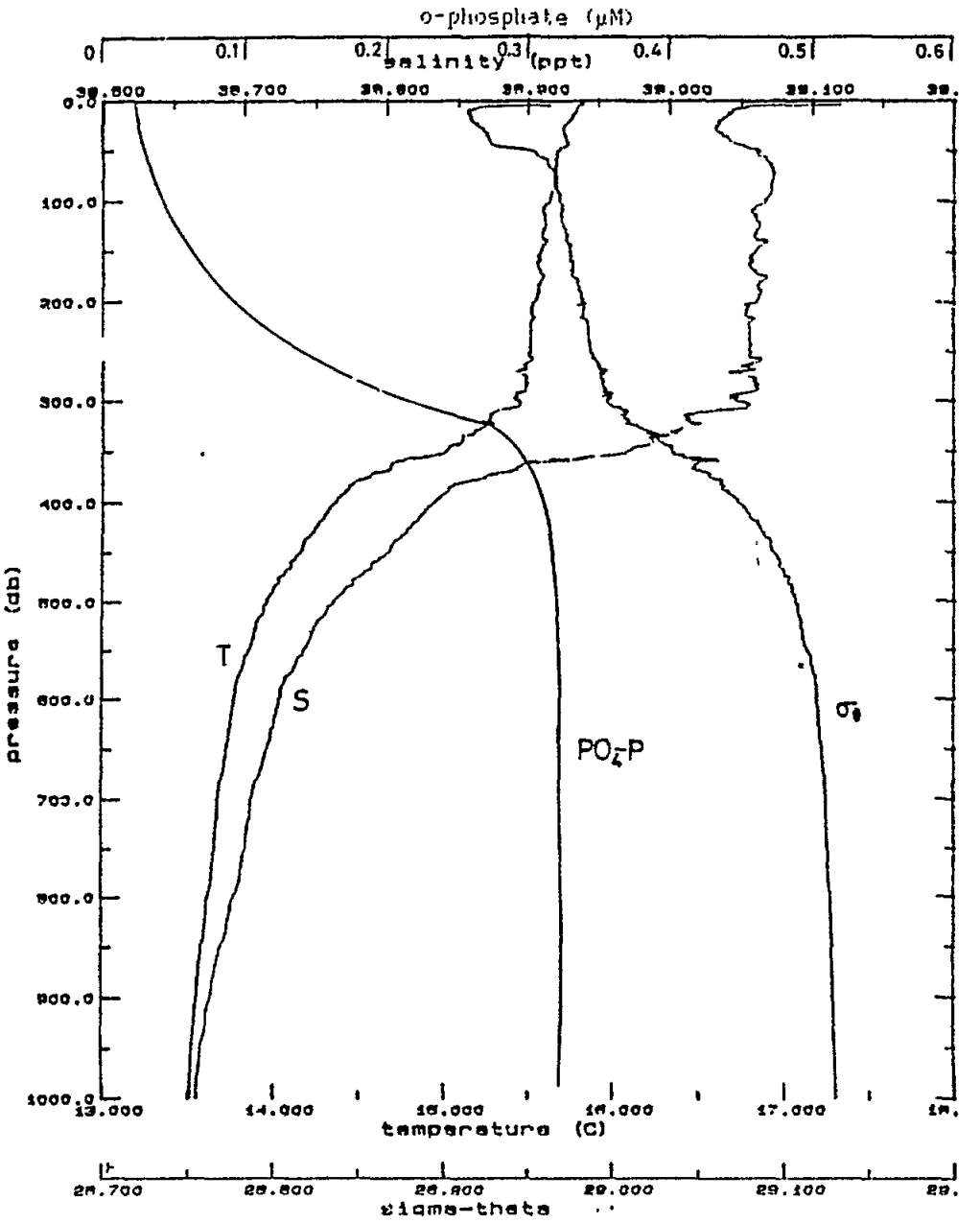

Fig.4 Vertical variation of temperature (T), Salinity (S), Sigma-theta (σ_θ), and o-PO_4 at station G10N30 located in downwelling region - March, 1989

Salihoglu *et al.* (1990) showed that the maximum *Chl-a* concentrations was found around a depth of 100 m. Therefore the biological activity in the NLW is effective down to this depth level. It is well known that biological activity strips out the water column from its nutrient components, hence the near zero levels of nutrient salts at the upper 100 metres is explained within the instrumental detection limits.

Below the photic zone, the dissolved nutrient concentrations gradually increase down to a depth of 400-500 metres and below 500 metres the levels remain nearly constant. The characteristic nutrient levels below 500 m depth for PO_4 are around 0.3 µM, for NO_3 are 6 µM and for silicates 8-10 µM. The increase in the concentrations of nitrates and phosphates is much more pronounced than that for silicates.

The vertical profiles given in Fig.4, however, exhibit a significant difference from the above situation. The striking feature of the temperature salinity density and dissolved nutrient profiles is the presence of a two-layer structure. The surface layer with 39.0-39.1 ppt salinity, 15.5-16.0°C temperature 28.95-29.0 sigma-τ and almost near zero level nutrient concentrations extend down to 300-400 metres. This layer is then separated from the deeper levels by a well-defined interfacial transition zone having a thickness of 100-200 m. Below this zone the dissolved nutrient levels increase sharply to their respective maximum concentrations observed at this part of the northern Levantine Sea.

Another interesting point which has been indicated by Ozsoy *et al.* (1989), is the horizontal distribution of depth of 5 ml/l oxygen as a typical indication of surface water saturated with atmospheric oxygen (Fig.5).

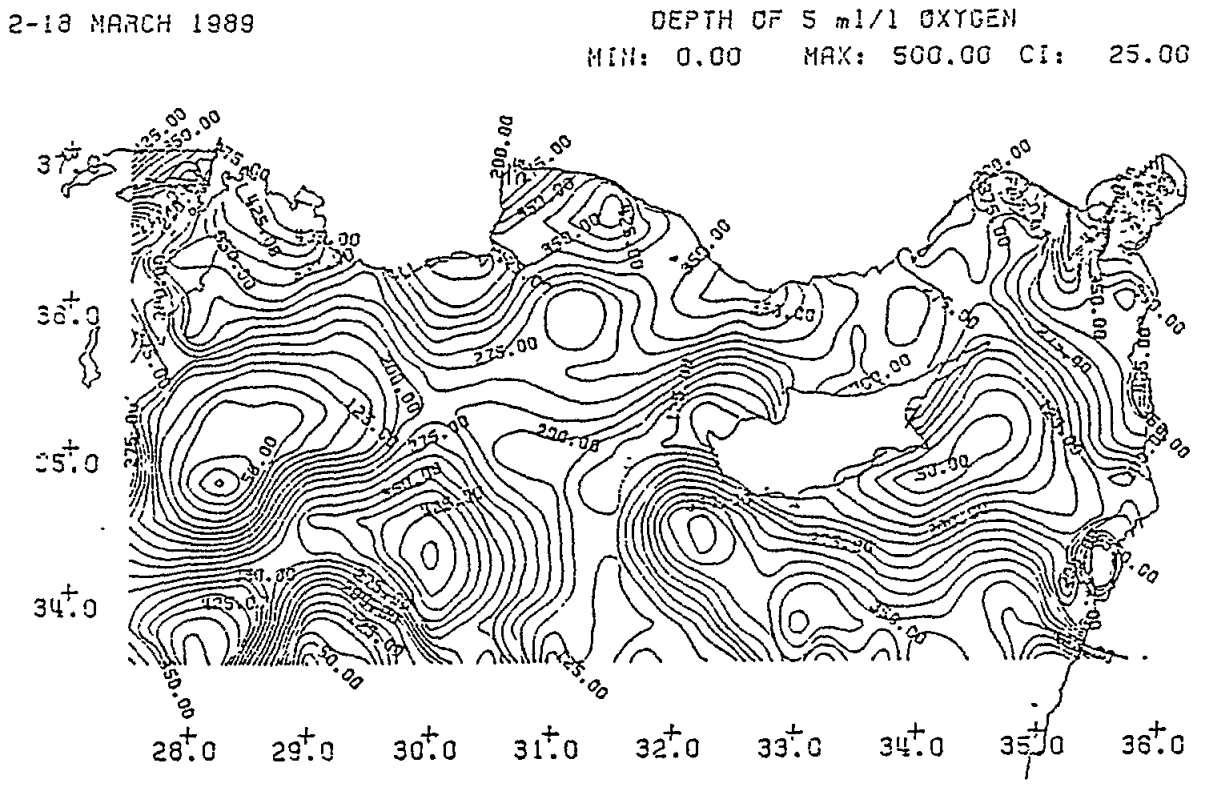

Fig.5 The distribution of the depth of 5ml/l oxygen along the NE Levantine Basin

In the cyclonic regions, the depth of 5 ml/l oxygen is within a 50 metre depth range as observed at 35EN, 28E30'E and 35EN, 34E30'E, whereas, in the anticyclonic regions the depth of 5 ml/l oxygen reaches down to a depth of 300-450 m, which implies a good ventilation of the region. The absence of nutrients in these regions clearly shows that the convective transport of LIW cannot be the source of nutrients for the deep water of the Eastern Mediterranean Sea.

This immediately brought up the question of the source of the nutrients present in the deep layers of the Eastern Mediterranean. If the formation of LIW cannot supply the nutrient loss due to upwelling at the cyclonic gyres, there must be some other source for the feedback of the nutrients in the deep layers. It is worth mentioning here that a large nutrient source should not be looked for as a source of nutrients, since the Mediterranean Sea is known to be the most impoverished large body of water in the world in terms of its nutrient concentrations. Riverine input cannot be expected to supply such concentrations alone, which leaves the atmospheric input of nutrients as the sole input source for the Eastern Mediterranean Sea. Loye-Pilot *et al.* (1989) has also stressed the importance of the Saharan dust input as a major source of detritus material to the open sea or at least in the same range as land-based sources, which also include direct sewage discharges to the sea. Martin *et al.* (1989) has also concluded that total N would be equally supplied by rivers and the atmosphere in the Western Mediterranean.

3. ATMOSPHERIC PARTICULATE SAMPLING

A 20 metre high atmospheric sampling tower has been constructed at the harbour jetty of IMS/METU (Fig.6), the geographic location of which is shown in Fig.1. The tower will incorporate an Aanderrea meteorological station to record atmospheric conditions (at present under repair in Norway). The location of the tower is by no means an ideal place for a collection tower but, because of logistics, the site proved to be a good choice. The collection tower is made of the skeletons of commercial containers welded on top of each other, and secured with steel wires to the harbour rocks. The tower is painted for better rust prevention. The top of the collection platform is made of plain wood, and the mesh is further raised from the platform by 3 metre wooden poles. During 1990 the atmospheric samples were collected with 300µ size mesh techniques. Two Sierra-Anderson type Sa23101051 hi-vol samplers, and one Sierra-Anderson hi-vol type SAUV-14H-1 cascade impactors equipped with flow controllers and pressure transducers for flow recording were ordered, together with one automatic APS acid precipitation collector. These instruments have arrived at the institute, and will be operational as from May 1991.

Since the beginning of 1990, atmospheric particulates were collected with mesh having a $1m^2$ area to the incoming wind in all directions. The collection periods, the associated dust loadings and the observed colour of the filters are tabulated in Table 1.

It is known that the mesh collects size-fractionated particulates but, when large particulates dominate the population, both high-vol and mesh samples are of the same material (Saydam, 1981).

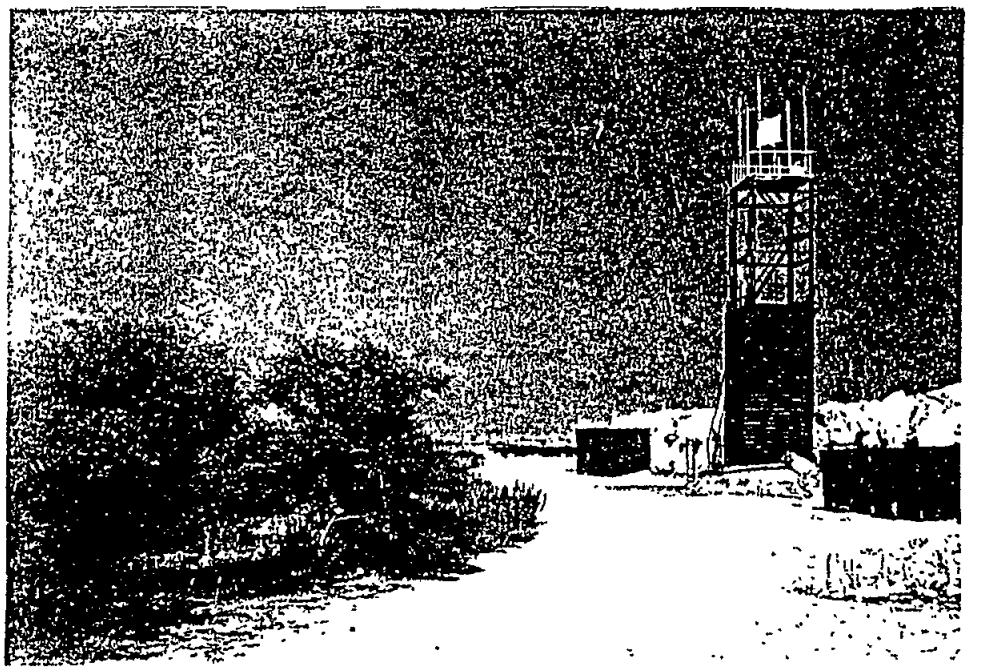

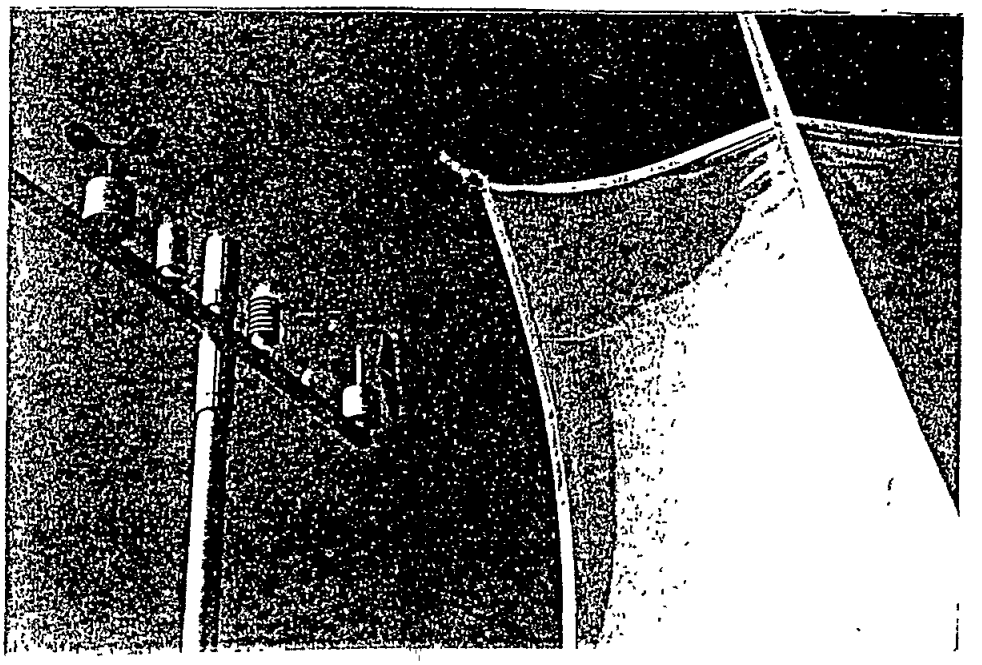

Fig.6 Atmospheric collection tower

Table 1

Atmospheric dust loadings, collection dates and colour of samples

Date of collection	g/day	Colour	Date of collection	g/day	Colour	Date of collecton	g/day	Colour
12-26/07/89	1.2	Light brown	16-20/04/90	0.9	Brown	10-14/08/90	0.8	Light brown
22-29/08/89	1.1	Brown	20-23/04/90	0.5	Light brown	14-17/08/90	1.0	Light brown
29/08-04/09/89	1.3	Dark brown	23-26/04/90	0.1	Light brown	17-23/08/90	1.1	Light brown
04-08/09/89	1.2	yellowish brown	26-30/04/90	0.2	Light brown	23-27/08/90	2.0	Light brown
04-12/01/90	0.2	Black	01-02/05/90	0.04	Black	27-31/08/90	1.1	Light brown
12-18/01/90	0.2	Black	02-07/05/90	0.3	Light brown	31/08-04/09/90	0.6	Light brown
18-22/01/90	1.6	Black	07-14/05/90	0.1	Black	04-05/09/90	0.7	Dark brown
22-26/01/90	2.1	Black	14-21/05/90	0.5	Brown	05-10/09/90	0.8	Light brown
26-31/01/90	1.7	Black	21-28/05/90	0.6	Light brown	10-12/09/90	0.6	Dark brown
31/01-02/02/90	9.1	Light black	28/05-04/06/90	2.4	Light brown	12-17/09/90	1.0	Light brown
02-06/02/90	0.4	Black	04-07/06/90	1.2	Brown	17-20/09/90	0.4	Light brown
06-09/02/90	10.1	Light black	07-11/06/90	0.7	Light brown	20-24/09/90	0.5	Light brown
09-15/02/90	0.3	Light black	11-15/06/90	0.5	Light brown	24-27/09/90	0.7	Light brown
15-20/02/90	0.2	Black	15-19/06/90	1.6	Light brown	27-29/09/90	0.6	Light brown
20-23/02/90	0.2	Black	20-25/06/90	0.4	Light brown	30/09-01/10/90	0.2	Dark brown
23-26/02/90	0.1	Black	25-29/06/90	0.5	Light brown	01-04/10/90	0.3	Light brown
26/02-02/03/90	0.1	Black	29/06-06/07/90	0.6	Light brown	04-08/10/90	0.2	Light brown
02-06/03/90	0.2	Black	06-11/07/90	0.5	Light brown	08-10/10/90	0.4	Light brown
06-20/03/90	0.2	Black	11-13/07/90	0.7	Light brown	10-12/10/90	0.5	Light brown
22-26/03/90	0.2	Brown	13-16/07/90	0.6	Brown	12-15/10/90	0.2	Yellowish brown
26-29/03/90	0.5	Brown	16-19/07/90	0.7	Light brown	15-16/10/90	1.5	Yellowish brown
29/03-02/04/90	0.3	Brown	19-21/07/90	0.6	Light brown	16-18/10/90	1.3	Yellowish brown
02-04/04/90	0.2	Brown	21-26/07/90	0.8	Light brown	18-22/10/90	1.7	Yellowish brown
04-06/04/90	0.3	Brown	26-29/07/90	0.9	Light brown	22-23/10/90	1.1	Yellowish brown
06-09/04/90	0.2	Brown	29/07-02/08/90	1.0	Light brown	23/10/90	0.4	Yellowish brown
09-11/04/90	0.2	Yellowish brown	02-07/08/90	0.8	Light brown	23-24/10/90	1.6	Light brown
12-16/04/90	1.2	Brown	07-10/08/90	0.9	Light brown	24-31/10/90	0.7	Brown

Table 1

(Continued)

Date of collection	g/day	Colour	Date of collection	g/day	Colour	Date of collecton	g/day	Colour
31/10-02/11/90	0.7	Black	19-23/11/90	1.1	Light brown	12-13/12/90	4.6	Light brown
02-05/11/90	0.3	Brown	23-26/11/90	1.2	Light brown	14-19/12/90	0.4	Light brown
05-07/11/90	0.3	Brown	26-28/11/90	0.6	Light brown	19-24/12/90	0.3	Light black
07-09/11/90	0.2	Brown	28-30/11/90	1.1	Light brown	24-28/12/90	0.5	Light brown
09-14/11/90	0.3	Light black	30/11-03/12/90	4.3	Light brown	28-31/12/90	1.2	Light black
14-16/11/90	0.6	Brown	03-10/12/90	0.3	Light black	31/12/90-02/01/91	0.3	Black
16-19/11/90	1.0	Brown	10-12/12/90	0.2	Light black			

4. ANALYTICAL PROCEDURES

The mesh collected (soil-sized) sample was washed from the mesh in redistilled water and sub-samples dissolved in HNO_3/HF mixture in PTFE beakers and stored in polystyrene bottles. The analysis of elements was performed by using Varian AA-6 AA equipped with deuterium background correction using the flame technique. BCR-142 light sandy soil was used to check the accuracy and the sensitivity of the digestion method (Saydam, 1981). The water soluble nutrient salts were analyzed, using a Technicon Autoanalyzer, for their soluble nutrients.

5. RESULTS AND DISCUSSION

5.1 Meteorological conditions

Because of the malfunctioning of the Aanderrea meteorological station, the meteorological conditions prevailing in the area during the 1990 collection period were recorded by a meteorological station at Alata. The frequencies of wind trajectories showed that the prevailing winds affecting the region have an evident SW and S origin (Fig.7).

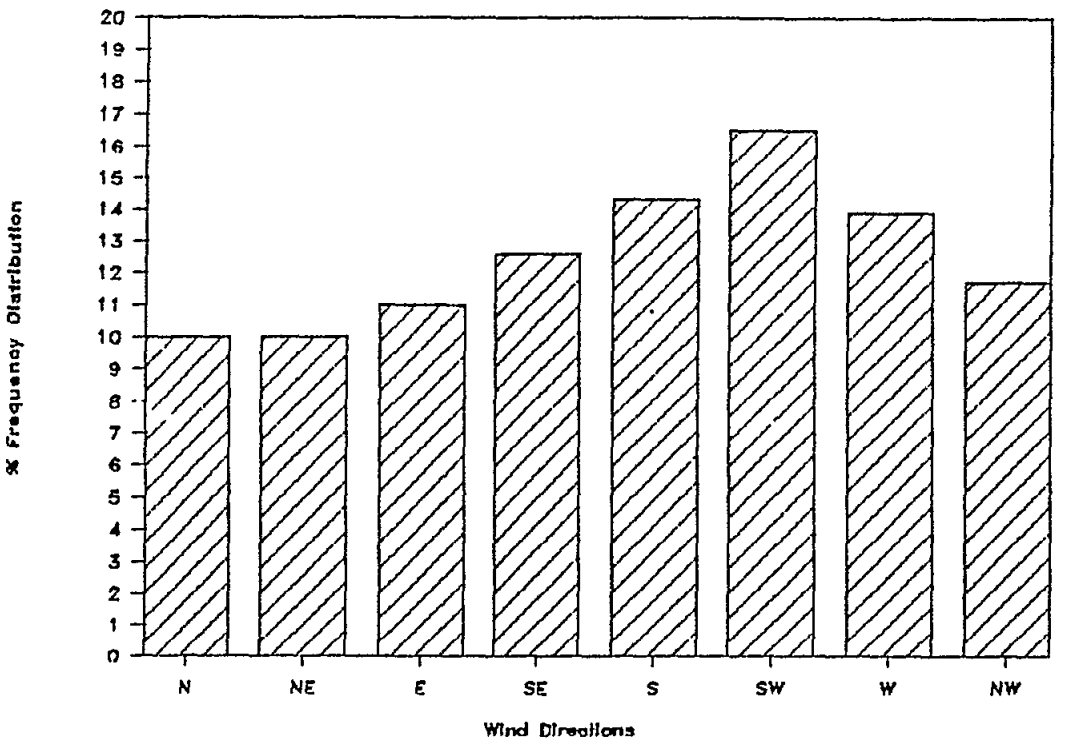

Fig.7 Frequency of wind trajectories observed at Alata Meteorological station

The frequencies of wind direction for each season are given in Fig.8. During the warm, dry season of the year, i.e. July-August-September, the wind was coming from the direction of the South-Southwest and West with a negligible or no contribution from the North and a negligible contribution of East winds. The January-February and March period (as shown in Fig.8), is mainly governed by the South and Southwest regimes with important North and Northwest components in it.

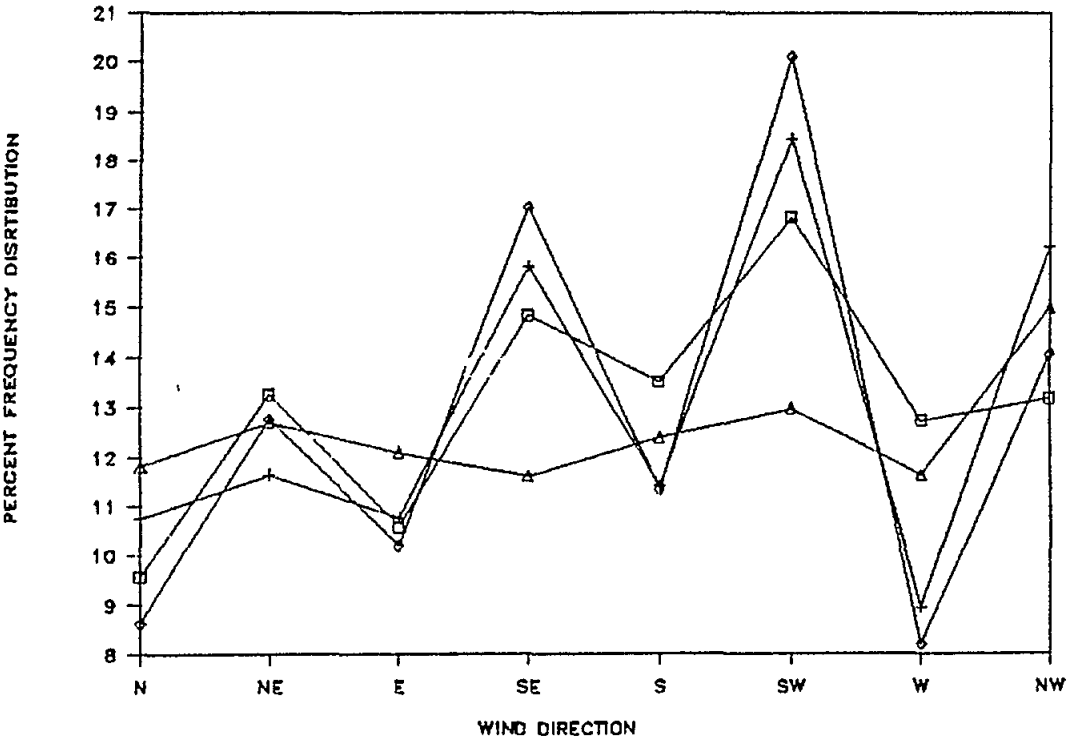

Fig.8 Frequency (%) of wind trajectories observed during Jan-Dec 1990

5.2 Dust loadings

The annual distribution of the dust loadings for the 1990 collection period is given in Fig.9. It can be seen that the variation at the dust loadings reaches a maximum during winter and late autumn. During the period March-June, the dust loading starts to build up and almost reaches the 1g/day level. It is interesting to note that during this period, the maximum wind speeds observed at Alata meteorological station gradually decreased to 5 m/s and there were no observations of storm events. September is the time of the year when the first strong winds are observed after long, calm, weather conditions, which is also the start of the decrease of the dust loadings from levels of 1g/day to 0.2 g/day until October. The period mid-October to January is associated with great fluctuations at the dust loadings, with episodes having dust loadings of 1.5 g/day and lasting for about a week. Dust loadings with levels greater than 3g/day, are associated with strong storm events and contain strong signs of sea spray which have affected the dust loadings. Although these events have not been taken into account, they are shown in Fig.10 for convenience. It can be seen that, out of 97 collections made during 1990, only four were affected by the sea-salt. This shows that the height of the collection tower is good enough to avoid the effect of the sea-spray.

The colour of the dust collected by the mesh technique is also given in Table 1. It can be seen that the dominant colour of the samples is black during the period January-April. During March-April the colour has turned to brown and to light-brown, which was the dominant colour of the atmospheric particulates from mid-June to November. From mid-November, the colour of the samples became darker and the black colour started to appear again.

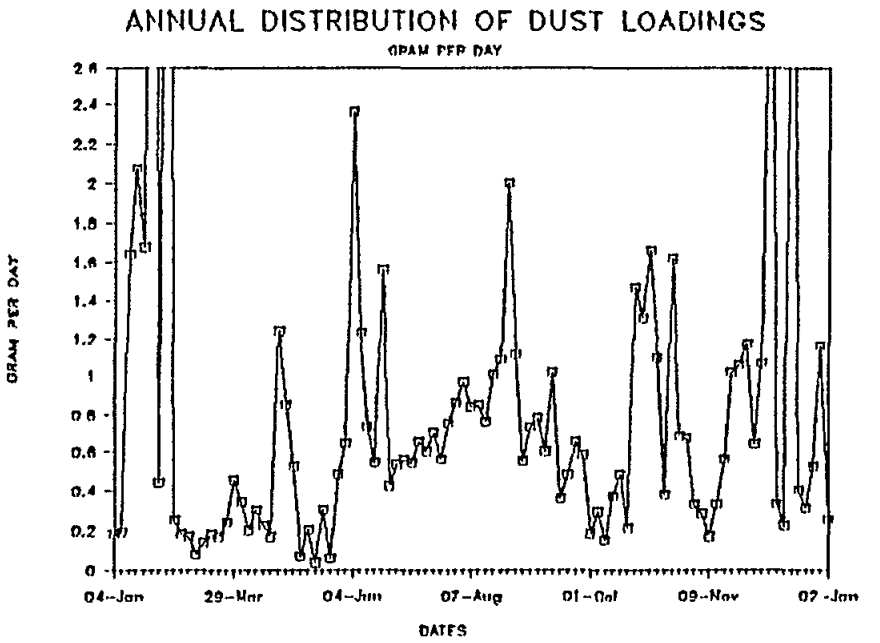

Fig.9 Annual distribution of dust loadings

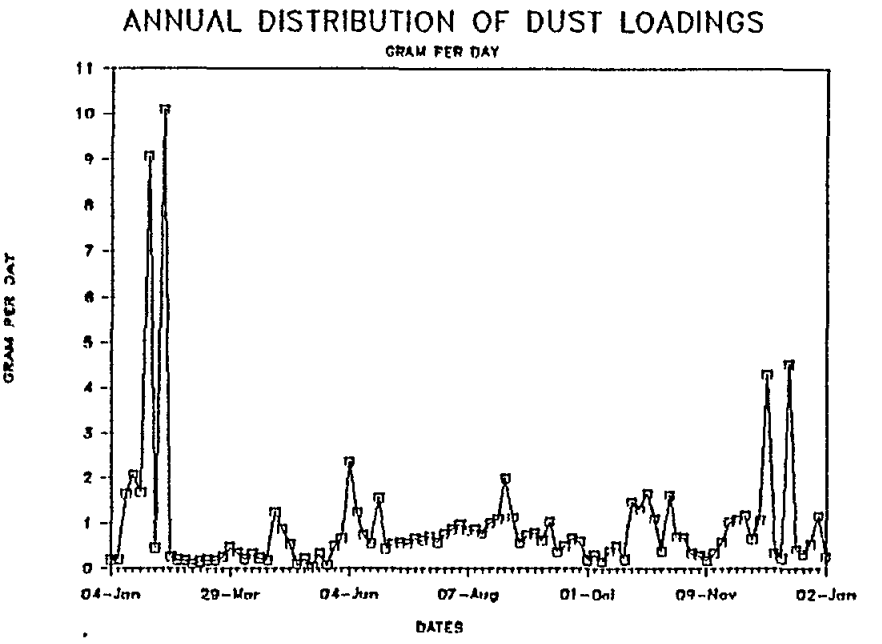

Fig.10 Annual distribution of dust loadings and the sea-salt spray

5.3 Annual distribution of nutrient salts in rainwater

The rainwater samples collected during the rainy periods were analyzed for their nutrient content and their pH's. The results of the analysis are shown in Fig.11. It can be seen that the nitrates in the rainwater were the most important nutrients detected. Loye-Pilot *et al.* (1989) reported that the concentrations of dissolved nitrogen compounds for polluted rain samples are greater than 25 $\mu mol.l^{-1}$ and the typical value is around 46.6. The observed N concentrations in the Northeastern Levantine are less than in the polluted samples, and are within the range of oceanic and Sahara-related samples. The two exceptionally high N concentrations which were observed can be classified as polluted, which must have been affected from local sources. The average pH of the rainwater was calculated as 6.8 and was within the range of the Sahara-related samples.

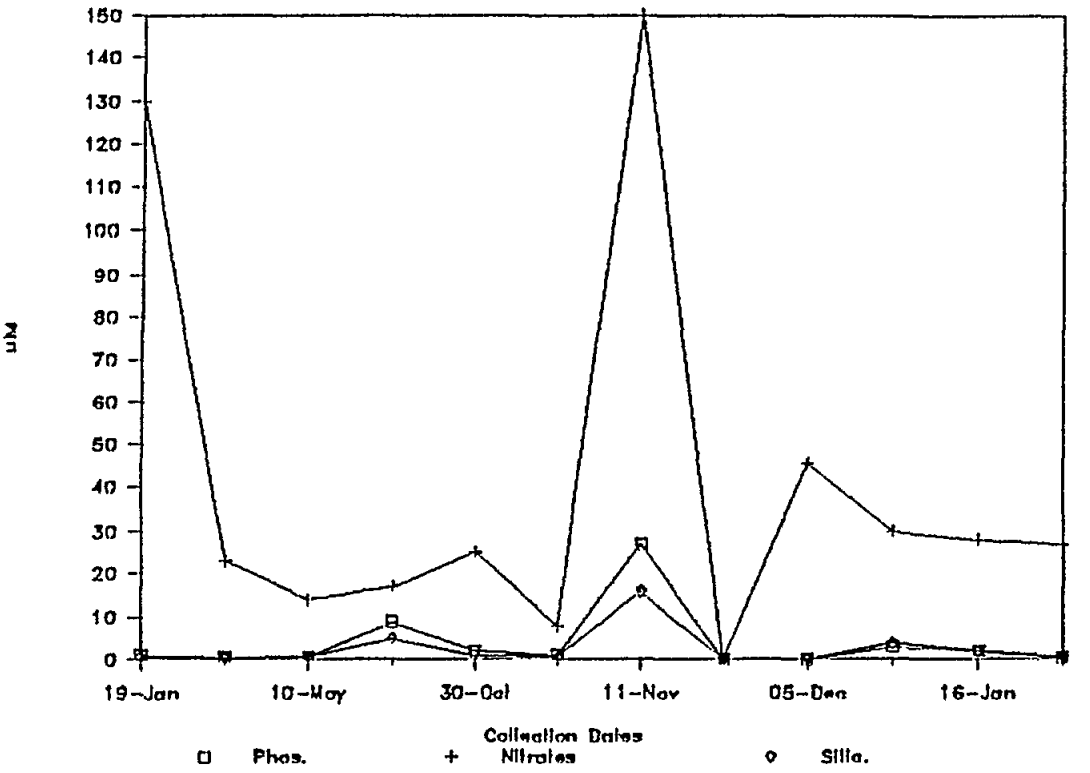

Fig.11 Nutrient salts in rainwater

5.4 Elemental composition of atmospheric particulates

To under certain characteristics of the Eastern Mediterranean airborne samples, the elements Al, Fe, Mn, Cr, Co, Ni, Cu, Pb, Zn and Cd were analyzed for samples collected during the period January 1 and August 15, 1990. The remainder of samples are still in the process of being analyzed. The result of the analyses of the elements are given in Table 2. An accepted way of characterizing the provenance of atmospheric particles is by the use of Crustal Enrichment Factors (Rahn *et al.*, 1979). For this study Al is used as a reference element. The EFs of Saharan and world aerosols as given by Rahn *et al.* (1979) are also shown in Table 3. In general the elements have been divided into three classes according to their EF values, i.e. enriched, intermediate and non-enriched. The boundaries between the classes have been chosen as >10, 10-2 and <2 respectively.

Table 2

The elemental concentrations of atmospheric particulates.
Al and Fe are in mg/g, others in µg/g

Date of collection	Al	Fe	Mn	Cr	Cu	Co	Ni	Zn	Pb	Cd
12-26/07/1989	32824	21554	542	181	40	10	92	185	64	0.59
22-29/08/1989	322248	20859	488	177	38	10	12	208108	9152	1.10
28/08-04/09-1989	18610	12126	269	116	28	6	78	118	65	0.63
04-08/09/1989	33423	17178	405	179	28	12	85	422	93	0.51
04-12/01/1990	12033	10181	243	212	30	8	81	573	181	0.95
12-18/01/1990	17067	16615	388	158	67	15	69	84	nd	2.65
19-22/01/1990	1738	1770	54	21	4	nd	26	31	13	0.11
22-26/01/1990	3957	2139	56	14	7	nd	22	137	117	0.11
26-31/01/1990	4751	5503	181	47	41	7	62	80	nd	0.76
31/01-02/02/1990	10070	3968	101	19	11	4	37	787	145	0.14
02-06/02/1990	18190	13880	310	136	67	nd	78	94	nd	1.22
06-09/02/1990	2174	2609	64	23	19	nd	24	22	nd	0.21
09-15/02/1990	2117	1471	45	15	6	nd	11	44	25	0.1
15-20/02/1990	3736	2877	87	34	12	4	31	66	46	0.57
20-23/02/1990	6854	6065	126	93	19	nd	47	237	90	0.79
23-26/02/1990	11025	9497	234	212	33	14	110	42	43	0.96
26/02-02/03/1990	3014	2295	69	67	12	nd	30	86	126	0.35
02-06/03/1990	5745	4669	175	219	13	nd	56	326	152	0.69
06-20/03/1990	11742	9777	271	171	39	nd	77	148	96	0.71
22-26/03/1990	27311	17313	497	206	35	9	112	283	143	0.48
26-29/03/1990	43297	25601	687	493	53	16	114	161	107	0.73
29/03-02/04/1990	24510	16401	402	417	34	15	73	151	87	0.99
02-04/04/1990	13756	9862	481	100	24	nd	58	53	71	1.63
04-06/04/1990	22538	14799	529	410	28	13	73	16	111	1.1
06-09/04/1990	22022	15759	292	73	28	12	78	47	70	0.97
09-11/04/1990	31312	18290	292	74	35	nd	104	42	13	0.53
12-16/04/1990	7949	5446	137	30	20	nd	30	51	50	0.07
16-20/04/1990	8761	6330	155	31	18	3	37	92	71	0.26
20-23/04/1990	19409	15873	248	78	30	8	78	76	98	0.60
23-26/04/1990	33845	23015	552	108	44	nd	91	90	115	0.28
26-28/04/1990	21769	14444	372	52	33	nd	82	nd		1.54
28-30/04/1990	11971	14019	317	18	nd	122	311			0.6

Table 2

(Continued)

Date of collection	Al	Fe	Mn	Cr	Cu	Co	Ni	Zn	Pb	Cd
01-02/05/1990	7468	6209	161	36	16	nd	56	80	41	0.73
02-07/05/1990	16619	10177	270	74	40	13	72	145	142	2.18
07-14/05/1990	25507	19110	486	210	47	10	94	251	215	0.42
14-21/05/1990	33701	22854	521	303	56	14	128	239	125	0.50
21-28/05/1990	28240	17674	391	155	28	9	86	148	61	0.72
28/05-04/06/1990	27561	20753	455	273	38	nd	108	114	92	0.28
04-07/06/1990	30636	24282	492	285	46	14	115	171	118	1.14
07-11/06/1990	34182	21370	588	122	45	7	91	117	65	0.25
11-15/06/1990	12650	10407	267	71	19	8	69	69	38	0.48
15-19/06/1990	24331	20358	368	288	39	10	121	197	208	1.52
20-25/06/1990	25458	21577	607	197	36	10	114	172	103	2.00
25-29/06/1990	32511	23808	513	320	42	13	117	167	140	0.26
29/06-06/07/1990	39834	26822	631	143	56	24	109	183	116	0.56
06-11/07/1990	23873	14247	359	75	26	10	61	139	50	0.40
11-13/07/1990	31468	19227	483	98	40	10	77	215	80	0.76
13-16/07/1990	37826	26473	701	175	39	21	111	242	76	0.37
16-19/07/1990	29702	25385	583	199	38	16	101	205	100	0.82
19-21/07/1990	41156	25580	692	99	40	9	92	315	87	0.44
21-26/07/1990	35615	22663	599	129	32	15	88	116	62	0.51
26-29/07/1990	25397	19428	512	154	30	9	87	114	79	1.49
29/07-02/08/1990	40901	26140	579	274	38	15	99	146	92	0.65
02-07/08/1990	33508	21164	456	136	28	8	72	96	69	0.41
07-10/08/1990	31944	21722	558	162	39	11	87	133	81	1.01
10-14/08/1990	38618	23240	529	199	39	9	95	143	65	0.54
14-17/08/1990	68701	43874	1403	247	165	20	113	825	370	1.57
17-23/08/1990	30561	19792	431	97	23	9	81	66	33	0.83

Table 3

The enrichment factors of atmospheric particles

Date of collection	Fe	Mn	Cr	Cu	Co	Ni	Zn	Pb	Cd
12-26/07/1989	1	1	5	2	1	3	6	13	14
27-29/08/1989	1	1	4	2	1	8	8	19	14
29/08-04/09-1989	1	1	5	2	1	5	7	19	6
04-08/09/1989	1	1	4	1	1	3	4	13	32
04-12/01/1990	1	2	14	4	2	7	41	52	63
12-18/01/1990	1	2	8	6	3	4	39	71	26
18-22/01/1990	1	3	10	3		16	57		12
22-26/01/1990	1	1	3	3		6	9	22	65
26-31/01/1990	2	3	8	13	5	14	34	164	6
31/01-02/02/1990	1	1	2	2	1	4	9		27
02-06/02/1990	1	1	6	5		5	51	53	39
06-09/02/1990	2	2	9	13		12	51		19
09-15/02/1990	1	2	6	4		6	12		62
15-20/02/1990	1	2	7	5	4	9	14	45	47
20-23/02/1990	1	2	11	4		8	11	45	35
23-26/02/1990	1	2	16	4	4	11	25	54	47
26/02-02/03/1990	1	2	18	6		11	16	95	48
02-06/03/1990	1	3	31	3		11	18	146	25
06-20/03/1990	1	2	12	5		7	33	86	7
22-26/03/1990	1	2	6	2	1	5	6	23	7
26-29/03/1990	1	1	9	2	1	3	8	22	16
29/03-02/04/1990	1	1	14	2	2	3	8	29	48
02-04/04/1990	1	3	6	3		5	13	32	20
04-06/04/1990	1	2	15	2	2	4	3	21	18
06-09/04/1990	1	1	3	2	2	4	1	34	7
09-11/04/1990	1	1	2	2		4	2	15	4
12-16/04/1990	1	1	3	4		4	6	11	12
16-20/04/1990	1	1	3	3	1	5	7	38	13
20-23/04/1990	1	1	3	2	1	4	6	24	3
23-26/04/1990	1	1	3	2		3	3	19	29
26-30/04/1990	1	1	2	2		4	5	35	20

Table 3

(Continued)

Date of collection	Fe	Mn	Cr	Cu	Co	Ni	Zn	Pb	Cd
01-02/05/1990	2	2		2		11	30	36	39
02-07/05/1990	1	2	4	3		8	12	57	53
07-14/05/1990	1	1	4	4	3	5	10	30	7
14-21/05/1990	1	2	7	3	1	4	12	25	6
21-28/05/1990	1	1	7	3	1	4	8	14	10
28/05-04/06/1990	1	1	8	2		4	5	22	4
04-07/06/1990	1	1	8	2	2	4	7	26	15
07-11/06/1990	1	1	3	2	1	3	4	13	3
11-15/06/1990	1	2	5	2	2	6	6	20	15
15-19/06/1990	1	1	10	2	1	5	10	57	25
20-25/06/1990	1	2	6	2	1	5	8	27	32
25-29/06/1990	1	1	8	2	1	4	6	29	3
29/06-06/07/1990	1	1	3	2	2	3	5	19	6
06-11/07/1990	1	1	3	2	1	3	7	14	7
11-13/07/1990	1	1	3	2	1	3	8	17	10
13-16/07/1990	1	2	4	2	2	3	8	13	4
16-19/07/1990	1	2	5	2	2	4	8	22	11
19-21/07/1990	1	1	2	1	1	3	9	14	4
21-26/07/1990	1	1	3	1	1	3	4	12	6
26-29/07/1990	1	2	5	2	1	4	5	21	23
29/07-02/08/1990	1	1	6	1	1	3	4	15	7
02-07/08/1990	1	1	3	1	1	2	3	14	5
07-10/08/1990	1	1	4	2	1	3	5	17	13
10-14/08/1990	1	1	3	2	1	3	4	11	6
14-17/08/1990	1	2	3	4	1	2	14	36	9
17-23/08/1990	1	1	2	1	1	3	3	7	11

It can be seen that elements like Fe, Mn, Co and Cu definitely fall into the non-enriched category as shown in Figs.12 and 13 respectively. Elements like Cr and Ni (Fig.14) exhibit large variations during the period January-April 1990, and their EFs fluctuate around 10. From the beginning of April, the EFs of Cr and Ni fall below 10 and a steady decrease was observed till August 15.

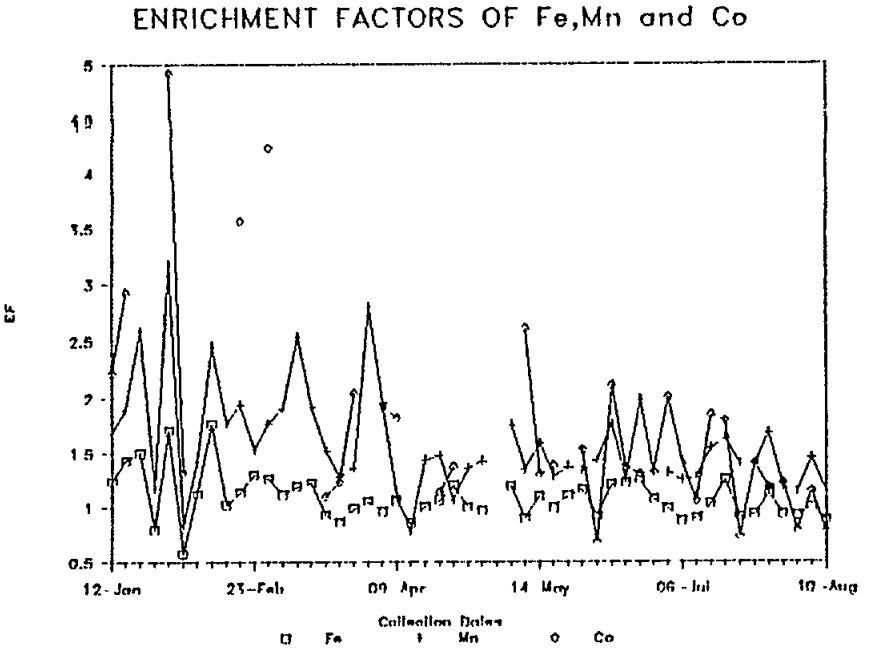

Fig.12 EFs of Fe, Mn and Co

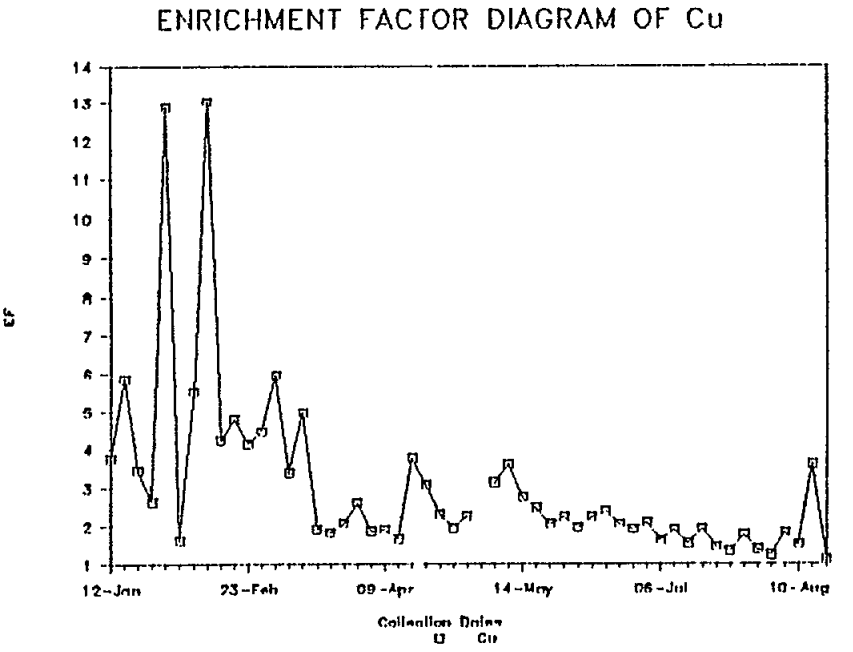

Fig.13 EFs of Cu

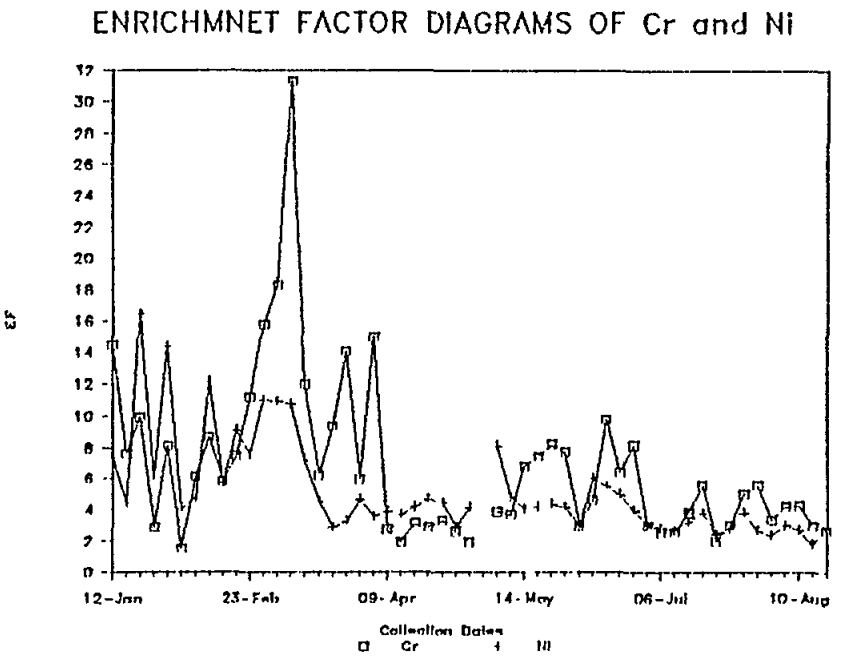

Fig.14 EFs of Cr and Ni

The same picture is also observed for Zn as shown in Fig.15. During the winter period the observed EFs were all above 10. From mid-march the EFs decreased sharply and continued like this until August 15.

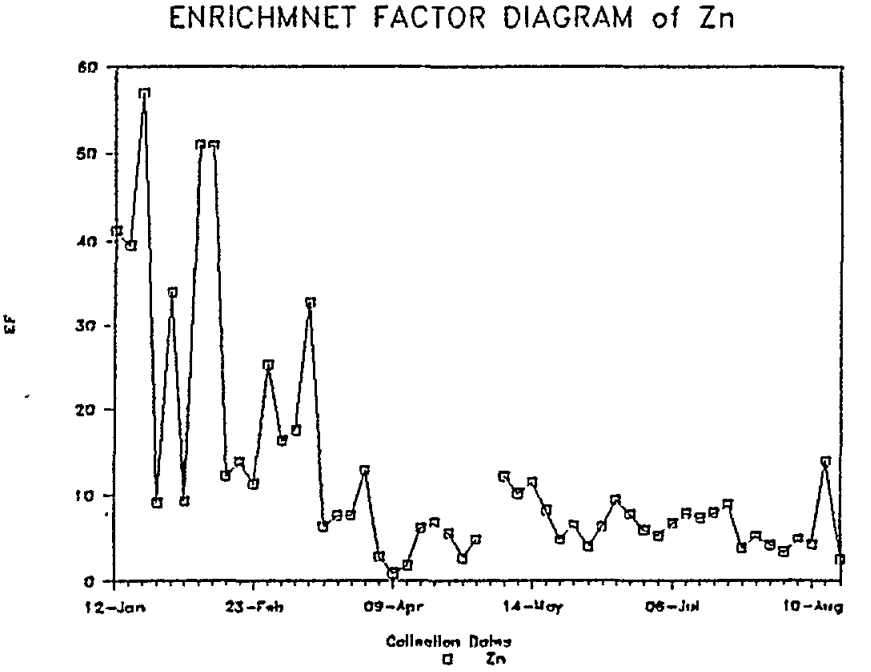

Fig.15 EFs of Zn

The EF diagrams for Pb and Cd are shown in Fig.16. It can be seen that the EFs of both of these elements have great similarities, indicating a common origin.

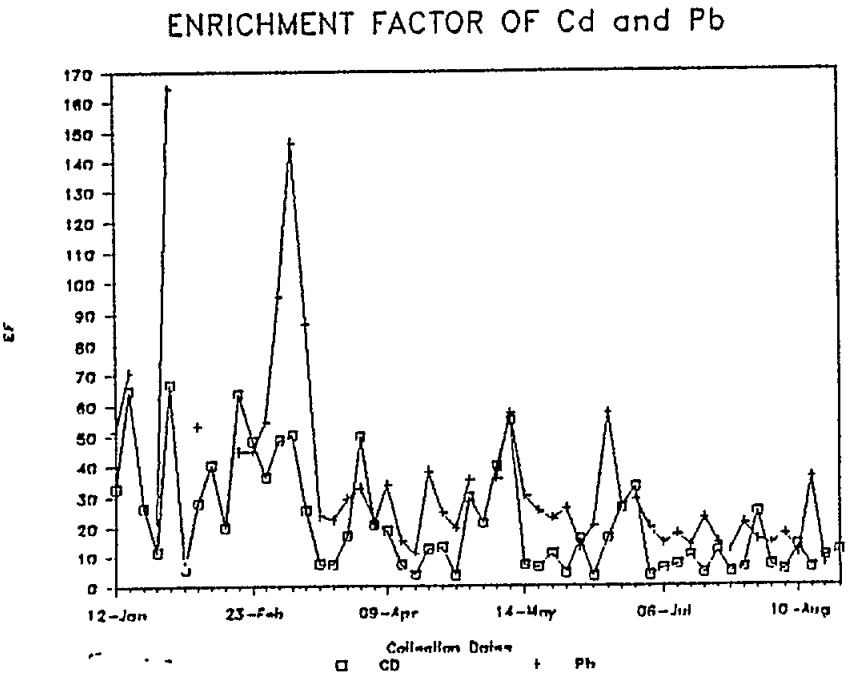

Fig.16 EFs of Cd and Pb

It can be concluded from the initial results of the 1990 collections, that the northern Levantine Basin is mainly affected by the Saharan crust-dominated component. The effect of the Saharan input is much more pronounced during spring and autumn whereas the European urban dominated component has its fingerprints on the region during winter and late autumn.

5.5. Pollution from the Gulf

The latest environmental pollution, which resulted from the burning of the crude oil wells at Kuwait, was also recorded by the remote sensing facilities existing at the IMS. The typical IR picture of the episode for 13 and 16 February 1991 respectively, can be seen in Figs.17 and 18.

On 13 February 1991 the burning fields were not as extensive as recorded on 16 February 1991. This picture can still be observed by the IR pictures taken from the NOAA satellites. The IR pictures obtained from the NOAA satellites and the visual pictures taken from the METEOR satellites, show that the prevailing winds in that area clearly transported the smoke towards the Persian Gulf. This must have increased the already petroleum-loaded system with even more debris coming from the atmospheric fallout.

During the period 3-4 March 1991, black rainfall was recorded in the southeast of Turkey. The atmospheric conditions prevailing at higher levels were the cause of the westerly transport of this oil smoke towards Turkey (Adana Meteorological Office, Personal. comm.

1991). The thunder showers recorded during this period at the southern coast of Turkey, caused the precipitation of the smoke as black rain at some specific parts of the region. The samples taken from Adana and Yumurtalik close to the Bay of Iskenderun were all black in colour, but these events were not recorded anywhere else and certainly not at the atmospheric collection tower at Erdemli. This proves that the event was confined to a small part of the region.

Fig.17 The IR picture of the burning Kuwait oilfield at 13 February 1991

Fig.18 The IR picture of the burning Kuwait oilfield at 16 February 1991

The odours emanating from the rainwater were typical of gasoline. The GC chromatography of the rainwater and Kuwait crude oil was extracted with hexane and analyzed with a capillary column coated with SE-54. The chromatograms of the extracts are shown in Fig.19. The low-chain hydrocarbons were not observed in the rain sample, indicating the loss of these low-chain hydrocarbons during burning and/or during the transport process. However, the important point is that the extent of the catastrophe has already started to affect the environment and, in the near future, the global effects might be traced to even larger distances due to wind transport at high elevations.

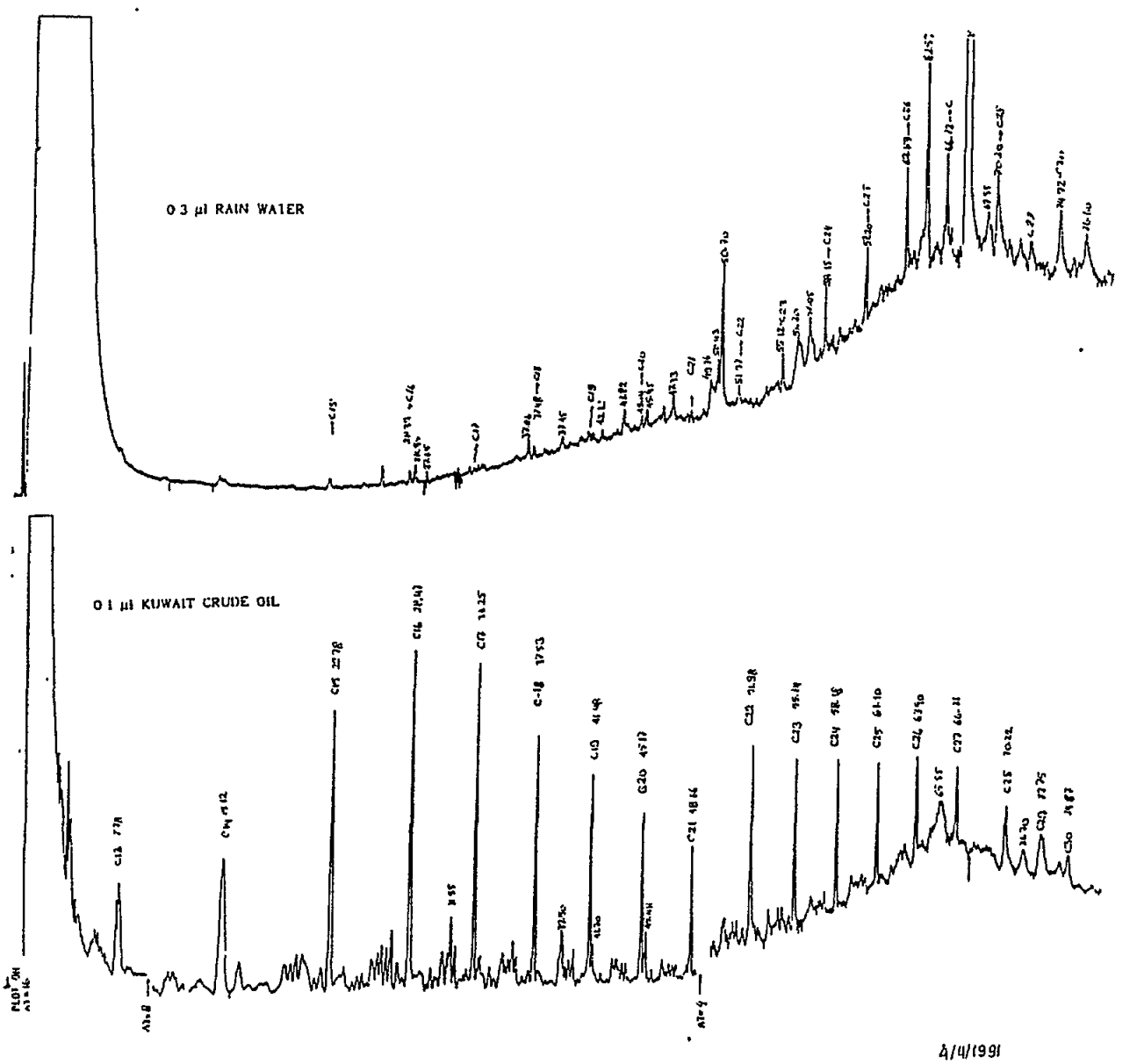

Fig.19 The gas chromatograms of Kuwait crude oil and rainwater samples

6. CONCLUSION

During 1990, the main objectives of the atmospheric dust collection programme were greatly achieved. It was observed that the region is mainly affected by the crustal component. Therefore, as pointed out by Rahn *et al.*, 1979, it would be more realistic to use the local crustal composition. Thus, through continuation of the collection programme, it would be possible to construct a Turkish Background Reference Standard for settling particles. This will enable us to pinpoint the anthropogenically contaminated samples using the EF method.

7. REFERENCES

Karein, A.A. (1977). Coastally trapped waves in the atmosphere. *Quart.J.R.Met.Soc.,* 103:431-440.

La Violette, P. (1987). Portion of Western Mediterranean circulation experiment EOS. *Trans. Amer. Geophys. Union*, 68(9):123-124.

Loye-Pilot, M.D., J.M. Martin and J. Morelli (1989). Atmospheric input of particulate matter and inorganic nitrogen to the northwestern Mediterranean. *Water Pollution Research Reports, EROS 2000*, Eds. J.M. Martin and H. Barth, pp.453.

Martin, J.M., F. Elbaz-Poulichet, M.D. Guieu, M.D. Loye-Pilot and G. Han (1989). *Water Pollution Research Reports, EROS 2000*, Eds. J.M. Martin and H. Barth, pp.453.

Mediterranean Pilot (1976). Volume 5, Hydrographer of the Navy, England.

Oguz, T., M. Abdul Latif, E. Ozsoy and U. Unljata (1989). The intermediate water formation in the warm core eddies of the Northern Levantine Basin of the Eastern Mediterranean Sea. Submitted to JPO, 1990.

Ozsoy, E. (1981). On the atmospheric factors affecting the Levantine Sea. European Centre for Medium Range Weather Forecasts. Technical Report No.25, 29pp.

Ozsoy, E., A. Hecth and U. Unljata (1989). Circulation and hydrography of the Levantine Basin. Results of POEM coordinated experiments 1985-1986. *Prog. Oceanog.*, 22:125-170.

Pollak, M.J. (1951). The source of the deep water of the Eastern Mediterranean Sea. *J. Marine Res*., V.10, 1:128-152.

Rahn, K.A. (1976). The chemical composition of the atmospheric aerosol. Technical Report, University of Rhode Island, Kingston.

Reiter, E.R. (1975). Handbook for forecasters in the Mediterranean weather phenomena of the Mediterranean Basin, Part 1: General description of meteorological processes, environmental prediction research facility, Naval Postgraduate School, Monterey, California. Technical Paper No.5-75, 344pp.

Salihoglu, I., C. Saydam, O. Basturk, A. Yilmaz, D. Gocmen, E. Hatipoglu and A. Yilmaz (1990). Transport and distribution of nutrients and chlorophyl-*a* by mesoscale eddies in the northerneastern Mediterranean. *Marine Chemistry*, 29:375-390.

Saydam, C. (1981). The elemental chemistry of the Eastern Mediterranean atmospheric particulates. Ph.D. Thesis, University of Liverpool, Faculty of Science, Department of Oceanography.

Unljata, U. (1986). A review of the physical oceanography of the Levantine and the Aegean basins of the Eastern Mediterranean in relation to monitoring and control of pollution. Institute of Marine Science, Middle East Technical University, Erdemli-Icel, Turkey. 55pp.

ON THE USE OF LONG-RANGE TRAJECTORIES TO EVALUATE THE ATMOSPHERIC TRANSPORT AND DEPOSITION OVER THE NORTHWESTERN MEDITERRANEAN

By

M. ALARCON and A. CRUZADO

Centre d'Estudis Avançats de Blanes (CEAB)
Cami de Santa Bàrbara
17300 Blanes, Spain

1. INTRODUCTION

Photosynthetic organisms in the marine environment depend for their development on the availability of light and nutrients. Light is plentiful in the surface layer down to depths which vary depending on the solar radiation (seasonally changing), the density of the phytoplankton population itself, and the turbidity caused by other. Nutrients are made available to the surface phytoplankton by various mechanisms: vertical mixing, continental runoff, *in situ* biological regeneration and atmospheric deposition.

Among the various nutrients (nitrate, nitrite, ammonia, silicate, phosphate), those which seem to have a greater atmospheric component are the nitrogen compounds generated by anthropogenic as well as natural processes. Among the latter, lighting, combustions, and excretion by marine and terrestrial organisms may be considered to be the most important ones. Among the anthropogenic processes, fuel combustion and the use of fertilizers are probably the most important.

Atmospheric nutrient inputs to the marine environment are carried out with dry and wet deposition. Dry deposition is produced when aerosol particles fall over the sea surface of when the air above the sea comes in contact with the surface water. Wet deposition takes place when rain droplets containing particles trapped, or dissolved gaseous components fall onto the sea.

Monitoring of the atmospheric aerosol by filtration or by other techniques is used to assess the concentrations of particular matter contained in the air masses, as well as its size distribution and composition. This technique has also been used to identify the sources (natural or anthropogenic) where the air masses come from.

These measurements provide a good basis for the evaluation of the amount of substances contained in the atmospheric aerosol over coastal areas, but measurements practically do not exist for open sea areas.

A first approximation of the dry deposition over marine areas can be done through the application of combined air-mass trajectory and diffusion-deposition models.

In general, air masses get their nutrient loads at the atmospheric boundary layer or when convection brings air from the lower troposphere into the upper troposphere. Most of the sources being located on land rather than at sea, there is a vertical gradient of particle and

reversed over the sea. As an air mass moves from land to sea, it stops getting new nutrient emissions while, through deposition, it continues to lose particles and nutrient concentrations must certainly decay. The rate of decay of the nutrient concentrations with distance from the coast, depends on the residence time of the air mass over the sea. As a consequence, air masses over the oceans, particularly the Pacific Ocean, see their particle and nutrient levels reduced to what is considered as background.

Computation of air parcel trajectories is a very powerful tool to estimate the long-range transport of substances when combined with diffusion-deposition models, thus providing an estimate of the fluxes over the sea of substances of particular interest, such as nutrients.

2. METHODS

2.1 Sampling and analysis

Sampling by filtration of the atmospheric aerosol with high volume samplers located on the roof of the Centre d'Estudis Avançats de Blanes (CEAB) has been used to quantify their particle contents. Total particulate matter retained by the filters was determined by the weight gain after pumping air through them for 24 hours. Parts of the filters were soaked with distilled water for 24 hours, and dissolved nutrient concentrations (nitrate, nitrite, ammonia, phosphate and silicate) were determined, after dilution, by usual autoanalyzer techniques.

2.2 Trajectory models

- **ARL Model**

The ARL model developed by Heffter *et al.* (1975) has been used here to compute long-distance trajectories. It is a purely kinematic model which computes the air mass backward or forward trajectories on the basis of wind-field data. The model inputs are latitude-longitude data grids (2.5 degrees) of wind analyses, every 12 hours, at several standard pressure levels.

Trajectories are computed by three-hour segments through an averaged wind in a layer (50m to 4,000m) from the winds linearly weighted according to the height:

$$V_i = \frac{\Sigma_j (H_j \, . \, V_j)}{\Sigma_j H_j} \qquad \text{(Equation 1)}$$

To compute the wind value at the segment origin, a bilinear interpolation is made between the four grid points containing that origin. Eight three-hour segments are needed to compute a one-day trajectory.

$$TS = V.\Delta t \qquad \text{(Equation 2)}$$

Where TS is the trajectory segment Δt is the time interval, and V is the interpolated wind velocity at the segment origin.

The duration of the trajectories has been limited to 5 days since the trajectories are interpreted individually, and there is a loss of reliability beyond thee or four days.

- **Isentropic model**

Due to the large numbers of meteorological data and to the calculations required for the simulation of atmospheric trajectories, the purely kinematic models for horizontal trajectory computation are very useful and easy to apply, as they only need some easily measurable or derived meteorological variables, and require relatively little computational time. For these reasons they are much used, particularly for long-range trajectory computation.

However, because of their poor representation of the tridimensional motion, they cannot be applied to meteorological situations with strong convection, proximity of fronts, across orographic barriers, or when some mesoscale phenomena need to be considered.

The best representation of tridimensional air-mass motion would be the simulation by wet adiabatic trajectories. Since the stratified nature of the humidity fields required is seldom given by current analysis methods, a good approximation to tridimensional transport is computation by dry adiabatic (isentropic) trajectories. This method, however, underestimates the vertical motion by neglecting the diabatic processes.

An isentropic model has been developed and its output has been compared with the trajectories obtained from the ARL model.

Trajectories are computed forward or backward in time from their origin, at a convenient height above the ground to simulate the transport of pollutants. A trajectory is integrated by 12-hour segments further divided in time steps (e.g. with a time increment of 900 s, 48 time steps are required to integrate a 12-hour segment).

The input data are fields of analyzed variables in a grid of 2.5 degrees of latitude-longitude, at seven standard levels between 1,000 and 100 hPa. The variables are geopotential height, temperature and horizontal components of the wind velocity at 00 UTM and 12 UTM.

The analyzed meteorological data are transformed to isentropic coordinates by Duquet's procedure (Duquet, 1984).

If T_j, P_i are known at two adjacent levels:

Temperature:

$$T_j = \frac{\Theta_j \, (T_i - B.P_i^k)}{\Theta_j - B.1000^k} \qquad \text{(Equation 3)}$$

where

$$B = \frac{T_{i+1} - T_i}{P_{i+1}^k - P_i^k} \qquad \text{(Equation 4)}$$

Pressure:

$$P_j = \frac{1000}{(\theta j / T_j)^{1/k}} \qquad \text{(Equation 5)}$$

Height:

$$z_j = z_i + \frac{c_p}{g} \cdot \frac{T_i \pi_j - T_j \pi_i}{\pi_j - \pi_i} \cdot \ln \frac{\pi_i}{\pi_j} + T_i - T_j \qquad \text{(Equation 6)}$$

where $\pi = (p/1000)^k$

Wind velocity:

$$u\ u_i + \frac{u_i - u_{i+1}}{z_i - z_{i+1}} \cdot (z - z_i) \qquad \text{(Equation 7)}$$

Trajectories are then computed by using the values of these fields in isentropic surfaces, forcing the air parcel to travel along constant potential temperature surfaces: $T_p = T(1000/p)^K$.

The isentropic approximation reduces a tri-dimensional trajectory computation to a bi-dimensional problem. Although only the horizontal components of the wind velocity are used, the vertical motion of the parcel is not ignored. It is implicitly taken into account through the contour and the temporal variation of the isentropic surface.

Trajectories are constructed in the isentropic framework from the movement equations, where the pressure fields are represented by the Montgomery stream function, $\Psi = c_p T + gz$.

Trajectories are computed applying an explicit system of equations based on the theory of the "discrete model" developed by Greenspan (1972), to the atmospheric equations of the movement.

The model calculates parcel positions in time steps of 900 s, integrating trajectory segments after 48 time steps. The process is repeated to complete a 12-hour trajectory segment.

First time step:

$$\alpha_X^{(o)} = - \frac{\Delta\psi^{(o)}}{\Delta X} f^{(o)}.U \qquad \text{(Equation 8)}$$

$$\alpha_Y^{(o)} = - \frac{\Delta\psi^{(o)}}{\Delta Y} f^{(o)}.U \qquad \text{(Equation 9)}$$

$$v^{(o)}=v^{(o)}+a_y^{(o)}.\Delta t \qquad \text{(Equation 10)}$$

$$u^{(1)}=u^{(o)}+a_x^{(o)}.\Delta t \qquad \text{(Equation 11)}$$

$$x^{(1)}=x^{(o)}+1/2(u^{(o)}+u^{(1)}).\Delta t \qquad \text{(Equation 12)}$$

$$y^{(1)}=y^{(o)}+1/2(v^{(o)}+v^{(1)}).\Delta t \qquad \text{(Equation 13)}$$

Next time steps:

$$a_x^{(n)}=-\frac{\Delta\psi^{(n)}}{\Delta x}+f^{(n)}.vel_x^{(n)} \qquad \text{(Equation 14)}$$

$$a_y^{(n)}=-\frac{\Delta\psi^{(n)}}{\Delta y}-f^{(n)}.vel_y^{(n)} \qquad \text{(Equation 15)}$$

$$u^{(n+1)}=vel_x^{(n)}+(3/2a_x^{(n)}-1/2a_x^{(n-1)}).\Delta t \qquad \text{(Equation 16)}$$

$$v^{(n+1)}=vel_y^{(n)}+(3/2a_y^{(n)}-1/2a_y^{(n-1)}).\Delta t \qquad \text{(Equation 17)}$$

$$x^{(n+1)}=x^{(n)}+1/2(u^{(n+1)}+u^{(n)}).\Delta t \qquad \text{(Equation 18)}$$

$$y^{(n+1)}=y^{(n)}+1/2(v^{(n+1)}+v^{(n)}).\Delta t \qquad \text{(Equation 19)}$$

where

$$vel_x^{(n)}=1/2(u_{(I)}^{(n)}+u^{(n)}) \qquad \text{(Equation 20)}$$

$$u_{(I)}^{(n)}=u^{(o)}+\frac{u^{(F)}-u^{(o)}}{t}.\Delta t.n \qquad \text{(Equation 21)}$$

- **Diffusion-deposition models**

The diffusion-deposition is computed along the ARL trajectories through the application of a gaussian scheme (Heffter *et al*, 1975). Level ground concentrations are computed on boxes of 0.5 x 0.5 degrees size from a continuous point source located at the trajectory origin.

The concentrations due to advection-diffusion are calculated from the equation:

$$\chi_g = \frac{Q}{\pi.\sigma_y.(\,2K_z t\,)^{1/2}.u} \exp(-y^2/2\sigma_y^2) \qquad \text{(Equation 22)}$$

Where χg is the ground level air concentration (Kg/m^3), Q is the emission rate (Kg/s), σ_y is the crosswind standard deviation of the plume (m), u is he wind speed affecting the plume (m/s), y is the crosswind distance from the trajectory segment, K_z is the vertical diffusion coefficient, and t is the plume travel time (s).

- **Dry deposition**

Fallout of aerosol particles depends very much on various factors such as density and size of the particles, turbulence of the air, wind speed and other parameters. The size of the particles is to a large extent related to the fact that they alternate between wet and dry conditions. The soluble components of particles included in a water droplet rather dissolve then coalesce with other water droplets, and finally dry up to make a larger particle. As a result, aerosol particles change their size distribution depending on the atmospheric conditions and the tie spent in their travelling from the source to the locality of deposition. Giant particles, with sizes above 50 µm, may be produced in this way.

Amounts involved in dry deposition are calculated, along a trajectory, using the dry deposition velocity:

$$D_d = \chi_g.V_d.\Delta t \qquad \text{(Equation 23)}$$

Where D_d is the amount deposited per unit area during the internal Δt, χ_g is the ground level air concentration, V_d is the deposition velocity and Δt is the time interval.

- **Wet deposition**

Relatively little is known about the rainfall that takes place over the sea. Convection of the air over the sea is substantially different from that over the land. As a consequence, there is a basic difficulty in extrapolating the rates of wet deposition over the sea from those measured along the coastline. On the other hand, the concentration of nutrients in rainfall vary greatly with time after the onset of rain events. However, according to Migon *et al.* (1989), the same amounts of nitrogen compounds are deposited with rain during a dry year as during a wet one. If this is so, the rate of rainfall would be irrelevant for the computation of the yearly wet deposition rates. This however requires further study.

Wet deposition amounts at a grid point along a trajectory have been computed from the ARL model as:

$$D_\omega = E.P.\chi_g.(\pi K_z t)^1/2(\Delta z)^{-1}.\Delta t \qquad \text{(Equation 24)}$$

Where E is the average scavenging ratio, $E=\chi_\omega/\chi_a$ between the concentration in rainwater at the ground (χ_ω) and the mean concentration in the column of air from the ground to the top of the rain-bearing layer (χ_a); P is the precipitation rate; Δz is the thickness of the rain layer.

- **Combined diffusion-deposition**

Incorporating the effects of wet and dry deposition in the diffusion model as source depletion terms, surface air concentrations along the trajectory are:

$$\chi_g = \frac{Q.\exp(-2u_d t^{1/2}(\pi k_z)^{-1/2} - EPt(\Delta z)^{-1})}{\pi\sigma_y(2K_z t)^{1/2}u} \exp(-y^2/2(\sigma_y)^2) \qquad \text{(Equation 25)}$$

3. RESULTS

Deposition of nutrients by particle settling and/or rainfall can be estimated to be of the same order of magnitude as the eddy diffusion transport from below the euphotic zone in highly stratified waters (Table 1). Assuming the upper water layer to be perfectly mixed down to a depth of about 10 metres, the atmospheric nutrient will generate a vertical gradient in the water column in equilibrium with the rate of deposition: $dC/dz = F/k_z$, where F is the rate of deposition and k_z is the vertical eddy diffusion coefficient.

Table 1

Nitrogen fluxes from the atmosphere into the ocean
(μmol N/m^2 d)

	WET		DRY		TOTAL		
	NO_3^-	NH_4^+	NO_3^-	NH_4^+	NO_3^-	NH_4^+	T-N
Sargasso Sea(1)	10-20	10-15	5-15	0.2-1	15-35	10-16	25-51
Sargasso Sea(2)	23						
Pacific Ocean(1)	3-6	2-10	2-6	0.2-1	5-12	2-11	7-23
Pacific Ocean(2)	23						
NW Mediterranean(3)	120-144		0.2-67	0-100			
		Av.	5	26			120-300

(1) Duce (1983)
(2) McCarthy and Carpenter (1983)
(3) Wet deposition: Migon *et al.* (1989)
Wet deposition: Alarcon and Cruzado (1989)

For F=100 µM N/m^2/day and K_z=100 cm^2/s (2000 m^2/day) the gradient should be of the order of 0.05 µM N/m^4, about 1000 times smaller than the gradient at the nitracline (about 50 µM N/m^4) (see Table 2). This difference is a function of the difference in K_z between the surface and the sub-thermocline waters.

An indirect way of estimating the impact of the atmospheric nutrient inputs, is the growth of the phytoplankton biomass supported by their flux. They phytoplankton growth supported in the upper mixed layer is equivalent to:

F µM N/m^2/day . 1.272 mg C/15 µM N/h m

Table 2

Vertical nitrate fluxes at the base of the euphotic zone
in oligotrophic areas of the oceans

LOCATION	GRADIENT (µmol m^{-4})	DEPTH RANGE m	FLUXES * µMOL M^{-2} D^{-1}	SOURCE
Sargasso Sea			22-135	(1)
North Pacific Gyre			60-520	(1)
Costa Rica Dome			380-1760	(2)
Trop. North Pacific			180	(3)
SW Sargasso Sea	0.05	100-160	80-400	(4)
NW Mediterranean	0.09	70-120	160-800	(4)
Ionian Sea	0.03	100-200	50-150	(5)
Levantine Sea	0.005	100-200	8-40	(6)

(1) McCarthy and Carpenter (1983)
(2) King and Devol (1979)
(3) Anderson (1978)
(4) Cruzado and Velasquez (1986)
(5) Souvermezoglu (1986)
(6) Yilmaz *et al.* (1986)

(*) Minimum and maximum values computed with K_z=1.7 and 8.5 m^2 d^{-1} equivalent to 0.2 and 1.0 cm^2 d^{-1}

For F=100 µM N/m^2/day the increase in productivity in the upper h m of the upper mixed layer would be of the order of about 10 mg C/m^2/day. These figures are equivalent to those obtained for the vertical eddy diffusion fluxes below the thermocline, therefore doubling the "new" productivity integrated over the water column. However, the excess primary productivity of 1 mg C/m^3/day generated by the atmospheric input at any point within the upper 10 m layer may be difficult to compare to the total carbon uptake estimated to range between 1 and 7 mg C/m^3/day in the very poor surface waters of the Sargasso Sea, for example.

On the other hand, only large deposition events could be followed by a noticeable increase in dissolved nutrient concentrations in the surface seawater (Migon *et al.*, 1989) since, for the greatest part, steady state deposition goes through the plankton system without large development of phytoplankton. On the other hand, large deposition events (stormy rainfall) are usually accompanied by strong winds that alter the vertical diffusion pattern and may bring deep nutrients to the upper layers, thus making the impact of the atmospheric input even more difficult to detect.

We have applied the ARL combined diffusion-deposition model along the trajectory to simulate a continuous point source located in Blanes, in order to calculate the air-to-sea fluxes in a grid box over the Mediterranean Sea due to simple diffusion and due to diffusion-deposition, for several days.

We have selected days when the meteorological situation was particularly favourable for the land-to-sea transport from the source. We have assumed an emission of 0.005 Kg/s, which produces a vertical flux on the range 10-100 μM N/m^2/day near the source, corresponding to the same order of magnitude as the fluxes calculated in Blanes from data obtained with high volume samplers (Table 1).

Fig.1 shows the meteorological maps at 700 hPa (00 UTC) corresponding to 16, 17 and 18 February 1989, where the synoptic situation shown is favourable for transport from the Catalan coast into the Mediterranean Sea.

Fig.2(a) shows the ARL trajectories for 16 February and the fluxes (μmol/m^2/day) of nitrogen due to the diffusion-deposition combined (taking into account the depletion by dry and wet deposition). Fig.2(b) shows the same, but only with diffusion (without depletion by dry and wet deposition). Figs.3 and 4 show the same data for 17 and 18 February respectively.

Figs.5 and 6 show isentropic back-trajectories for 13 and 21 February 1989 from the Catalan coast (Northwestern Mediterranean). The transport has been focused on the isentropes of 295 K, 300 K and 305 K, because these surfaces intersect the layer comprised between the ground and the top of the boundary layer in the Mediterranean area.

Aerosol aluminium is used here as an indicator of desert dust. Aerosol samples have been obtained in the CEAB station, and aluminium analyses were carried out at the University of Liverpool for the period 1-21 February 1989. The values show two different situations, one that corresponds to a day with high aluminium concentration (about 1,440 ng/m^3), and a second that corresponds to a day with very low aluminium concentration (about 397 ng/m^3).

Examples of back-trajectories from the Blanes area are typical of days when North African air masses arrive at the Northwestern Mediterranean region. Fig.7 shows 3 isentropic back-trajectories following 3 different potential temperature surfaces (290 K, 300 K and 310 K) from Blanes, for 21 February at 12 UT.

4. CONCLUSION

It is possible to conclude that the atmospheric inputs of nutrients may be of great importance for the primary productivity in such an inland sea as the Mediterranean, equivalent to the vertical fluxes achieved by the eddy diffusion transport at the nitracline.

It is however difficult to measure the impact of the nutrient input because of the mixing of surface water layers, which makes atmospherically generated nutrient concentration gradients practically non-existent after large deposition events, provided there is no other transport mechanism that has been altered by the event.

In the future, it seems to be suitable to carry out systematic studies of the trajectories and deposition taking into account the emission and/or the monitoring data. For estimating the overall nutrient inputs over a relatively large sea such as the Mediterranean, the observed decay of the concentration in air due to deposition over the sea should also be taken into consideration.

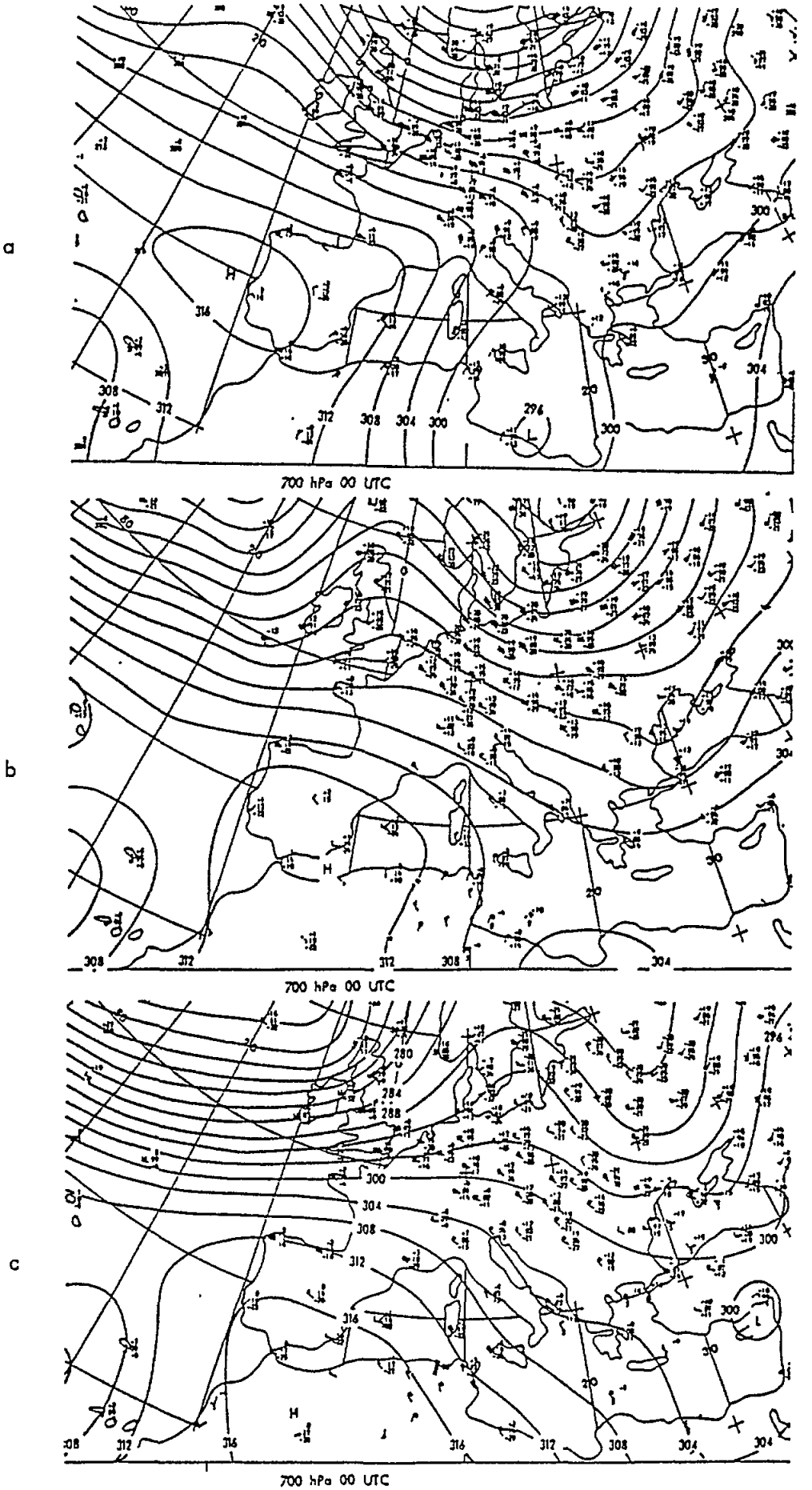

Fig.1 Synoptic situation at 700 hPa over Europe for (a) 16, (b) 17 and (c) 18 February 1989

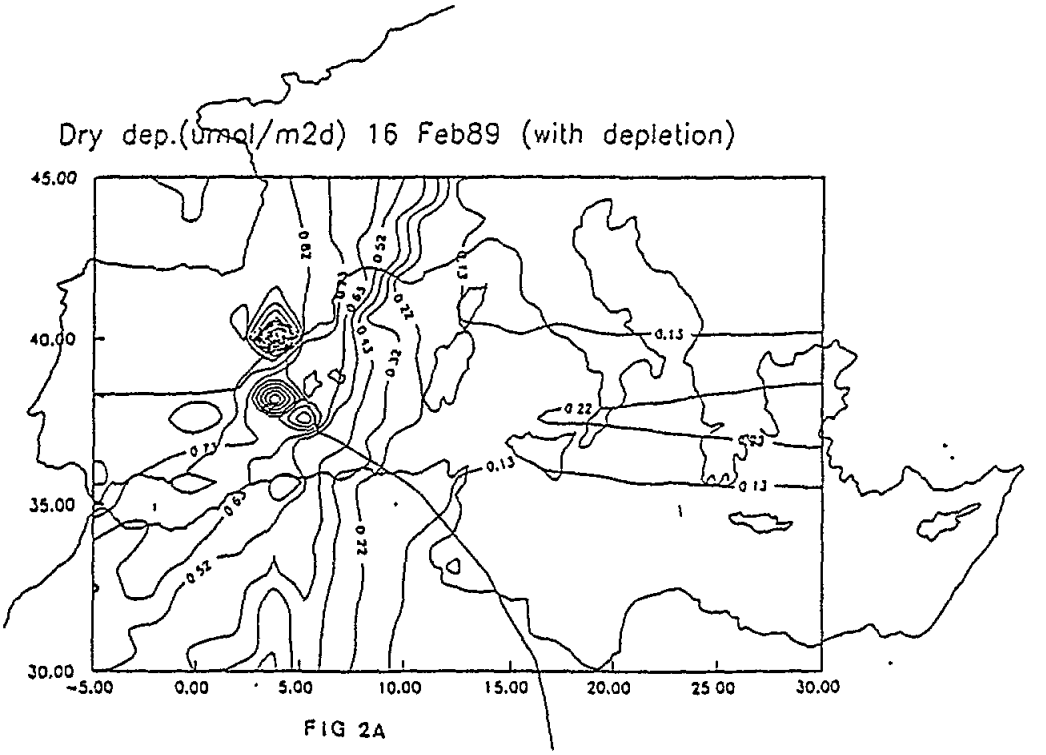

FIG 2A

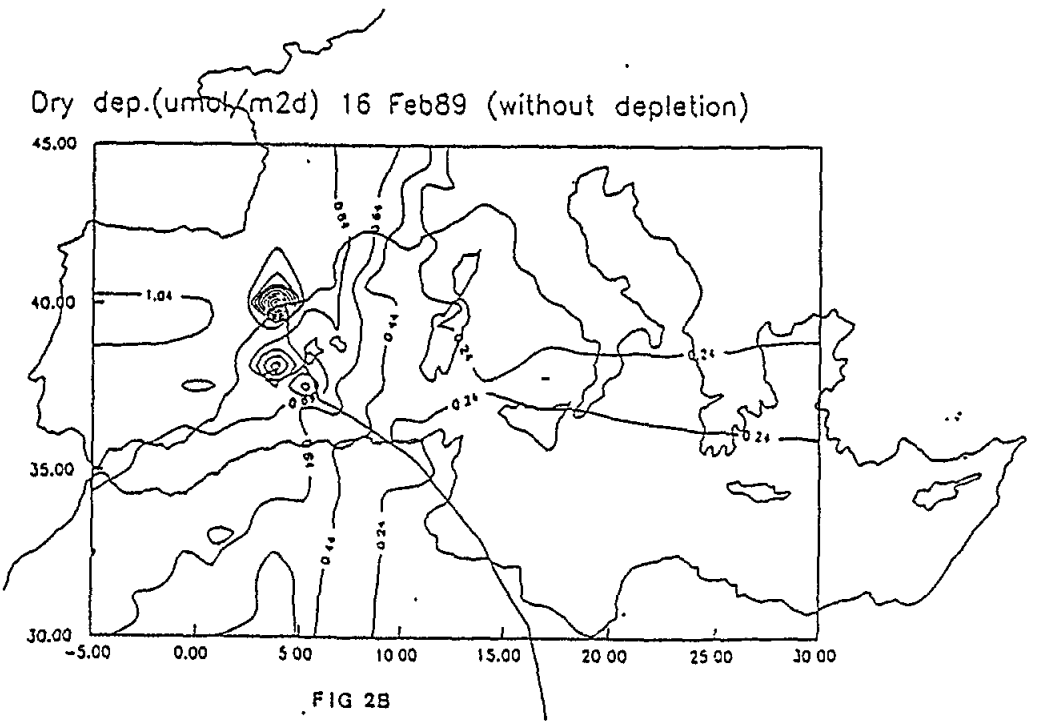

FIG 2B

Fig.2 Calculated ARL trajectories and fluxes of nitrogen for 16 February 1989 (a) allowing for depletion by dry and wet deposition, and (b) without depletion by dry and wet deposition.

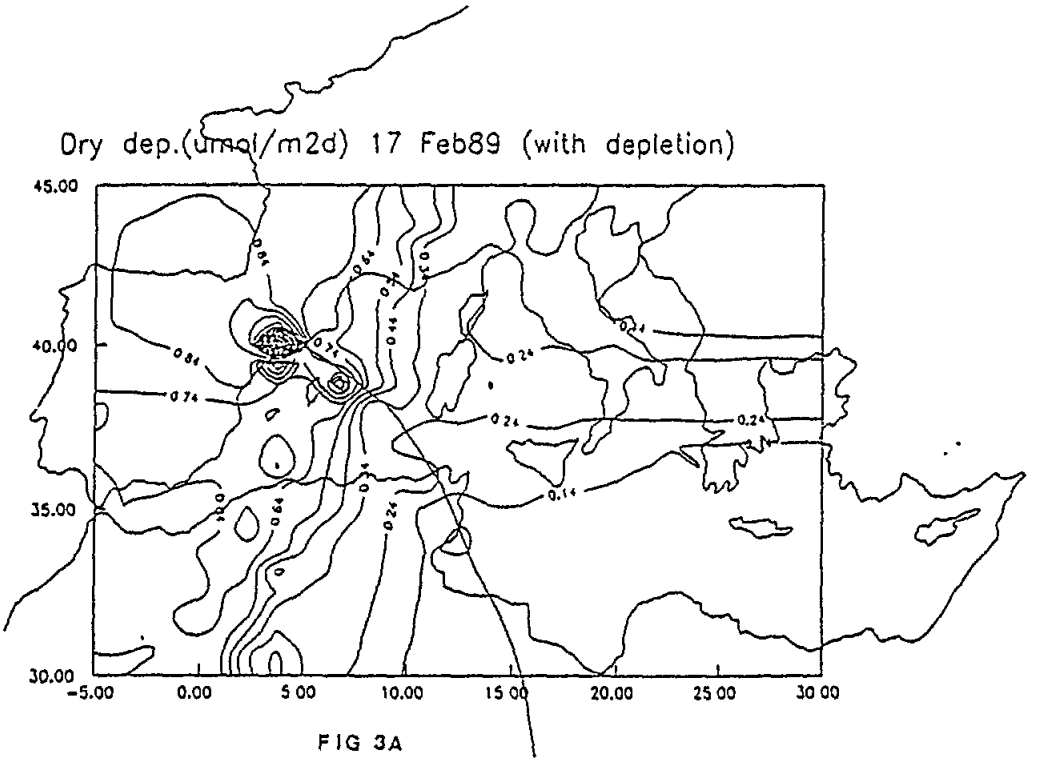

FIG 3A

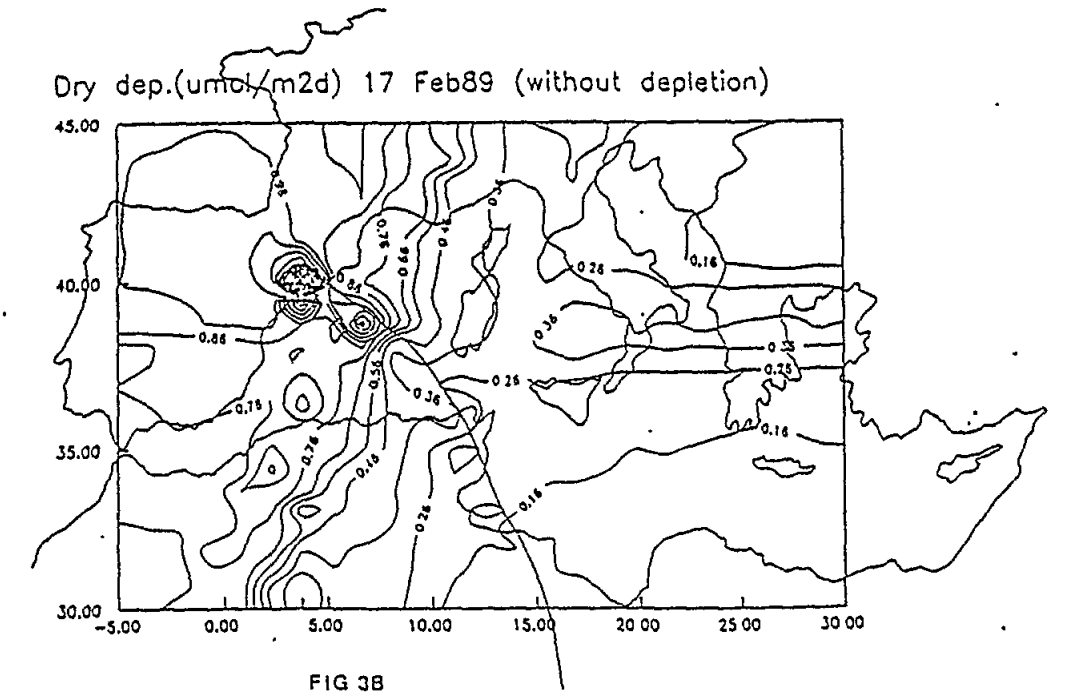

FIG 3B

Fig.3 Calculated ARL trajectories and fluxes of nitrogen for 17 February 1989 (a) allowing for depletion by dry and wet deposition, and (b) without depletion by dry and wet deposition.

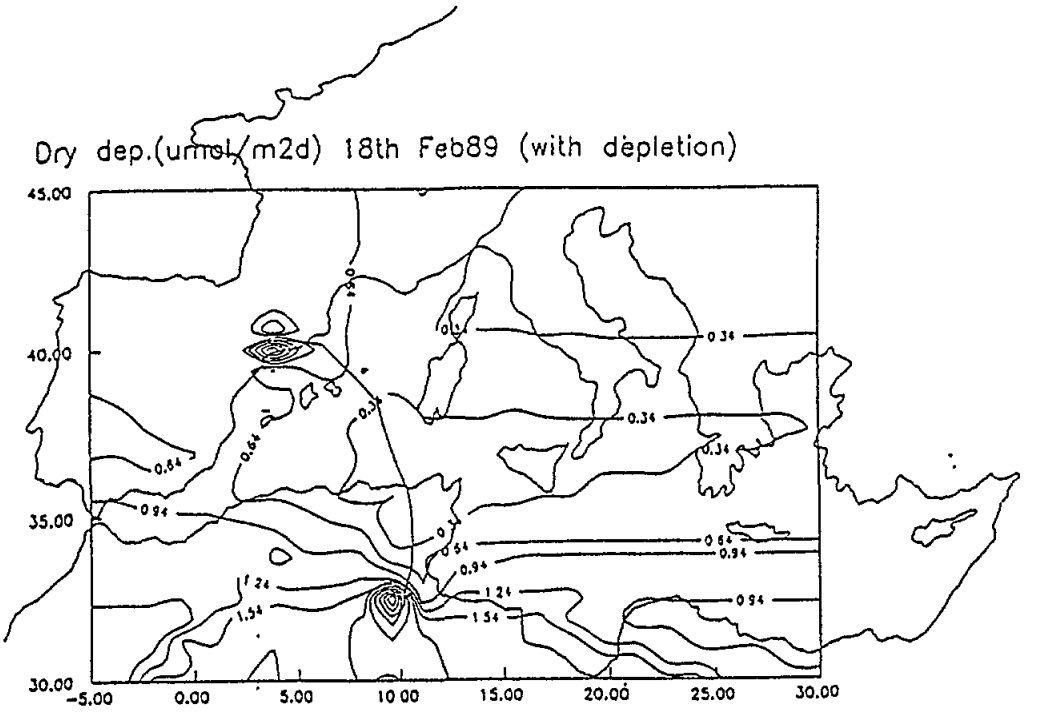

FIG 4A

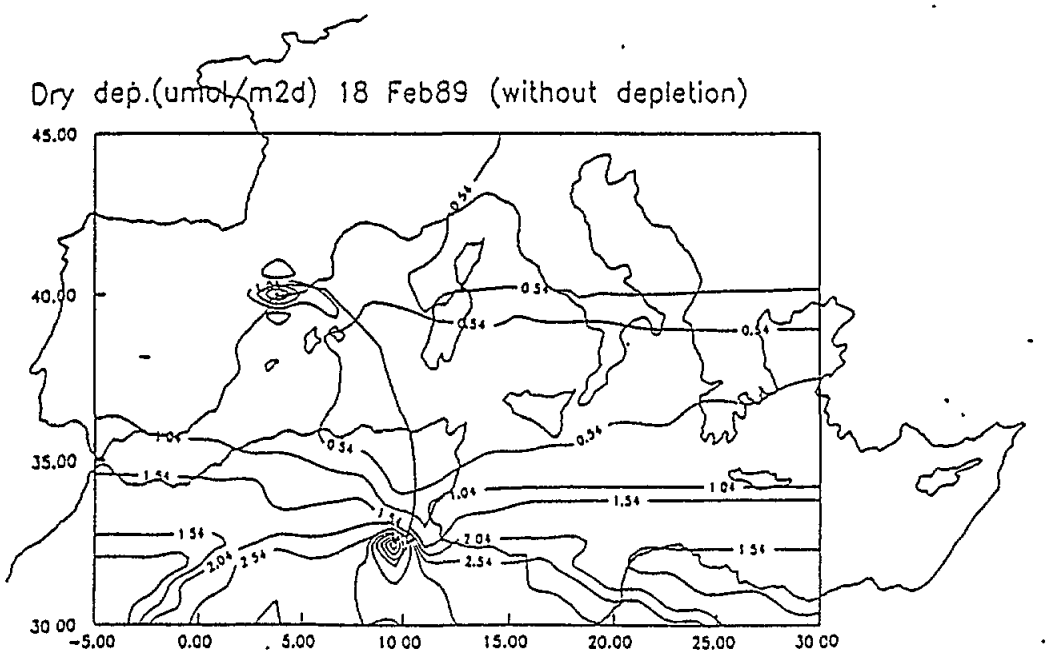

FIG 4B

Fig.4 Calculated ARL trajectories and fluxes of nitrogen for 18 February 1989 (a) allowing for depletion by dry and wet deposition, and (b) without depletion by dry and wet deposition.

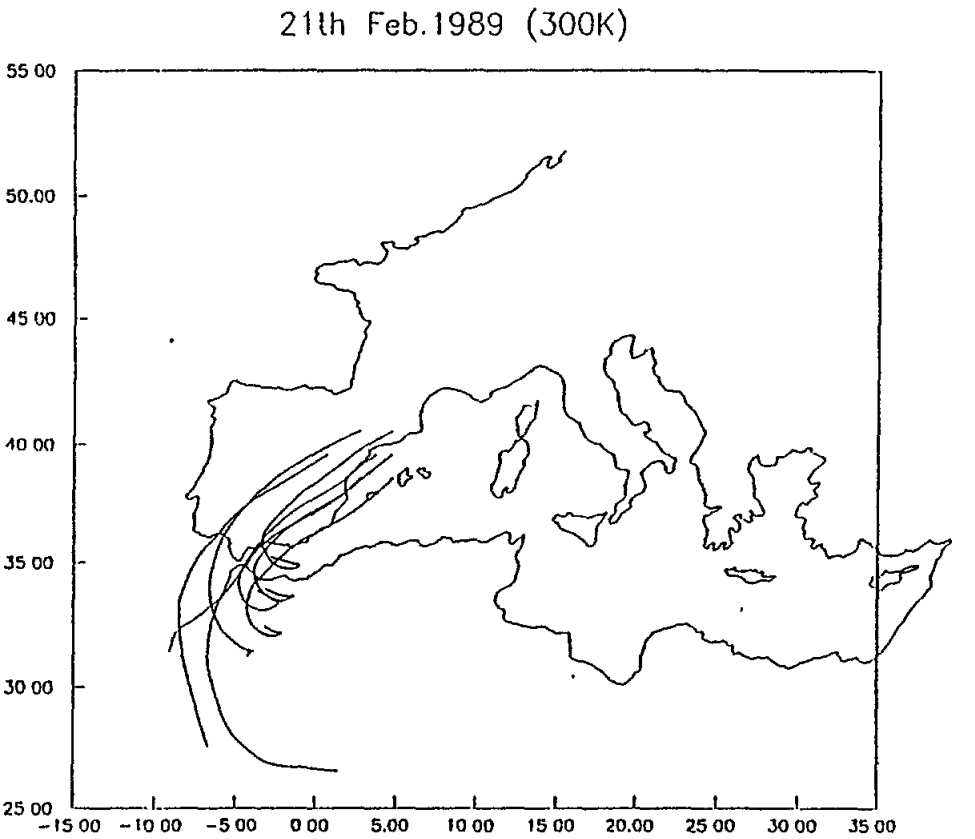

Fig.5 Isentropic back-trajectories from the Catalan coast for 21 February 1989.

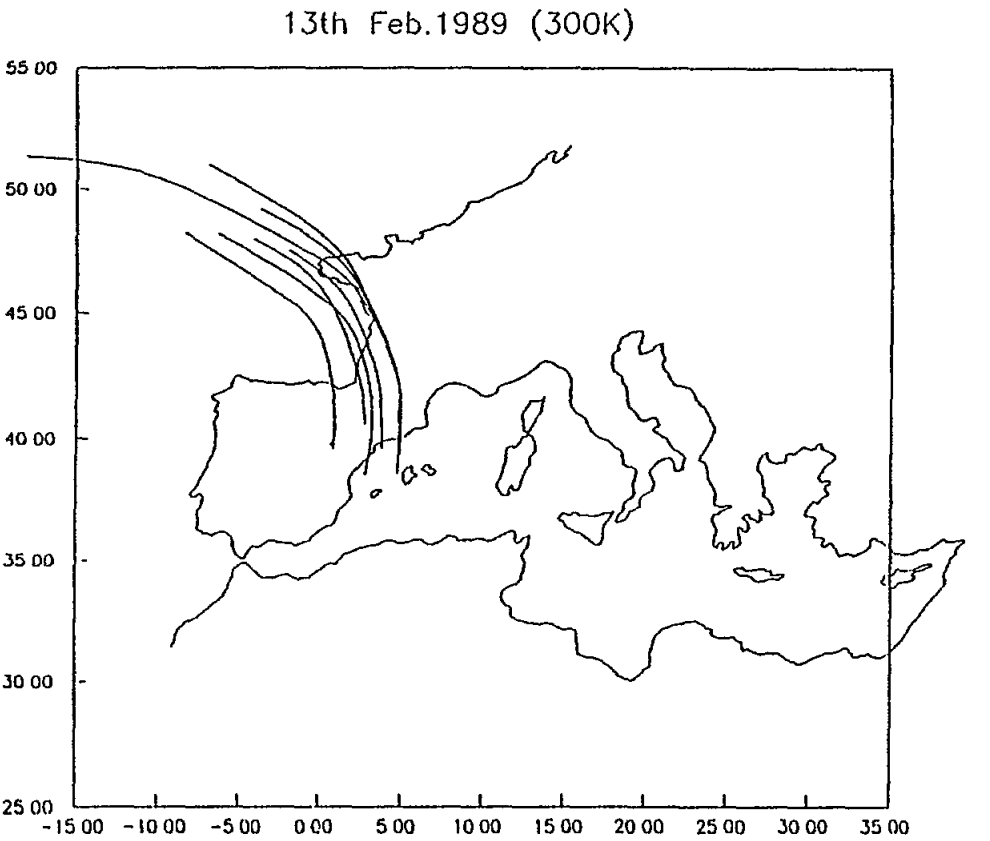

Fig.6 Isentropic back-trajectories from the Catalan coast for 13 February 1989.

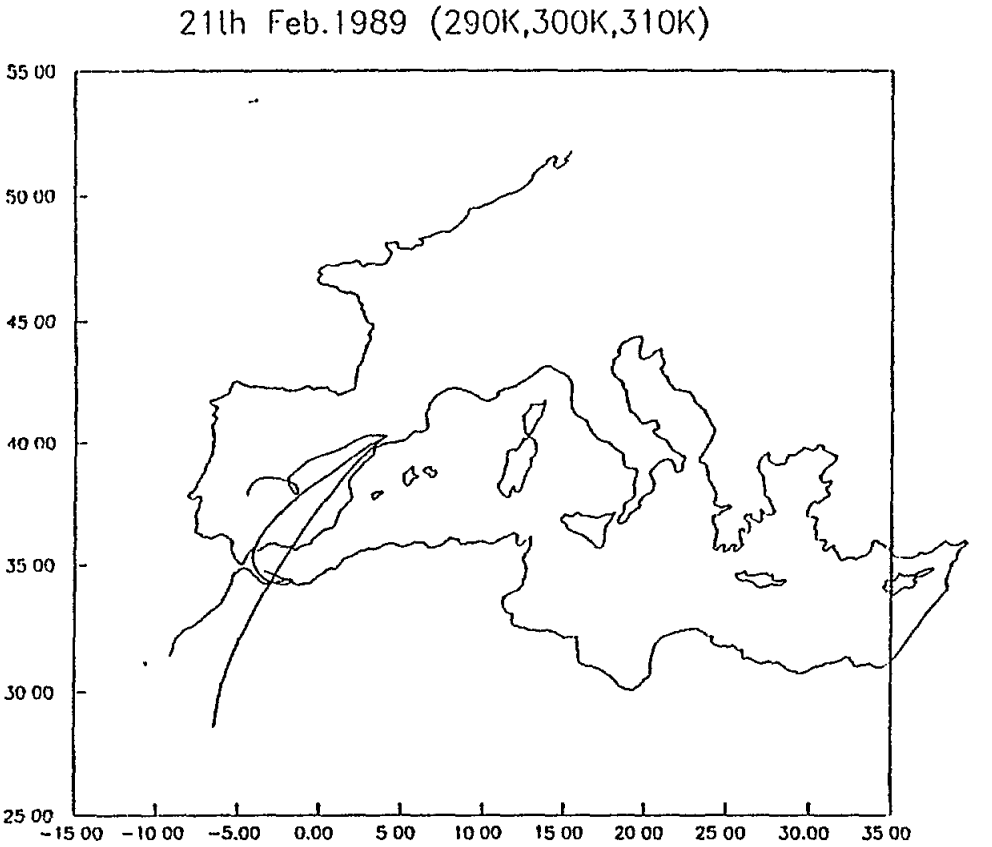

Fig.7 Isentropic back-trajectories from Blanes for 21 February 1989.

5. REFERENCES

Alarcon, M. and A. Cruzado (1989). *Atmospheric dry deposition of nutrients at a Catalan coastal site of Northwestern Mediterranean.* Proceedings de la XXII Reunion Bienal de la real Sociedad Espanola de Fisica. Universitat de les Illes Balears.

Anderson, G.C. (1978). *Deep ocean mining and the ecology of the Tropical North Pacific.* Dept. of Oceanography, University of Washington Special Report 81:1-123.

Cruzado, A. and Z.R. Velasquez (1986). Upward nutrient flux in the Western Mediterranean Sea. XXX Congress-Plenary Assembly of ICSEM, Palma de Mallorca, 20-24 October 1986.

Duce, R.A. (1983). Biogeochemical cycles and the air-sea exchange of aerosols. In: *SCOPE 21.* The major biochemical cycles and their interactions. Vol.16 (Eds. Bolin, B; Cook, R.B.), John Wiley and Sons, Chichester, 427-456.

Duquet, R.T. (1964). Data processing for isentropic analysis. Tech. Rep. No.1, contract No. (30-1)-3317, Air Force Cambridge Research Laboratories.

Greenspan, D. (1972). A new explicit discrete mechanics with applications. *J. Franklin Inst.*, 294:231-240

Heffter, J.L., A.D. and G.J. Ferber (1975). A regional continental scale transport, diffusion and deposition model. *NOAA Tech. Mem. ERL ARL-50*.

King, F. and A. Devol (1979). Estimates of vertical eddy diffusion through the thermocline from phytoplankton nitrate uptake rates in the mixed layer of the Eastern Tropical Pacific. *Limnol. Oceanogr.*, 24(4):645-651.

McCarthy, J.J. and E.J. Carpenter (1983). Nitrogen cycling in the near-surface waters of the open ocean. In: *Nitrogen in the marine environment*, (Eds. Carpenter, E.J; Capone, D.G.), Academic Press, New York, 487-571.

Migon, C., G. Copin-Montégut, L. Elégant and J. Morelli (1989). Etude de l'apport atmosphérique en sels nutritifs au milieu côtièr mediterranéen et implications biogéochimiques. *Oceanol. Acta.*, 12(2):187-192.

Petersen, R.A. and L.W. Uccellini (1979). The computation of isentropic atmospheric trajectories using a "discrete model" formulation. *Mon. Wea. Rev.*, 107:566-574.

Souvermezoglu, E., I. Pampidis, E. Hatzigeorgiou and K. Siapsali (1986). *Dissolved oxygen and nutrients in the Northeast Ionian Sea*. XXX Congress-Plenary Assembly of ICSEM, Palma de Mallorca, 20-24 October 1986.

Yilmaz, A., D. Ediger, A.C. Saydam and O. Basturk (1986). *Fluorescence characteristics due to phytoplankton chlorophyll and optical transparency of Northeast Mediterranean waters*. XXX Congress-Plenary Assembly of ICSEM, Palma de Mallorca, 20-24 October 1986.

ACID PRECIPITATION IN THE NORTHERN ADRIATIC

By

VESNA DURIÈIÆ and SONJA VIDIÈ

Centre for Meteorological Research
Hydrometeorological Institute of Croatia
Zagreb, Yugoslavia

A B S T R A C T

The high emission release from industrial stacks (oil refinery, cokery, thermal power plant), urban emissions and heavy traffic, associated with unfavourable meteorological conditions often cause high levels of SO_2 concentrations, episodes of acid precipitation, as well as sulphate and nitrate depositions at Kvarner Bay area in the Northern Adriatic.

The aim of this paper is to discuss air and precipitation pollution level in this part of the Adriatic coast. SO_2 average daily concentrations and the three main components (pH, SO_4^{2-} -S, NO_3^- -N) in daily precipitation samples during the five-year period 1985-1989 were statistically analyzed.

It has been shown that 5-15% of average daily SO_2 concentrations at Rijeka are higher than the legislated limit value; average five year daily mean was about 100 µg/m^3, and peak value reaching even 500 µg/m^3. 42% of precipitation samples were acid, with sulphur wet deposition about 25-44 kg/ha per year and nitrogen wet deposition about 10 kg/ha per year. The comparison of data from an urban, industrially developed area (Rijeka) and two rural regions (Zavižan, at 1,594 metres above sea level, and Veli Lošinj, on the island of Lošinj at sea level) indicates that the long-range transport of pollution from the Western Mediterranean contributes to the overall pollution in this area, especially in the case of acid rain episodes.

1. INTRODUCTION

The settlement of various types of emission sources at coastal areas used to be rather frequent. The presence of diverse unfavourable conditions associated with industrial development has been disregarded or neglected in many instances, hence the air, water and soil pollution has been a common problem in these areas.

This is also the case at Kvarner Bay in the Northern Adriatic. The city of Rijeka, in the centre of the area, has developed into the largest shipyard and harbour on the Yugoslav Adriatic coast. Besides, the greatest number of pollution sources is assembled here: oil refinery and petroleum industry, cokery, thermal power plant, local industrial sources, heavy traffic, domestic heating. A variety of pollutants, continuously emitted into the atmosphere, associated with prevailing meteorological conditions (strong solar radiation receipt, diurnal land-sea breeze pattern, internal boundary layer development) related to the orographically induced processes,

resulted in a rise of serious air pollution problems. Exhibiting all these conditions, Kvarner Bay has grown to one of the most polluted areas on the Yugoslav coast.

Moreover, the problem is enhanced by the fact that there is considerable regional transport of pollution across the sea from industrially well developed Northern Italy. In connection with the strong cyclogenetic activity in the Western Mediterranean, especially in the lee of the Alps, moist air masses accompanied by considerable precipitation events at coastal areas and inland, come from that region (Klein, 1957; Radinoviæ, 1962; Speranza, 1975; Tibaldi, 1980; Tibaldi *et al.*, 1983).

The purpose of this paper was to analyze the precipitation pollution data in Rijeka, together with the date of two stations representing the industrially unaffected surrounding area. One of these is the regional station operating within the framework of the EMEP/MED POL monitoring programme (Zavižan - 1,594 metres above sea level), while the other is a station within the Children's Hospital for Allergic Diseases in Veli Lošinj.

No systematic analysis of air and precipitation pollution in this area has been done until now. The first sampling of SO_2 concentrations started in the seventies, while sampling of chemical compounds in precipitation started in the early eighties. The emission control is still rather poor, and is not supported by the meteorological observational system. The continuous emission monitoring system, although planned, has not yet been established. Hence, an attempt has been made to relate the pollution rates generated by a large industrial urban area to those in the surrounding areas. Based on the statistics, the degree to which precipitation quality in the area depends on locally-generated, as opposed to important, pollutants, has still to be found.

The results indicate that the considered area is very polluted. The SO^2 concentrations (from daily samples) at 3 considered urban sites have mean values of about 100 µg/m^3 and maxima exceeding 500 µg/m^3. Precipitation acidity is also high; 42% of the precipitation samples have a pH level below 5.6, while sulphur deposition is 25-44 kg/ha per year.

Taking all factors into consideration, pollution of the area under investigation arises as a result of several joint effects: local pollution, pollution imported by regional and long-range transport, as well as unfavourable meteorological conditions enhanced by complex topography features. The problem of air pollution transport into the Mediterranean region from the Kvarner Bay area, will be included in future work. The detailed analyses of similar problems have been discussed in a number of papers (Högstrom, 1974; Benarie, 1976; Davies, 1976; Zanetti *et al.*, 1976; Lamb *et al.*, 1978; Reid, 1978; Carroll *et al.*, 1979; Clark *et al.*, 1988).

2. MATERIAL AND METHODS

2.1 Study area

The topography of the Kvarner Bay area in the Northern Adriatic is rather complicated. The area behind it, from the Northwest to the East, are enclosed by mountains which exceed a height of 1,000 metres to the Northeast, while Krk, Cres, Lošinj and a few smaller islands lie to the front of it. The urban area (Rijeka) with its industrial sources extends about 20 km in a Northwest-Southeast direction in the narrow coastal region. The overall position of the area, major topographic features, location of pollution sources and sampling sites are shown in Fig.1.

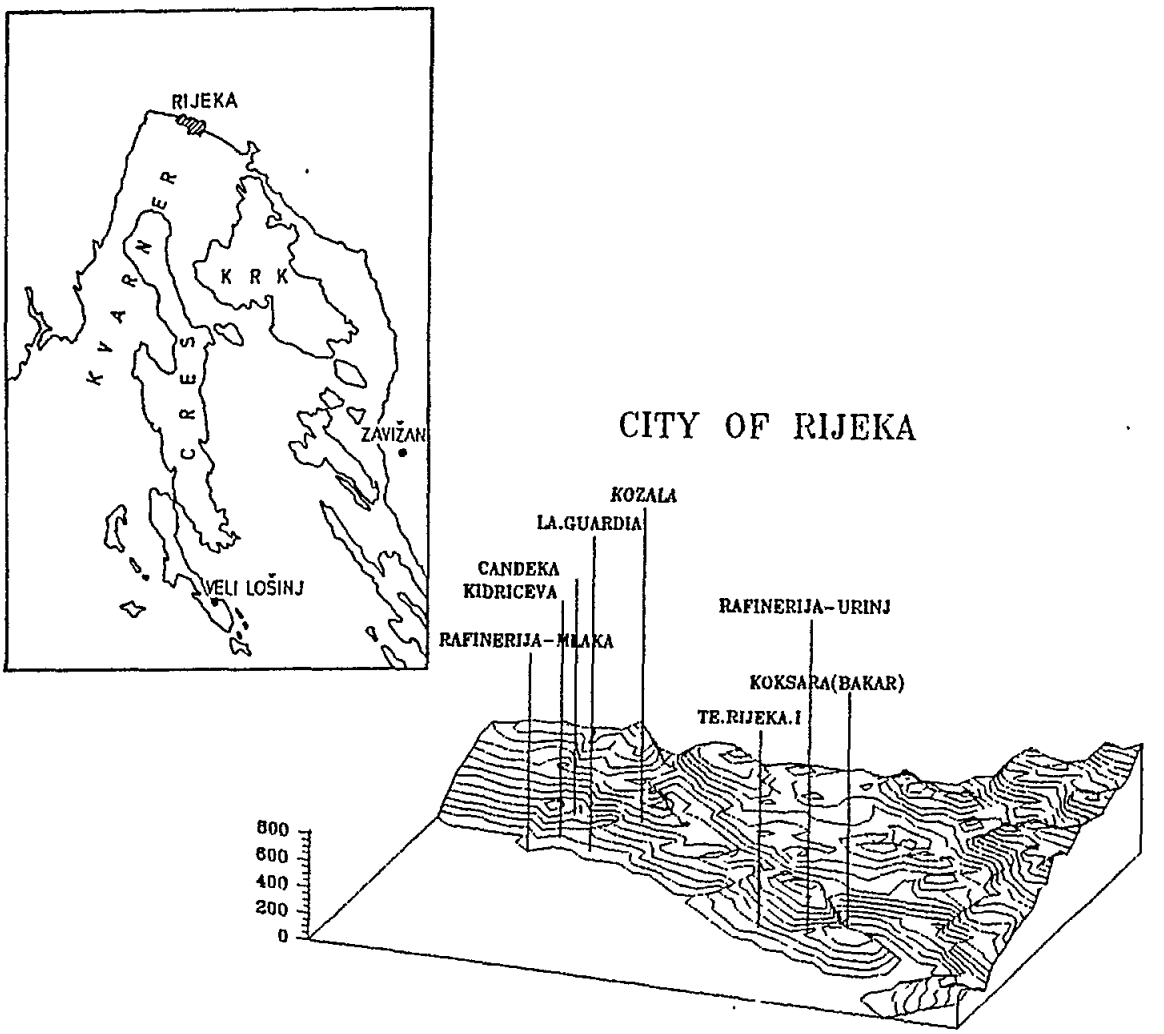

Fig.1 Locations of main sources of pollution, sampling sites and topography of the area.

2.2 Data

- Emission data

Main pollution sources are placed at three locations, at a distance of approximately 5-7 km from each other (Fig.1): at the centre of Rijeka-Mlaka (low level oil refinery sources), at the small peninsula Urinj (low and 80 m high oil refinery sources and thermal power plant with 180 m high stack), and at the small Bakar gulf area (cokery with uncontrolled low exhausts and 250 m high stacks). Moreover, a number of other sources of different types are comprised here; therefore the influence of primary and secondary generated pollutants is present. Some crude emission data, which is estimated on the basis of general fuel consumption, is shown in the following table:

Oil Refinery		Thermal Power	Cokery	Urban emissions
Rijeka-Mlaka	Rijeka-Urinj	Urinj	Bakar Gulf	Traffic
70,000 tons of oil per year (oil with 2.5-4% of S)	140,000 tons of oil per year (oil with 2-3% of S)	160,000 tons of oil per year (oil with 2-3% of S)		
	160,000 tons of oil gas per year (0.5% of H_2S)	30 mil. Nm^3 of gas-coke (with 4-7g of H_2S/Nm^3)	330 mil. Nm^3 of gas-coke (with 6.5 g H_2S/Nm^3)	
350 tons of SO_2/year	16,000 tons of SO_2/year	18,000 tons of SO_2/year	740 tons of SO_2/year	150 tons of SO_2/year

All estimates are made by the industrial personnel

It is to be recognized that all emission sources lie at the narrow coastal area, which is no larger than 70 km^2; therefore the total emission rate of SO_2 can be estimated as 500 tons per year per km^2.

- **Air and precipitation quality data**

Concentration data were provided by two networks. One, installed and surveyed by the Public Health Institute of Rijeka, operates with the programme of sampling 24-hr concentration values, mainly SO_2, using methods recommended by WMO. The other was established with the purpose of controlling the precipitation data quality in Croatia. It is under the survey of the Hydrometeorological Institute of Croatia in Zagreb. The sampling methods used are those recommended by WMO. These data are insufficient, as collected precipitation samples are "bulk", and contain both wet and dry deposition.

Here we reviewed data from 3 urban sites that have the greatest SO_2 concentration levels in the whole region. We also examined precipitation quality data from 3 sites, one in the centre of an urban area and two sites further from it (Zavižan, regional EMEP/MED POL station, and Veli Lošinj on the island of Lošinj).

The data available for the present analysis were collected over a five-year period (1985-1989), with the exception of Veli Lošinj (1987-1989) where the first sampling began in 1987. Three compounds were analyzed in precipitation: pH, SO_4^{2-}-S and NO_3^--N (sites P1-P3), and SO_2 (24-hr) air concentration data (sites S1-S3). Their positions are shown in Fig.1.

2.3 Climate conditions

The Kvarner Bay area has a generally mild climate, with an average yearly temperature of about 14EC and relative humidity of 62%. The average yearly rainfall is between 1,250 and 1,500 mm. For the period 1985-1989, this was about 1,400 mm (Tables 1(a) and 1(b)). Violent small-scale convective storms with intensive rain showers occur in summer and early autumn due to the high rate of evaporation associated with orographically induced effects.

Table 1(a)

Monthly and annual means of precipitation amounts (mm) and variability (%) for Rijeka, 1958-1977

Month	I	II	III	IV	V	VI	VII	VIII	IX	X	XI	XII	Year
Mean (mm)	131	124	110	122	104	103	101	103	186	148	185	157	1574
Variable (%)	269	260	272	165	202	151	172	202	153	311	130	268	80

Table 1(b)

Monthly and annual totals of precipitation (mm) for Rijeka, 1985-1989

Year	I	II	III	IV	V	VI	VII	VIII	IX	X	XI	XII	Total
1985	188	95	234	130	71	118	31	66	27	54	193	129	1336
1986	116	112	124	152	122	140	74	120	74	103	144	154	1435
1987	178	139	50	116	121	94	63	99	91	270	323	48	1592
1988	184	130	158	85	74	123	25	119	215	259	13	61	1446
1989	1	59	92	195	30	229	62	164	64	63	150	112	1221

The prevailing wind directions are from North to Northeast, with a little seasonal variation. A peculiarity of the area is a strong Northeasterly wind Bora (with speeds of about 10-20 m/s and hourly gusts that can exceed 35 m/s). Its duration can be a few days and even more, in the cold season. Most frequently, Bora wind conditions develop together with strong cyclogenetic activity in the Western Mediterranean, causing the creation of the high pressure gradients along the coast (Jurčec, 1989; Bajić, 1989; Vučetić, 1988). However, the low wind speed conditions (< 3 m/s) predominate in the area. A seabreeze effect, characteristic of the area, has been detected by examining the evolution of the wind roses obtained over this period of with speeds less than 3 m/s (Fig.2); downslope, winds occur during the evening and morning hours. On an average, atmospheric stability conditions, defined according to Pasquill's criteria, are neutral (stable - 32%, neutral - 30%, unstable - 38%). The frequency of unstable conditions, particularly in summer, increase mainly in association with winds blowing from the sea.

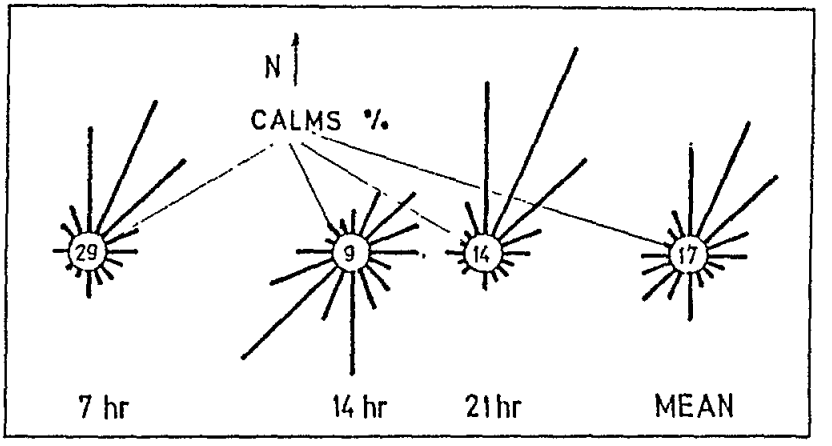

Fig.2 Term wind rose for Rijeka (1981-1988)

3. RESULTS AND DISCUSSION

Identification of the large industrial emissions' share in the total deposition rate at the investigated area, as well as at inland continental areas, became of great interest. The question which arose is how much of the sulphur emissions are deposited within the region, which is the forest resource in Croatia (Gorski, Kotar, 10-50 km away in a Northeast direction) (Fig.1). The results of some investigations indicated a progressive process of forest decay (Šojat *et al*., 1990).

This problem has been investigated by many authors (Smith, 1991; Cehak and Chalupa, 1985; Lisac, 1986; Ciattaglia and Cruciani, 1989; Charlson and Rodhe, 1982; Galloway *et al*., 1982, etc.). Högstrom (1974) studied the wet fallout of sulphurous pollutants around the city of Uppsala (Sweden) and concluded that almost all of the emitted sulphur dioxide was deposited as SO_4^{2-} in the first 50-100 km. Benarie (1976) concluded that gaseous and particulate dry depositions from sources in Paris, France, remained within the region of a 37 km radius. Davis (1976) claimed that precipitation had little effect on airborne SO_2 concentrations in an industrial area of England; however, since the SO_4^{2-} were not measured, no firm conclusion has been reached regarding total sulphur deposition rates.

Since no comprehensive study of this problem has been exhibited until now, the analysis of available data for the period 1985-1989 and 1987-1989 has been done. The basic statistical parameters of considered compounds in the air and precipitation are presented in Table 2. The annual course of daily samples and frequency distributions are given in Figs.3-12. It must be mentioned that at Rijeka (site P1) 83% of precipitation samples, at Zavižan (site P2) 98%, while at Veli Lošinj (site P3) only 59% of the samples were available for analysis. A summary of statistic results is presented in Table 2.

! Sulphur dioxide

According to the basic statistics, daily concentration values of SO_2 at three urban sites are high for the period under consideration, an average of about 100 µg/m^3 and with maxima that exceed 500 µg/m^3 (Table 2). The maximum occurs in winter, but there is a second one in summer (Fig.7). Although 3 urban sites are not far from one another, they show differences in the annual course (Fig.1). The site S1 is placed at 120 m above sea level in the vicinity of the oil refinery (Rijeka-Mlaka, at sea level) indicating the highest concentrations in the area during the whole year. Two other sites (S2, S3) are influenced by traffic, showing more regular annual concentration cycles (Fig.7).

At Veli Lošinj (site P3), with measurement site inside the Children's Hospital for Allergic Diseases, which is surrounded by forests and distant from pollution sources, the SO_2 concentration level is much lower (Fig.11, Table 2). More than 95% of the time concentrations are below the value of 50 µg/m^3. Only 1% of the data obtained values higher than 67 µg/m^3, so we assumed that the observed maximum of 193 µg/m^3 was the result of some unusual local activity. Annual course shows periodicity, with the higher winter and lower secondary summer maximum (in 1987 and 1988 - Fig.11).

Meteorological and climate conditions associated with complex topographic conditions at Kvarner Bay are favourable for high air pollution episodes. Natural ventilation of the area is generally weak (prevailing low winds and calms with frequency of 25%) and connected with the strong Bora wind occurrence from the Northeast.

Table 2

Statistical parameters of air and precipitation pollution at Rijeka, Zavižan and Veli Lošinj

Site	N	C_{avg}	σ	mode	C_{25}	C_{50}	C_{75}	C_{95}	C_{99}	Max	Min	iqr
					SO_2 (μg/m^3)							
S1	1733	98	60	105	60	83	121	211	327	510	3	61
S2	1776	68	41	55	40	58	85	146	205	381	3	45
S3	1731	108	47	108	76	101	132	196	248	460	3	56
P3	1285	14	15	3	3	9	21	41	67	193	1	18
					pH							
P1	371	5.57	0.96	6.3	4.9	5.9	6.4	7.2	8.1	8.4	3.8	1.5
P2	680	5.99	0.77	6.0	5.6	6.2	6.6	7.0	7.3	8.4	3.5	1.0
P3	101	5.47	0.94	6.1	4.9	5.9	6.4	7.1	7.3	7.3	4.0	1.5
					SO_4^{2-}-S							
P1	366	3.64	5.13	1.67	1.46	2.56	3.99	8.44	30 3	52.1	0	2.53
P2	672	1.91	2.25	0	0.66	1.29	2.46	6.11	8.30	26.4	0	1.80
					NO_3^--N							
P1	353	1.47	1.52	0.85	0.65	1.01	1.61	4.08	8.55	11.1	0	0.96
P2	679	1.66	4.47	0.36	0.29	0.44	0.77	10.1	16.9	69.0	0	0.48

N = sample size; C_{avg} = average; mode = mode; max = maximum; min = minimum; iqr = inter-quartile range

C_{25} - lower quartile; C_{50} - median; C_{75} - upper quartile; C_{95} - 95 percentile; C_{99} - 99 percentile

P1 - Rijeka (pH, SO_4^{2-}-S, NO_3^--N)
P2 - Zavižan (pH, SO_4^{2-}-S, NO_3^--N)
P3 - Veli Lošinj (pH, SO_4^{2-}-S, NO_3^--N SO_2)
S1 - urban site 1 (SO_2) - čandeka
S2 - urban site 2 (SO_2) - Kidričeva
S3 - urban site 3 (SO_2) - La Guardia

Note that c_{avg} for pH is precipitation-weighted mean, and for other compounds arithmetic mean

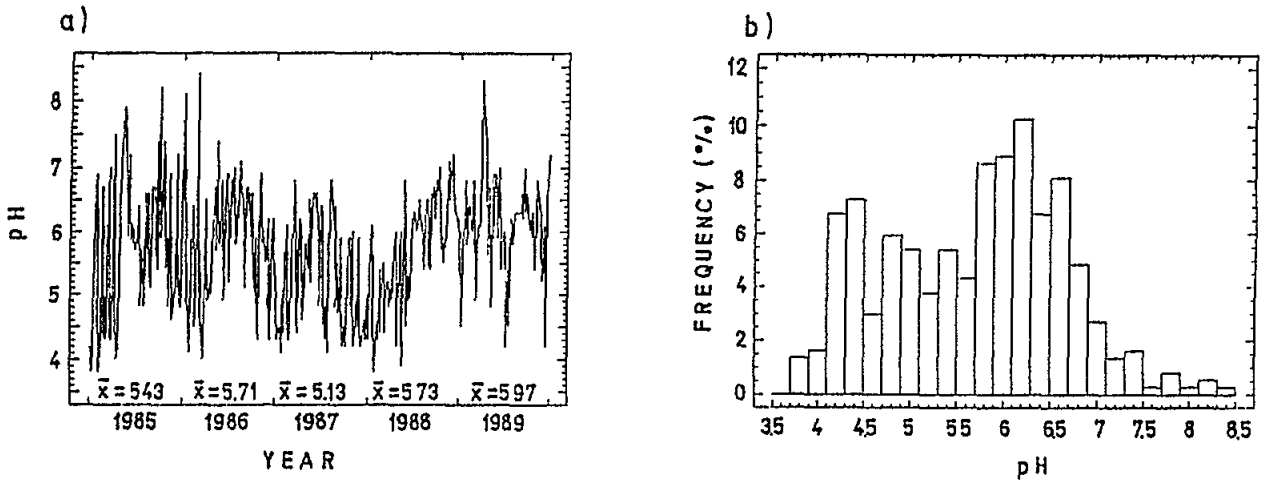

Fig.3 Annual course (a) and frequency histogram (b) of pH values from daily samples at Rijeka for the period 1985-1989. (Numbers on figure (a) are annual precipitation-weighted means).

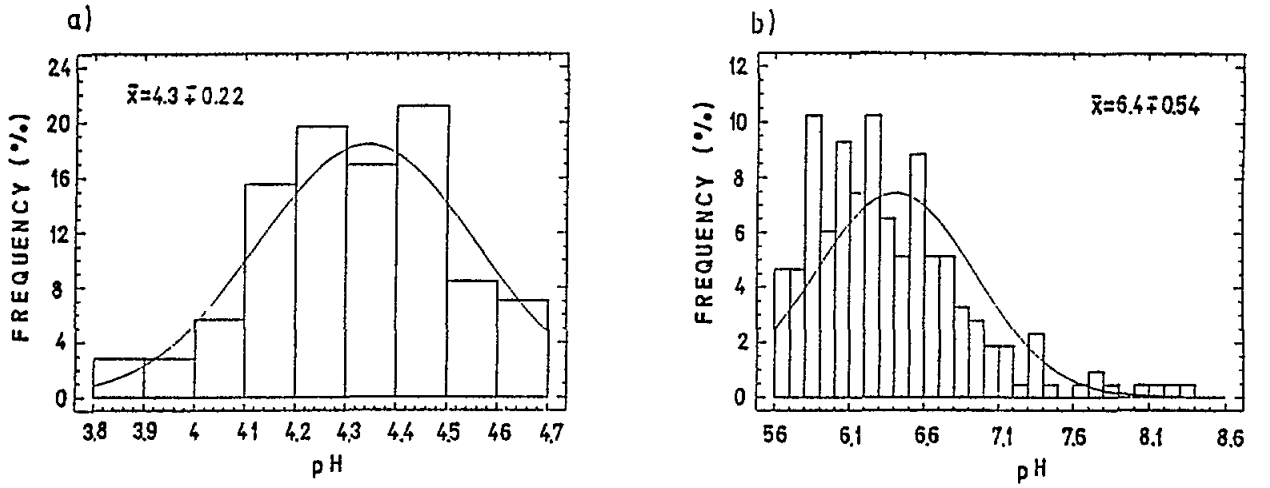

Fig.4 Normal distribution fitted to pH values from daily samples at Rijeka for the period 1985-1989.

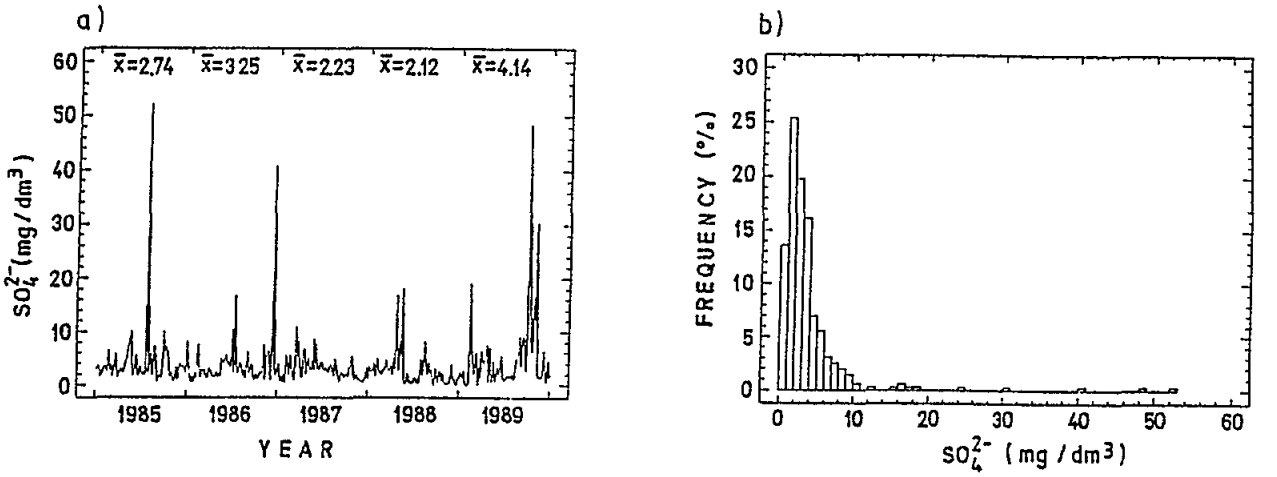

Fig.5 Annual course (a) and frequency histogram (b) of sulphate ion concentrations in daily samples at Rijeka for the period 1985-1989. (Numbers on the figure (a) are annual precipitation-weighted means).

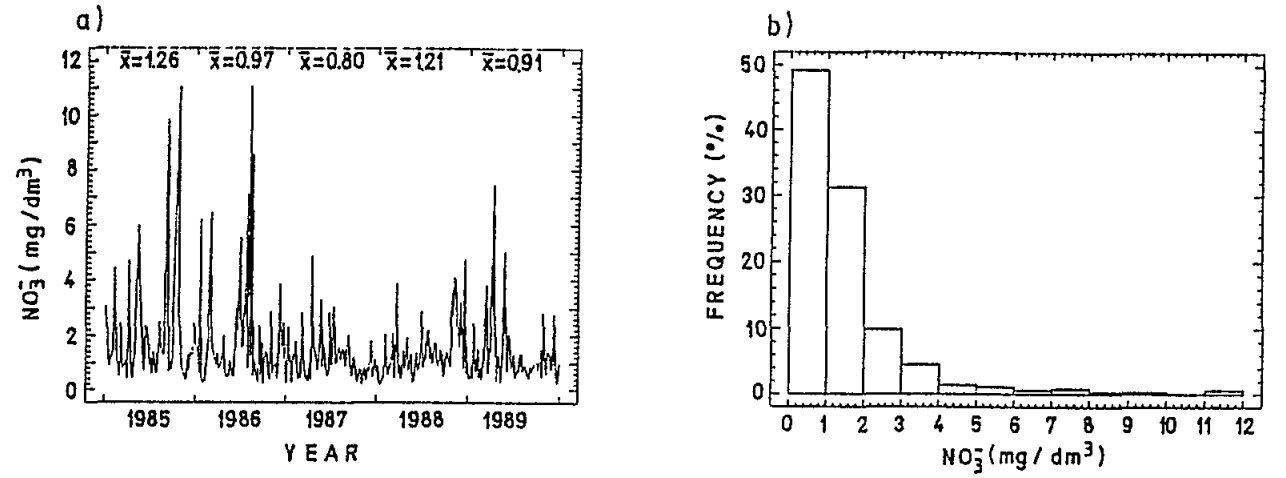

Fig.6 Annual course (a) and frequency histogram (b) of nitrate ion concentrations in daily samples at Rijeka for the period 1985-1989. (Numbers on the figure (a) are annual precipitation-weighted means).

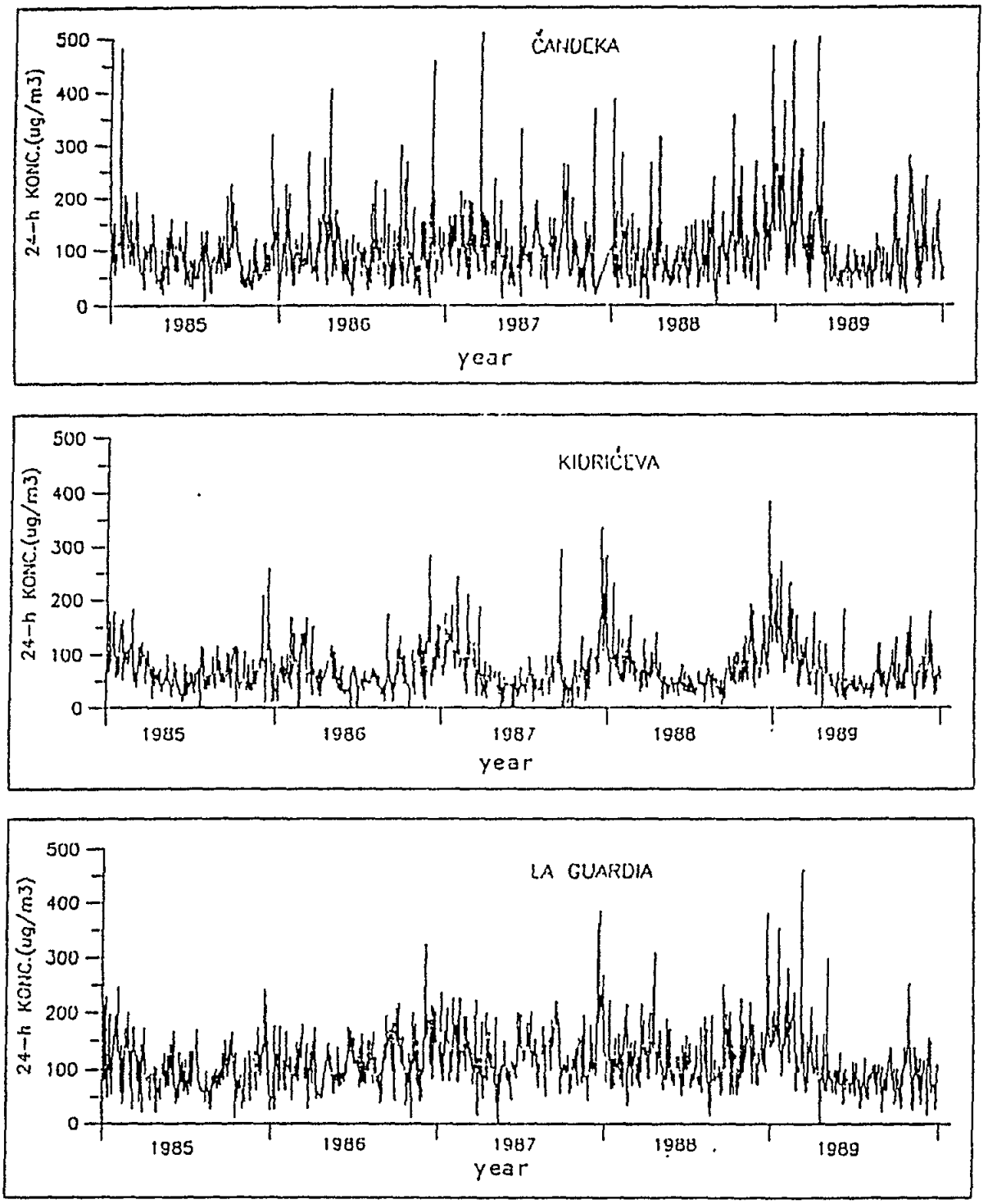

Fig.7 Annual course of mean daily SO_2 concentrations at three urban measuring sites at Rijeka for the period 1985-1989.

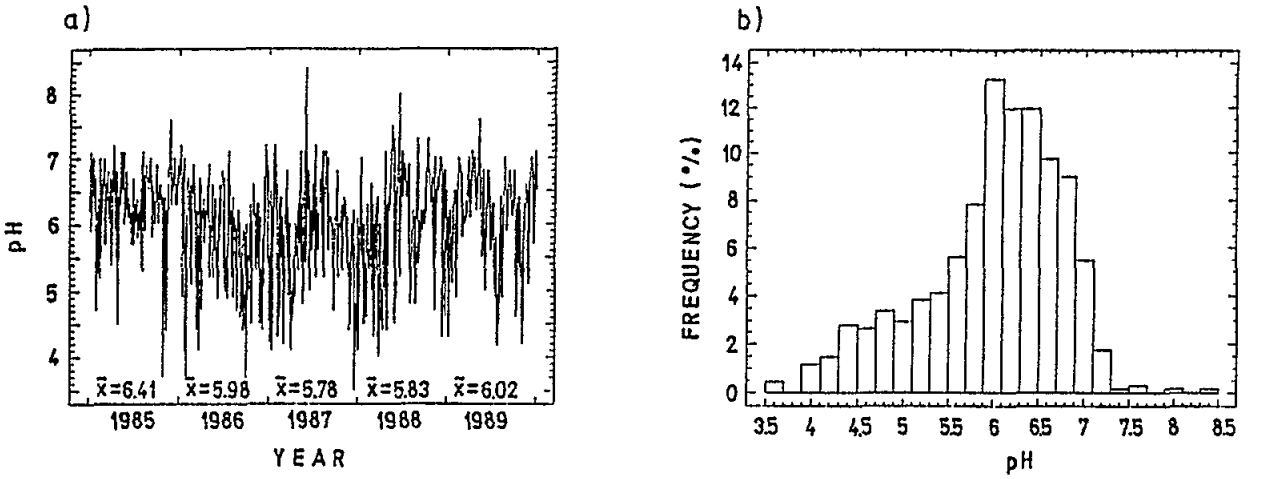

Fig.8 Annual course (a) and frequency histogram (b) of pH values from daily samples at Zavižan (1,594 m) for the period 1985-1989. (Numbers on the figure (a) are annual precipitation-weighted means).

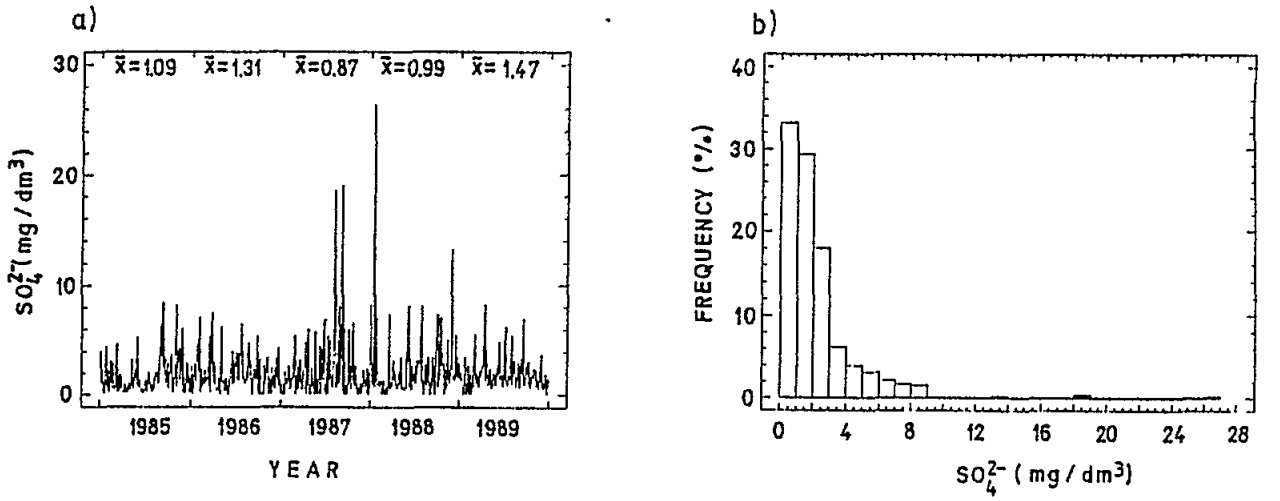

Fig.9 Annual course (a) and frequency histogram (b) of sulphate ion concentrations in daily samples at Zavižan (1,594 m) for the period 1985-1989. (Numbers on the figure (a) are annual precipitation-weighted means).

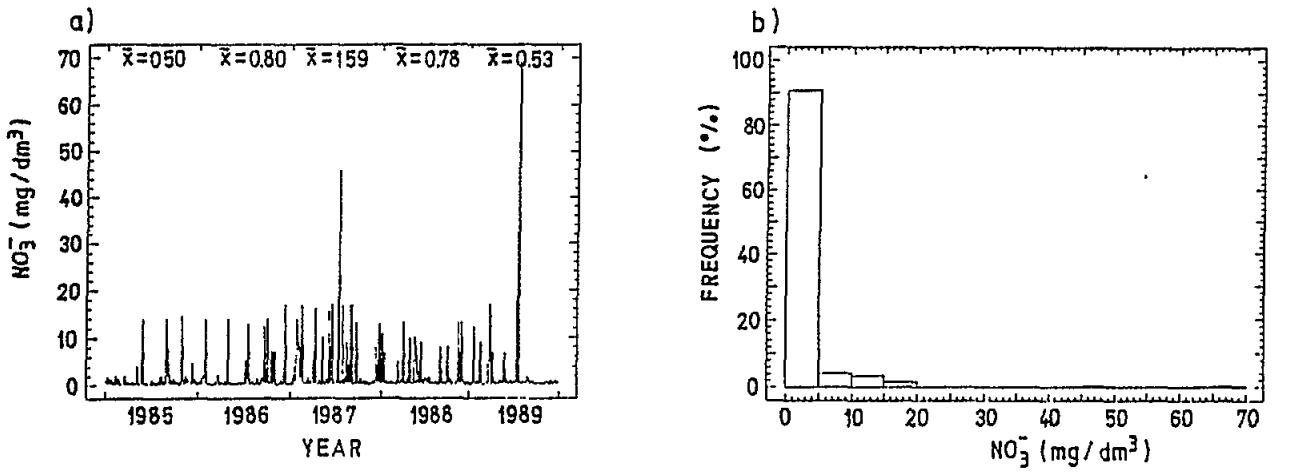

Fig.10 Annual course (a) and frequency histogram (b) of nitrate ion concentrations in daily samples at Zavižan (1,594 m) for the period 1985-1989. (Numbers on the figure (a) *are annual precipitation-weighted means*).

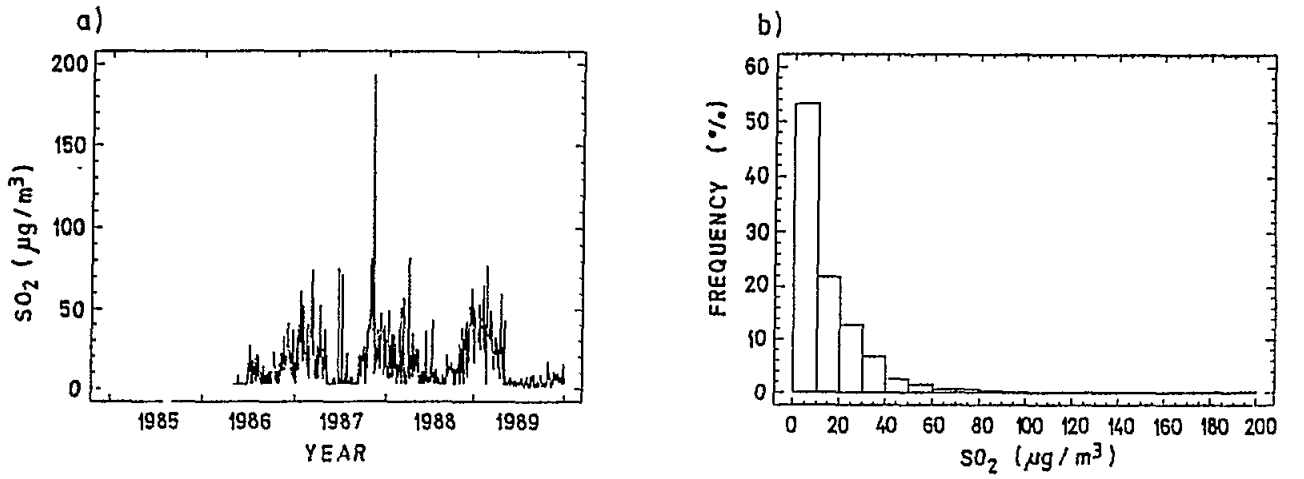

Fig.11 Annual course (a) and frequency histogram (b) of SO_2 daily mean concentrations at Veli Lošinj for the period 1986-1989.

! pH

On the basis of cumulative frequency distribution of pH data from precipitation samples (Fig.12), it can be seen that the acidity of precipitation at urban (P1-Rijeka) and island (P3-Veli Lošinj) sites differ slightly. Considering the fact that one is located in the centre of the polluted area (Rijeka) while the other one (Lošinj) is almost 100 km away from the coast, it could be assumed that precipitation acidity is not generally under the influence of locally generated pollution. However, under certain meteorological conditions, especially during the cold season, there are episodes of acid precipitation (pH < 4) at the urban area, being the result of local air pollution episodes persisting for several days.

The acidity of precipitation at Zavižan (P2) is generally lower than at Rijeka; however, pH > 7 are found more often at Rijeka than at two other sites (Fig.12). The lowest pH average values (Table 2) are found at Veli Lošinj (P3). The reason for this could be the two-year shorter data record. Nevertheless, it is significant to note that, according to the statistics, two sets of data (P1, P3) correspond as regards the acidity of precipitation.

Frequency distributions of pH values at sites P1 and P2 are presented in Figs.3, 4 and 8. The observed pH values are between 3.8-8.4 at Rijeka and 3.5-8.4 at Zavižan respectively. Precipitation-weighted annual mean at P1 was the lowest in 1987 (5.13) and the highest in 1989 (5.97). Most frequent were precipitation samples with pH values from 6.1-6.3 and 5.7-5.9, but it should be recognized that values of pH between 4.1-4.5 were often frequent too. The acid precipitation frequency (pH < 5.6) over the period of five years is 42%; particularly, the frequency of data in the range of 3.8-4.7 is about 17%.

The detailed analyses of pH frequency distribution data showed that, by dividing the sample in two parts, two normally distributed samples are obtained: precipitation data with pH less or equal to 4.7 are normally distributed, with an average of 4.3 and a standard deviation of 0.22, and precipitation samples with pH greater or equal to 5.6 are normally distributed too with an average of 6.4 and standard deviation of 0.54 (Fig.4). Bimodal frequency distributions of pH data are found also at Tamnava (Radiæ and Dudiæ, 1988) and Zagreb-Griè (in the centre of the city of Zagreb) stations (Lisac, 1986). It has been shown that frequency distributions of pH data which have an acid precipitation on average, obtain two pick values: one of 6.5 and the second of 4.5-5.

Some authors suggest that the pH of 5.6 is not appropriate to be the reference value for the rainwater without human influences (Charlson and Rodhe, 1982). In remote temperature regions of the world, the average rainfall acidity was found to be about 4.9 with individual episodes ranging from 4.0-6.0 (Galloway *et al.*, 1982). Those measurements, and a consideration of the natural sulphur cycle (Charlson and Rodhe, 1982) suggested that, in the absence of human activity, natural long-term mean acidity should be of the order of 5.0. As a result of man-made excess acidity, the pH values in industrial areas range between 4-5 (Georgii, 1981), depending on regional distribution of anthropogenic and natural pollution sources. The analyses of pH mean values in the European network exhibited the ranges from 4.2 in Sweden to 5.4 in France (Lisac, 1986, from NILU). Recent data analyses showed that the annual average acidity of the rain over Europe and the USA range from 4.1-5.1 (Smith, 1991).

Although industrially developed and locally polluted, Kvarner Bay area is on average still prevented from precipitation acidity. Nevertheless, episodic conditions occur. It has still to be proved that this area as a whole generates unfavourable pollution episodes and acid precipitation inland, causing forest decay. Regarding the precipitation acidity on the island

of Lošinj, it has also to be decided whether, and how often it happens as a result of the long-range transport of pollutants across the Adriatic Sea or as a consequence of pollution transport orientated towards the Mediterranean from the Kvarner Bay industrial area.

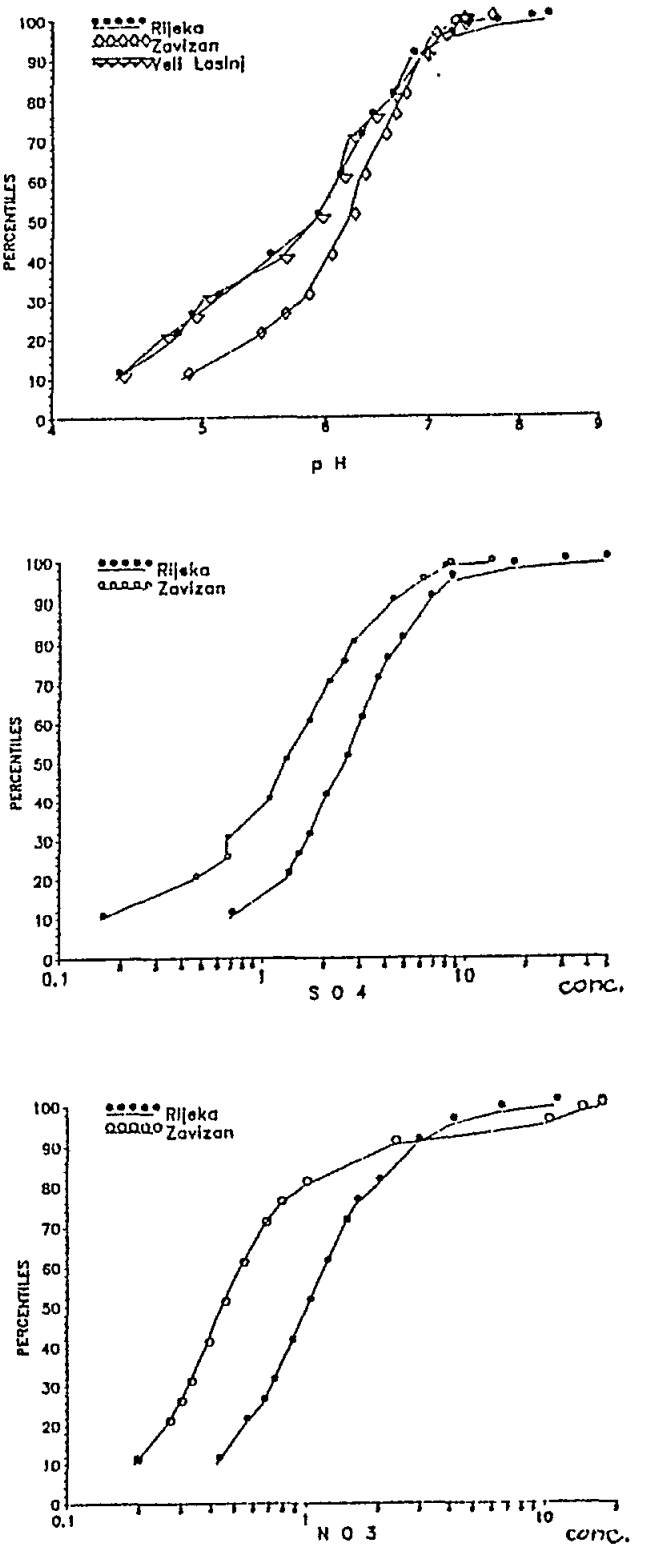

Fig.12 Distribution of percentile values for Rijeka, Zavižan and Veli Lošinj

! Sulphates

Concentrations of SO_4^{2-}-S ions in precipitation at Rijeka (P1) are in the high range of values (Fig.5a). The highest concentrations were found in 1989, the lowest in 1988. Extremely high concentrations were rarely sampled. Most frequent were concentrations of 1-2 mg/dm^3 (Fig.5b). Only 1% of daily samples have values higher than 30.3 mg/dm^3 during the whole period. The concentrations of SO_4^{2-}-S ions at Zavižan (P2) were almost two times lower than that at Rijeka (Figs.9(a) and 12). Only 1% of data were greater than 8.3 mg/dm^3, so the extreme values are rare (Fig.9(b).

SO_4^{2-}-S mean concentrations observed in the European network (1978-1982) varied from 0.21 mg/dm^3 in Norway to 2.65 in Yugoslavia. Sulphate concentrations lower than 1 mg/dm^3 were found in Ireland, Iceland, Norway, Sweden and Portugal, and greater than 2 mg/dm^3 in Yugoslavia, Romania, Hungary, Germany, Czechoslovakia and at 1 station out of 5 in France (NILU, 1984).

Annual mean sulphate concentrations at a rural station Retz (Austria) with no industry around were about 3-3.5 mg/dm^3, with the maximum in 1978 (5.89). It has been shown that in the year with the minimum amount of total precipitation, concentrations of SO_4^{2-}-S, NO_3^--N, NH_4^+-N, Ca^{2+}, Cl^- and other components were extremely high (Cehak and Chalupa, 1985). This was also the case at Rijeka: maximum sulphate concentrations were found in 1989 - the year with the minimum amount of total precipitation during the whole period. To avoid the impact of precipitation amount on the average of sulphate ion concentrations, the precipitation-weighted means are calculated as well (shown in Fig.5(a); the same for nitrates in Fig.6(a).

In the whole range of data, concentrations of sulphates in precipitation at Rijeka are significantly greater than those measured at Zavižan (Fig.12), which was expected.

! Nitrates

Concentrations of nitrate ions range between 0 and 11.06 mg/dm^3 (Fig.6(a)). The highest values are found in 1985 and the lowest in 1987. Most frequent were concentrations up to 1 mg/dm^3 (Fig.6(b)).

It is interesting that at Zavižan, the regional station, nitrate concentrations are greater than at Rijeka. Pick values are six times higher than that observed at Rijeka. Mean values are similar (Table 2) but frequency distributions show that higher concentrations occur more often at Zavižan. 5% of the samples have nitrate concentrations between 10 and 20 mg/dm^3 while at Rijeka only 1% of data have values greater than 8.55 (Fig.10(b), Fig.12).

For the comparison, the annual NO_3^--N concentration value at the rural station Retz (Austria) over the period of 26 years was about 0.70 mg/dm^3 and maximum (1978) was 2.32 mg/dm^3 (Cehak and Chalupa, 1985). At the Bavella Pass site (South Corsica) in November 1985, the analysis of 3.1 mm of rainfall sample showed a pH of 3.89, SO_4^{2-}-S concentration of 10.9 mg/dm^3 and NO_3^--N concentration of 8.1 mg/dm^3 (Loye-Pilot *et al.*, 1989). In this case, Authors showed that the atmospheric input was from the European continent.

4. CONCLUSION

Our analyses show that the area of Rijeka is rather polluted, especially from sulphur compounds (in the air as well as in precipitation), while pH values and nitrates are in the range of some other published results.

One of the main purposes of pollution analyses is to study the effects on the soil, vegetation and the human environment. In the case of precipitation, these effects can be followed through the sulphate and nitrate deposition rates. Deposition rates of sulphur in sulphates and nitrogen in nitrates for Rijeka and Zavižan are given in Table 3.

Table 3

Total annual deposition of sulphur from sulphates (S) and nitrogen from nitrates (N) (kg/ha) for Rijeka and Zavižan, 1985-1989

Site	1985		1986		1987		1988		1989		Totals	
	S	**N**	**S**	**N**	**S**	**N**	**S**	**N**	**S**	**N**	**S**	**N**
P1	30	13	35	10	32	11	25	14	44	10	165	59
P2	17	8	20	12	17	30	17	13	22	8	92	72

The permitted limit for annual wet sulphur deposition is 2-5 kg/ha (Acid Magazine, 1987). At Rijeka, deposition is for the order of magnitude higher. For instance, in the Atlantic Provinces of Canada, wet sulphate deposition exceeds 20 kg/ha per year (Beattie, Shaw and Whelpdale, 1987). At Zavižan, wet sulphur deposition was about two times lower than at Rijeka, but still much over the limited.

Nitrate depositions at both stations were in the range of 10-30 kg/ha, depending on the year.

One of the reasons for obtaining deposition values of that order might be the sampling method used (bulk samples).

According to data, it appears that the area of Kvarner Bay is rather polluted, especially the town of Rijeka itself. Because of the prevailing Northeast wind, the transport of pollution towards the Northern Adriatic could be significant. The analyses of meteorological conditions associated with air and precipitation pollution episodes are needed.

5. ACKNOWLEDGMENTS

We are very grateful to the Public Health Institute of Rijeka for providing the data of Veli Lošinj, and to colleagues in the Chemical Laboratory of the Hydrometeorological Institute of Croatia, for data and useful information provided. This work was partially supported by the Union for Scientific Research of Croatia.

6. REFERENCES

Aic Magazine (1987). No.1, Solna, Sweden, 13pp.

Bajiæ, A. (1989). Severe Bora on the Northern Adriatic, Part I: Statistical analysis, Papers, No.24, Zagreb, 1-9.

Bajiæ, A. (1989). Transport of pollutants considered from the point of view of a short and medium-range material balance. *Water, soil and air pollution*, 6:329-338.

Benarie, M. (1976). Transport of pollutants considered from the point of view of a short and medium-range material balance. *Water, Air and Soil Pollution*, 6:329-3338.

Carroll, J.J. and R.L. Baskett (1979). Dependence of air quality in a remote location on local and mesoscale transports : A case study. *Journal of Appl. Met.*, 18:474-486.

Cehak, K. and K. Chalupa (1985). Observations of various chemical contaminants of the precipitation at a BAPMoN station in the Eastern Pre-Alpine region. *Arch. Met. Geoph. Biocl. Ser*. B.35:307-322.

Ciattaglia, L. and L. Cruciani (1989). Review of chemical data by the Italian Meteorological Service, Airborne Pollution of the Mediterranean Sea, Report and Proceedings of a WMO-UNEP Workshop, MAP Technical Reports Series No.31:101-123.

Charlson, R.J. and H. Rodhe (1982). Factors controlling the acidity of natural rainwater. *Nature*, 295:683-685.

Clark, A.I. *et al.* (1988). Statistical analysis of gaseous air pollutant concentrations at urban, rural and motorway locations, *Env. Tech. Letters*, 9:1303-1312.

Davies, T.D. (1976). Precipitation scavenging of sulfur dioxide in an industrial area, *Atm. Env.*, 10:879-890.

Eliassen, A. *et al.* (1988). Estimates of airborne transboundary transport of sulphur and nitrogen over Europe, EMEP/MSC-W Report 1/88, Oslo, Norwegian Met. Inst.

Georgii, H.W. (1981). Review of the activity of precipitation according to the WMO-network, Idojaras, *Journal of the Hungarian Meteorological Service*, 35:1-9.

Högstrom, U. (1974). Wet fallout of sulfurous pollutants emitted from a city during rain or snow, *Atm. Env.*, 8:1291-1303.

Irvin, J.G. and M.L. Williams (1988). Acid rain : Chemistry and Transport, *Environmental Pollution*, 50:29-59.

Klein, W.H. (1957). Principal tracks and mean frequencies of cyclones and anticyclones in the Northern Hemisphere, *Res. Pap. Weather Bureau*, US Dept. of Commerce, Washington D.C., No.40.

Lamb, B.K., A. Lorenzen and F.H. Shair (1979). Atmospheric dispersion and transport within coastal regions - Part I: Tracer study of power plant emissions from the Oxnard plain. *Atm. Env.*, 12:2089-2100.

Lisac, I. (1986). The acid rain statistic over broader area of the city of Zagreb, ICAM, Rauris, Sept. 1986.

Logan, J.A. (1983). Nitrogen oxides in the troposphere : global and regional budgets. *J. Geophys. Res.*, 88:-785-807.

Loye-Pilot, M.D., J. Morelli and J.M. Martin (1989). Results related to rain chemistry in South Corsica, Airborne Pollution of the Mediterranean Sea, Report and Proceedings of a WMO/UNEP Workshop, MAP Technical Reports Series No.31:125-138.

Müller, D. (1984). Estimation of the global man-made sulphur emission. *Atm. Env.*, 18:19-27.

NILU (1984). Summary report from chemical coordinating centre for the second phase of EMEP, EMEP/CCC - Report 2/84, Apr. 1984, 119.

Novakoviæ, J. *et al.* (1983). Meteorološka podloga za izradu idejnog projekta željezniènog èvorišta Rijeka (Analysis of meteorological data used for the project for railway crossing, Rijeka), Hydrometeorological Institute of Croatia, Zagreb.

Radiæ, N. and V. Dudiæ(1988). Kiselost padavina na teritoriji SR Srbije za period 1982-1987 (Acid precipitations at Serbia for the period 1982-1987), I Jug.savetovanje "Tehnièka kultura u zaštiti i unapredenju èovekove sredine, Belgrade, June 1988.

Radinoviæ, Ð. (1962). Analysis of the cyclogenetic effects in the Western Mediterranean, Bled, VI Congress Internat. Meteor. Alpine, 33-40.

Reid, J.D. (1978). Studies of pollutant transport and turbulent dispersion over rugged mountainous terrain near Climax, Colorado. *Atm. Env.*, 13:23-28.

Smith, F.B. (1991). An overview of the aic rain problem. *The Meteor. Magaz.*, 120:77-91.

Speranza, A. (1975). The formation of baric depression near the Alps. *Annali di Geof.*, 28:3-29.

Tibaldi, S. (1980). Cyclogenesis in the lee of orography and its numerical modelling with special reference to the Alps, Orographic effects in planetary flows, GARP Publications Series, No.23, Chapter 7, WMO, June 1980.

Vidiè, S. i sur. (1991). Meteorološki monitoring rijeèkog podruèja (Meteorological monitoring of the area of Rijeka), Idejni projekt, Centar za meteorološka istraživanja, Hydrometeorological Institute of Croatia, Zagreb, 78 pp.

Vuèetiæ, V. (1988). Analiza vjetrovnog režima na mostu preko Rjeèine (The analyses of wind regime on the Rjeèina bridge), Hydrometeorological Institute of Croatia, Zagreb.

Zannetti, P., P. Melli and E. Runca (1977). Meteorological factors affecting SO_2 pollution levels in Venice. *Atm. Env.*, 11:605-616.

WMO (1978). International operations handbook for measurement of background atmospheric pollution, Geneva, No.491.

TROPOSPHERIC OZONE IN THE ADRIATIC REGION

By

J. JEFTIÆ, LJ. PAŠA-TOLIÆ, D. SRZIÆ, D. TILJAK, T. CVITAŠ and L. KLASINC

Rudjer BoškoviæInstitute
YU-41001 Zagreb
Croatia, Yugoslavia

A B S T R A C T

Tropospheric ozone was monitored in 5 places along the Adriatic coast during the summer of 1990. The places were chosen so as to be representative of tourist resorts at different distances from larger pollution sources. One site was in Rovinj, a small Mediterranean town and important tourist centre in the northern Adriatic, one was on the island Krk in Malinska relatively close to the city of Rijeka, another was on the island of Iz in the central Adriatic which can be considered as isolated from larger pollution sources, and two were in the southern Adriatic in Makarska on the coast and in Hvar on the island Hvar, both tourist resorts. The incidence of high ozone concentrations was found to be much greater in the north than in the south of the Adriatic. The analysis shows that, even in relatively remote sites, such as Iz, high ozone concentrations could be measured on a few occasions. By taking into account the time of day and wind directions during the peak ozone concentrations, it appears that ozone is formed locally at such sites and that significant amounts of precursors must therefore be present.

1. INTRODUCTION

While considerable attention has been paid to the pollution of the sea, the photochemical pollution of the air in the Mediterranean region has largely been neglected. However, during the summer months, considerable pollution is being formed within and close to the urban centres. Well known examples of such photochemical pollution are Athens(Cvitaš *et al.*, 1985; Güsten *et al.*, 1988), Tel-Aviv (Ganor *et al.*, 1975; Steinberger *et al.*, 1980) and Jerusalem (Steinberger *et al.*, 1980).

Reports on air pollution measurements have been sporadic and far too few (Giovanelli *et al.*, 1981; Deželjin *et al.*, 1981; Butkoviæ*et al.*, 1990; Zerefos *et al.*, 1989; Bouscaren, 1991). Hardly any reports have been published on measurements of components of photochemical air pollution in non-urban areas of the Mediterranean region (Božièviæ*et al.*, 1978; Cvitaš and Klasinc, 1979; Novak and Sabljiæ, 1981; Rušèiæand Srziæ, 1981; Kovaè and Marèec, 1983), although it is well known that ozone as the dominant component of photochemical smog can be transported over long distances (Güsten, 1986). An adequate coverage of the Mediterranean region with respect to photochemical pollution monitoring is not envisaged, even in the recent international environmental research and monitoring programmes (Keune, 1991). Based on ground-level measurements, it is known that the average tropospheric ozone concentration is increasing in the northern hemisphere (Hough and Derwent, 1990). By comparing data obtained

from measurements at the end of the last century with present ones, it can be seen that tropospheric ozone concentrations have more than doubled (Volz and Kley, 1988; Lisac and Grubišiæ, 1991). In the Mediterranean region this can be expected to be even worse since, especially during the summer months, the population density and anthropogenic emissions increase here more than elsewhere in Europe.

In an attempt to obtain an insight into the level of tropospheric ozone concentrations outside urban centres in the Adriatic region, we monitored ozone at four sites for short periods of time (10-14 days) and in one site for almost three months (86 days) during the summer of 1990. This is a report of the results obtained.

2. MEASUREMENTS

Ozone was monitored at five places along the Adriatic coast. The places were chosen so as to be representative of tourists resorts at difference distances from larger pollution sources. Starting from the north, one site was in Rovinj, a small Mediterranean town and important tourist centre in the northern Adriatic. The monitoring took place there from 21 August to 2 September 1990. The second site, where monitoring took place between 7 and 17 August, was on the island Krk in Malinska, relatively close (25 km SSE) to the city of Rijeka. The main monitoring site was on the island of Iz in the central Adriatic, which can be considered as isolated from larger pollution sources. Ozone was monitored on Iz during 86 days from 27 April to 21 July 1990. Two further sites were in the southern Adriatic in Makarska on the coast and in Hvar on the island Hvar, both important tourist resorts. The instrument was installed in Hvar from 25 July to 7 August and then transferred to Makarska to be used there from 10 to 20 August. The monitors used were of commercial origin: Dasibi AH 1003 and 1008 PC based on UV absorption used in Iz, Hvar and Makarska, and Bendix 8002 based on the chemiluminescent reaction of ozone with ethylene used in Malinska and Rovinj. The Dasibi instruments have a reliable internal calibration system, and the Bendix instrument was calibrated against a Dasibi and the neutral potassium iodide method (Hodgeson *et al.*, 1971). The measured values have been plotted on a chart recorder and the hourly average ozone volume fractions in the air have been determined therefrom.

3. RESULTS AND DISCUSSION

Fig.1 shows the average diurnal behaviour of ozone volume fraction during the corresponding monitoring periods at the respective sites. The values obtained in the northern region (top diagrams) are considerably higher than those in the southern sites (bottom diagrams).

The characteristic diurnal behaviour with maximum values around noon are indicative of photochemical production. The autocorrelation functions (Fig.2) show it more explicitly, except in the case of Rovinj where exceptionally high values have been measured almost during the whole monitoring period.

When interpreting the data with respect to the wind directions, it was found that in the short monitoring periods (shorter than one month) too few data points were collected to draw reliable conclusions. We shall therefore focus our discussions on the data obtained for the island Iz.

A more complete description of the data than that provided by the average diurnal behaviour is shown in Fig.3 by the so-called "box and whiskers" representation (Jeftić and Cvitaš, 1991). It can be seen from the asymmetry of the vertical bars that there must have been days with significantly higher than average concentrations. Indeed, if the deviations from average behaviour are analyzed and the days classified accordingly, it can be seen that there was a period of 6 consecutive days (6-11 May) when ozone volume fractions exceeded 90 ppb, the peak values ranging from 95 to 106 ppb between 13 and 18 hours of the day. The wind blew mainly from the southwest, i.e. from the sea, at 2-5 ms^{-1}, as is usual for that part of the day. Since there are no major sources of ozone precursors to the southwest of Iz and peak values are observed in the early afternoon, it can be concluded that ozone has been produced locally. Obviously, relatively large amounts of precursors seem to be present even in remote sites of the Adriatic, so that significant amounts of ozone can be formed photochemically under favourable conditions.

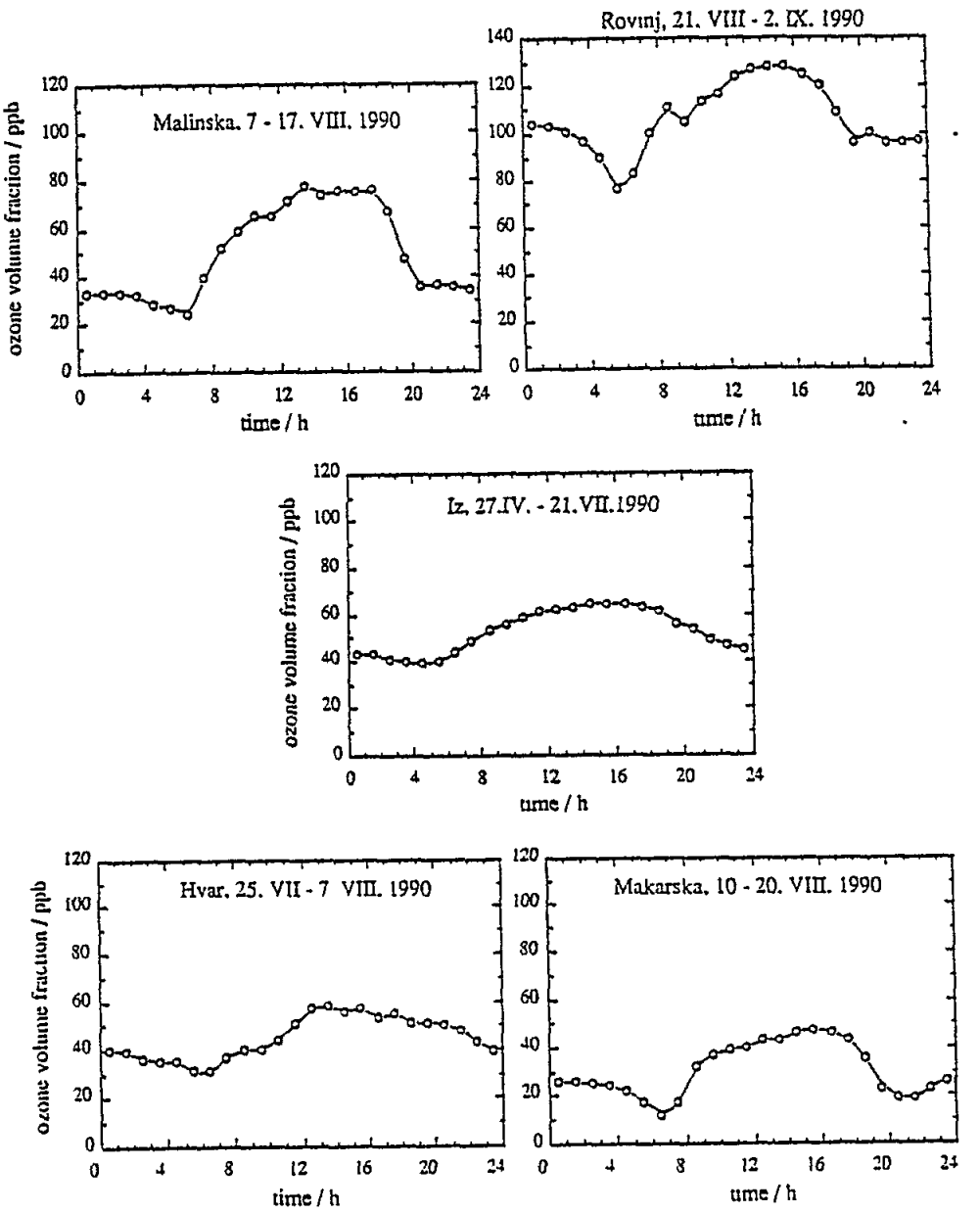

Fig.1 Average diurnal behaviour of ozone volume fractions at five sites on the Adriatic Sea

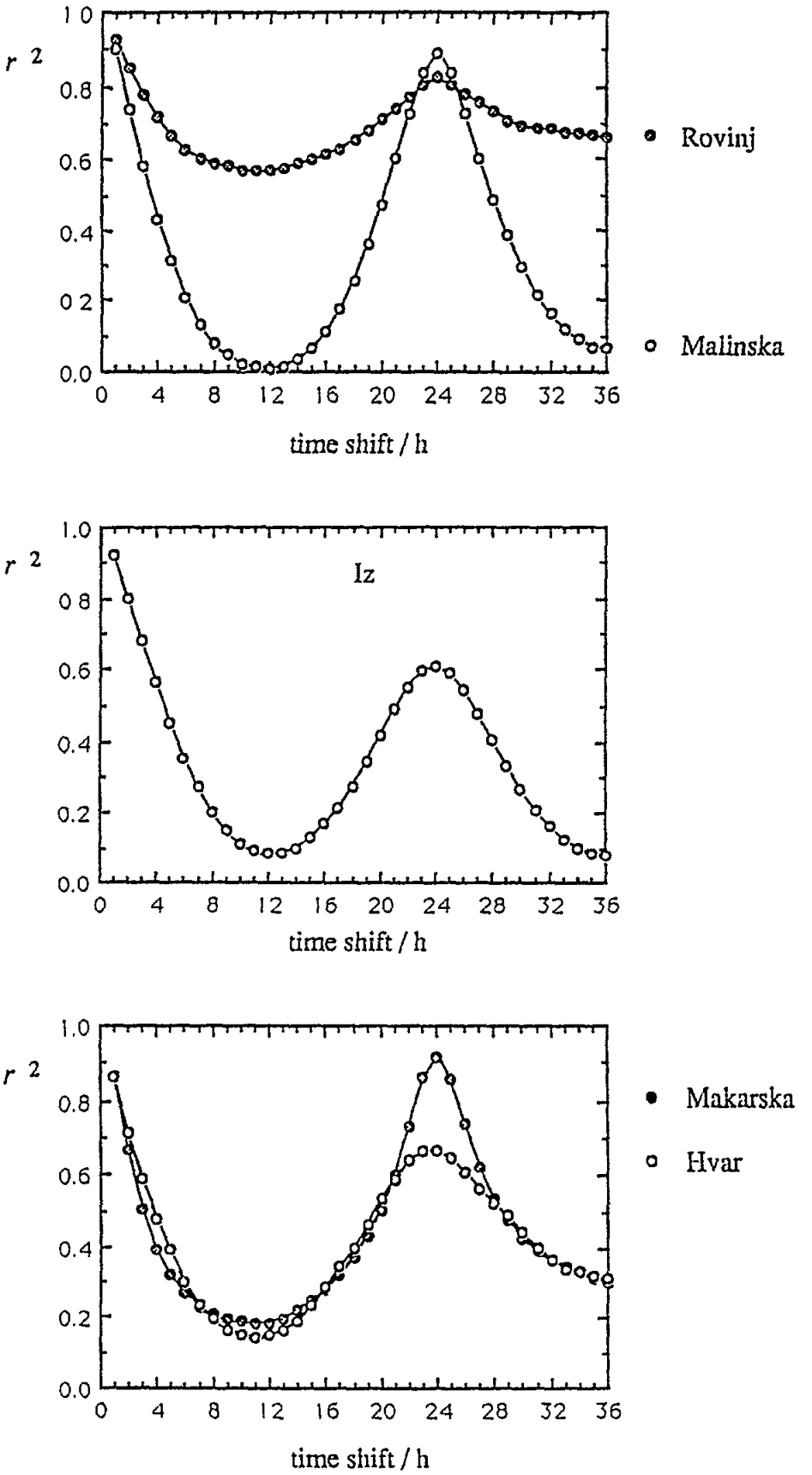

Fig.2 Autocorrelation functions for the hourly average ozone data obtained at five monitoring sites.

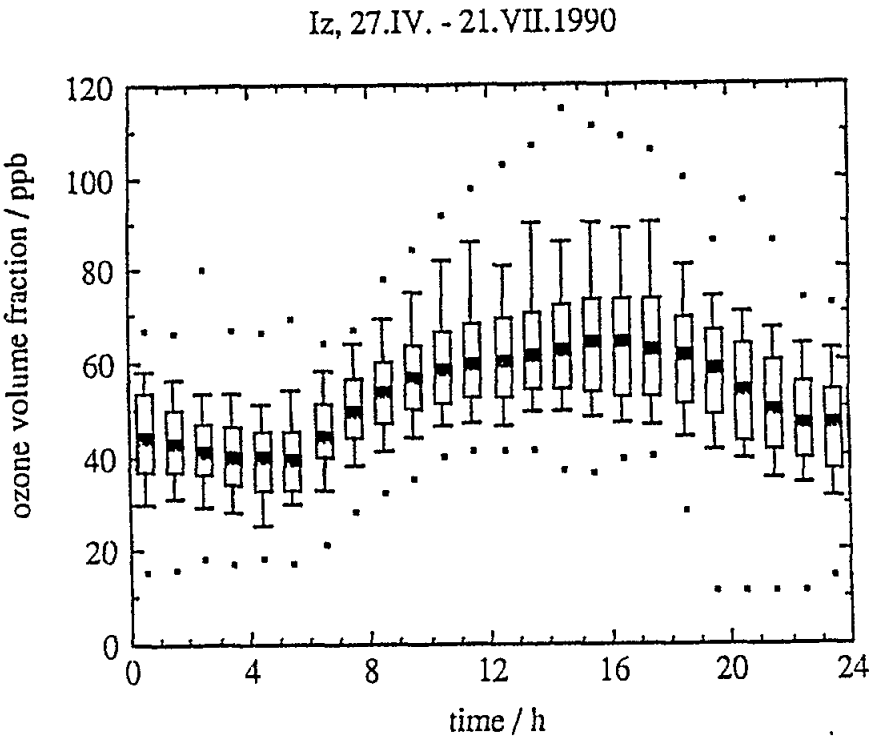

Fig.3 Diurnal behaviour of ozone volume fractions at Iz. The black central squares indicate the median, the bottom and top edges of the rectangles the first and third quartiles, the bottoms and tops of the bars the first and ninth deciles, and the dots the minimum and maximum values respectively.

The wind rose measured in Sibenik during the monitoring period is shown in Fig.4 (top). If the average ozone volume fractions during each wind direction are plotted as a function of wind direction, a diagram is obtained which indicates that the average values are between 40 and 50 ppb when the wind blows from the north to south-southeast, and above 60 ppm when it blows from south-southwest to west (Fig.4, bottom left diagram). However, one has to take into account that the wind pattern in coastal areas has also a diurnal behaviour in that it blows from the sea during the day and from the land during the night. We therefore plotted the average relative deviations from typical behaviour, as given in Fig.1 (centre), as a function of wind direction (Fig.4, bottom right). It can be seen that positive deviations are associated with the winds from the southwest, but on the average they are less than 10% and mainly caused by the behaviour on the six mentioned days in early May. No major positive deviations from typical behaviour were observed that could be associated with the wind from the Yugoslav mainland.

4. CONCLUSIONS

Based on relatively short monitoring periods, it can be concluded that ozone concentrations are higher in the northern than in the southern part of the Adriatic. This conclusion has however to be verified during longer and simultaneous monitoring periods.

Ozone volume fractions of over 100 ppb could be measured even in remote sites unaffected by nearby urban areas on 5 to 10% of the days. These high values are caused

by local production from precursors which seem to be present in sufficient amounts in most of the area. Further studies of ozone concentrations and preferably also of its precursors in background stations in the Mediterranean region, are desperately needed in order to understand the problems of photochemical pollution in this area.

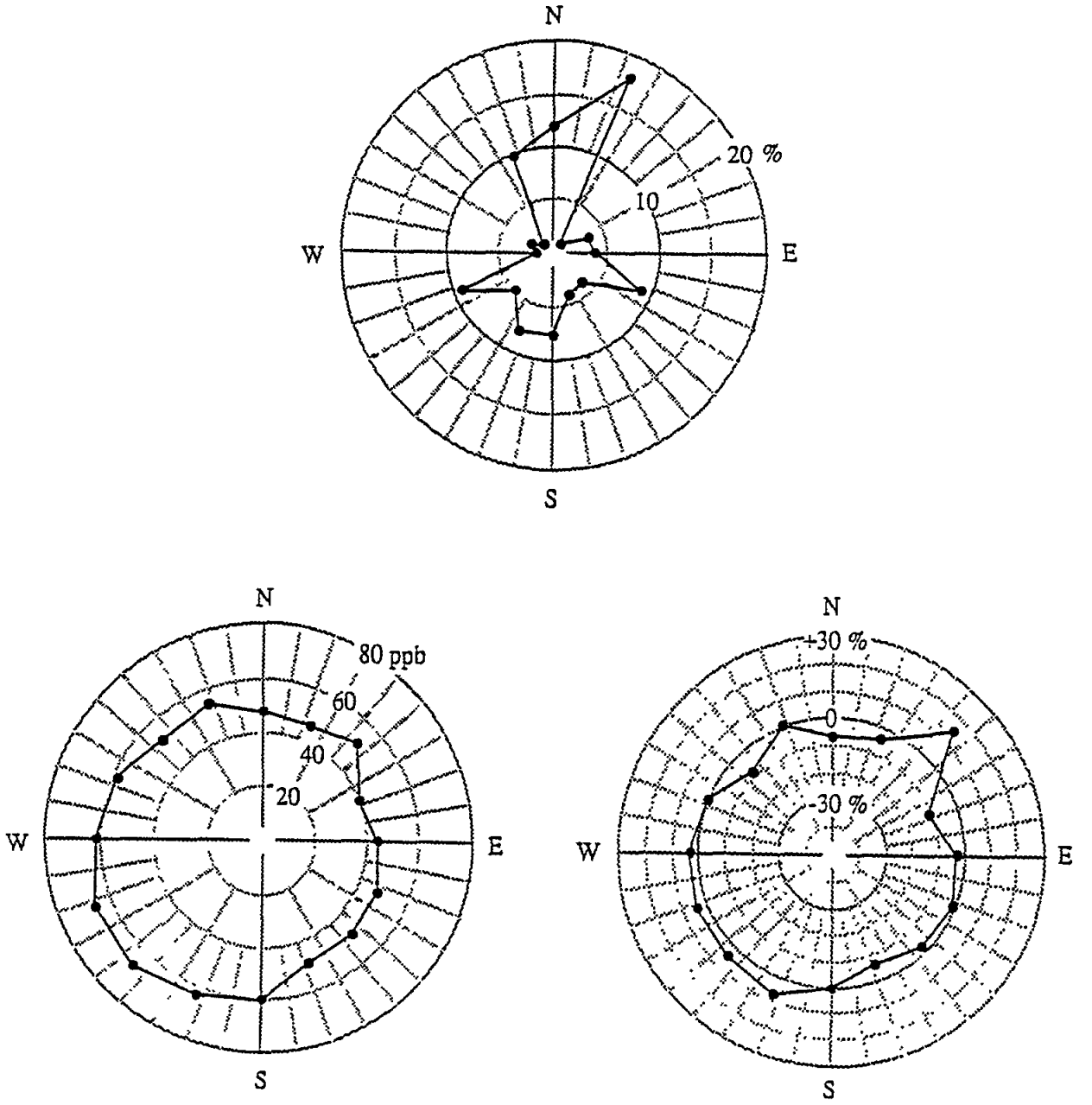

Fig.4 The wind rose for Sibenik during the period 27 April - 21 July 1990 (at the top), average ozone volume fractions for different wind directions at Iz (bottom left) and average relative deviations from typical behaviour for different wind directions at Iz.

5. REFERENCES

Bouscaren, R. (1991). The problems related with the photochemical pollution in the southern EC member states. *CITEPA Report 071-4/4/91*, Centre Interprofessional Technique d'Etudes de la Pollution atmosphérique, 3 Rue Henri Heine, 75016 Paris, 1991.

Božièeviæ, Z., T. Cvitaš and L. Klasinc (1978). Ozone in the lower atmosphere at Omisalj. *Proc. 5th Int. Symposium* "Chemistry of the Mediterranean", Rovinj, 1978.

Butkoviæ, V. T. Cvitaš and L. Klasinc (1990). Photochemical ozone in the Mediterranean. *Sci. Tot. Environ.*, 99:145-151.

Cvitaš, T. and L. Klasinc (1979). "Trenutni snimak" zagadjenja zraka u Kvarnerskom zaljevu. *Zastita atmosfere*, 15:13-16.

Cvitaš, T., H. Güsten, G. Heinrich, L. Klasinc, D.P. Lalas and M. Petrakis (1985). Characteristics of air pollution during the summer in Athens, Greece. *Staub-Reinhalt. Luft. 45*, 297pp.

Deželjin, S., V. Gotovac and T. Cvitaš (1981). Ozon u Splitskom zraku, *Kem. Ind. (Zagreb)*, 30:57-61.

Ganor, E., Y.(R.E.) Beck and A. Donagi (1978). Ozone concentrations and meteorological conditions in Tel-Aviv, 1975. *Atmos. Environ.*, 2:1081-1085.

Giovanelli, G., F. Fortezza, L. Minguzzi, V. Strocchi and W. Vandini (1981). Photochemical ozone transport in an industrial coastal area, *Proc. Second Symposium*, Varese, Italy, 1981. Physico-chemical behaviour of atmospheric pollutants, D. Riedel Publ. Co., Dordrecht.

Güsten, H. (1986). Formation, transport and control of photochemical smog. In: *The Handbook of Environmental Chemistry, Vol.4/Part A*, Springer Verlag, Berlin 1986, pp.53-105.

Güsten, H., G. Heinrich, T. Cvitaš, L. Klasinc, B. Rušèiæ, D.P. Lalas and M. Petrakis (1988). Photochemical formation and transport of ozone in Athens, Greece. *Atmos. Environ.*, 22:1855-1861.

Hodgeson, J.A., R.E. Baumgardner, B.E. Martin and K.A. Rehne (1971). Stoichiometry in the neutral iodometric procedure for ozone by gas-phase titration with nitric oxide. *Anal. Chem.*, 43:1123-1125.

Hough, A.M. and R.G. Derwent (1990). Changes in the global concentration of tropospheric ozone due to human activities. *Nature*, 344:645-648.

Jeftiæ, J. and T. Cvitaš (1991). Analysis of ozone monitoring data. *J. Math. Chem.*, 9 (in press).

Keune, H. (1991). *A survey of environmental monitoring and information management programmes of international organizations*, 2nd edition, UNEP-HEM Office, GSF, Ingolstädter Landstr. 1, D-8042 Neuherberg, 1991.

Kovaè, B. and R. Marèec (1983). "Trenutni snimak" zagadjenja zraka u Kvarnerskom zaljevu 1981. *Kem. Ind. (Zagreb)*, 32:569-574.

Lisac, I. and V. Grubišiæ(1991). An analysis of surface ozone data measured at the end of the 19th century in Zagreb, Yugoslavia. *Atmos. Environ.*, 25A:481-486.

Novak, I. and A. Sabljiæ(1981). "Trenutni snimak" zagadjenja zraka u Kvarnerskom zaljevu 1979. *Kem Ind. (Zagreb)*, 30:5-8.

Rušèiæ, D. and D. Srziæ(1981). "Trenutni snimak" zagadjenja zraka u Kvarnerskom zaljevu 1980. *Nafta*, 32:641-646.

Steinberger, E.H. and E. Ganor (1980). High ozone concentrations at night in Jerusalem and Tel-Aviv. *Atmos. Environ.*, 14:221-225.

Volz, A. and D. Kley (1988). Evaluation of the Montsouris series of ozone measurement made in the nineteenth century. *Nature*, 332:240-242.

Zerefos, C.S., I.C. Ziomas, A.C. Bais, G.T. Amanatidis and A.G. Kelessis (1989). Chemical oxidants in air of northern Greece in relation to meteorological and solar flux conditions. *Toxicol. Environ. Chem.*, 20-21:3-9.

POTENTIAL AIRBORNE LONG-RANGE CADMIUM TRANSPORT INTO THE MEDITERRANEAN REGION

By

SLOBODAN NIČKOVIĆ[1], ZAVIŽA I. JANJIĆ[2], MILAN DRAGOSAVAC[3]*
SLAVKO PETKOVIĆ[3], SVETLANA MUSIĆ[3] and BORIVOJE RAJKOVIĆ[4]

(1) Institute of Physics, Atmospheric Research Laboratory, Zemun.
(2) Institute of Meteorology, University of Belgrade.
(3) Federal Hydrometeorological Institute, Belgrade.
(4) Institute of Meteorology, University of Belgrade.

1. GENERAL OVERVIEW

It is generally recognized that long-range atmospheric transport of various contaminants can contribute significantly to the pollution of the Mediterranean Sea. In this respect, the major industrial centres on the European continent are obvious first suspects as potential sources.

Contaminants of major concern are heavy metals and metaloids such as Pb, Cd, Hg, As and Sn, petroleum hydrocarbons, chlorinated hydrocarbons and pathogenic micro-organisms. The atmospheric lifetime of such materials is typically long enough (more than one day) to allow them to be transported far from their sources by synoptic scale processes (greater than 1,000 km). In this context, the lower part of the atmosphere is presumably the preferred transport environment.

Apart from chemical and photochemical transformations, the important process affecting the distribution of the contaminant in the atmosphere are: turbulent mixing, advection (horizontal and vertical) and deposition (dry and wet). It should be noted that sophisticated forecasting models already include parameterizations of a number of relevant physical processes, such as turbulence and precipitation. Thus, they represent a natural, and potentially very powerful tool for studying the propagation of the contaminants in the atmosphere. However, due to the computational resources needed, and many uncertainties concerning the initial distribution of the contaminants and the properties of the major sources, as well as the complexity of the transformation processes, this Eulerian approach has not been extensively used, particularly in routine applications.

Instead, a simpler, Lagrangian (or trajectory) method is often applied in order to estimate the long-range atmospheric transport. For this purpose, analyzed or prognostic wind fields are used as large-scale driving parameters. The computed trajectories may be either only horizontal or 3-dimensional, depending on whether the vertical velocity component is included. The trajectories may be computed forward and/or backward in time. With forward calculation, the trajectory starts at the source of the contaminant and follows the path of the contaminated air parcel. On the other hand, starting from the location of interest, the backward trajectories give the information on the possible origins of the contamination.

---

* Current affiliation, ECMWF, Reading, U.K.

In spite of very crude assumptions concerning the turbulent mixing and deposition, the simple Lagrangian models produced remarkably good results in some applications (e.g., Eliassen and Saltbones, 1983).

2. OBJECTIVES AND BASIC APPROACH

The general objective of the present study is to provide preliminary information relevant for the investigation of the synoptic scale horizontal transport of a pilot tracer into the Mediterranean region. Following the suggestions of GESAMP (GESAMP, 1985), cadmium was chosen as the tracer.

Within the framework of the study, horizontal trajectories were calculated at 920 and 850 hPa pressure levels. Two groups of the trajectories were considered:

(a) Forward trajectories starting from several major cadmium sources in Europe (Fig.1, heavy dots) identified in the report by Pacyna (1985); and

(b) Backward trajectories starting from the points regularly spaced in the longitudinal direction along the European coast of the Mediterranean Sea (Fig.1, crosses).

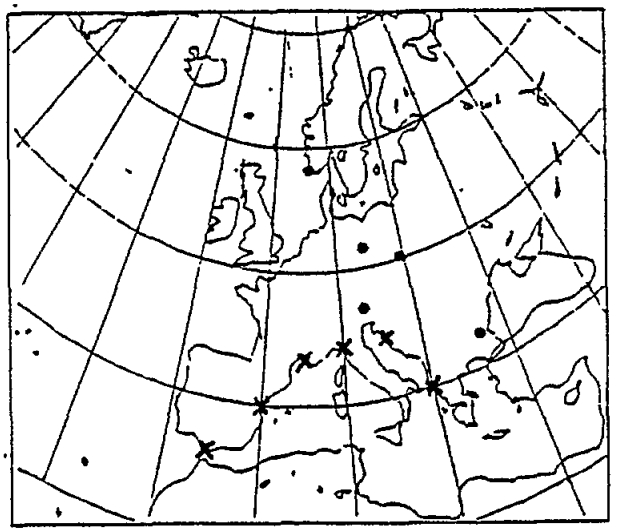

Fig.1 Cadmium sources in Europe for which the forward trajectories are calculated (•), and the arrival points of the backward trajectories (X).

3. THE MODEL USED TO PRODUCE THE DRIVING WIND FIELD AND THE TRAJECTORY COMPUTATION

The operational sigma coordinate version of the HIBU (Hydrometeorological Institute and Belgrade University) limited area model is used to produce overlapping sequences of the forecast wind fields with the forecast period of up to 36 hours. The model is defined on a semi-staggered Arakawa E grid. The technique for preventing the elementary grid separation (Mesinger, 1973, 1974; Janjić, 1974, 1979) is used in combination with the split-explicit time differencing scheme (e.g., Janjić, 1979). The horizontal advection scheme has a built-in strict non-linear energy cascade control (Janjić, 1984). Special care was taken to reduce the pressure gradient force error in the sigma system in the presence of steep mountains (Janjić, 1977, 1980). As usual, a simple brute-force method is used at the lateral boundaries. In addition, upstream advection is applied at several rows of grid-points along the boundaries. In order to increase the computational efficiency, the model uses the rotated latitude-longitude coordinate system.

This version of the model has a very simple physical package consisting of straight-forward formulations of the surface drag and vertical turbulent transport of momentum. The dry convective adjustment is also included. Realistic representation of mountains is used. The model is dry.

The integration domain, shown in Fig.2, covers the West Atlantic, most of the European continent and the Mediterranean region. The horizontal resolution is about 170 km. The model has eight equidistant layers in the vertical, and the top of the model's atmosphere is located at the 200 hPa level. The restricted amount of the forecast products of the European Centre for the Medium-range Weather Forecasts was used to specify the lateral boundary conditions.

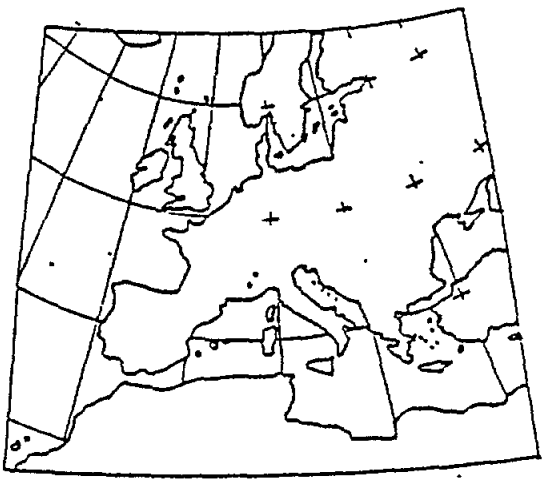

Fig.2 The integration domain

The model produced forecast data are recorded every three hours during the forecast period. After completion of the forecast calculations, the data from the model history file are converted from sigma to pressure coordinate system, and the pressure coordinate file thus

obtained is then used as the interface for various applications, including the trajectory calculations.

The forward/backward trajectories are calculated using "first-forward/backward-then-centered" time differencing technique. Namely, the preliminary location of the point on the trajectory at the end/beginning of each three-hour time step is calculated forward/backward by the formula:

$$x^*(t\pm\Delta t) = x(t)\pm\Delta t\, u[x(t),y(t)]$$

$$y^*(t\pm\Delta t) = y(t)\pm\Delta t\, v[x(t),y(t)]$$

Here, x and y are the horizontal coordinates, t is time, Δt is the time step, u and y are the velocity components, and the asterisks denote the preliminary values of the horizontal coordinates. The values of velocity at the beginning/end of the period, and at the preliminary ending/starting point area averaged, and this average velocity is then used to calculate the final location of the ending/starting point, i.e.:

$$x(t\pm\Delta t) = x(t)\pm\Delta t\{u[x(t),y(t)] + u[x^*(t\pm\Delta t),y^*(t\pm\Delta t)]\}/2$$

$$y(t\pm\Delta t) = y(t)\pm\Delta t\{v[x(t),y(t)] + v[x^*(t\pm\Delta t),y^*(t\pm\Delta t)]\}/2$$

Within this process, the check is made whether a model mountain is intersecting the forward/backward trajectory. If so, it is assumed that the particle reaches/comes from the obstacle. The particle does not move further until the wind direction is changed.

If a particle reaches the boundary of the integration domain, the trajectory calculation is terminated.

The routine calculation of the trajectories reported here commenced on 1 October, 1987 and ended on 30 September 1988. The forward and backward trajectories were calculated at the 920 and 850 hPa levels. After converting the coordinates of the points on the trajectories from the transformed coordinate system used in the model, into the regular latitude-longitude coordinates, the trajectories were accumulated in a specially designed database needed for subsequent processing.

4. EXAMPLES OF THE RESULTS

The analysis of the results of the forward trajectory calculations is performed separately for the four seasons. The seasons are defined as "Autumn" - 1 October to 31 December; "Winter" - 1 January to 31 March; "Spring" - 1 April to 30 June; and "Summer" - 1 July to 30 September.

The percentages of the trajectories reaching the Mediterranean Sea for the five locations considered (Stavanger, Norway; Dresden, FRG; Kraków, Poland; Salzburg, Austria; and Dimitrovgrad, Bulgaria) are summarized in Table 1 according to the starting point, pressure level and season.

As an illustration, summer trajectories for Stavanger (Fig.3), Salzburg (Fig.4) and Dimitrovgrad (Fig.5) are displayed. As can be seen from Fig.3, Stavanger is apparently too far away to be able to influence the transport on the time-scales considered.

The Salzburg trajectories at the 920 hPa level are missing in all seasons. This is because the model topography extends above this level at this point. Fig.4 shows that the 850 hPa trajectories reaching the Mediterranean region in summer are channelled mainly through the Viennese Door.

In summer, an increased fraction of the Dimitrovgrad trajectories reach the Mediterranean region. As can be seen from Fig.5, most of them cross or end in the Aegean Sea.

Table 1

Summary of the percentages of the trajectories reaching the Mediterranean region for various seasons and pressure levels

Season / Place	Stavanger		Dresden		Kraków		Salzburg		Dimitrovgrad	
Level	850	920	850	920	850	920	850	920	850	920
Autumn	0.00	0.00	11.72	7.03	14.06	2.34	28.13	0.00	51.56	22.66
Winter	0.72	0.00	7.19	3.60	6.47	5.04	31.65	0.00	30.94	23.74
Spring	0.00	0.00	3.39	0.00	5.08	5.08	15.25	0.00	28.81	22.03
Summer	0.00	0.00	4.26	0.00	2.84	1.42	29.79	0.00	59.57	41.84

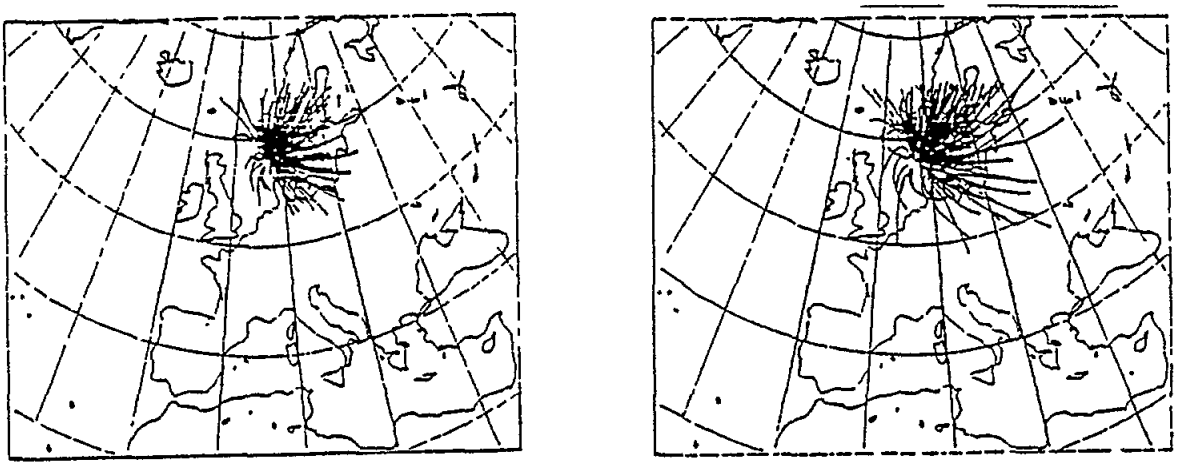

Fig.3 Summer forward trajectories for Stavanger at 920 hPa (left panel) and 850 hPa levels (right panel)

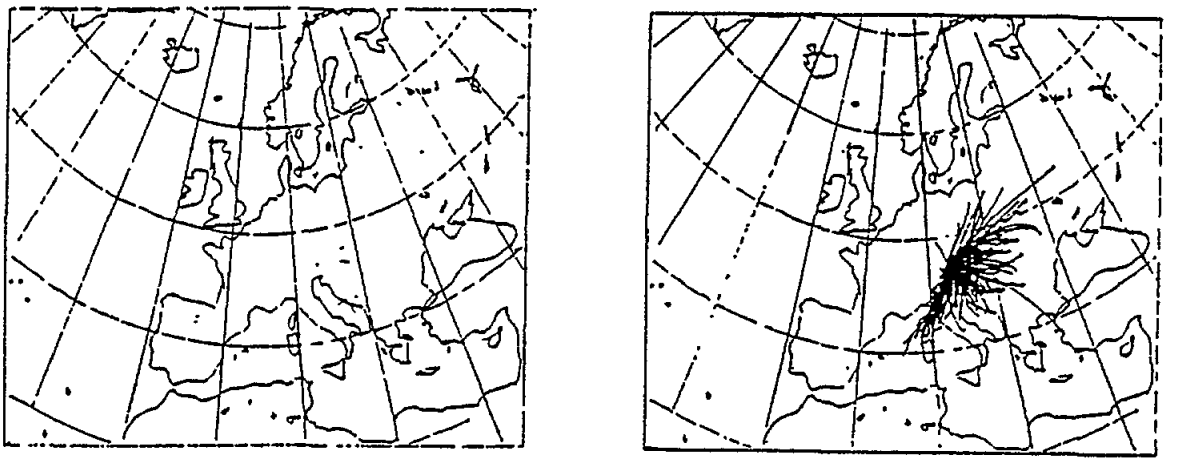

Fig.4 Summer forward trajectories for Salzburg at 920 hPa (left panel) and 850 hPa levels (right panel)

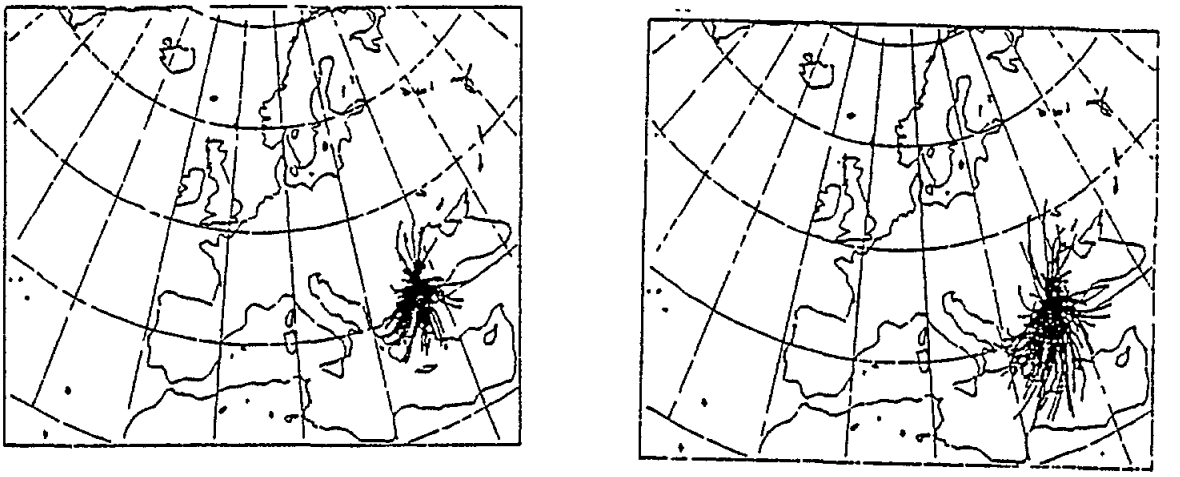

Fig.5 Summer forward trajectories for Dimitrovgrad at 920 hPa (left panel) and 850 hPa levels (right panel)

The backward 36 hour trajectories were calculated at six points regularly distributed with respect to the longitude along the northern coast of the Mediterranean Sea. They were located at 5°W (near Gibraltar), 0°E (near Valencia), 5°E (near Marseille), 10°E (near Genoa), 15°E (near Rijeka) and 20°E (near Corfu). As before, the results were considered separately for the four previously defined seasons.

As an example, the winter backward trajectories are displayed in Fig.6 for the point in the Northern Adriatic, near Rijeka. Due to more vigorous synoptic scale processes, the

trajectories are generally reaching further away from the Mediterranean Sea than in the other seasons.

As can be seen from the figure, generally speaking, the 920 hPa trajectory patterns are strongly channelled by the mountains along the northern coast of the Mediterranean Sea. The blocking effect of the Alps is clearly seen.

The Alps are a significant obstacle even at the 850 hPa level. The channelling effect of the Viennese Door is clearly visible. Similar effect can be seen along the Pyrenees and in the case of the major mountain gap in the South of France.

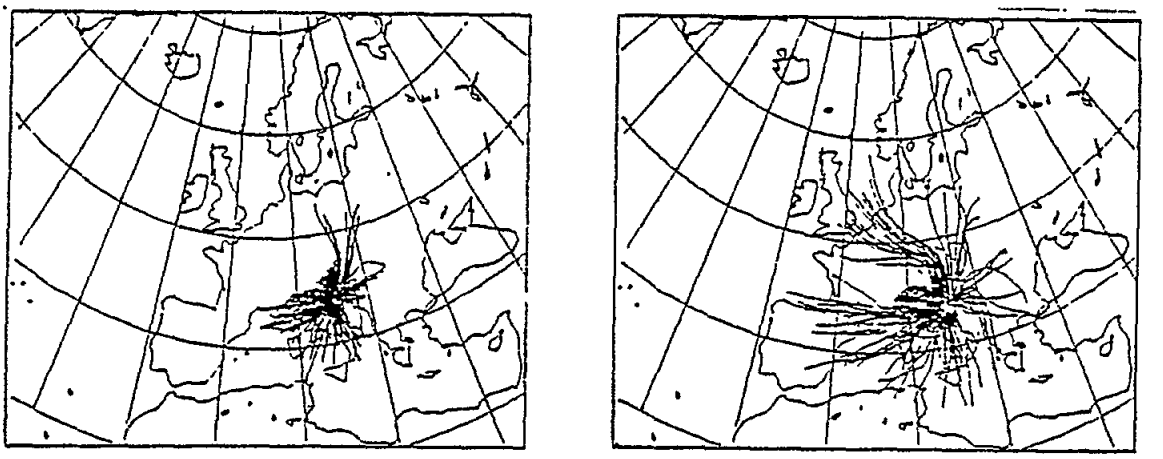

Fig.6 Winter background trajectories for the point near Rijeka at 920 hPa (left panel) and 850 hPa levels (right panel)

5. CONCLUSIONS

In spite of the limited objectives of the present study, and the limitations of the method employed, the results discussed in the preceding two sections suggest that:

1. A considerable fraction of the pollution emitted in Europe can reach the Mediterranean Sea by the long-range atmospheric transport within the time-scale of 1 to 2 days, particularly in the colder part of the year when the atmospheric circulation is more vigorous. However, in the case of Dimitrovgrad, the percentage of the forward trajectories reaching the Mediterranean Sea sharply increases in summer, particularly at the 920 hPa level. The reason for this may be the increased heights of the pressure levels considered and, therefore, reduced blocking effects of the mountains.

2. Assuming that the pollution is transported at the 850 hPa level, in the colder part of the year the contribution of the pollution sources in Europe located south of about 44°N, and west of about 40°E, are potentially most important on the time-scale considered. If the pollution is transported at the 920 hPa level, the boundaries of this area should be shifted to about 50°N, and west to about 30°E.

3. There are preferred pathways of the flow towards the Mediterranean Sea on the two pressure levels considered. They are determined by the blocking and channelling effects of the major mountain ranges in Europe. The most striking channelling effect observed is the splitting of the flow around the Alps. Further east, another channelling effect can be seen in the Morava and Vardar river valleys.

4. Due to the channelling effects, the trajectories originating in Europe tend to group:

   (a) along the Pyrenees and through the gap between the Pyrenees and the Alps:

   (b) through the Viennese Door, and towards and across the northern Adriatic Sea and the Dinaric Alps; and

   (c) across northern Yugoslavia and the Morava and Vardar valleys towards and across the Aegean Sea.

5. Judging by the preferred pathways of the trajectories, potentially most affected areas by the long-range transport of pollution originating from the sources in Europe are the Gulf of Lyon, the Gulf of Genoa, the northern Adriatic Sea and the Aegean Sea. For this reason, these areas may be convenient for monitoring the contribution of the long-range atmospheric transport of the pollutants.

6. ACKNOWLEDGMENTS

This research was supported by the WMO and the Yugoslav Federal Fund for Fostering Scientific and Technological Development.

7. REFERENCES

Eliassen, A. and J. Saltbones (1983). Modelling of long-range transport of sulphur over Europe : at two-year model run and some experiments. *Atmos. Env.*, 17:1457-1473.

GESAMP (1985). IMO/FAO/UNESCO/WMO/WHO/IAEA/UN/UNEP Joint Group of Experts on the Scientific Aspects of Marine Pollution. *Atmospheric transport of contaminants into the Mediterranean Sea*. Reports and Studies, GESAMP, No.26, p.41.

Janjiæ, Z.I. (1974). A stable centered difference scheme free of the two-grid-interval noise. *Mon. Wea. Rev.*, 102:319-323.

Janjiæ, Z.I. (1977a). Pressure gradient force and advection scheme used for forecasting with steep and small scale topography. *Contrib. Atmos. Phys.*, 50:186-199.

Janjiæ, Z.I. (1979). Forward-backward scheme modified to prevent two-grid-interval noise and its application in sigma coordinate models. *Contrib. Atmos. Phys.*, 52:69-84.

Janjiæ, Z.I. (1980). Numerical problems related to steep mountains in signa coordinates. *Workshop on Mountains and Numerical Weather Prediction*. ECMWF 1979, Shinfield Park, Reading, U.K., 48-89.

Janjiæ, Z.I. (1984). Non-linear advection schemes and energy cascade on semi-staggered grids. *Mon. Wea. Rev.*, 112:1234-1245.

Mesinger, F. (1973). A method for construction of second-order accuracy difference schemes permitting no false two-grid-interval wave in the height field. *Tellus*, 25:44-458.

Mesinger, F. (1974). An economical explicit scheme which inherently prevents the false two-grid-interval wave in the forecast fields. *Proc. Symp. on Difference and Spectral Methods for Atmosphere and Ocean Dynamics Problems*, Novosibirsk, 17-22 September 1973, Acad. Sci., Novosibirsk, Part II, 18-34.

Pacyna, J.M. (1985). Spatial distributions of As, Cd, Pb, V and Zn emissions in Europe within 1.5E grid net. Norwegian Institute for Air Research, Report 60/85.

AEROSOL INTRUSION EVENTS INTO THE MEDITERRANEAN BASIN

By

U. DAYAN[1], J. HEFFTER[2], J. MILLER[2] and G. GUTMAN[3]

(1) Israel Atomic Energy Commission, Soreq Nuclear Research Centre, Yavne, Israel.
(2) Air Resources Laboratory, National Oceanic and Atmospheric Administration, Silver Springs MD, USA.
(3) National Environmental Satellite, Data and Information Service, National Oceanic and Atmospheric Administration, Washington DC, USA.

A B S T R A C T

In this study seven aerosol intrusion events were identified and analyzed in the central and eastern part of the Mediterranean Sea beginning August 1988 and ending September 1989. In order to locate their sources, characterize their mode, and determine atmospheric transport levels, air flow back trajectories were calculated using the BAT Model (Heffter, 1983) for two layers (300-2000 m; 1500-3000 m) in conjunction with the synoptic situations prevailing during these dust outbreak events. Aerosol mass loading and horizontal visibility were derived for each of these seven cases from optical thickness values as analyzed by visible and near infrared radiances measured with the NOAA-9 and NOAA-11 satellite borne radiometers. Optical thickness is displayed in composite weekly charts over the Mediterranean.

The analysis has shown that transport of Saharan dust occurring in the western and central part of the Mediterranean are usually rather intensive in their atmospheric mass loading capacity and take place in deeper atmospheric layers for a longer duration (approximately 2-4 days) than eastern Mediterranean dust events. The eastern transport usually originates from the Arabian Desert for short periods (approximately 1 day) and is restricted to a rather shallow atmospheric transport layer featured by low optical depth values.

1. INTRODUCTION

This report is the result of mutual efforts of a coordinated research group consisting of three subgroups: the National Oceanic and Atmospheric Administration (NOAA) Air Resources Laboratory (ARL), for the generation of backward trajectories to track dust sources using Long-Range Transport (LRT) models; NOAA's National Environmental Satellite, Data and Information Service (NESDIS), for aerosol remote sensing with AVHRR data from the NOAA satellites; and the Soreq Nuclear Research Center (SNRC) meteorological unit for reduction of synoptical and ground truth data for each aerosol intrusion event selected for analysis.

1.1 Impacts

Atmospheric aerosols play an important role in neutralizing acidic airborne deposition over the Mediterranean Basin of land source origin (Mamane *et al*., 1980), affecting the pH of cloud water and rain. In addition, because of their complex chemical nature, aerosols are important to many biogeochemical cycles after being deposited in the sea. Aerosol climatology over the Mediterranean Basin has applications such as:

(1) Governing the extinction of radiation (scattering and absorption) above the sea during clear sky conditions and acting as cloud condensation nuclei (CCN) and ice nuclei (IN) during cloudy atmospheres, hence influencing the processes of cloud formation.

(2) Computing regional energy budget above this semi-enclosed sea.

(3) Understanding transport mechanisms.

(4) Estimation of visibility and visual range

(5) Assessment of deposition rate of dust to air pollution modelers.

(6) Controlling effects of haze layers on aviation operations.

1.2 Objectives

The overall objective of this study was to identify extreme aerosol intrusion events in the Mediterranean Basin, to detect and map their sources, to characterize their mode of transport in the atmosphere making usage of long-range transport models and satellite measurements, and to analyze the synoptical conditions leading to these anomalous episodes. The main goal is to assist modelers in climate simulation of a water body which serves as a sink for airborne particles originating mainly from natural sources.

2. AEROSOL EVENT DETECTION METHODOLOGY

2.1 General methodology

The region of interest in the study, i.e., the Mediterranean Sea basin, lies between 30EN and 46EN and between 5.5EW and 36EE. The period being considered for sandstorm and duststorm intrusions to this Mediterranean region was about one year (August 1988 through September 1989). Duststorms moving from the Sahara and the surrounding desert to the eastern Mediterranean usually occur between October and May, but mostly from December to April (Lunson, 1950; Katsnelson, 1970; Ganor, 1975).

The methodology adopted here was to retrieve on a real time basis as much information as possible regarding each duststorm intrusion. These data included IR and VIS satellite imagery for location of the storm, surface synoptic charts, and aerosol attenuation optical thickness as analyzed by visible and near-infrared radiances measured with the Advanced Very High Resolution Radiometer (AVHRR) on NOAA-9 and NOAA-11 satellites. Optical thickness is displayed in composite weekly charts over the Mediterranean.

2.2 Satellite pictures

The visible and infrared satellite pictures of each dust outbreak above the Mediterranean was obtained by the Meteosat geostationary and NOAA-9 and NOAA-11 polar orbiting environmental satellites. The intensity of brightness in infrared images served as an indication of the degree of upward extension of the haze in the atmosphere whereas visible images gave a more precise description of location and orientation of the dust outbreak propagation above the sea. Observation of these spells in the visible spectrum appeared as a grayish/white area resembling the high cloud but with softer boundaries.

2.3 Synoptic charts

In order to understand the generation and dissipation of sandstorms or duststorms above the Mediterranean Sea an analysis of the synoptical conditions leading to these anomalous aerosol episodes is necessary. Therefore, surface synoptic charts of the Mediterranean region were obtained for each event.

Synoptically the majority of wind-spread duststorms which occur above the Mediterranean over the year are of the pressure gradient type caused by an increasing surface pressure gradient (Morales, 1979, pp. 187-193). They are usually associated with the passage of either a cold or a warm low pressure system. Saharan depressions of this kind develop most readily when a polar or Arctic air mass from the northwest (maritime polar, maritime Arctic) or northeast (continental polar or continental Arctic) flows behind dry desert air. When this happens usually in winter and early spring, there is a corresponding induced flow of continental tropical air northwards, often bringing dust with it. The duststorms cease, usually when the wind veers to a northerly direction. This finding will be shown later by atmospheric trajectories which were computed individually for each storm.

2.4 Aerosol optical depth charts

The concept of determining aerosol loading of the atmosphere using reflectivity patterns obtained from satellite radiance measurements is of a primary interest for the evaluation of mass concentration associated with the Mediterranean dust outbreaks. This method, however, needs further validation for several reasons:

(1) The standard technique employs the linear correlation between upwelling radiance and aerosol optical depth noted by Griggs (1975). These retrieval methods have been developed prompted by theoretical studies which showed the relationship between aerosol optical depth (δ), intensity of radiation (I) and aerosol column density assuming certain adopted albedo values which are not necessarily true for every region (Meckler *et al*., 1977).

(2) All of the three above-mentioned quantities are dependent on the particular aerosol model used in the retrieval algorithm.

(3) Usage of Junge aerosol size distribution (between radius limits of 0.1µm and 20µm) does not account for bigger aerosol particles although scarce above water bodies.

(4) Assumptions of aerosol shape as spherical particles.

In this study, ôvalues could not be obtained for each dust intrusion event due to: (a) an inappropriate solar zenith angle; (b) clouds in the field of view during the event; and technical difficulties during transition from NOAA-9 TO NOAA-11 AVHRR.

Optical thickness data were derived from radiance values obtained from the satellites. These data were used to produce composited weekly values over the Mediterranean at the wavelength of 0.5 µm on a 100 km grid for which contours were generated by computer-based objective analysis techniques.

2.5 Relationship of optical observations to aerosol mass loading as measured in the Mediterranean and around the world

2.5.1 Eastern Mediterranean

In 1977 Meckler *et al*., developed a technique for deriving relative atmospheric aerosol content over water, using satellite observations of ERTS type. This study was prompted by theoretical methods which showed the relationship between aerosol optical thickness (δ), intensity of radiation (I) and aerosol column density. Their investigations were validated by ground truth observations which were performed at the same time that satellite observations were taken over the eastern part of the Mediterranean Sea for few spells when abnormally low visibility was reported. The optical thickness obtained by Meckler *et al*., based on photometry results and computed radiance results are displayed in Table 1. Also in columns 3 and 4 are the ground visibility and the aerosol mass loading, respectively.

Table 1

Optical thickness as a function of ground visibility for the Eastern Mediterranean region

Date of haze intrusion observed	Optical thickness (δ) (at 0.56 µm)	Ground visibility (VV) (km)	*Aerosol mass loading (µg/m^3)
8-9 May 1973	0.76	4-8	100-350
10-13 June 1973	0.61	5.8	100-200
24 August 1973	0.09	>20	<50

* The corresponding aerosol mass loading to visual range is based on daily monitoring of these two elements at the same time as supplied by the Israel National Air Quality Monitoring Network

2.5.2 Central and Western Mediterranean

Aerosol optical depth, particle concentrations and visibility were measured simultaneously in the central and western part of the Mediterranean by the U.S.S. America ship for a 12 day cruise (Fig.1) and analyzed (Haggerty and Durkee, 1988), (Fig.2). The results displayed in Fig.2 seem to be relatively in good agreement with Meckler's few observations for the eastern Mediterranean.

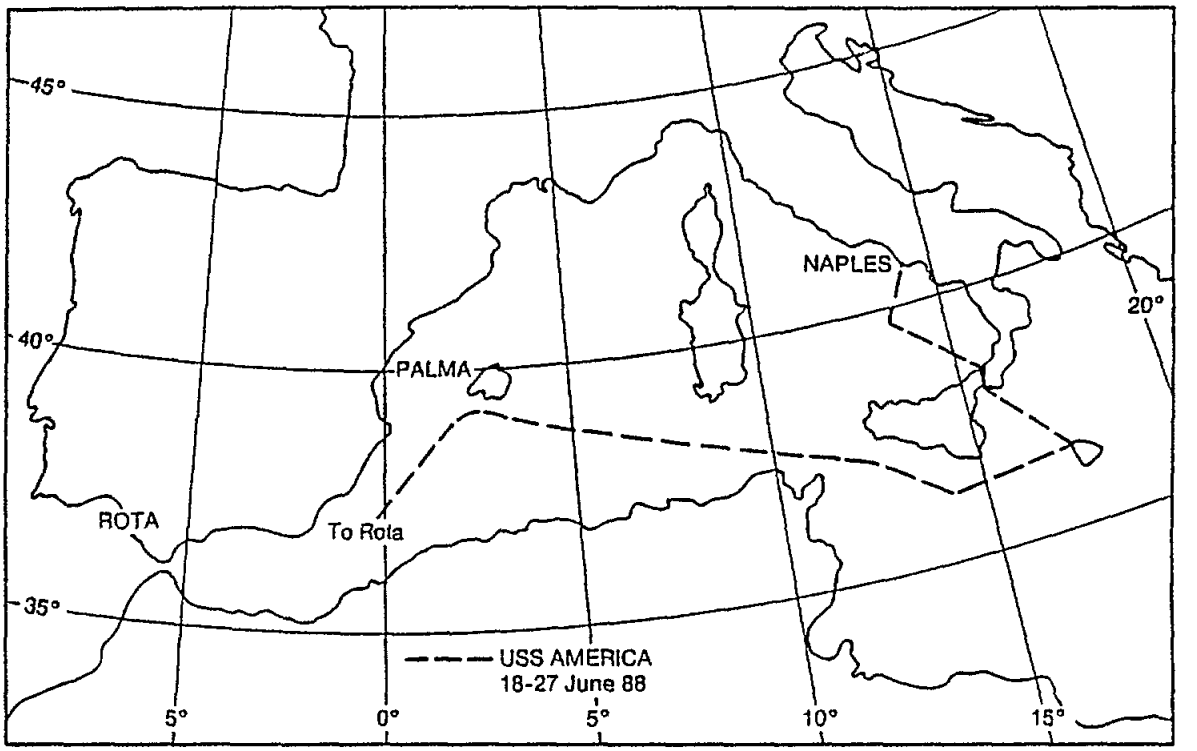

Fig.1 U.S. America cruise in the central and western Mediterranean (from Haggerty and Durkee, 1988)

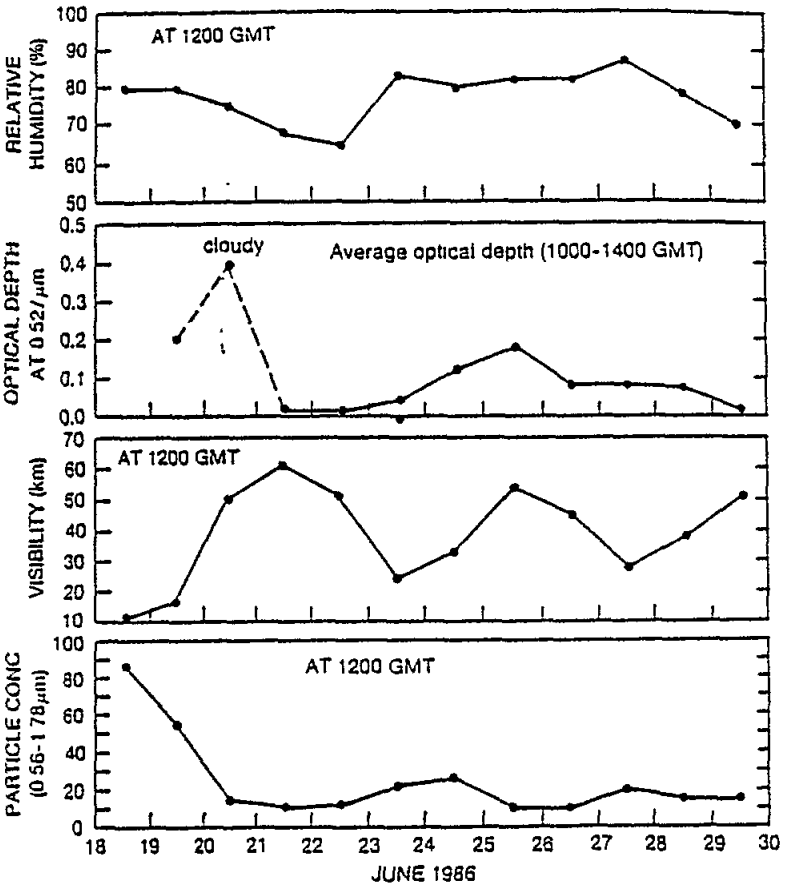

Fig.2 Relative humidity, optical depth, visibility, particle concentration as measured during the U.S. America cruise in the central and western Mediterranean (from Haggerty and Durkee, 1988

Unfortunately all the results shown so far above the Mediterranean Sea are related to weak hazy weather conditions rather than massive dust outbreaks, the visibility never being below 3-4 km consisting therefore of rather low aerosol optical thickness values.

In order to gain insight into the relationship of these two parameters: ô and VV a short overview of some more results as measured around the world is presented. Kaufman and Fraser (1983) measured optical thickness (ô) from the surface during the summer of 1980 and 1981 near Washington, DC derived from solar transmission measurements and meteorological parameters (i.e., visual range) of the surface air (Table 2).

Junge (1958), Curcio *et al*. (1961), Fett (1967) and Charlson *et al*. (1969) show a typical mass loading value of 70 µg/m^3 for a visibility of 25 km, which is typical for continental rural areas. A much lower value is probably expected above water bodies.

Table 2

Optical thickness as a function of ground visibility in Washington DC

ô(0.56 µm)	Visibility (km)
0.7 - 1.0	5-7
0.4 - 0.7	7-15
0.2 - 0.4	15-25
0.0 - 0.2	25-40

2.6 Trajectories

The trajectories in this report were calculated using the Branching Atmospheric Trajectory (BAT) model (Heffter, 1983). The model uses average observed winds in a layer and inverse distance squared wind weighting with the modified Euler technique for advection. Input winds for the model were obtained from global upper-air observations archived at ARL starting 1981 to the present. Two transport layers were chosen to be representative of dust transport in the Mediterranean Basin; a lower layer of 300 to 2000 m to represent the planetary boundary layer (PBL) (UNEP, 1989) and a higher layer of 1500 to 3000 m for the lower "free troposphere" just above the PBL. Trajectories were run in a backward-in-time mode from a receptor using a time step of 3-h. It should be noted that the scan radius for including observations in a 3-h advection step was increased from 4Elat to 6Elat to compensate for the irregular, and often sparse, upper-air observation network in the Mediterranean Basin.

3. AEROSOL EVENT CASE STUDIES

3.1 General concepts

The following aerosol intrusion events to the Mediterranean Sea were analyzed based on satellite pictures (in the visual and I.R. spectrum), synoptic charts, composite weekly optical depth charts and backward trajectory computations. These events were divided into two distinctive categories: (a) Duststorms in the central Mediterranean Basin with their sources originating mainly from Africa, and (b) Duststorms in the eastern Mediterranean Basin for which

their sources originate both from Africa and from Asia. This division is based on several features characterizing each storm category such as origin of dust, appropriate atmospheric layers in which dust is transported, its spatial propagation, and its duration.

3.2 Description of the data base and selection of the cases

In the 13-month monitoring period, August 1988 - September 1989, 15 duststorms or sandstorms were detected in the Mediterranean. The majority of them occurred during winter and early spring, mainly in the north African coast. This finding is in good agreement with the air flow climatology evaluated in the western Mediterranean (Miller *et al.*, 1987) and in the eastern Mediterranean (Dayan, 1986, 1987) in conjunction with seasonal weather types.

Table 3 summarizes the location, chronology and types of the 15 dust outbreaks. Out of the total number of events for this period, seven intrusions to the Mediterranean Basin were selected for analysis--the other eight cases were ruled out because the duststorm could not be observed distinctly due to the poor quality of the satellite pictures.

Table 3

Summary of dust events in the Mediterranean Basin with the backward trajectory start location for those events selected for analysis.

Sub-section	Date	Location	Latitude	Longitude
3.4.a	Sep. 29, 1988	Eastern	34EN	34EN
3.3.a	Oct. 23, 1988	Central	34EN	22EE
	Dec. 9, 1988	Central		
3.4.b	Feb. 9, 1989	Eastern	35EN	35EE
	Feb. 10, 1989	Eastern		
	Feb. 17, 1989	Eastern		
	Feb. 20-23, 1989	Central		
3.3.b	Feb. 25-28, 1989	Central	35EN	25EE
	Mar. 1, 1989	Central		
3.3.c	Mar. 21, 1989	Central	34EN	19EE
	Mar. 24, 1989	Eastern		
3.4.c	Mar. 25, 1989	Eastern	35EN	33EE
3.3.d	Apr. 5, 1989	Central	39EN	17EE
	Apr. 16, 1989	Eastern		
	Apr. 30, 1989	Central		

3.3 Aerosol intrusion events into the central Mediterranean Sea

(a) October 23, 1988 (Case No. 3.3.a)

In the NOAA-9 AVHRR visible image, a distinctive dust layer is observed oriented south-north above the Libyan coast and the adjacent Mediterranean Sea (Fig.3a). This dust intrusion is caused by the presence of a deep barometric low (1010 mb) (Fig.3b) in the center of Libya with a flow of continental tropical air northward. Backward trajectories (Fig.3c) indicate that the origin of the dust on the October 23 satellite picture was most likely from the

south in the lower layer, and from the southwest if the dust extended to the higher layer. Furthermore, the trajectories indicate the event had a duration of about 2 to 3 days since transport in both layers from october 23 to 25 continued from the south to the southwest while transport on October 22 and 26 was clearly from the north, bringing in dust-free air. The weekly composite contour map (Fig.3d) of τ displays a spot of 0.2, a rather low value, corresponding to a 7-day average of approximately a 25 km range visibility (Table 2).

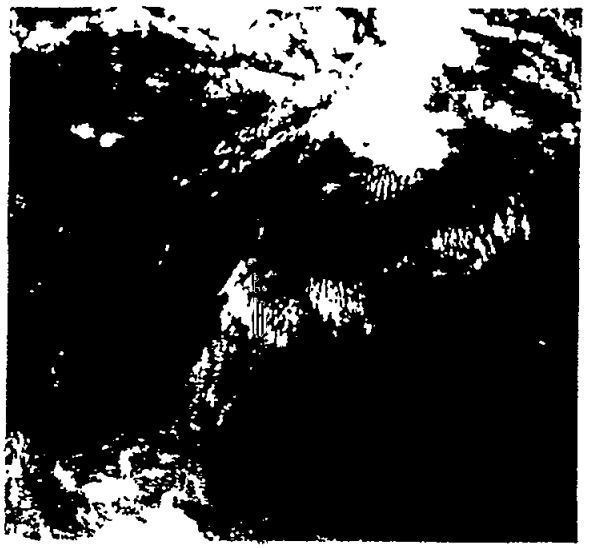

Fig.3(a) Satellite picture of the aerosol intrusion event

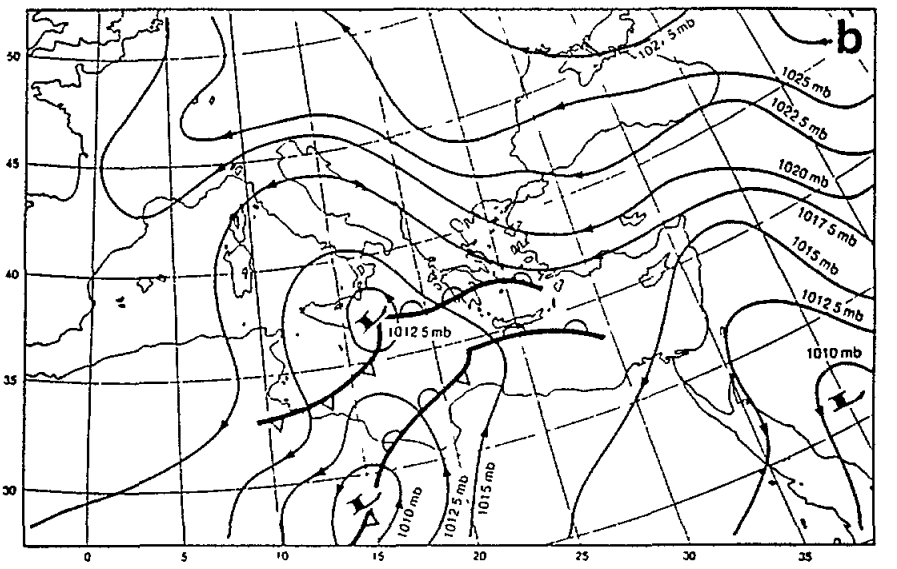

Fig.3(b) Surface synoptic chart

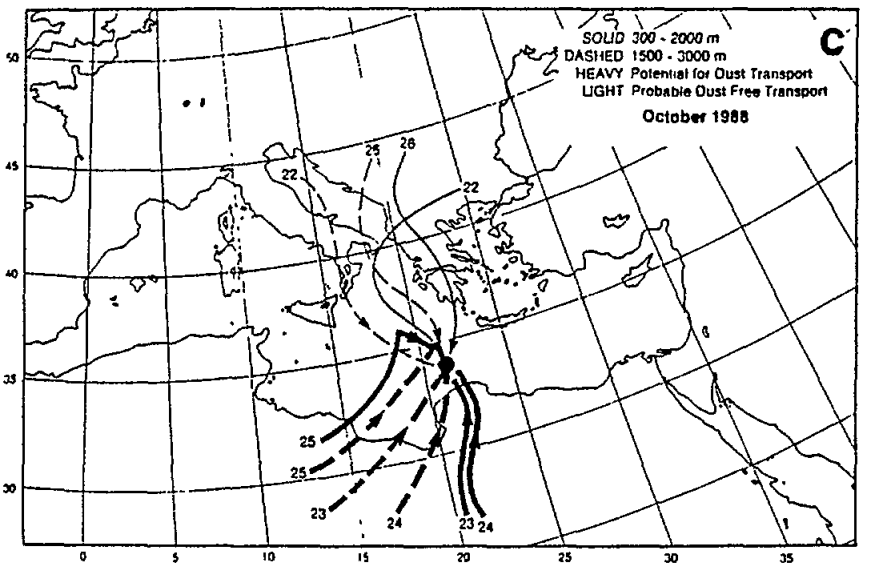

Fig.3(c) Back trajectories for the central Mediterranean aerosol intrusion event

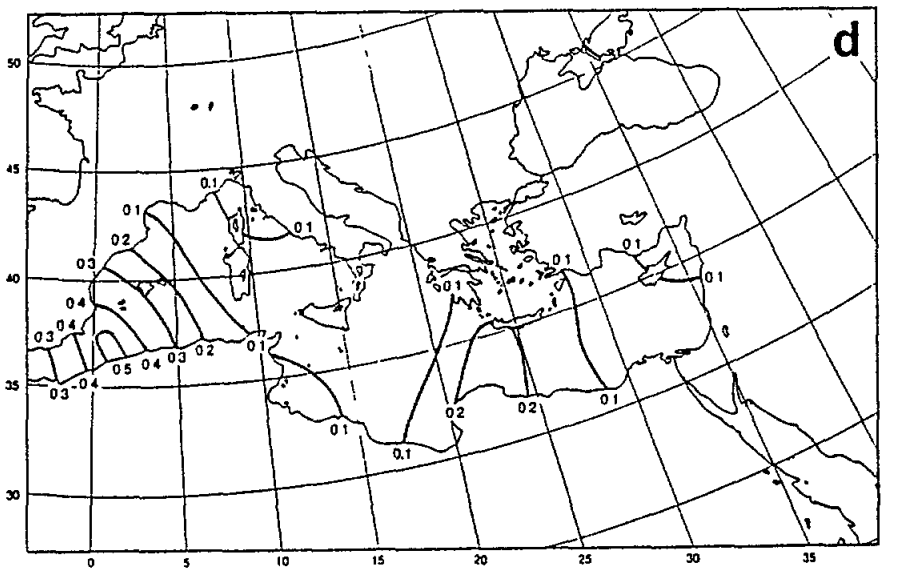

Fig.3(d) Weekly composite contour map of aerosol optical thickness over the Mediterranean Basin for the week ending October 27, 1988

(b) February 25-28, 1989 (Case No. 3.3.b)

The Meteosat visible spectrum satellite photograph for February 27 shows an outbreak of dust crossing the Mediterranean Sea in a southwest-northeast track (Fig.4a). This dust layer originates from the southern border of the Saharan Desert. The steepening of the surface pressure gradient shown in Fig.4b lasted for 3 days (25-28 Feb.) moving duststorms from the Sahara toward the Aegean Sea.

The airflow displayed in the trajectory chart (Fig.4c) suggests that both the lower and higher layers contributed to the transport of dust and that this episode lasted 2-3 days. The dust concentrations derived from the weekly averaged optical depth values correspond to about 50 µg m^{-3} (Fig.4d and Table 1).

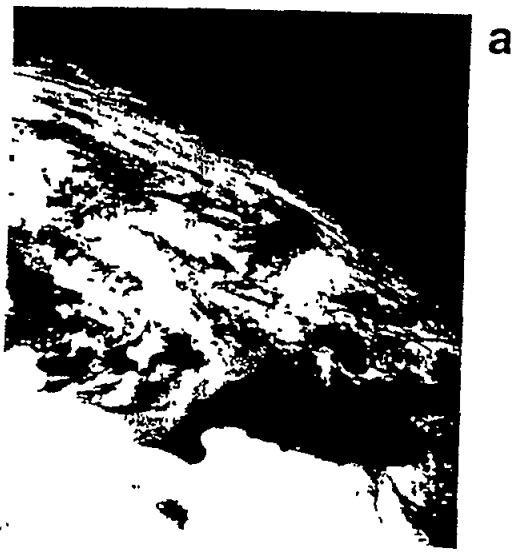

Fig.4(a) Satellite picture of the aerosol intrusion event

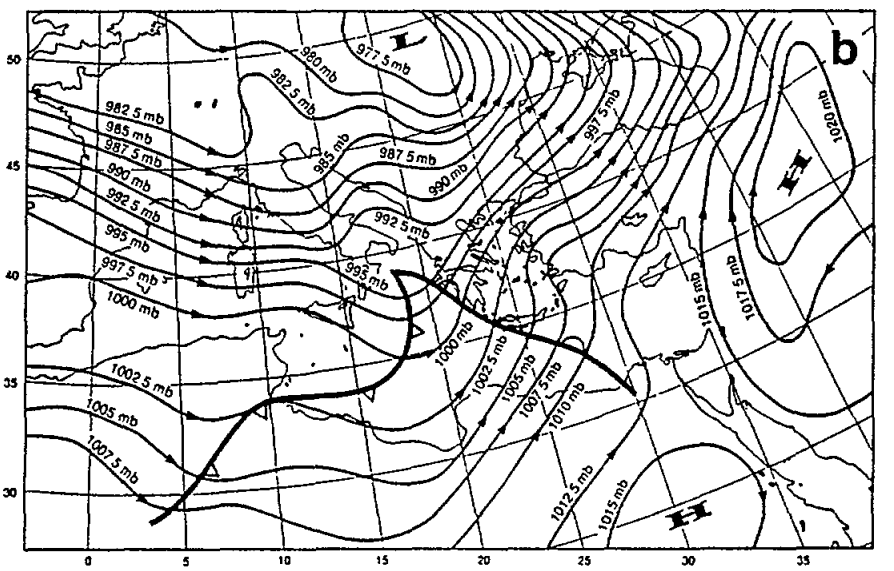

Fig.4(b) Surface synoptic chart

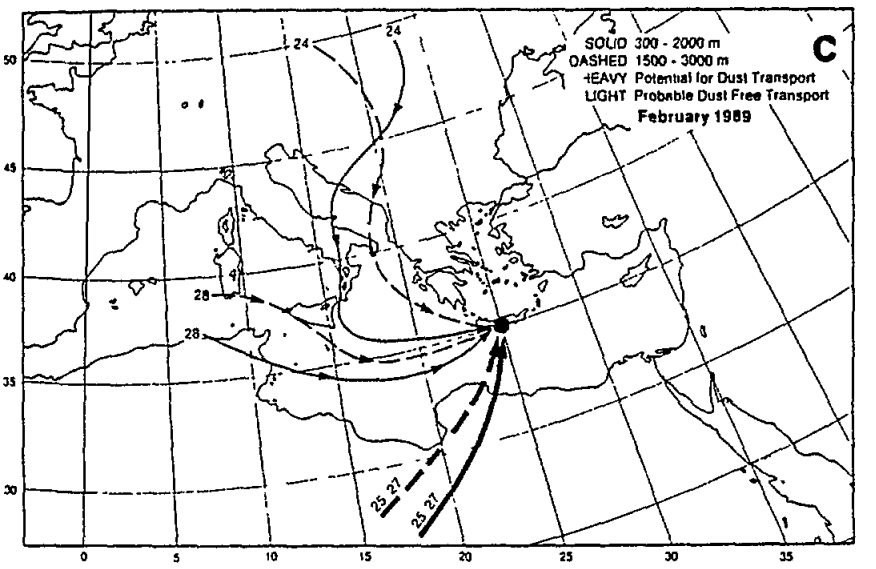

Fig.4(c) Back trajectories for the central Mediterranean aerosol intrusion event

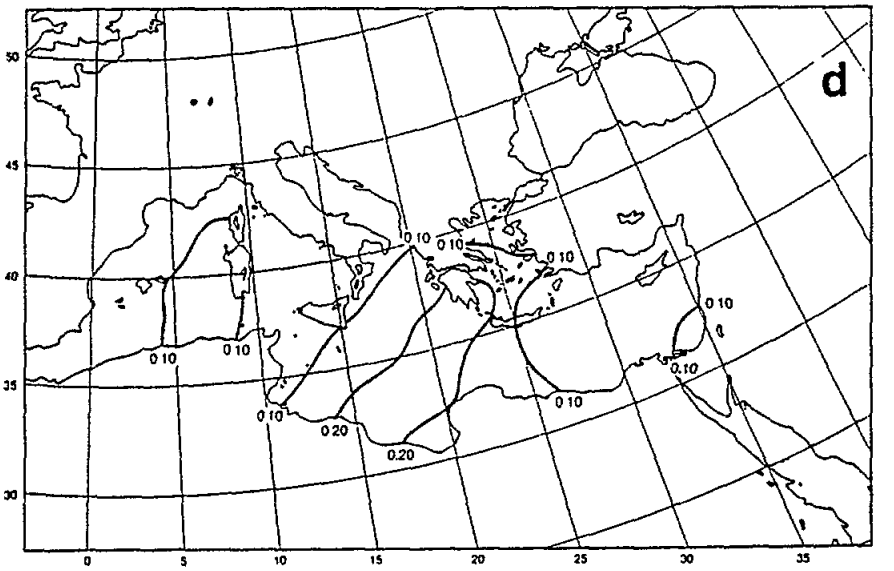

Fig.4(d) Weekly composite contour map of aerosol optical thickness over the Mediterranean Basin for the week ending March 2, 1989

(c) March 21, 1989 (Case No. 3.3.c)

In the NOAA-8 satellite picture of March 21, two distinct dust layers can be observed (Fig.5a). The highest one had a brighter reflectivity measured in the visible spectrum and a southwest-northeast orientation, and the second a shallow layer indicating movement more toward the north. This superposition of dust layers is supported by the trajectories (Fig.5c). The onset of the event cannot be established since sparse or missing observed wind data near the trajectory origin prevented calculations for several days prior to March 22 for the lower layer and March 20 for the higher layer. On March 21, the day of the satellite picture, the brightest reflectivity is clearly related to transport at the higher layer from the south. It is

suggested that the event probably lasted 3 to 4 days with dust coming more from the southwest at the lower layer as the event progressed. The weekly composite optical thickness values show two spots of elevated τ values of 0.3 and 0.2 for the Libyan coast and Ionian Sea, respectively, corresponding to an average of about 50-80 $\mu g\ m^{-3}$ mass loading of particulates within each of these two layers (Fig.5d).

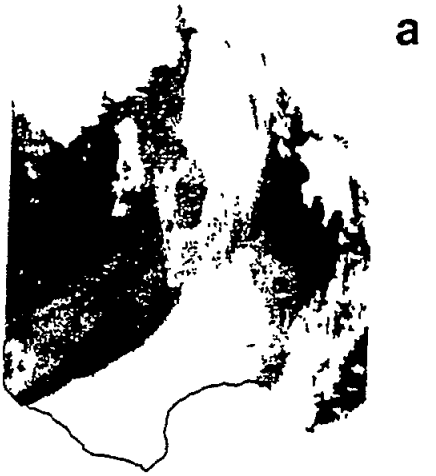

Fig.5(a) Satellite picture of the aerosol intrusion event

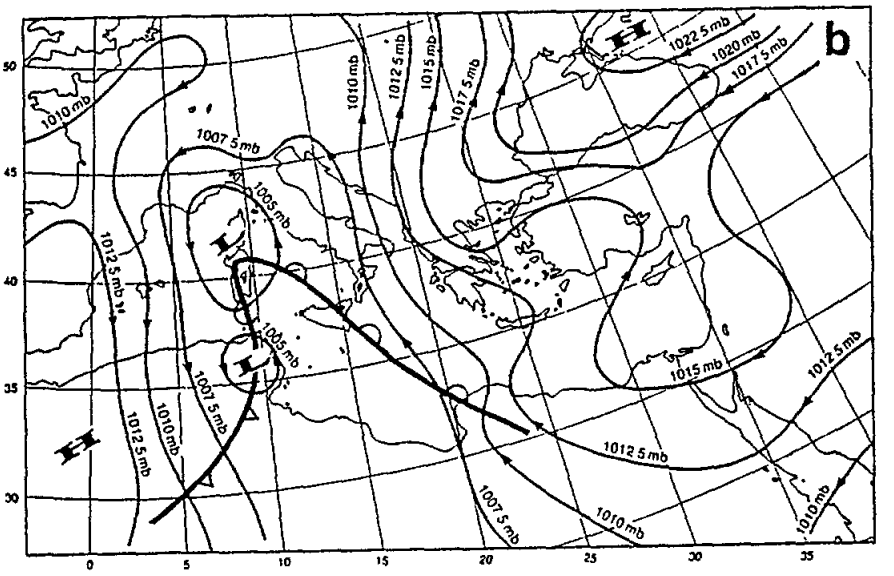

Fig.5(b) Surface synoptic chart

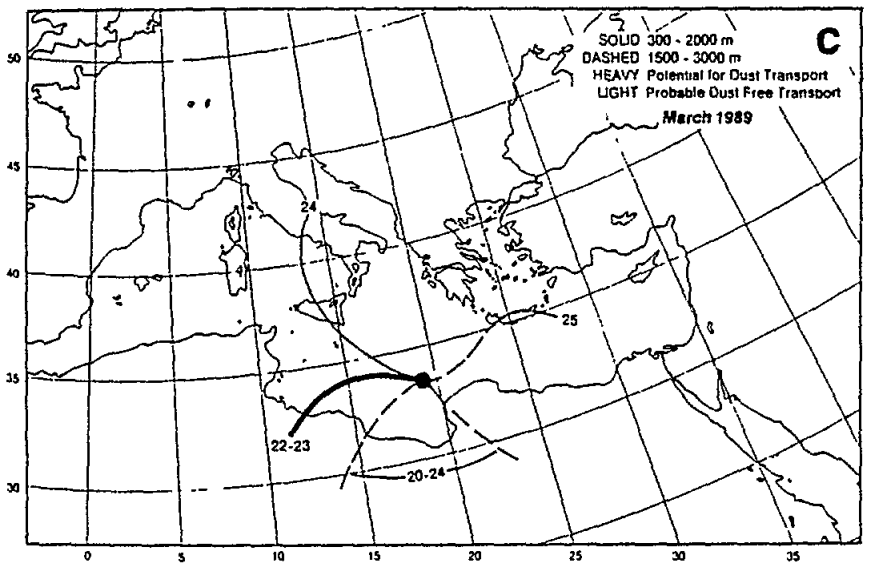

Fig.5(c) Back trajectories for the central Mediterranean aerosol intrusion event

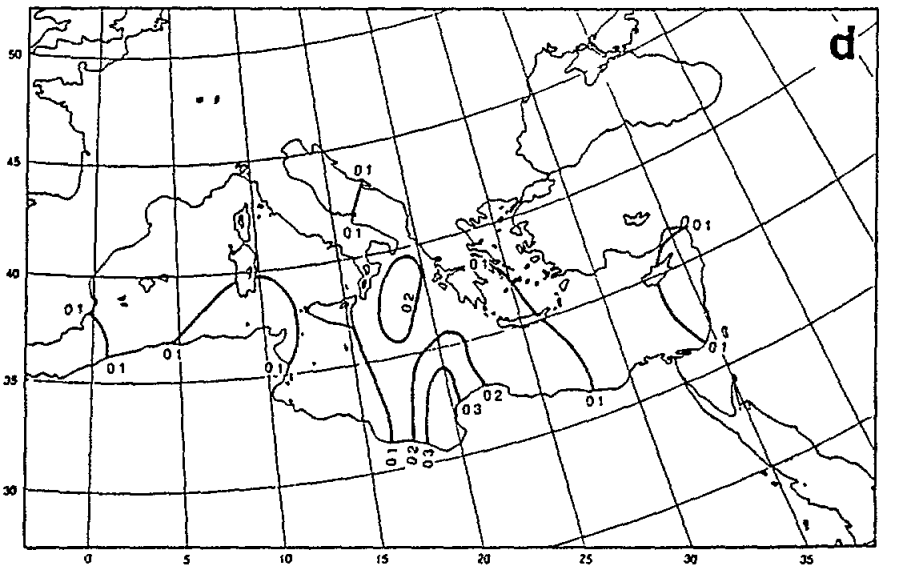

Fig.5(d) Weekly composite contour map of aerosol optical thickness over the Mediterranean Basin for the week ending March 23, 1989

(d) April 5, 1989 (Case No. 3.3.d)

The depression, which caused this event (Fig.6b), affects the central and eastern Mediterranean region usually during the spring season (Ganor and Mamane, 1982). Saharan depressions of this kind develop mostly when a polar or Arctic air stream from the northwest flows behind dry desert air. When this happens, as for this April 5 case, there is a corresponding induced flow of continental tropical air northward into a deep atmospheric layer, often bringing dust with it (lower and higher layer in Fig.6c). The trajectories indicate that the event duration was about 2 days. The highest optical thickness values observed as

averaged for the week ending April 6 (Fig.6d) are 0.4 corresponding to a horizontal visibility of about 15 km and a mass loading concentration of about 60-80 μg m^{-3}.

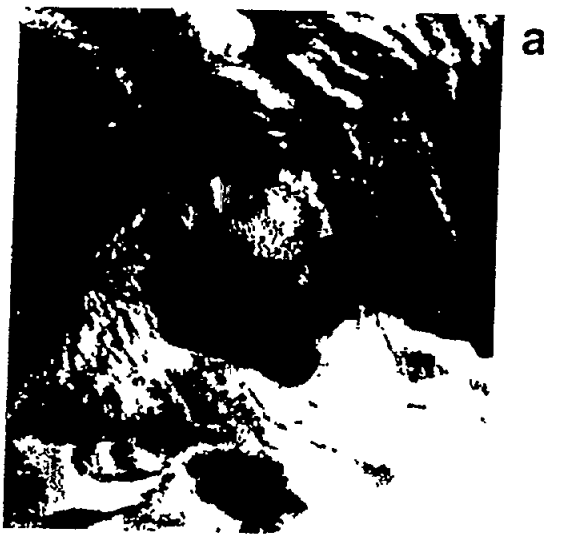

Fig.6(a) Satellite picture of the aerosol intrusion event

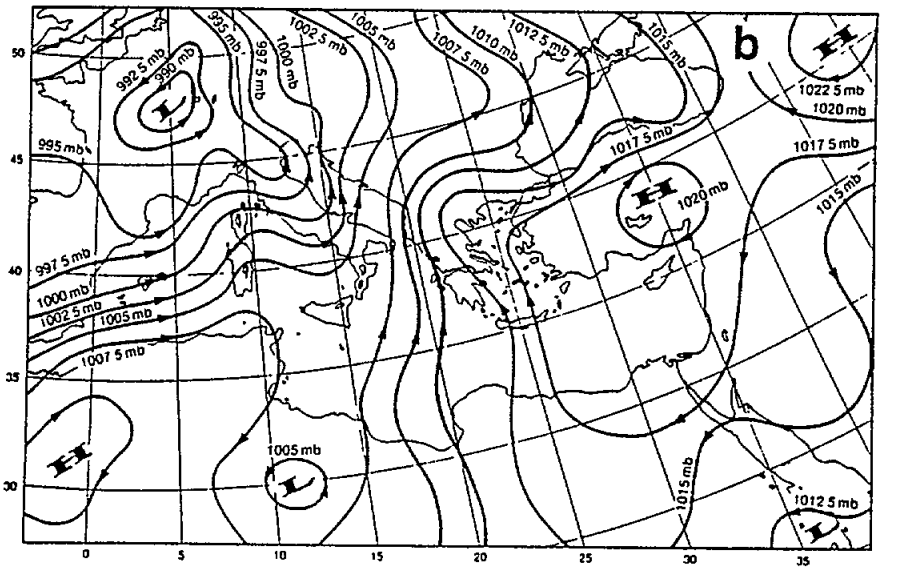

Fig.6(b) Surface synoptic chart

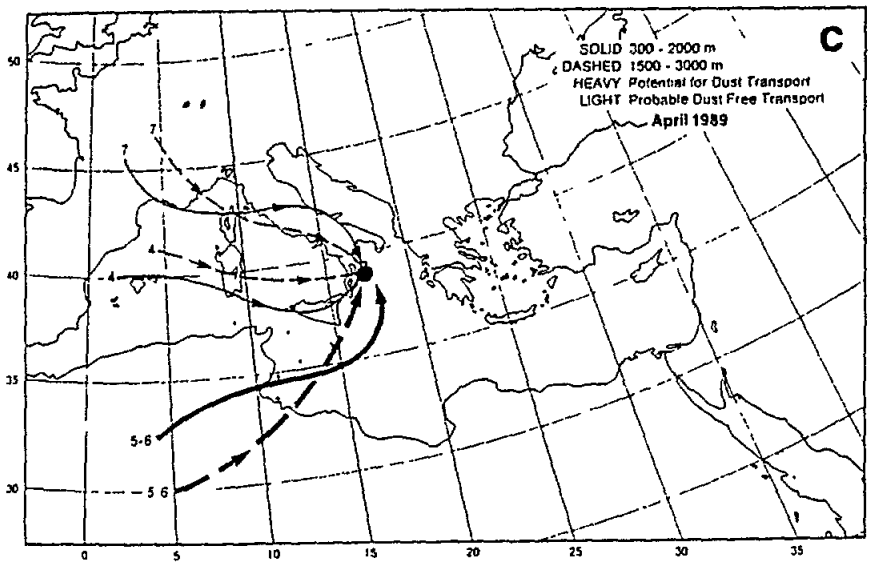

Fig.6(c) Back trajectories for the central Mediterranean aerosol intrusion event

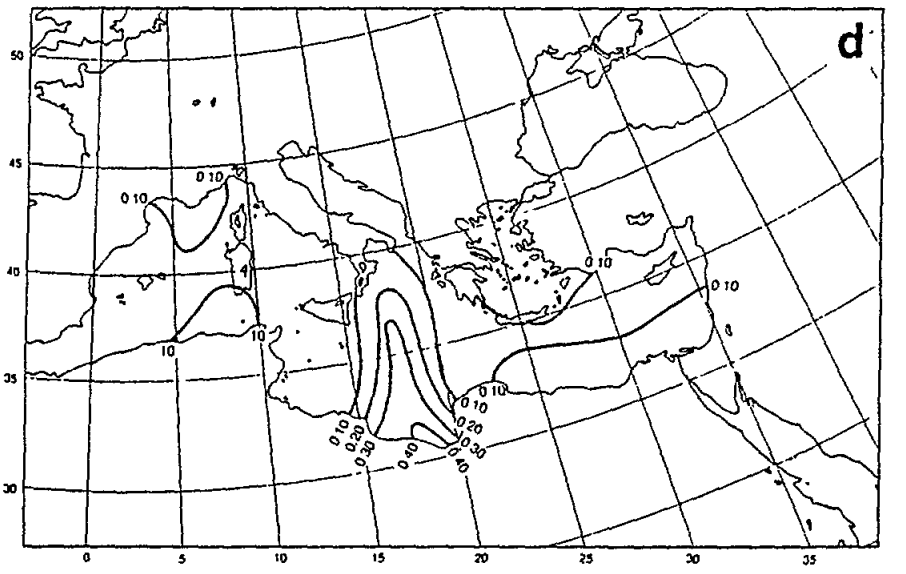

Fig.6(d) Weekly composite contour map of aerosol optical thickness over the Mediterranean Basin for the week ending April 6, 1989

3.4 Aerosol intrusion events into the eastern Mediterranean Sea

(a) September 29, 1988 (Case No. 3.4.a)

As mentioned in section 2, during the eastern Mediterranean aerosol intrusion events, the dust originates from western Asia (mainly the Arabian Peninsula) or from Africa (mainly the Saharan Desert). The most common synoptic situation in conjunction with eastern dust origins is a shallow barometric trough penetrating from the Red Sea toward the north up to Syria and the Cyprus Island (i.e., the Red Sea Trough) (Fig.7b). This trough is associated with the invasion of northeast or southeast winds of continental tropical origin. During the

September 29 episode, characterized by a relatively short duration, the atmospheric transport layer of dust was confined to the lower layer only as shown in Fig.7c. This dust layer, arriving from a northeastern source, is confirmed by the NOAA-7 satellite reflection pattern as displayed in Fig.7a. The composite weekly τ values displayed in Fig.7d were quite low probably due to the fact that this spell did not last for more than one day.

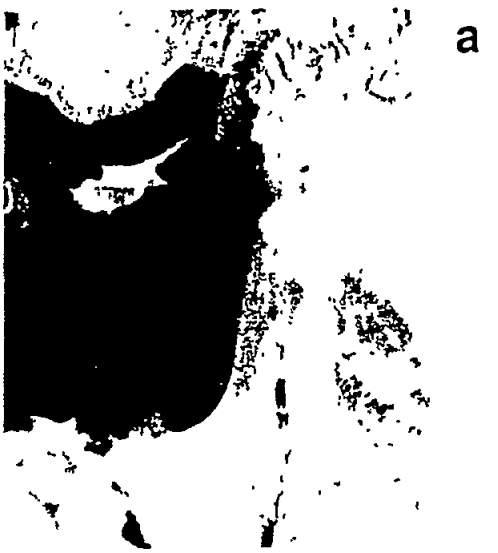

Fig.7(a) Satellite picture of the aerosol intrusion event

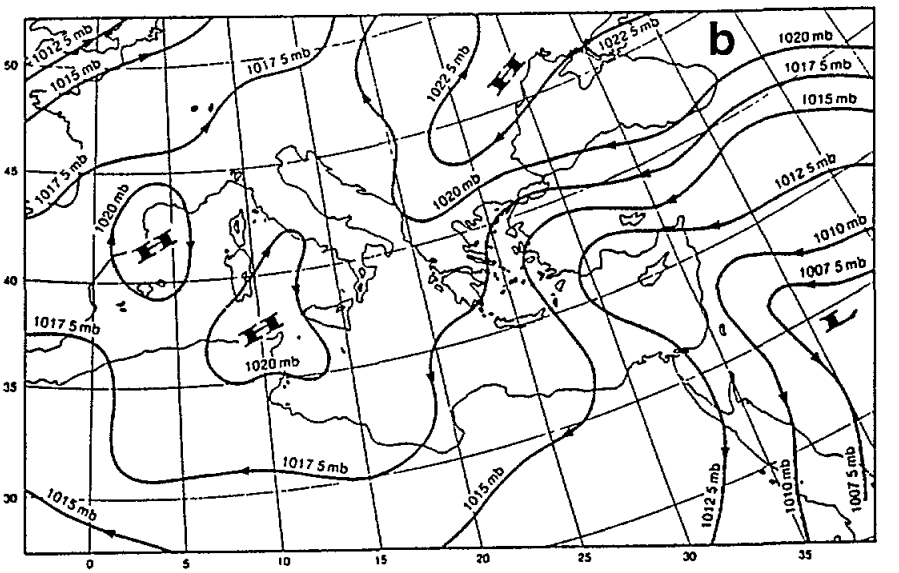

Fig.7(b) Surface synoptic chart

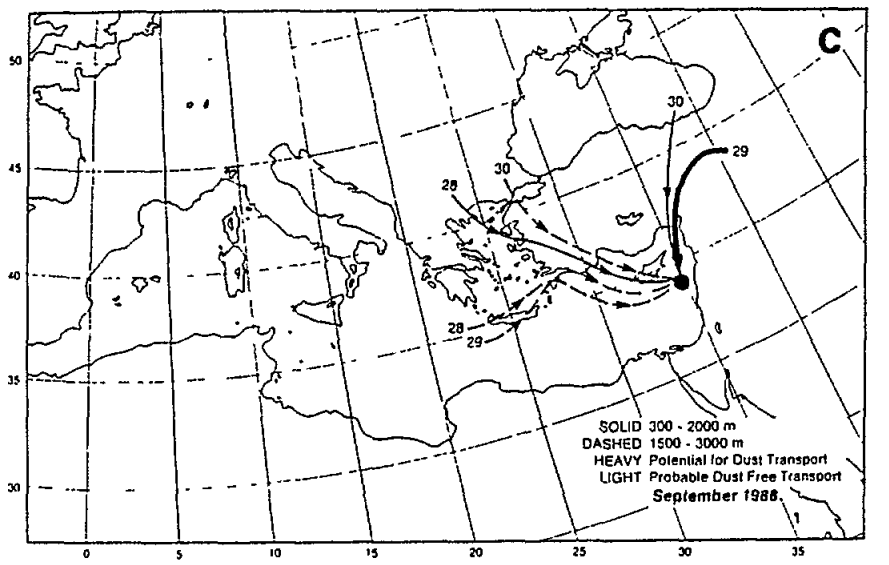

Fig.7(c) Back trajectories for the eastern Mediterranean aerosol intrusion event

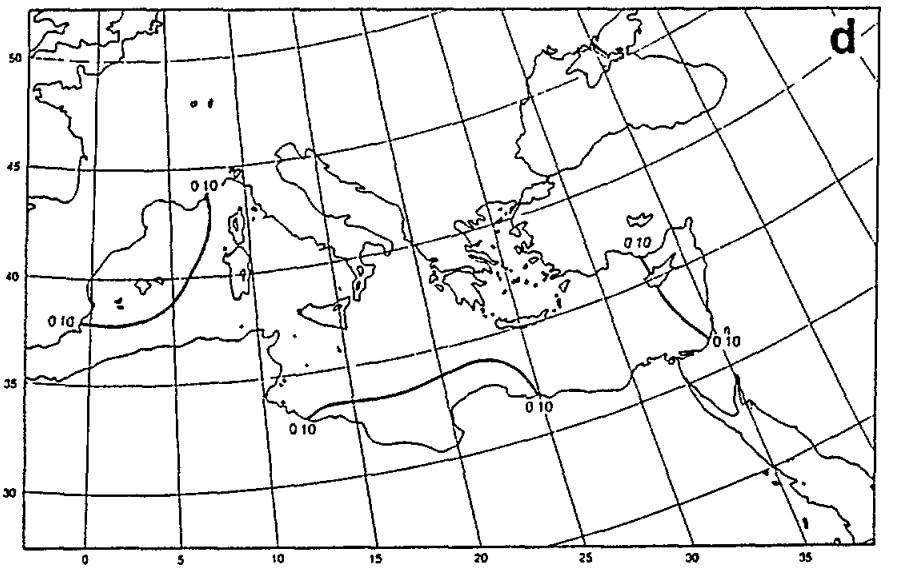

Fig.7(d) Weekly composite contour map of aerosol optical thickness over the Mediterranean Basin for the week ending September 29, 1988

(b) February 9, 1989 (Case No. 3.4.b)

This event resembles the previous eastern event (Sept. 29) in that dust is transported in the lower layer under an easterly flow regime characterizing the first 1500 m above ground as observed regularly during the influence of the Red Sea Barometric Trough (Fig.8b). The trajectories calculated for the higher atmospheric layer show a persistent northerly component origin before, during, and after the event day; whereas the shallow trajectories computed, veer sharply to an easterly component during the event (Fig.8c).

Fig.8(a) Satellite picture of the aerosol intrusion event

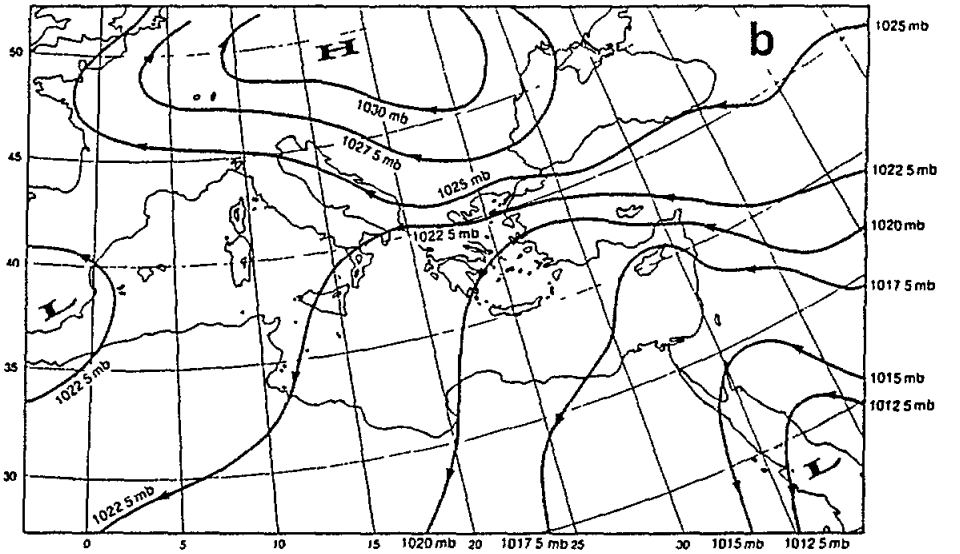

Fig.8(b) Surface synoptic chart

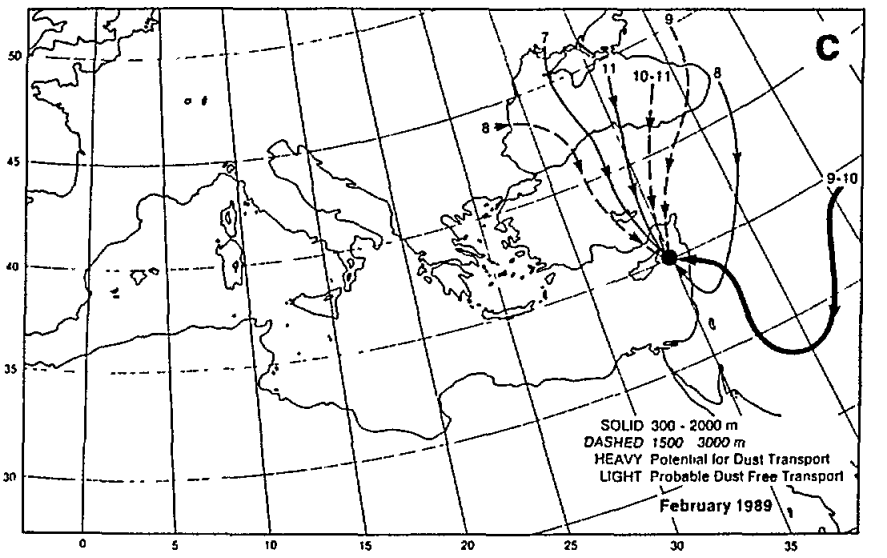

Fig.8(c) Back trajectories for the eastern Mediterranean aerosol intrusion event

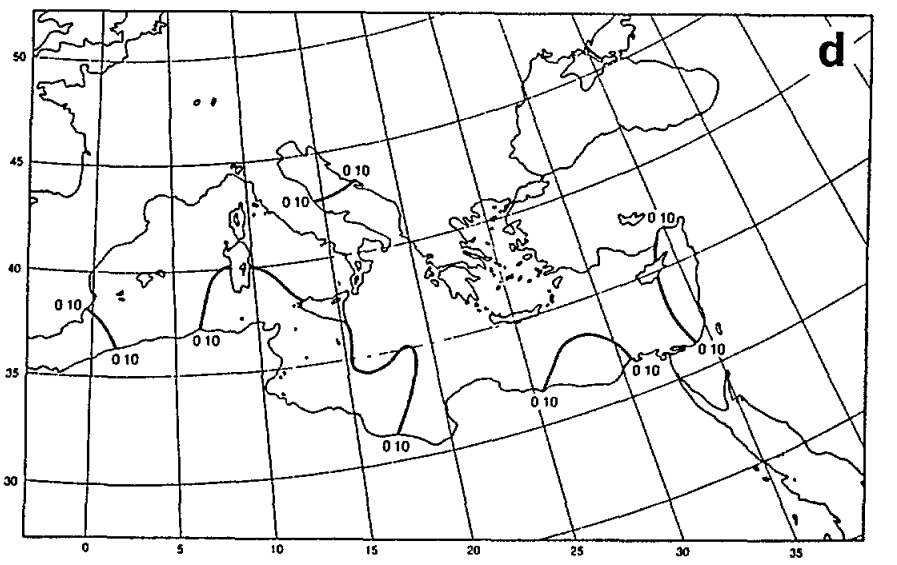

Fig.8(d) Weekly composite contour map of aerosol optical thickness over the Mediterranean Basin for the week ending February 9, 1988

(c) March 25, 1989 (Case No. 3.4.c)

The NOAA-8 visual spectrum satellite photograph for March 25 illustrates a massive dust intrusion from the south to the eastern Mediterranean region. The penetration northward is shown in the picture (Fig.9a) according to the superimposed haze layers having a much steeper gradient above the east-west axis than along the north-south axis. Inspection of this picture reveals increased reflectivity associated with increased dust concentrations in each atmospheric layer.

This duststorm is generated by strong southerly winds caused by a steep surface pressure gradient in the presence of a deep barometric depression formed over a relatively northern latitude (Fig.9b).

Fig.9(a) Satellite picture of the aerosol intrusion event

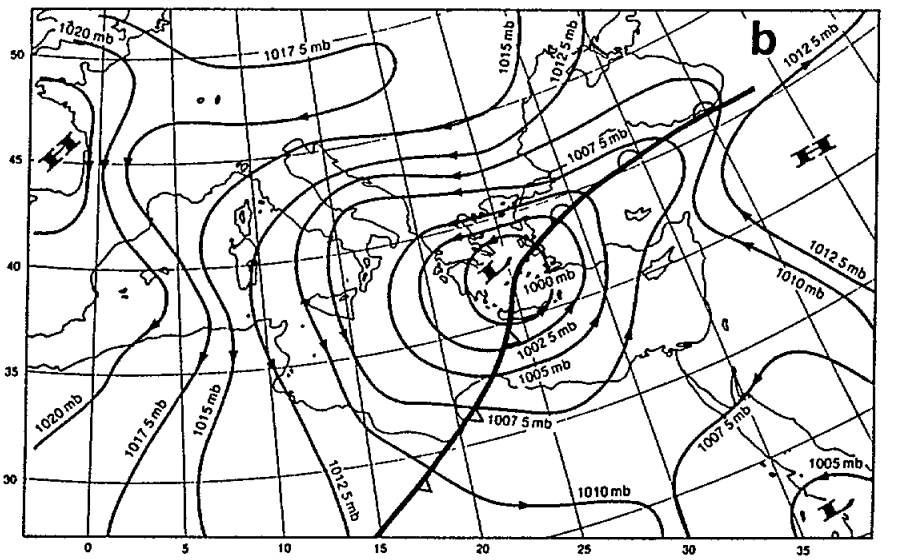

Fig.9(b) Surface synoptic chart

In this event, brightness patterns, as displayed in the multi-layer satellite picture, as well as the back trajectory (Fig.9c), give evidence that this intrusion occurred simultaneously in a deep atmospheric layer. The trajectories plus satellite data imply that the event duration at the lower level probably lasted about 3 days ending March 28 with transport from the north. The higher layer transition to dust-free transport from the north came earlier (a somewhat complex transition trajectory on March 27, not shown in Fig.9c) indicating a more gradual cessation of the vertical extent of dust. The composite weekly optical thickness values displayed in Fig.9d show an isopleth pattern which fits the orientation of this dust spell.

Table 4 summarizes each of the selected events.

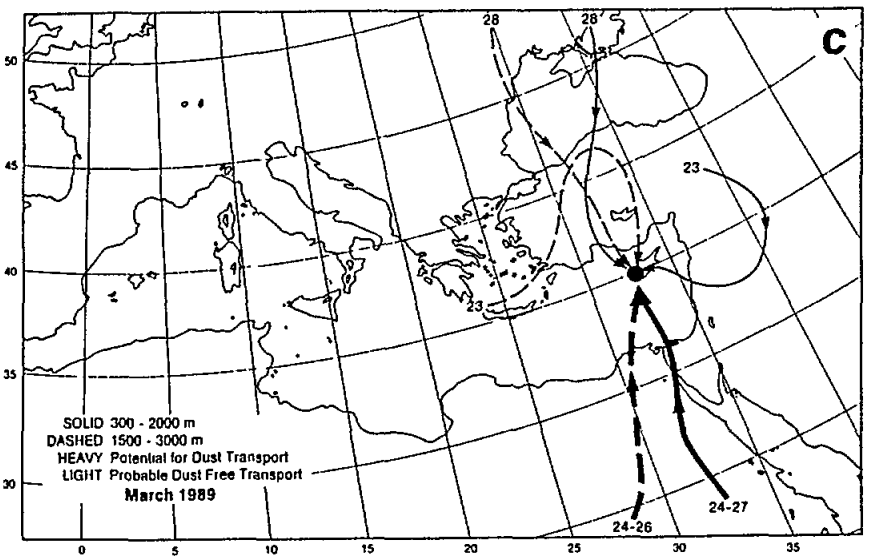

Fig.9(c) Back trajectories for the eastern Mediterranean aerosol intrusion event

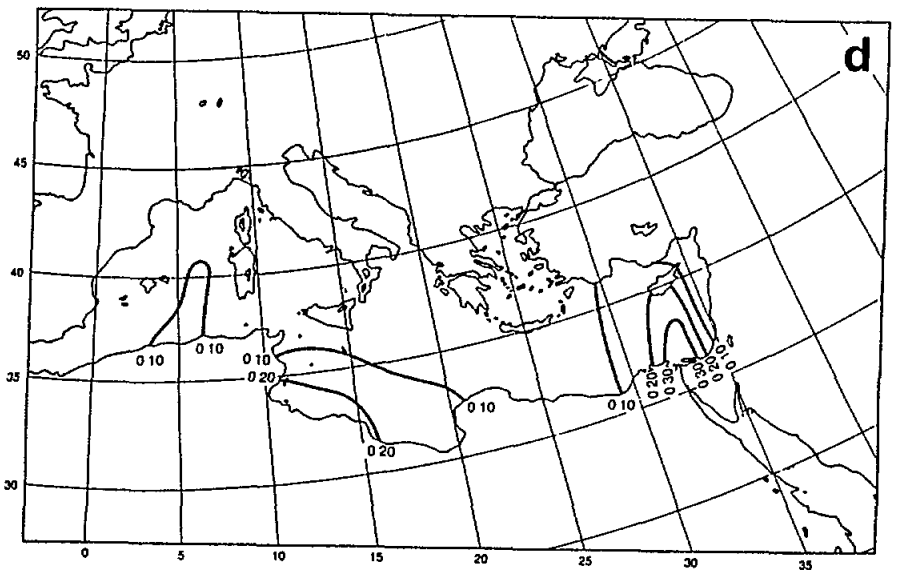

Fig.9(d) Weekly composite contour map of aerosol optical thickness over the Mediterranean Basin for the week ending March 30, 1989

Table 4

Summarization of analyzed dust events

Sub-section	Date	Surface synoptic conditions	Location*	Satellite type and spectrum	Layer-Origin	Event duration (days)	Optical depth (?)	Visibility range (km)
3.3.a	Oct. 23, 88	Cold depression over the centre of Libya	C	NOAA-9 Visible	Lower - S	2-3	.3	<25
3.3.b	Feb. 25-28, 89	Deep depression over the Ionian Sea	C	Meteosat Visible	Lower and higher - SW	2-3	.2	<25
3.3.c	Mar. 21, 89	Developed trough over Libya and Italy	C	NOAA-8 Visible	Lower - S Higher - SW	3-4	.3	15-25
3.3.d	Apr. 5, 89	Shallow Saharan depression	C	NOAA-8 Visible	Lower and higher - SW	2	.4	10-20
3.4.a	Sep. 29, 88	Well developed trough from Red Sea	E	NOAA-7 Visible	Lower - NE	1	.1	<30
3.4.b	Feb. 9, 89	Red Sea trough	E	Meteosat Visible	Lower - ESE	1	.1	<30
3.4.c	Mar. 25, 89	Deep cold depression over the Aegean Sea	E	NOAA-8 Visible	Lower and higher - S	2-3	.3	15-25

* C = Central Mediterranean E = Eastern Mediterranean

4. CONCLUSIONS

The 7 aerosol intrusion events selected for analyses were divided into two distinctive categories--four events occurring in the central Mediterranean region and three events occurring in the eastern Mediterranean Basin.

The analyses presented in Figs. 3-9 and summarized in Table 4 reveal several interesting features of these dust outbreaks. The central Mediterranean events differ distinctly from those in the eastern Mediterranean in their origin of dust sources, their atmospheric transport layers and their duration. Synoptically, all the central events are characterized by deep barometric depressions extending from the ground up to higher atmospheric layers (3000 m or more) with a strong gradient on their east side leading to air flow originating from a southern direction; i.e., the Saharan Desert. The eastern dust events occur mainly when a shallow barometric trough extends north from the Red Sea depression, with its north-south axis lying over the eastern Mediterranean region and accompanied by easterly winds. Therefore, the central events are usually characterized by deeper atmospheric layers as observed in subsections 3.3.b, 3.3.c, and 3.3.d. This is confirmed by the trajectories for each event considering the two transport layers shown. Another interesting difference between the central and eastern dust events is their duration; 2 days or more for the former and short for the latter (see subsections 3.4.a and 3.4.b). An exception should be noted for subsection 3.4.c which lasted for over a day and is explained by the occurrence of a synoptic condition similar to the central dust events (i.e., deep, cold barometric low).

The main conclusion is that transport of Saharan dust usually extends into deeper atmospheric layers and is characterized by a regional extension all over the Mediterranean Basin with longer duration compared to Arabian Peninsula dust where origins are rather short in time and affect only the eastern part of the Mediterranean Sea and are usually restricted to a lower atmospheric layer above ground (up to 2000 m a.s.l.).

5. RECOMMENDATIONS

This work represents an initial step in determining the requirements for the most effective combination of remote sensed data and ground truth data for the assessment of aerosol intrusion events into the Mediterranean Basin. It still remains to be shown, by more extensive comparisons between dust outbreak observations and trajectory simulations, that such events could be monitored more precisely by remote sensing methods in order to assist environmental modelers in the aerosol climatology of the Mediterranean Basin. This task might be achieved in a future study considering some of the following recommendations:

A. Improvement of the spatial and temporal resolution of the optical thickness values above the Mediterranean Sea

(1) Develop a better procedure for determining ô values from satellite brightness maps through upgrading the radiative transfer model.

(2) Characterize more accurately the Mediterranean aerosol size spectrum including particle radii above Junge's limits of 20 μm.

(3) Develop an appropriate algorithm to enable ruling out high cloud overcast conditions from aerosol radiance calculations.

(4) Improve the validation of satellite data for selected dust spells by ground truth observations, transmissometers, nephelometers, and reported visibility.

B. Improvement of trajectory calculations

(1) Expand the vertical resolution of the transport layers in the BAT model.

(2) Use a multilayer gridded LRT model for trajectory generation to overcome problems of data sparsity featuring the southern part of the Mediterranean Basin.

6. ACKNOWLEDGMENTS

The authors are grateful to I. Marcus and B. Ziv from the Israel Meteorological Satellite Center for their interest and encouragement and for supplying the satellite pictures. They would also like to thank A. Hildebrand from the NOAA/Visual Service for assistance in satellite picture reproduction, and B. Wells for typing the manuscript.

7. REFERENCES

Charlson, R.J., N.C. Ahlquist, H. Selvidge and P.B. MacCready (1969). Monitoring of Atmospheric Aerosol Parameters with the Integrating Nephelometer. *J. Air Poll. Control Assoc.*, *19*, pp. 937.

Curcio, J.S., G.L. Knestrick and T.H. Cosden (1961). Atmospheric Scattering in the Visible and Infrared. NRL Rpt. 5567, U.S. Naval Research Laboratory, Washington, DC.

Dayan, U. (1986). Climatology of Back Trajectories from Israel Based on Synoptic Analysis. *J. of Clim. and Appl. Meteor.*, 25:591-595.

Dayan, U. (1987). Sandstorms and Duststorms in Israel - A Review. IAEA IA Report 1419, Jan. 87, pp. 32.

Fett, W. (1967). *Beitr. Phys. Atmos. 40*, p. 262.

Ganor, E. (1975). *Atmospheric Dust in Israel - Sedimentological and Meteorological Analysis of Dust Deposition*. Ph.D. Thesis, 224 pp. The Hebrew University of Jerusalem.

Ganor, E. and Y. Mamane (1982). Transport of Saharan Dust Across the Eastern Mediterranean. *Atmos. Environ.*, 16:581-587.

Griggs, M. (1975). Measurements of Atmospheric Aerosol Optical Thickness over Water Using ERTS-1 Data. *J. Air Poll. Control Assoc.*, 25:622-626.

Haggerty, J.A. and P.A. Durkee (1988). Estimating Aerosol Optical Depth from Satellites for Navy Applications. Presented at the *Workshop on NOAA Experimental Aerosol Products*, 25-26 April 1988, World Weather Building, Camp Springs, MD 20746.

Heffter, J.L. (1983). Branching Atmospheric Trajectory (BAT) Model. NOAA Tech. Memorandum ERL ARL-121, NOAA, Air Resources Laboratory, Silver Spring, Maryland, U.S.A.

Junge, C.E. (1958). Atmospheric Chemistry. *Advances in Geophysics*, 4:1.

Katsnelson, J. (1970). Frequency of duststorms at Beer-Sheva. *Isr. J. Earth-Sci.*, 19:69-76.

Kaufman, Y.J. and R.S. Fraser (1983). Light Extinction by Aerosols during Summer Air Pollution. *J. of Clim. and Appl. Meteor.*, 22:1694-1706.

Lunson, E. (1950). Sandstorms on the Northern Coasts of Libya and Egypt. Gr. Brit. Meteorol. Off., *Professional Notes*, 102:1-12.

Mamane, Y., E. Ganor and A.E. Donagi (1980). Aerosol Composition of Urban and Desert Origin in the Eastern Mediterranean, I. Individual Particle Analysis. *Water, Air and Soil Poll.*, 14:29-43.

Meckler, Yu., H. Quenzel, G. Ohring and I. Marcus (1977). Relative Atmospheric Aerosol Content from ERTS Observations. *J. Geophys. Res.*, 82:967-970.

Miller, J.M., D. Martin and B. Strauss (1987). A Comparison of Results from Two Trajectory Models Used to Produce Flow Climatology to the Western Mediterranean. NOAA Tech. Memorandum ERL ARL-151, NOAA, Air Resources Laboratory, Silver Spring, Maryland, U.S.A.

Morales, C., (Editor) (1979). *Saharan Dust*. Scope 14, John Wiley and Sons, New York.

UNEP (1989). Meteorological and Climatological Data from Surface and Upper Air Measurements for the Assessment of Atmospheric Transport and Deposition of Pollutants in the Mediterranean Basin: A Review. MAP Technical Report Series No. 30, UNEP, Athens, 137 pp.

AFRICAN AIRBORNE DUST MASS OVER THE WESTERN MEDITERRANEAN FROM METEOSAT DATA

By

FRANÇOIS DULAC[1], PATRICK BUAT-MÉNARD[1], DIDIER TANRÉ[2] and GILLES BERGAMETTI[3]

[1] Centre des Faibles Radioactivités, Centre National de la Recherche Scientifique/Commissariat à l'Energie Atomique, Gif-sur-Yvette Cedex, France.
[2] Laboratoire d'Optique Atmosphérique, Université des Sciences et Techniques de Lille, Villeneuve d'Ascq Cedex, France.
[3] Laboratoire de Physico-Chimie de l'Atmosphère, Université de Paris 7, Paris Cedex 05, France.

A B S T R A C T

This paper is a shortened version of a paper on the assessment of the mass of African dust present over the Western Mediterranean during a transport episode from northwestern Africa, which occurred in early July 1985 (Dulac *et al.*, 1991a). The method is based on the use of a desert aerosol model, an earth-atmosphere radiative transfer model and data from Meteosat Visible channel. Optical properties of the desert aerosol, and a proportionality factor between aerosol optical thickness and aerosol atmospheric load have been calculated using the Mie theory and the background desert aerosol model of particle size distribution from Shettle (1985), found to be consistent with mass-particle size distribution of desert particles as derived from cascade impactor and dry deposition sampling. Using the radiative transfer model of Tanré *et al.* (1990), we were able to simulate the Meteosat signal. The atmospheric aerosol optical thickness was adjusted in order to fit Meteosat observations. This allows the estimation of the integrated aerosol load per unit area. Calculated values range between 0.1 and 2.3 g m^{-2}. Uncertainties have been carefully evaluated, with particular emphasis on the relationship between atmospheric dust load and aerosol optical thickness. The lack of knowledge of the actual particle mass-size distribution, particularly for particles larger than 10 µm in diameter, is the major source of uncertainty. Also important uncertainties in the spatial extrapolation of the data may come from the presence of clouds. Overall, we estimate that such an approach predicts the mass of desert dust transported within a factor of 3.

1. INTRODUCTION

Previous studies have shown that long-range atmospheric transports of desert dusts are responsible for sporadic but intense aerosol concentration peaks in areas several thousands of kilometres away from source regions. In the Western Mediterranean, atmospheric transport of soil dust from Africa is responsible for sporadic but intense aerosol concentration peaks, with daily mean values greater than background by up to 2 order of magnitude (Arnold *et al.*, 1982; Chester *et al.*, 1984; Tomadin *et al.*, 1984; Dulac *et al.*, 1987; Bergametti *et al.*, 1989a; Corregiari *et al.*, 1990). These events control the atmospheric input to the sea of major particulate elements, such as Al, Si or Fe (Bergametti *et al.*, 1989b), and play a significant role in the pH of associated precipitations (Lo-e-Pilot *et al.*, 1986; Losno *et al.*, 1988). Moreover, they are

followed by significant increases of elemental concentrations and fluxes in the upper water column (Buat-Ménard *et al.*, 1989). Meteorological satellites offer the opportunity for making long-term and large-scale studies of such transports. It has been shown that accurate measurements of the aerosol optical thickness may be derived from satellite data in the visible range over the ocean, due to the low value of oceanic surface albedo (e.g. Rao *et al.*, 1988). However, up to now, very few attempts have been made to derive the mass of aerosols being transported from such remotely sensed data. Such information would be extremely useful to assess the geochemical significance of such transport and deposition events, especially over open ocean areas.

We report here results based on the use of Meteosat data to estimate the mass of suspended desert dust particles over the Western Mediterranean, with special reference to a dust transport event which occurred in early July 1985. Aerosol optical depth over the basin is estimated from Meteosat Vis data using an earth-atmosphere radiative transfer model, and a relationship between aerosol optical depth and aerosol mass is computed. This work has already been described. For a detailed discussion of the method and of its uncertainties, complementary figures and colour pictures, the reader can refer to Dulac *et al.*, (1991a).

2. THE DATA SET

2.1 Field sampling and analytical methods

Atmospheric aerosol samples were collected at Capo Cavallo (43E31N, 8E40E), Corsica Island. The sampling site has an unimpeded view onto the sea, is 700 m from the shore and at an altitude of about 300 m. Noon to noon daily aerosol samples were collected between April 1985 and December 1987, at the top of a 10 m high meteorological tower, on 0.4 µm porosity Nuclepore® filters. Samples of total deposition (wet + dry) were also collected there during the same period, on a ten to twenty-day basis, using a hemisphere collector with an area of $0.1 m^2$. The deposition samples were acidified using HNO_3 01.N, and filtered on 0.4 µm porosity Nuclepore® filters. Details of sampling location and conditions have already been published elsewhere (Bergametti, 1987; Bergametti *et al.*, 1989a; Dulac *et al.*, 1989). We focus here on the late June-early July 1985 period, during which a transport of dust particles from Africa was recorded (Bergametti *et al.*, 1989b). Date include: (1) daily atmospheric concentrations of Al and Si from June 21-22 to July 10-11, excluding two missing samples on June 27-28 and July 9-10; and (2) Si total deposition, integrated from June 21, 11:00, from July 1, 10:00 to July 11, 11:40, and from July 11, 11:40 to August 1, 11:00. Rain occurred during the first deposition sampling period but the two other deposition samples corresponded to dry deposition only.

Al and Si were considered as tracers of soil dust particles. X-ray fluorescence was used for Al and Si analyses of aerosol samples (Losno *et al.*, 1987). Si was analyzed by X-ray fluorescence in the undissolved fraction of total deposition samples, and by colorimetry in the filtered solution. Analytical precision was better than ± 10% for the considered samples.

2.2 Meteorological data

Capo Cavallo used to be a French meteorological station, and the basic meteorological parameters (wind velocity and direction, cloud coverage, precipitation) were recorded on a six-hour time step. Local precipitation amounts were also obtained from French Mediterranean coastal synoptic meteorological stations: Perpignan, Montpellier-Frejorgues, Marseille-Marignane, Toulon, Nice, Bastia-Poretta, and Ajaccio. Vertical soundings of the atmosphere were performed at 0 and 12h GMT at the meteorological station of Ajaccio, Corsica. Vertical profiles of temperature and relative humidity were obtained from the ground level up to 500 hPa (about 5,900 m) at 12h GMT from July 1 to July 6.

In order to trace the transport of aerosol particles back from their source regions, air mass trajectories have been computed by the Service des Etudes Spéciales, Météorologie Nationale, Paris (Martin *et al.*, 1987; Bergametti *et al.*, 1989a; Martin *et al.*, 1990). Three-dimensional, four-day back trajectories, finishing at the sampling point and at the mid-time of each daily sampling time, and arriving at the 925-, 700- and 500-hPa final levels, have been computed from the analyzed wind fields of the European Centre for Medium-Range Weather Forecasts of Reading, England. Forward trajectories leaving the source region, as identified from Meteosat data, were also computed.

2.3 Satellite data

Digital data from both visible (VIS: 0.35-1.1 µm) and thermal infrared (IR: 10.5-12.5 µm) channels of the operational meteorological satellite Meteosat 2 were obtained from the European Space Operation Centre, Darmstadt, Federal Republic of Germany. A sequence of 8 VIS and 8 IR images have been considered, corresponding to Meteosat slot 24 (11h-11h30 observation) and slot 25 (11h30-12h observation) on 1 to 4 July 1985. Data were coded over 8 bits, so that numerical values were integers ranging between 0 and 255. However, the raw VIS data used to be originally coded over 6 bits and arbitrarily extended to 8 bits using a random process (ESOC, 1987). We set to 0 these two VIS, non-significant, low order bits, so that numerical values were integers ranging from 0 to 252 by step of 4.

The resolution of full Earth disk images is 5000 pixels by 2500 lines in the VIS channel, and 2500 pixels by 2500 lines in the IR one. We performed a sampling of 1 pixel over 2 of VIS data in order to have coincident VIS and IR images, and extracted 510 pixels x 510 line windows approximately centered on Algiers, and covering Spain, Southern France, Italy, the western Mediterranean and northwestern Africa (Fig.1).

3. METHODS

3.1 Cloud distribution

Because of the high albedo of clouds, aerosol optical thickness should be inferred from cloud free pixels. A simple adjusted multispectral thresholding on VIS and IR counts is insufficient to discriminate cloud covered pixels, so that more complex tests are necessary (Schiffer and Rossow, 1983; Saunders and Kriebel, 1988). Coackley and Bretherton (1982) have shown that water or ice clouds and dust clouds may be discriminated by differences in local standard deviation of pixel values, determined over square areas of some pixels. This is due to the difference in spatial homogeneity of water and dust clouds.

Fig.1 Meteosat VIS image (July 3, 1985, slot 24) showing the presence of a dust plume over the western Mediterranean basin. The dust front is located over Corsica and Sardinia. The grey scale is linear between the numeric count 0 and 60, thresholded in the outer range.

In order to detect cloudy pixels, we applied an objective discrimination method, based on four different thresholding tests. The first three were respectively applied to the VIS count, to the IR count, and to the VIS local variance calculated over a 3 by 3 pixels square area. Respective threshold values were optimized by visual examination of the images so that evident cloud contaminated pixels were marked out, and pixels at the limit between homogeneous areas of dust pixels of different luminances were saved. Pixels were discarded as cloudy pixels when: (1) their VIS count was greater than 60, which otherwise would have led to aerosol optical thickness values greater than 3.5; (2) their IR count was lower than 120, corresponding to a radiative temperature lower than 5°C according to the IR sensor calibration (MEP, 1985); and (3) their VIS variance was greater than 8. This spatial coherence test was the most severe one, as verified by Jankoviak and Tanré (1990) from Meteosat data over the Atlantic. Quite a few likely cloud pixels in large-scale cloud structures and in scattered cloud fields were not discarded. However these few pixels appeared to have a significant influence when interpolating pixel values over masked areas (see Section on

Integration over the basin). We discarded these pixels using an edge filter which retains a pixel P if at least six of the pixels adjacent to it have the same value as P, and otherwise eliminates P.

3.2 Determination of the aerosol optical depth over the sea

! **Earth-atmosphere radiative transfer model**. Because surface seawater has a low and fairly constant albedo, we retrieved aerosol optical depth only over the sea, from Meteosat VIS data, and using an Earth non-cloudy atmosphere radiative model derived from the model "Simulation of the Satellite Signal in the Solar Spectrum" (5S), available from the Laboratoire d'Optique Atmosphérique, Université des Sciences et Techniques de Lille, France (Tanré *et al.*, 1990). Briefly, this computer code allows the estimation of the satellite signal due to the backscattering of the light in the solar spectrum by the ground-atmosphere system, assuming a cloudless atmosphere. It includes accurate analytical descriptions of the absorption by aerosol particles and atmospheric gases H_2O, O_3, O_2 and CO_2, and of the scattering by gas molecules and aerosols, as well as an approximate handling of the interaction between the two phenomena. The apparent reflectance as seen by the satellite is expressed as a function of the intrinsic atmospheric reflectance, the actual target reflectance, and the target environment reflectance. The relative contributions of the direct and diffuse transmittances on the sun-ground and ground-satellite paths, of the spherical albedo of the atmosphere and of the environment of the target are calculated, as well as the transmission multiplicative factor related to the absorption by atmospheric gases and particles. Input parameters include geometrical and spectral conditions, atmospheric gaseous composition, aerosol type and concentration and ground reflectance. Our geometric and spectral conditions were defined by Meteosat 2 position and filter function (Morgan, 1981). The VIS channel has a non-zero transmission between 0.35 and 1.1 µm, with a spectral integrated value of 0.39. The LOWTRAN standard mid-latitude summer atmosphere was used to define the gaseous composition of the atmosphere (McClatchey *et al.*, 1971; Kneizys *et al.*, 1980). Corresponding O_3 and H_2O columnar densities are 6.83 g m^{-2} and 2.93 g cm^{-2} respectively. The spectral reflectance of seawater was 0.024 (Viollier, 1980).

! **Aerosol model**. We had to consider a specific desert aerosol model and to implement it in 5S, because optical properties of the WCP standard dust-like aerosol component (WCP 112, 1986) included in the 5S package are significantly different from optical properties of desert aerosol (Shettle, 1984; D'Almeida, 1987).

Fitting data from seven cascade impactor samples of African dust performed in Corsica and at sea during several oceanographic cruises, has yielded a single mode for particle size distribution, with a mass-median diameter (MMD) ranging from 2.3 to 5.2 µm (typically 2.5 µm), and a geometric standard deviation (ó) ranging from 1.1 to 4.5 (typically 2.0), the largest values being derived from samples collected along the African coast (Bergametti *et al.*, 1987; Dulac, 1987; Dulac *et al.*, 1989; Gomes *et al.*, 1990). However, our cascade impactors allow the sampling of particles in a limited range of size, probably from 0.05 to 15 µm in diameter. Moreover, the optical properties of these aerosols have not been studied. Because of this lack of relevant data from African dust plumes over the Mediterranean, we considered the standard continental desert aerosol models which were available from Shettle (1984) and D'Almeida (1987). By selecting different number-particle size distribution models of from the literature, these authors have determined optical properties for several standard models of desert aerosol. Each proposed model is composed of 3 log-normal modes. There are significant differences in the mass-size distribution parameters of the different modes between comparable models

by Shettle and D'Almeida. This is also the case for the total distributions when the 3 modes are summed up. The mass-particle size distribution of the background desert aerosol model used by Shettle (1984) seems well adapted to our observations, because it presents a single mode in the particle size range where cascade impactors efficiently collect particles. The following parameters have been calculated from the number distributions of Shettle's background desert aerosol model, assuming spherical particles of density 2.5:

Mode	MMD (µm)	ó	% of total mass
1	0.0110	2.13	$2.6\ 10^{-4}$
2	2.52	3.20	78.1
3	42.3	1.89	21.9

The mode at 2.52 µm accounts for about 78% of the total particle mass. The contribution of the sub-micronic mode to both aerosol mass and optical properties is negligible. On the other hand, there is observational evidence that giant mineral particles (of 50 µm diameter or more) from desert areas are transported over very long distances (Prospero *et at.*, 1970; Jaenicke and Schütz, 1978; Carder *et al.*, 1986; Betzer *et al.*, 1988; Coudé-Gaussen, 1989). Microscopic investigations of alumino-silicate particles in aerosol samples also indicate that large particles are present in African dust plumes over the Mediterranean (Coudé-Gaussen, 1989). Moreover, from microscopic investigations of 558 mineral particles in a dry deposition sample which was obtained during another African dust transport event in Corsica from Corsica, Dulac *et al.* (1991b) could retrieve the relevant airborne mass concentration of particles (dC/dLnD) by dividing the deposited mass of every particle by its deposition velocity, calculated using the model of Slinn and Slinn (1980). They could fit the resulting mass size distribution of airborne particles by a sum of 2 log-normal modes: $MMD_1 = 2 \pm 0.5$ µm, $MMD_2 = 13 \pm$ µm, $ó_1 = 2.0 \pm 0.1$, $ó_2 = 1.85 \pm 0.1$, and $C_1 = C_2 = 50 \pm 10\%$. The fine mode is typical of the mass-particle size distributions of Al observed in the Mediterranean from cascade impactor samples (Bergametti, 1987; Dulac *et al.*, 1989; Gomes *et al.*, 1990). Dulac)1986) also reported an overall MMD of about 13.5 µm for insoluble particles in a red rain collected at sea (40.62N-07.17E) in April 1981. Moreover, using a Coulter® counter, Guerzoni *et al.* (1991) measured mass-particle size distributions from a few rain and aerosol samples associated with southern origins, which were collected in southeastern coastal Sardinia. Their results suggest an overall MMD of about 15 µm in two different rain samples, and the presence of two modes in one aerosol sample. These modes are about 3 and 15 µm in diameter, and the large mode contribution to the total mass is about 40%. The background desert aerosol model used by Shettle states that the relevant large mode has a mass-median diameter of 42.2 µm and accounts for 22.1% of the total mass. Any location in the western Mediterranean basin is within 1,500 km of the North African source region of dust for the episode considered (see Section 4.1), and Schütz's (1979) calculations, which consider only particles in the diameter range 0.2-40 µm, suggest that particles larger than 20 µm in diameter can contribute significantly to the total aerosol concentration in this range of distance from Saharan source areas. Therefore, in the absence of more quantitative data on very large particles, we assumed that the particle size distribution of the background desert aerosol model used by Shettle (1984) was adapted to describe the desert aerosol transported over the western Mediterranean. Moreover, derived radiative properties are in good agreement with optical ground-based measurements performed in Senegal during dust events (Tanré *et al.*, 1988b). Nevertheless, the radiative properties of D'Almeida's (1987) background model were also very consistent, and the consequence of using either mass-size distribution has been considered.

! **Aerosol optical depth**. All other parameters being fixed, the aerosol optical thickness at 550 nm ($\hat{o}_{550}$) was used to set the aerosol concentration, assuming that the atmospheric aerosol loading is directly related to $\hat{o}_{550}$. The approach we used was to look at the variations in the calculated Meteosat signal when varying $\hat{o}_{550}$, in order to fit the spectral aerosol optical depth dependence as a function of the Meteosat value for a given geometry.

The radiance at the top of the atmosphere (L^*, in W m^{-2} sr^{-1}) has been computed using the radiative properties of the aerosol model and the modified version of the 5S code, for several values of $\hat{o}_{550}$: 0.1, 0.2, 0.4, 0.6, 0.8, 1.0, 1.2, 1.4, 1.7, 2.0 and 2.5. The corresponding Meteosat value (N, a real positive number) was retrieved from L^*, as calculated by 5S, using $N = 2 + L^*/C$, where C = 0.575 W m^{-2} sr^{-1} 8-bit-$count^{-1}$, is the calibration constant of the Meteosat 2 VIS channel determined by Köpke (1983). Then a third order polynomial functions was fitted between $\hat{o}_{550}$ and N: $\hat{o}_{550} = a_0+a_1N+a_2N^2+a_3N^3$, the coefficients a_i depending on the geometrical conditions (hour of observation, and position of the pixel). Geometrical conditions corresponded to noon observations, at 11h45 and 12h15 GMT (corresponding to Meteosat slot 24 and 25 respectively) from July 1 to 4, and to 35 test pixels regularly distributed throughout the western Mediterranean area. The corresponding zenithal viewing angle ranged between 42E and 52E, while the sun zenithal angle ranged between 13E and 23E.

Moreover, for each image from the series considered (hour of observation fixed), the coefficients a_i (0#i$3) were fitted as $a_i=b_{0,i}+b_{1,i}A$, where A is the angle between OC and CP if O, C, and P are respectively the point of 0E latitude and 0E longitude, the centre of the Earth, supposed spherical, and the point of observation, and each $b_{0,i}$ a constant for that particular image. Thus $\hat{o}_{550}$ could be determined for every remaining dust pixel in Meteosat VIS images from its numerical count N and calculated angle A.

The accuracy of the overall fit of $\hat{o}_{550}$ in function of N and A was checked. Any test value of $\hat{o}_{550}$ was approximated within ±0.015. The relative precision was better than 1% for $\hat{o}_{550}$$0.6. The highest deviations between fitted and computed values were observed for $\hat{o}_{550}$=0.1 at the far South-West and North-East of the basin for slot 24 (maximum relative deviation of 4.5%) and at the far South-East for slot 25 (max. 8.5%).

3.3 Airborne dust mass

! **Columnar aerosol mass loading at the pixel scale**. It is generally accepted that the aerosol optical thickness $\hat{o}_ë$ at a wavelength ë, is proportional to the total aerosol mass loading (M, in g m^{-2}) in a vertical column (Volz, 1970; Carlson and Caverly, 1977): $M = R\ \hat{o}_ë$, where the proportionality factor R depends on aerosol properties. The mass M depends on the aerosol size distribution n (r,z), r being the radius of particles, supposed spherical, and z the altitude, and on the aerosol density d, while $\hat{o}_ë$ depends on the aerosol size distribution n (r,z) and on the Mie theory extinction cross section Q, itself depending on the aerosol particle size r and refractive index m, and on the wavelength ë.

Assuming d = 2.5 g cm^{-3} (Fraser, 1976; Carlson and Caverly, 1977), m = 1.55-0.005i (Patterson *et al.*, 1977), and a constant size distribution as a function of the altitude, we computed the ratio R_{550} between M and $\hat{o}_{550}$ range from 1.3 for the background desert aerosol model of Shettle up to 45 and 136 for sandstorm aerosol models. Such a spread of the results shows that the determination of M from $\hat{o}_{550}$ is very sensitive to the aerosol mass-size distribution, and therefore subject to large uncertainties. The computed value of 1.3 for the background desert aerosol model considered is in good agreement with the values of 1.3 and

1.5, reported for Saharan aerosol after Atlantic crossing, respectively by Volz (1970) and by Carlson and Caverly (1977) after measurements in the Caribbean and at Barbados. When only the intermediate mode of Shettle's background model is considered, the ratio R_{550} is 0.965. This value is 26% lower than when considering the three modes together, when 22% of the mass is due to the single third mode (see above table). This confirms that extinction is essentially due to the second mode, while the third mode also contributes significantly to the total mass. We also determined the value of R_{550} for the model derived from cascade impactor Mediterranean samples of African aerosol suggested above (MMD=2.5 µm; ó=2.0). This result is 1.13 and consequently very close to relevant values derived from Shettle's background model. As already mentioned, Shettle's background model fits our ground measurements, which cover a limited range of particle size, so that the value of 1.3 seems the most realistic one. Therefore, we used the relationship M (g m^{-2}) = 1.3 $\hat{o}_{550}$ to infer the columnar atmospheric dust loading from the atmospheric turbidity.

For comparison, let us also mention the value of 3.75 measured by Carlson and Caverly at Cape Verde Islands (off the West African coast) and the value of about 10, deduced from measurements performed by D'Almeida (1986) at Agadez assuming the thickness of the equivalent homogeneous Saharan air layer was 3 km. Although all these coefficients are deduced from optical thickness determined for different spectral conditions, authors agree that the dependence of ô on ë is weak n the case of desert aerosol (Carlson and Caverly, 1977; Shettle, 1984; D'Almeida, 1987) so that the different values of the ratio R from the literature may be compared to the value of R_{550} calculated in this work.

! **Integration over the basin**. The aerosol columnar densities were determined from a number of pixels, due to the presence of islands and clouds over the basin. In order to take into account the mass of dust present in the numerous pixels where raw data were not exploitable in terms of aerosol loading, we performed a linear interpolation of the discontinuous M fields. This is justified because the continuity of aerosol densities through areas that were masked suggest that water clouds did not significantly modify the structure of the dust front (Fig.1). Indeed, the meteorological reports from Ajaccio confirmed the presence of a partial coverage of the sky (<50%) by altocumulus clouds, but only at the highest altitude of the standard scale used for reports, i.e. over 2,500 m, during the passage of the cloud system over Corsica (July 4, 0 and 12h GMT reports), while clear skies were observed on the day before and after.

We used a standard distance weighted interpolation routine of the Uniras®/Unimap 2000® graphic display package (UNIRAS, 1988, 1989). The grid cell for interpolation was fitted to have one pixel per grid node. No smoothing of interpolated data was performed, so that the numerical values of unmasked pixels remained unchanged after the interpolation process.

4. RESULTS AND DISCUSSION

4.1 Atmospheric circulation

The Meteosat image displayed in Fig.1 shows the presence of a dust plume from North Africa to Europe over Corsica and Sardinia. The transport of this dust plume was associated with the eastward movement of a cyclonic cloud system over the basin. The 850 hPa meteorological synoptic charts from the European Meteorological Bulletin show the incursion of a cold polar air mass over the eastern Atlantic at the latitude of the Iberian

Peninsula in late June. An anticyclonic wedge was located over Tunisia and the southern part of the western Mediterranean Sea. Ground level charts report a NW-SE front, between the trough located over the eastern Atlantic and this anticyclonic wedge, generating strong winds ahead of itself in Northeastern Algeria. The eastward movement of the trough, which was located over the Iberian Peninsula on July 3 (Figs.1 and 2), generated a SW-NE circulation at 850 hPa in the western part of the western Mediterranean, propitious to dust transport from North Africa to the basin. Simultaneously, the front also moved eastward and was located over Corsica and Sardinia on July 3. Meteorological reports from Ajaccio and Capo Cavallo did not mention any precipitation during the passage of the front.

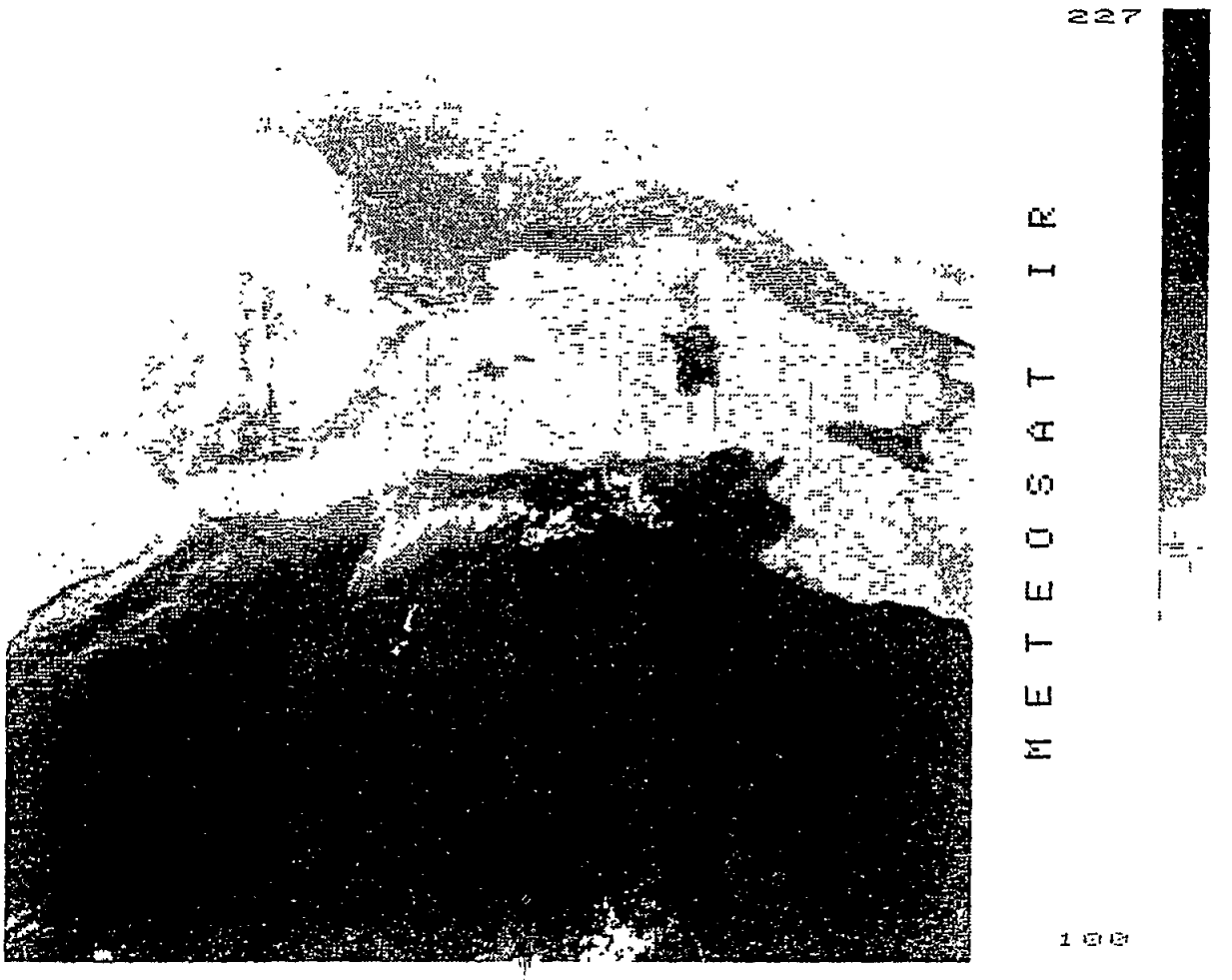

Fig.2 Meteosat IR image (July 2, 1985, slot 24) showing the dust source region in Northern Algeria. The grey scale is linear between the numeric count 100 (-6.5°C) and 227 (51°C), thresholded in the outer range.

Backward air mass trajectories, finishing at our ground sampling station at Capo Cavallo on July 4, at 700 and 925 hPa have shown that the upper air mass transported from Africa to Corsica experienced a mean continuous upward movement from the source region,

over a lower layer air mass coming from the Atlantic over France (Dulac *et al.*, 1991a). This is in agreement with the frontal character of African dust transport events over the western Mediterranean and western Europe (Prodi and Fea, 1979; Reiff *et al.*, 1986; Bergametti *et al.*, 1989a; Martin *et al.*, 1990). These trajectories suggest that the dust layer was transported at a mean altitude of about 3 km over Corsica. Moreover, rawind soundings performed at Ajaccio showed that the thickness of the dust layer over Corsica was up to 5,500 m on July 3 at 0h, and that an average thickness of about 3,500 m may be assumed for the dust layer during its presence over Corsica (Dulac *et al.*, 1991a).

Only a rough indication of the source region of the dust was given by finishing trajectories. However, Meteosat IR images taken on July 1 and 2 show that a dust rise occurred on the Algerian Atlas plateaux (Fig.2), where large summer dried marshes lie (Peters, 1989).

4.2 Ground based measurements

! Daily atmospheric concentrations. The atmospheric particulate concentrations of Al or Si are well known to be efficient tracers of the soil-derived dust component of the tropospheric aerosol (Rahn, 1976). The daily atmospheric particulate concentrations of Al and Si at Capo Cavallo from June 21-22 to July 12-13 are the following, in ng m^{-3}:

June	21-22	22-23	23-24	24-25	25-26	26-27	27-28	28-29	29-30	30-01
Al	138	101	42	175	106	149	-	206	333	373
Si	501	310	133	499	398	453	-	643	1020	1056

July	01-02	02-03	03-04	04-05	05-06	06-07	07-08	08-09	09-10	10-11	11-12	12-13
Al	296	1013	1595	2128	804	438	405	296	-	367	333	387
Si	933	2675	4495	5904	2770	1202	1308	851	-	1047	1035	1224

During this period, mean background levels were observed (100-400 ng m^{-3} for Al and Fe, and 300-1000 for Si). They correspond to background levels in this part of the western Mediterranean, as observed by Bergametti *et al.* (1989a). However, the samples collected on July 2-3 to July 5-6 exhibit much higher concentrations, up to 5,900 ng m^{-3} for Si on July 4-5. Such high atmospheric concentrations of soil-derived dust in this area are generally connected to African dust inputs (Chester *et al.*, 1984; Dulac *et al.*, 1987; Bergametti *et al.*, 1989a; Correggiari *et al.*, 1990). Rawind soundings at Ajaccio showed that changes in Al and Si concentrations were strongly correlated to changes in tropospheric air temperature. The temperature of air at an altitude of 2,000 m at Ajaccio was the following, in EC:

July	01-0h	12h	02-0h	12h	03-0h	12h	04-0h
T	12.4	13.6	13.2	16.1	16.8	16.9	20.3
	12h	05-0h	12h	06-0h	12h	07-0h	12h
	19.7	13.5	12.7	13.8	-	13.5	13.3

It is noteworthy that the concentration peak at ground level corresponded to the July 4-5 sample, while Meteosat images suggest that the dust layer had already passed Corsica and that the maximum integrated dust load over Corsica occurred during the time of the previous sample, i.e. July 3-4. This is probably due to the frontal character of the dust transport. Indeed, the observation of dust at ground level in Corsica when the dust layer was still at high altitude, on July 2.3, may be attributed to strong vertical mixing in the frontal zone. Then, maximum concentrations at ground level were observed, when the lowest part of the front passed over Corsica, allowing the presence of the dust layer at the sampling level. Results from the rawind soundings confirmed that the base of the warm and dry air layer regularly descended from about 550 m on July 3, 0h GMT, to the sea level on July 4, 12h GMT. This layer reached the level of the sampling station (about 300 m) late on July 3, and was no longer present on July 5, 0h GMT. High concentrations, still observed on July 5-6, were probably due to the setting of particles.

The evolutions of atmospheric concentrations (see above) and of the dust plume as seen on Meteosat images (Dulac *et al.*, 1991a), suggest that the presence of atmospheric dust at Capo Cavallo lasted from early July 3 to early 6, i.e. for 3 ± 0.5 days. In order to average the Si atmospheric concentration during that period, and because of the noon to noon sampling period, we assumed background Si concentrations of 1,000 and 1,200 ng m^{-3} respectively during the first half of the July 2-3 sampling period and the second half of the July 5-6 period. This yielded a mean atmospheric Si concentration of about 4,900 ng m^{-3} over the 3 days of presence of dust particles over Corsica. Using the mean Si concentration of 33% in average soil (Vinogradov, 1959; Bowen, 1966) as a reference for Si concentration in the aerosol, we estimated that an average concentration of dust of about 15,000 ng m^{-3} occurred at ground level during those 3 days.

! **Atmospheric deposition**. The total atmospheric deposition of Si measured at Capo Cavallo during the sampling period considered was (6.64 ± 0.42) 10^{-3} g m^{-2} d^{-1} from June 21 to July 1, (10.74 ± 0.33) 10^{-3} g m^{-2} d^{-1} from July 1 to July 11, and (3.13 ± 0.13) 10^{-3} g m^{-2} d^{-1} from July 11 to August 1. Precipitations were observed at Capo Cavallo on June 22 (9 mm) and June 23 (traces), i.e. during the first deposition sampling period. The two other samples corresponded to dry deposition only. While comparable background concentrations of atmospheric particulate Si were observed during the first and third deposition samples, the deposition flux was twice as intense during the first sample as during the third, due to the wet deposition event. These results confirm that wet deposition is more efficient at aerosol deposition than dry deposition (Slinn, 1983). Despite the absence of wet deposition, but due to the occurrence of the dust event considered, the atmospheric deposition of Si was still higher for the second total deposition sample. Approximating the contribution of background Si deposition during this sampling period (10.12 d) from a mean atmospheric Si concentration of 1,000 ng m^{-3} and a dry deposition velocity of 1 cm s^{-1} for background conditions (Dulac *et al.*, 1989), we calculated that a total of 0.10 g m^{-2} of Si was deposited due to the African dust plume itself. This corresponds to 92% of the Si deposition during the relevant total deposition sampling period. Using the mean Si concentration of 33% in average soil (Vinogradov, 1959; Bowen, 1966) as a reference for Si concentration in the deposited dust, we estimated that about 0.30 g m^{-2} of dust was deposited by dry deposition at the sea surface in the vicinity of Capo Cavallo, due to the African dust plume. Therefore, an average deposition of dust of about 0.10 g m^{-2} d^{-1} occurred during the three-day transit of the dust plume.

! **Deposition velocity of particles**. From the previous estimates of the average atmospheric dust load and deposition at Capo Cavallo, we inferred an average deposition velocity of the dust particles of 7.7 cm s^{-1} during the transit of the dust plume. In order to test our hypothetical aerosol model, we applied the Slinn and Slinn (1980) dry deposition model to the mass-particle size distribution of Shettle's background desert aerosol, divided into 100

successive size intervals, according to the method used by Arimoto *et al.* (1985) and discussed by Dulac *et al.* (1989). This yielded a very consistent dry deposition velocity of dust particles to seawater of 6.9 cm s^{-1}, controlled by gravitational settling, almost 94% of the deposition flux being due to the largest mode of the distribution (MMD = 42.2 µm). The deposition velocity being particularly sensitive to the contribution of large particles (Dulac *et al.*, 1989), the aerosol model of Shettle (1984) appears to be very well adapted to describe the whole mass-particle size distribution of the dust particles transported during this event. Indeed, using the model for mass-particle size distribution from Mediterranean cascade impactor samples mentioned above yielded a dry deposition velocity of only 0.1 cm s^{-1}.

The same approach applied to the mass-size distribution of D'Almeida's background aerosol, which yielded a dry deposition velocity of dust particles to seawater of 0.4 cm s^{-1}, more than 93% of the flux being due to the intermediate mode (MMD = 4.82 µm). Previous studies in the western Mediterranean yielded Al dry deposition velocities from 1.1 to 9.7 cm s^{-1} in case of transport from Africa, averaging between 3 and 4 cm s^{-1} (Dulac *et al.*, 1989). Published deposition velocities for dust particles are generally close to 1 cm s^{-1} (Duce *et al*., 1980; Giorgi, 1988; Schneider *et al.*, 1990), but concern longer range and larger scale transport than in this study.

4.3 Aerosol optical thickness

Fig.3 shows the calculated aerosol optical thickness ($\hat{o}_{550}$) over the western Mediterranean at 11h45 GMT on July 3. From July 1 to 4 respectively, values range from 0.14 to 1.77, 0.14 to 1.41, 0.13 to 1.70, and 0.14 to 1.04. Similar results have been obtained at 12h15 GMT using slot 25. Due to the solar and viewing geometry, the same Meteosat numeric count was produced by different aerosol optical thickness values in the northern and southern parts of the basin. On July 3 the front of the dust plume, extending from Tripoli, Libya to the Gulf of Genoa, correspond to the unique Meteosat numeric count of 16, while in Fig.3 a palette of greys covers the same area, corresponding to aerosol optical thicknesses increasing from 0.13 in the North to 0.23 in the South. This is due to the low sensitivity of the Meteosat visible sensor.

Different possible sources of errors in the determination of $\hat{o}_{550}$ have been listed and discussed in Dulac *et al.* (1991a), including the absolute calibration of the Meteosat VIS sensor and its limited sensitivity, the use of a standard gaseous atmospheric model to take into account Rayleigh scattering and gaseous absorption of the light, the sea surface reflectance, the stratospheric aerosol and non-desert background influence on the aerosol optical thickness, and aerosol physical properties, i.e. refractive index and size distribution. Jankowiak and Tanré (1991) estimated the overall relative uncertainty of the determination of $\hat{o}_{550}$ off western Africa from Meteosat imagery using an approach similar to ours, to be about ± 30% for any given pixel, by comparison with ground based measurements. We did not perform ground truth optical measurements to confirm this range of uncertainty over the Mediterranean basin. Since the relative uncertainty could be higher in our conditions due to greater uncertainty in the aerosol model after crossing the Mediterranean, we believe an overall relative uncertainty of ± 50% in the determination of $\hat{o}_{550}$ has to be considered as a maximum. Let us emphasize that this is the uncertainty in the value of any single pixel, so that any integration process should decrease it.

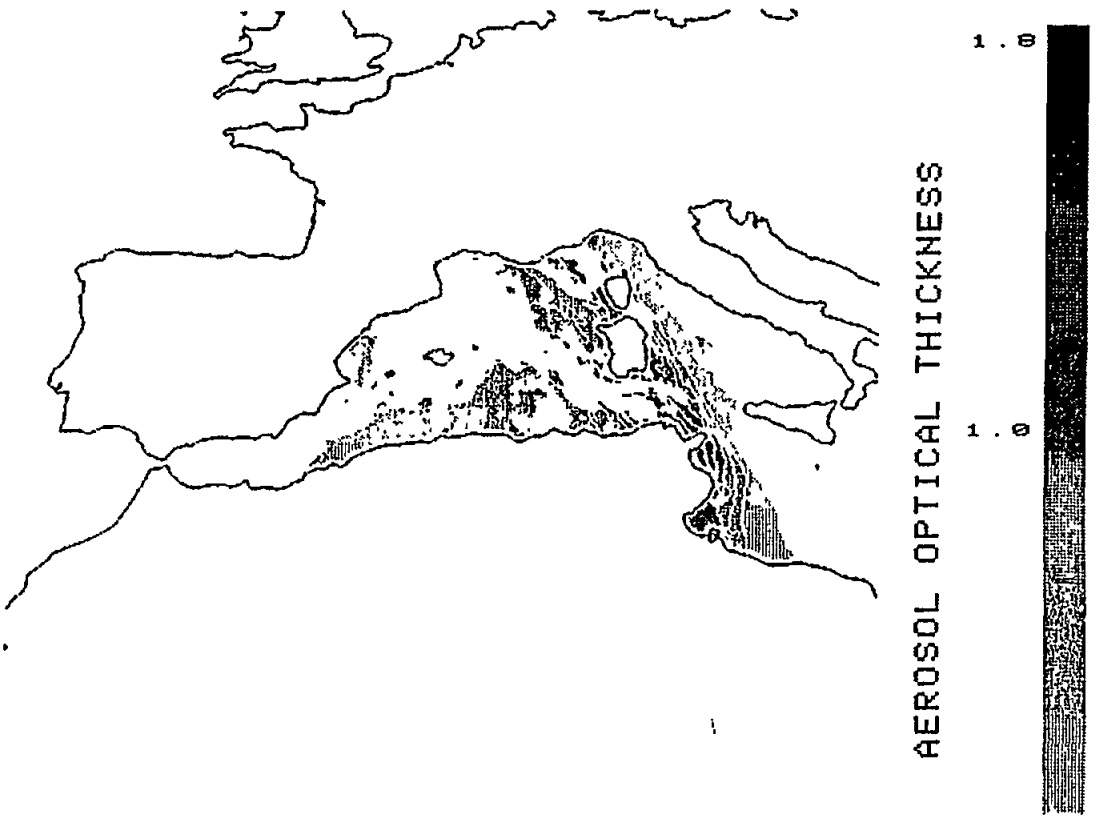

Fig.3 Calculated desert aerosol optical thickness over the western Mediterranean at 11h45 GMT on July 3, 1985. White pixels have been filtered out (see text).

4.4 *Airborne dust mass*

Results from our computation of desert aerosol columnar densities over the western Mediterranean at 11h45 GMT on July 3, 1985, are presented in Fig.4. Values range between 0.18 and 2.30 g m^{-2}. The interpolation is believed to give a good estimate of what would be the aerosol loading if clouds were not present, and to allow us to obtain the total mass of dust transported over the sea and islands by spatial integration. Using an average of 30.4 km^2 per pixel, we estimated the area covered by the dust plume over the western and central Mediterranean sea, including islands, and the mass of desert dust over the basin, from July 1 to 4, 1985, at 11h45 and 12h15 GMT. Results are as follows:

July	1-11h45	1-12h15	2-11h45	2-12h15	3-11h45	3-12h15	4-11h45	4-12h15
Area (10^3 km^2)	498	517	393	412	735	752	866	882
Mass (10^9 g)	309	330	300	314	574	580	379	418

The dust plume was spread over a few hundred thousand square kilometres, and was continuously expanding. The decrease in area and mass observed between July 1 and 2 was essentially due to the eastern part of the dust plume which was present over the Gulf of Gabes on July 1, and had returned over Africa on July 2, due to a southward circulation generated by the high cell over Tunisia. The related mass of dust transported back to Africa amounted to 45 10^9 g. Excluding this recycled part of the dust plume, the mass of dust over

the western basin continuously increased from July 1, 11h45 (259 10^9 g) to July 3, 12h15 (580 10^9 g).

There are several assumptions in the determination of the aerosol mass from the aerosol optical thickness. The numerous sources of errors in the determination of M have been discussed in Dulac *et al.* (1991a), including the proportionality coefficient R_{550} between τ_{550} and the columnar aerosol mass, hypotheses of spherical particles with a bulk density of 2.5 g cm^{-3}, and interpolation of the dust mass over the basin (the mass from interpolated pixels accounts for 45 to 75% of the total). The overall accuracy of the total dust mass determination was estimated to be about a factor of 3.

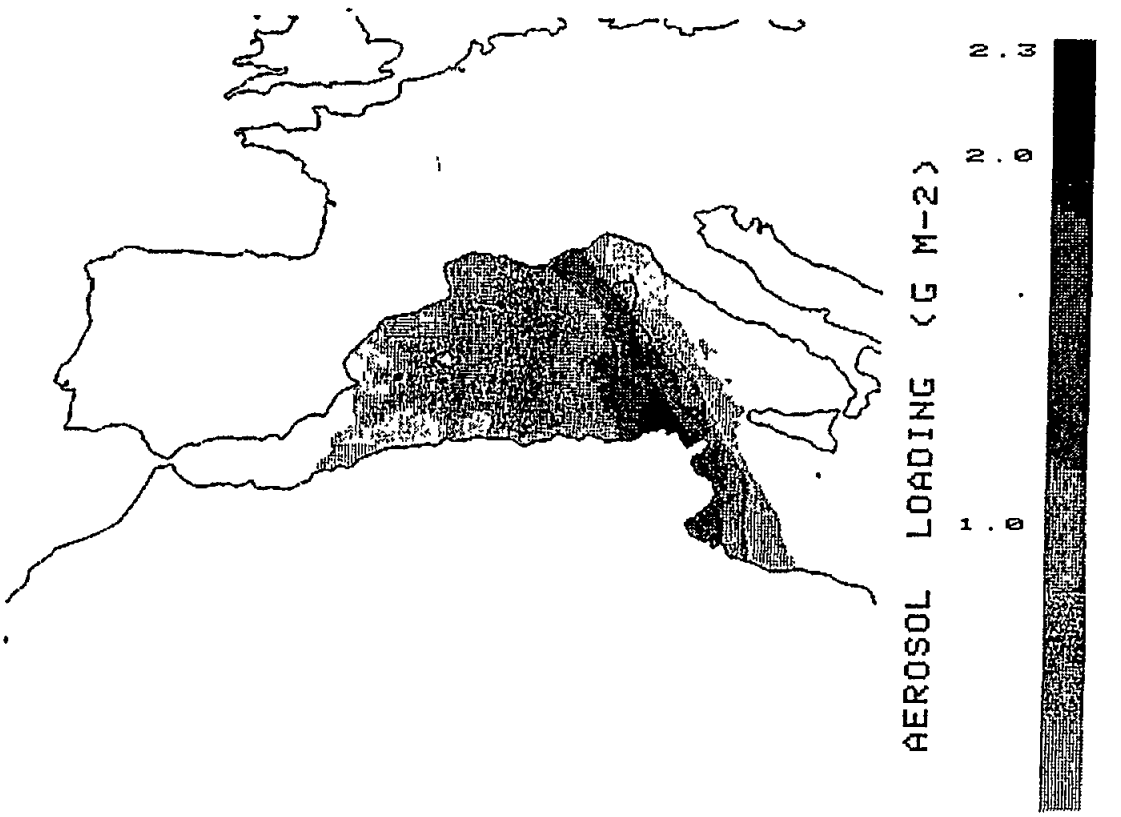

Fig.4 Computed desert aerosol columnar density (g m^{-2}) over the western Mediterranean at 11h45 GMT on July 3, 1985.

4.5 Total mass of dust exported from Africa

Averaging the atmospheric dust load over Corsica during the estimated deposition period yielded about 0.4 g m^{-2} (within a factor of 3). By comparison with the mean deposition of 0.1 g m^{-2} d^{-1} (see section 4.2), it turned out that an average of 25% of the dust would have been removed per day. Given this daily settling rate and the airborne dust mass calculations (see above), we calculated that an amount of about 0.4 10^{12}g of dust was deposited in the sea. Given the export of dust to continental Europe, as evidenced by Figs.1 and 4, it was roughly estimated that a total of 10^{12}g during the June-July period in 1981, and 4.44 10^{12}g in June-July 1982.

4.6 Comparison between dust removal rates derived from remote sensing and from ground based data

Taking into account the daily settling rate of 25% of the atmospheric dust mass during the transport, and assuming a 3,500 ± 500 m average thickness for the dust layer over Corsica yielded an apparent scavenging velocity of the dust particles from the dust layer of 1.0 cm s^{-1}, within the possible range 0.29-3.5 cm s^{-1}, including uncertainties on the average atmospheric load and average thickness of the dust layer. Despite this range, this net vertical transfer velocity is lower than the deposition velocity of particles to seawater, controlled by gravitational settling, which was measured at 7.7 cm s^{-1} using a surrogate surface (see Section 4.2). Either the aerosol model we used (Shettle, 1984) underestimates the contribution of large particles, or the gravitational settling of particles during transport is very limited. As discussed in Section 4.2, it is not likely that this aerosol model underestimates the mass of large particles, since the dry deposition velocity to surface seawater calculated using the model of Slinn and Slinn (1980) was found to be 6.9 cm s^{-1}. Moreover, reported observations of very long-range transport of giant mineral aerosol particles (see Section 3.2), contradicting model calculations (e.g. Schütz, 1979), strongly suggest that the scavenging of particles out from dust plumes is limited by physical mechanisms. Indeed, the air mass trajectories (Dulac *et al.*, 1991a) indicate that the African air layer was subject to a synoptic upward movement of 1.5 to 2 cm s^{-1} over the basin, which was likely to limit the gravitational settling of dust particles (Dulac *et al.*, 1991b). Assuming that gravitational settling was only limited by this process, yields a gravitational deposition velocity of dust particles averaging 2.5-3 cm s^{-1} within the possible range 1.8-5.5 cm s^{-1}. Moreover, upward air movements due to small scale convection processes associated with clouds (Gage *et al.*, 1990) may further limit the downward transfer of particles. Therefore, the method used in this work for assessing the mass of atmospheric desert dust over the sea from Meteosat data produced results consistent with our field measurements.

5. CONCLUSION

This work was focused on the use of Meteosat VIS data to estimate the mass of desert dust over the western Mediterranean during a transport event which occurred in early July 1985. A method based on a desert aerosol model and an earth-atmosphere radiative transfer model was developed to calculate aerosol optical depth over the sea from Meteosat VIS data. The cloud contaminated pixels of Meteosat images, as well as pixels over islands, were discarded, and masked pixels were interpolated for integrating the atmospheric load over the basin. The desert aerosol optical thickness was found to range between 0.1 and 1.8. A proportional coefficient of 1.3 was computed between the aerosol mass in g m^{-2} and the aerosol optical depth. Despite indirect validation of the aerosol model used, the lack of knowledge of the actual mass-size distribution of suspended dust particles was found to be the accuracy limiting factor. This points out the need for accurate characteristics of mass-particle size distributions of long-range transported desert aerosols, especially over 10 µm in diameter, emphasizing the need for adequate techniques of measurements that have already been mentioned (Dulac *et al.*, 1989). The mass of atmospheric particles from Africa present over the basin was estimated to reach about 0.6 10^{12}g at the maximum, and the total mass of dust exported from Africa to approximately 10^{12}g, within a factor ±3. Finally, we estimated a daily scavenging rate of 25% of the suspended dust mass over Corsica, a dry deposition to the sea of 0.4 10^{12}g, a net transfer velocity of particles from the dust layer of approximately 1 cm s^{-1}. The former result was derived from the comparison between vertically integrated atmospheric load and deposition at ground level, the latter from observations at ground level only. This net transfer velocity results from the

combination of the settling of dust particles with the competing synoptic upward movement of the associated African air mass, which was found to be uplifted over the basin at a velocity of the order of 2 cm s^{-1}. Given the large uncertainties in computation that were shown, the overall consistency between model computations from satellite data and results from ground based measurements is considered as a validation of the method used in this work.

6. ACKNOWLEDGEMENTS

We wish to thank the staff of the signal station at Capo Cavallo for their logistical support in Corsica. We also thank the French Marine Nationale for the free access to the signal station, and the French Direction of Météo-France, Ministère des transports, for the use of the meteorological tower at Capo Cavallo. We are grateful to B. Strauss, D. Martin and J.-M Gros, Service des Etudes Spéciales de Météo-France for providing air mass trajectories. This work was supported by the Centre National de la Recherche Scientifique and the Commissariat à l'Energie Atomique, and by grants from the PIREN/CNRS ATP "Aérosols Désertiques" and from the programme "Erosion Eolienne", and from the Programme National de Télédétection Spatiale.

7. REFERENCES

Arimoto, R. *et al.* (1985). Atmospheric trace elements at Enewetak Atoll, 2, Transport to the ocean by wet and dry deposition. *J. Geophys. Res.*, 90:2391-2408.

Arnold, M. *et al.* (1982). Geochemistry of the marine aerosol over the western Mediterranean Sea. In: *Proc. VIe Journées d'Etudes sur les Pollutions Marines en Méditerranée*, CIESM, Monaco, pp. 27-37.

Bergametti, G. (1987). *Apports de matière par voie atmosphérique à la Méditerranée occidentale: aspects géochimiques et météorologiques*, Thèse d'état, Univ. of Paris 7.

Bergametti, G. *et al.* (1989a). Seasonal variability of the elemental composition of atmospheric aerosol particles over the northwestern Mediterranean. *Tellus*, 41B:353-361.

Bergametti, G. *et al.* (1989b). Present transport and deposition patterns of African dusts to the northwestern Mediterranean. In: *Paleoclimatology and Paleometeorology: Modern and Past Patterns of Global Atmospheric Transport*, edited by M. Leinen and M. Sarnthein, Kluwer Academic Publishers, pp.227-252.

Betzer, P.R. *et al.* (1988). Long-range transport of giant mineral aerosol particles. *Nature*, 336:568-571.

Bowen, H.J.M. (1966). *Trace Elements in Biochemistry*, Academic, Orlando, Fla.

Buat-Ménard, P. *et al.* (1989). Non-steady-state biological removal of atmospheric particles from Mediterranean surface waters. *Nature*, 340:131-134.

Carder, K.L. *et al.* (1986). Dynamics and composition of particles from an aeolian input event to the Sargasso Sea. *J. Geophys. Res.*, 91:1055-1066.

Carlson, T.N. and R.S. Caverly (1977). Radiative characteristics of Saharan dust at solar wavelengths. *J. Geophys. Res.*, 82:3141-3152.

Chester, R. *et al.* (1984). Saharan dust incursion over the Thyrrhenian Sea. *Atmos. Environ.*, 18:929-935.

Coackley, J.A. and F.P. Bretherton (1982). Cloud cover from high-resolution scanner data: detecting and allowing for partially filled fields of view. *J. Geophys. Res.*, 87:4917-4932.

Corregiari, A. *et al.* (1990). Dust deposition in the central Mediterranean (Thyrrhenian and Adriatic Seas): relationships with marine sediments and riverine input. *Terra Nova*, 1:549-558.

Coudé-Gaussen G. (1989). Local, proximal and distal Saharan dusts: characterization and contribution to the sedimentation. In: *Paleoclimatology and Paleometeorology: Modern and Past Patterns of Global Atmospheric Transport*, edited by M. Leinen and M. Sarnthein, Kluwer Academic Publishers, pp.339-358.

D'Almeida, G.A. (1986). A model for Saharan dust transport. *J. Clim. Appl. Meteor.*, 25:903-916.

D'Almeida, G.A. (1987). On the variability of desert aerosol radiative characteristics. *J. Geophys. Res.*, 92:3017-3026.

D'Almeida, G.A. (1989). Desert aerosol: Characteristics and effects on climate. In: *Paleoclimatology and Paleometeorology: Modern and Past Patterns of Global Atmospheric Transport*, edited by M. Leinen and M. Sarnthein, Kluwer Academic Publishers, pp.311-338.

Duce, R.A. *et al.* (1980). Long-range atmospheric transport of soil dust from Asia to the tropical North Pacific: Temporal variability. *Science*, 209:1522-1524.

Dulac, F. (1986). *Dynamique du transport et des retombées d'aérosols métalliques en Méditerranée occidentale*, Thèse de doctorat, Univ. of Paris 7.

Dulac, F. *et al.* (1987). Atmospheric input of trace metals to the western Mediterranean Sea: factors controlling the variability of atmospheric concentrations. *J. Geophys. Res.*, 92:8437-8453.

Dulac, F. *et al.* (1989). Atmospheric input of trace metals to the western Mediterranean: uncertainties in modelling dry deposition from cascade impactor data. *Tellus*, 41B:362-378.

Dulac, F. *et al.* (1991a). Assessment of the African airborne dust mass over the western Mediterranean Sea using Meteosat data, revised version submitted to *J.Geophys.Res.*

Dulac, F. *et al.* (1991b). *Dry deposition of aerosol particles in the marine atmosphere: a critical evaluation of current field and modelling approaches*, fifth International Conference on Precipitation Scavenging and Atmosphere-Surface Exchange Processes, Richland, Washington, 15-19 July, 1991.

ESOC (1987). Magnetic Tapes and Files Description, Meteosat System Guide, 12, European Space Operation Center, Darmstadt, Germany.

Fraser, R.S. (1976). Satellite measurement of mass of Sahara dust in the atmosphere. *Appl. Opt.*, 15:2471-2479.

Gage, K.S. *et al.* (1990). Wind-profiling Doppler radars for tropical atmospheric research. *Eos, Trans. AGU*, 71:1851-1854.

Giorgi, F. (1988). Dry deposition velocities of atmospheric aerosols as inferred by applying a particle dry deposition parametrization to a general circulation model. *Tellus*, 40B:23-41.

Gomes, L. *et al.* (1990). Assessing the actual size distribution of atmospheric aerosols collected with a cascade impactor. *J. Aerosol. Sci.*, 21:47-59.

Guerzoni, S. *et al.* (1991). A new sampling station at the coastal site of Capo Carbonara (Sardinia, Central Mediterranean): preliminary data and technical proposal, Report of the Second WMO/UNEP Workshop on Airborne Pollution of the Mediterranean, Monaco, 8-12 April 1991, *MAP Technical Report Series*.

Jaenicke, R. (1985). Aerosol physics and chemistry. In: *Landolt-Börnstein Numerical Data and Functional Relationships in Science and Technology, V, 4b*, edited by G. Fischer, Springer-Verlag, pp.391-457.

Jaenicke, R. and L. Schütz (1978). Comprehensive study of physical and chemical properties of the surface aerosols in the Cape Verde Islands region. *J. Geophys. Res.*, 83:3585-3599.

Jankowiak, L. and D. Tanré (1991). Climatology of Saharan dust events observed from Meteosat Imagery over Oceans, Method and preliminary results. *J. Clim.* (in press).

Kneizys, F.X. *et al.* (1980). Atmospheric transmittance/radiance: Computer code LOWTRAN 5, Report AFGL-TR-80-0067, Air Force Geophysics Lab., Bedford, Mass.

Köpke, P. (1983). Calibration of the VIS-channel of Meteosat. *Adv. Space. Res.*, 2:93-96.

Losno, R. *et al.* (1987). Determination of optima conditions for atmospheric aerosol analyses by X-ray fluorescence. *Environ. Tech. Lett.*, 8:77-87.

Losno, R. *et al.* (1988). Zinc partitioning in Mediterranean rainwater. *Geophys. Res. Lett.*, 15:1389-1392.

Löye-Pilot, M.D. *et al.* (1986). Influence of Saharan dust on the rain acidity and atmospheric input to the Mediterranean. *Nature*, 321:427-428.

Martin, D. *et al.* (1987). Evaluation of the use of the synoptic vertical components in a trajectory model. *Atmos. Environ.*, 21:45-52.

Martin, D. *et al.* (1990). On the use of the synoptic vertical velocity in trajectory model: validation by geochemical tracers. *Atmos. Environ.*, 24A:2059-2069.

McClatchey, R.A. *et al.* (1971). Optical properties of the atmosphere, Report AFCRL-TR-71-0279, *Environ. Research Paper 354*, Air Force Cambridge Res. Lab., Bedford, Mass.

MEP (1985). Meteosat-2 calibration report: July-September 1985, Meteosat Exploitation Project Calibration Report, 13, ESOC, ESA, Darmstadt, Germany.

Morgan, M. (1981). Introduction to the Meteosat System, ESOC, ESA, Darmstadt, Germany.

Patterson, E.M. *et al.* (1977). Complex index of refraction between 300 and 700 nm for Saharan aerosols. *J. Geophys. Res.*, 82:3153-3160.

Peters, A. (1989). Peters Atlas of the World, Longman, 231 pp.

Prodi, F. and G. Fea (1979). A case of transport and deposition of Saharan dust over the Italian peninsula and southern Europe. *J. Geophys. Res.*, 84:6951-6960.

Prospero, J.M. *et al.* (1970). Dust in the Caribbean atmosphere traced to an African dust storm. *Earth Planet Sci. Lett.*, 9:287-293.

Rahn, K.A. (1976). *The chemical composition of the atmospheric aerosol*, Tech. Rep., University of R.I., Kingston, 275 pp.

Rao, C.R.N. *et al.* (1988). Development and application of aerosol remote sensing with AVHRR data from NOAA satellites, In: *Aerosols and Climate*, edited by P.V. Hobbs and M.P. McCormick, A. Deepak Publishing, pp.69-79.

Reiff, J. *et al.* (1986). African dust reaching northwestern Europe: a case study to verify trajectory calculations. *J. Climate Appl. Meteorol.*, 25:1543-1567.

Saunders, R.W. and K.T. Kriebel (1988). An improved method for detecting clear sky and cloudy radiances from AVHRR data. *Int. J. Remote Sensing*, 9:123-150.

Schiffer, R.A. and W.B. Rossow (1983). The International Satellite Cloud Climatology Project (ISCCP): the first project of the World Climate Research Programme. *Bull. Am. Met. Soc.*, 64:779-784.

Schneider, B. *et al.* (1990). Dry deposition of Asian mineral dust over the central North Pacific. *J. Geophys. Res.*, 95:9873-9878.

Schütz, L. (1979). Sahara dust transport over the North Atlantic Ocean - Model calculations and measurements. In: *Saharan Dust*, edited by C. Morales, SCOPE 14, Wiley and Sons, pp.267-277.

Shettle, E.P. (1984). Optical and radiative properties of a desert aerosol model. In: *Proc. Symp. on Radiation in the Atmosphere*, G. Fiocco (ed.), A. Deepak Publishing, Hampton, Va., pp.74-77.

Slinn, W.G.N. (1983). Air to sea transfer of particles. In: *Air-Sea Exchange of Gases and Particles*, edited by P.S. Liss and W.G.N. Slinn, Reidel, pp.299-396.

Slinn, S.A. and W.G.N. Slinn (1980). Prediction for particle deposition on natural waters. *Atmos. Environ.*, 14:1013-1016.

Tanré, D. *et al.* (1988b). Radiative properties of desert aerosols by optical ground-based measurements at solar wavelengths. *J. Geophys. Res.*, 93:14223-14231.

Tanré, D. *et al.* (1990). Description of a computer code to simulate the satellite signal in the solar spectrum: the 5S code. *Int. J. Rem. Sens.*, 2:659-668.

Tomadin, L. *et al.* (1984). Wind-blown dusts over the Central Mediterranean. *Oceanol. Acta.*, 7:13-23.

Uematsu, M. *et al*. (1985). Deposition of atmospheric mineral particles in the North Pacific Ocean. *J. Atmos. Chem.*, 3:123-138.

UNIRAS (1988). AGL/Interpolations: User guide and reference manual, Uniras, Søborg, Denmark.

UNIRAS (1989). AGS/Unimap 2000: Users manual, Uniras, Søborg, Denmark.

Vinogradov, A.P. (1959). *The geochemistry of rare and dispersed chemical elements in soils*, 2nd Edition, Consultants Bureau Inc., New York.

Viollier, M. (1990). *Télédétection des concentrations de seston et pigments chlorophylliens contenus dans l'océan*, Thèse d'état No.503, Univ. of Lille.

Volz, F. (1970). Spectral skylight and solar radiance measurements in the Caribbean: marine and Saharan dust. *J. Atmos. Sci.*, 27:1041-1047.

WCP 112 (1986). A preliminary cloudless standard atmosphere for radiation computation, *World Climate Programme Series Report No.112*, International Council of Scientific Unions and World Meteorological Organization (eds.).

THREE DIMENSIONAL MODELLING OF THE EFFECT OF SEA AND LAND BREEZES ON POLLUTION TRANSPORT IN THE EASTERN MEDITERRANEAN

By

Y. MAHRER

The Hebrew University of Jerusalem
Department of Soil and Water Sciences
Faculty of Agriculture
76100 Rehobot, Israel

A B S T R A C T

A three-dimensional numerical air quality model for the Eastern Mediterranean area is being developed and tested. The model is based on integrating three existing submodels: a mesoscale submodel, a dispersion and transport submodel, and a photochemistry and deposition submodel. The mesoscale model is based on the primitive equations of motion and on heat, humidity and continuity equations. Terrain features of the simulated area are considered. The mesoscale model output provides the necessary input for the dispersion submodel, which predicts ambient concentrations of inert pollutants originating from natural and anthropogenic sources. Detailed photochemical calculations are then performed in order to determine concentrations of primary and secondary pollutants. The air quality model was applied to the topography of Israel, where mesoscale phenomena are dominant, covering an area of 150 x 320 km. Initial conditions required to run the meteorological model include radiosonde data of air temperature and humidity, wind speed and direction as well as pressure. Operating data about the main pollution sources along the Israel coastline, viz. Haifa power plant (4 stacks, 400 MW), Haifa oil refineries, Hadera power plant (2 stacks, 1400 MW), Tel-Aviv power plant (1 stack, 500 MW), Ashdod power plant (5 stacks, 1200 MW), and Ashdod oil refineries, are needed for the dispersion calculations. The model was validated for two typical days during the summer and winter.

1. MODEL SIMULATION

The air quality model is applied to the topography of the coast of Israel, covering an area of 150 x 320 km. It consists of 30 x 32 grid points with a horizontal grid interval of 5 km in the x direction and 10 km in the y direction (Fig.1). The vertical grid of the model contains 14 unevenly spaced levels. The initial conditions include radiosonde data of air temperature and humidity, wind speed and direction, and pressure. These data are obtained from the Israel Meteorological Service in Bet-Dagan at 01.00 local time (23.00 GMT).

The output of this model included fields of wind speed and direction, temperature and horizontal and vertical eddy diffusion coefficients at all model grid points, and the height of the mixed layer. The second stage of modelling comprises the calculation of dispersion of inert pollution under the influence of the above predicted meteorological fields. The input of this model includes all the main pollution sources along the Israel coastline: Haifa power plant (4 stacks, 400 MW), Haifa oil refineries, Hadera power plant (2 stacks, 1400 MW), Tel-Aviv power plant (1 stack, 500 MW), Ashdod power plant (5 stacks, 1200 MW) and Ashdod

oil refineries. Additional input is the hourly SO_2 emission of each source, it's geographical location, height and radius of the stacks, gas exit velocity and temperature of the effluent gases (Table 1). At this stage no chemical reaction and no deposition of the pollutant constituents are considered.

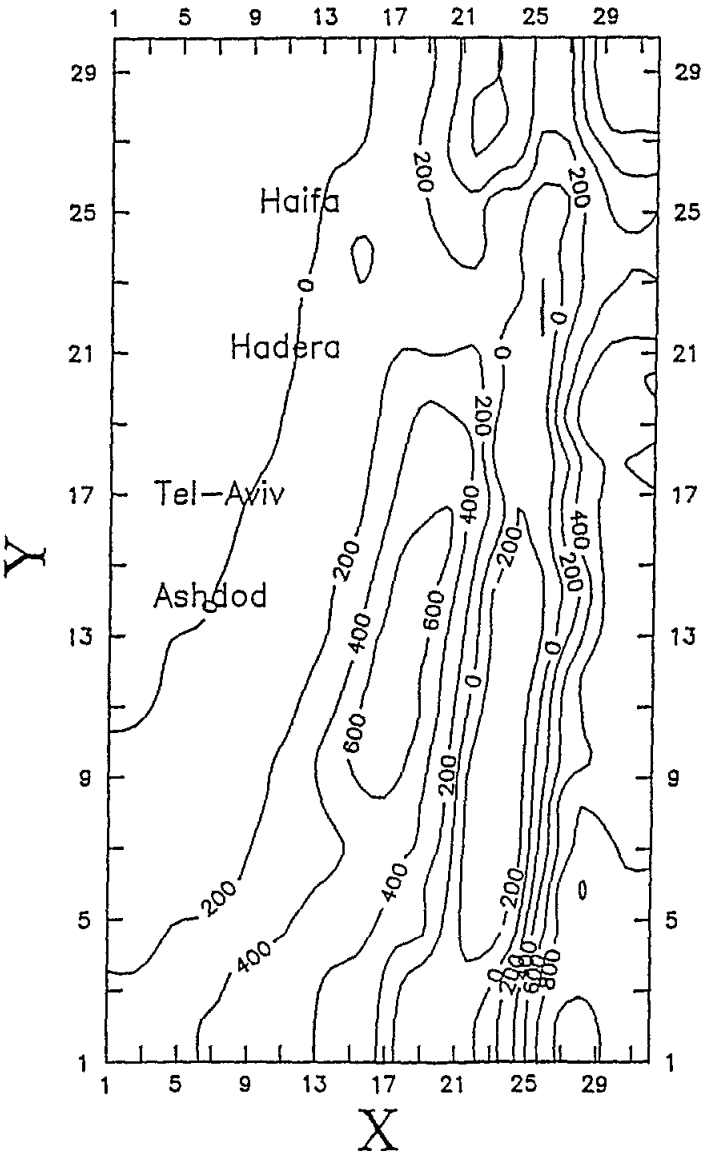

Fig.1 Topographic map of the simulated area

The model is validated for two typical days during summer and winter. The summer day is characterized by an annual Persian trough, combined with a barometric trough in the upper layers of the atmosphere (Table 2). During the night and early morning hours, the land breeze and the downslope flow from the mountain range are dominant in the area and generate an easterly flow. The Persian trough causes deepening of the convective layer and looping type of plume dispersion. The winter day is characterized by a Red Sea trough over the area with easterly winds in the lower layers of the atmosphere (Table 3).

Table 1

Pollution sources data

	STACK DATA			
Location	Height (m)	Radius Effective (m)	Speed of gases (m/sec)	Temperature of gases (Ek)
Haifa (Power plant)	80 80 80 80	2.0 2.0 1.5 1.5	9.7 9.7 26.8 26.8	443 443 443 443
Haifa (Oil Refinery)	60	2.0	8.0	400
Tel-Aviv	150	3.1	26.0	423
Ashdod (Power plant)	51 51 150 150	1.4 1.4 1.4 3.2 2.6	14.4 14.4 14.4 25.5 27.0	433 433 433 428 428
Ashdod (Oil Refinery)	40	2.0	5.0	400
Hadera	250 250	3.5 3.5	25.4 25.4	411 411

Table 2

Radiosonde data on 9 July 1990
Upper air data from radiosonde measurements at Bet-Dagan on the summer day

Height (m)	Pressure (mb)	Temperature (EC)	Dewpoint (EC)	Wind direction (degrees)	Wind direction (m/sec)
0	1005	21.0	18.2	0	0
40	1003	21.6	19.5	0	0
81	1000	22.3	20.9	0	0
128	995	23.6	23.7	0	0
720	930	23.4	9.3	280	1.5
763	925	23.2	9.1	280	1.5
1001	900	22.3	8.2	280	1.5
1226	877	21.4	7.4	260	3.5
1496	850	22.4	2.4	240	5.5
1965	805	21.4	1.6	200	11.0
2021	800	21.0	1.2	200	12.0
3156	700	12.3	-5.9	180	11.5
4424	600	2.4	-14.0	260	5.0
5084	552	-3.2	-18.7	260	5.0
5707	510	-6.3	-21.2	250	5.0
5868	500	-6.5	-21.6	250	5.0
7162	423	-8.5	-25.1	260	10.0
7602	400	-10.7	-26.1	260	13.0

Table 3

Radiosonde data on 29 December 1989
Upper air data from radiosonde measurements at Bet-Dagan on the winter day

Height (m)	Pressure (mb)	Temperature (EC)	Dewpoint (EC)	Wind direction (degrees)	Wind direction (m/sec)
0	1019	8.8	7.6	0	0
143	1007	14.3	11.1	0	0
153	1000	15.3	10.3	10	1.0
324	984	17.8	8.4	10	1.0
852	925	14.1	5.4	100	3.0
1082	900	12.4	4.3	100	3.0
1558	850	8.9	2.1	150	3.5
1898	816	6.4	0.7	180	4.5
2056	800	5.7	-8.8	190	5.0
2102	769	5.5	-11.5	190	5.0
3141	700	2.3	-18.1	280	6.0
4362	600	-7.7	-13.5	280	14.0
4746	571	-10.8	-12.0	280	15.0
5758	500	-15.5	-18.3	280	16.0
6706	440	-21.8	-31.2	280	16.0
7404	400	-28.0	-32.6	280	16.0

2. RESULTS

2.1 Summer day simulation

At 02.00 LT, light easterly winds at 10 metres height are dominant over the sea. Over the land, light northeasterly winds are presented in the Haifa area, while to the south of this area, winds are generally calm. Air pollutants emitted during this time will be transported inland in the Haifa area. South of the Haifa area, due to the calm winds in the lower part of the atmosphere, plume rise will be very high and no pollutants each the ground. In the upper levels (above the effective height) the pollution is transported offshore.

At 06.00 LT, winds over the sea are south-southwesterly while over the land they are southwesterly. Pollutants emitted at this time are being transported inland in the upper layers and spread in the lateral direction. Yet, no pollutants reach the ground, except in the Haifa area.

At 10.00 LT, winds are northwesterly over the entire area. Wind speeds have significantly increased and pollutants are entering further distances inland. Pollutants transported initially by the land breeze toward the sea, are now recirculated inland.

At 14.00 LT, winds are northwesterly with intensified speeds. Pollutants are being transported further inland leaving almost no trace over the sea.

At 18.00 LT, winds are very strong and pollution is spread all over the country.

Figs.2(a), (b), (c), (d) and (e) show the wind and pollutant fields in the simulated area for different hours during a summer day. The left drawing depicts isoplates of SO_2, the centre a horizontal view of particles' location (particles were released starting at 01.00 LT),

and the right the horizontal wind vector at a height of 50m (a one horizontal grid distance in the x direction (equal to 5 km) represents a wind speed of 10 ms^{-1})

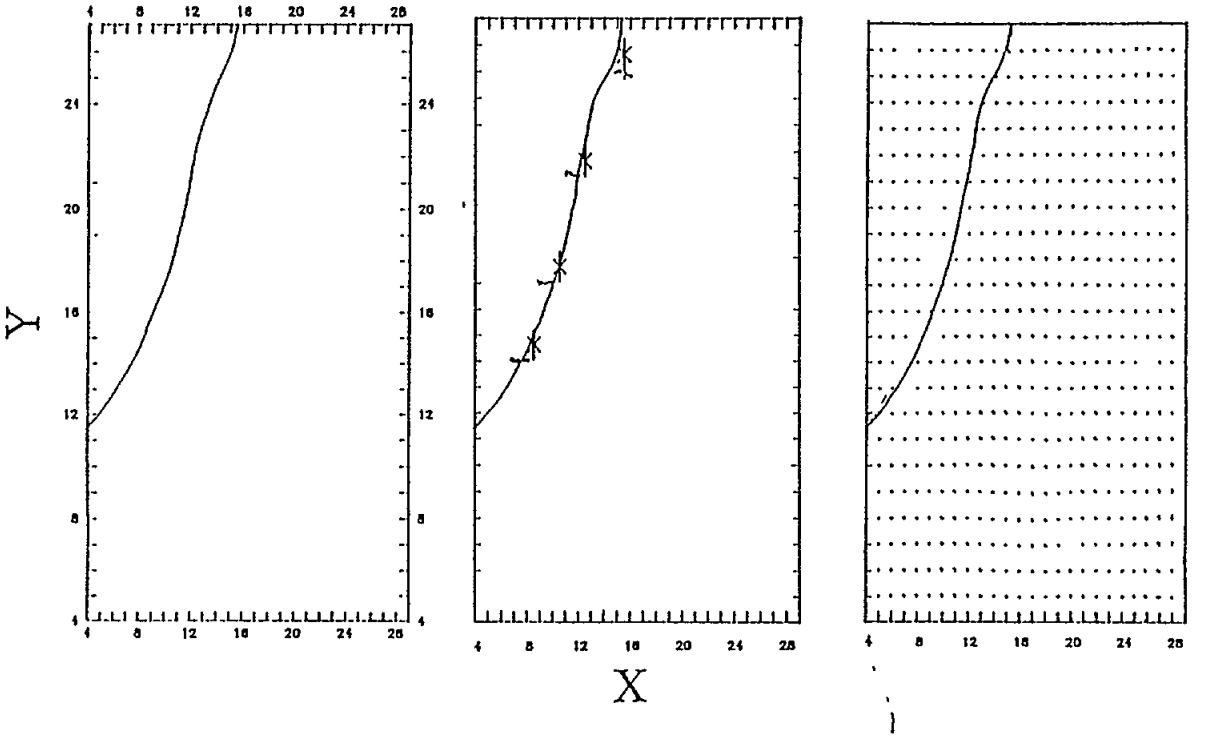

Fig.2(a) Local time = 02.00

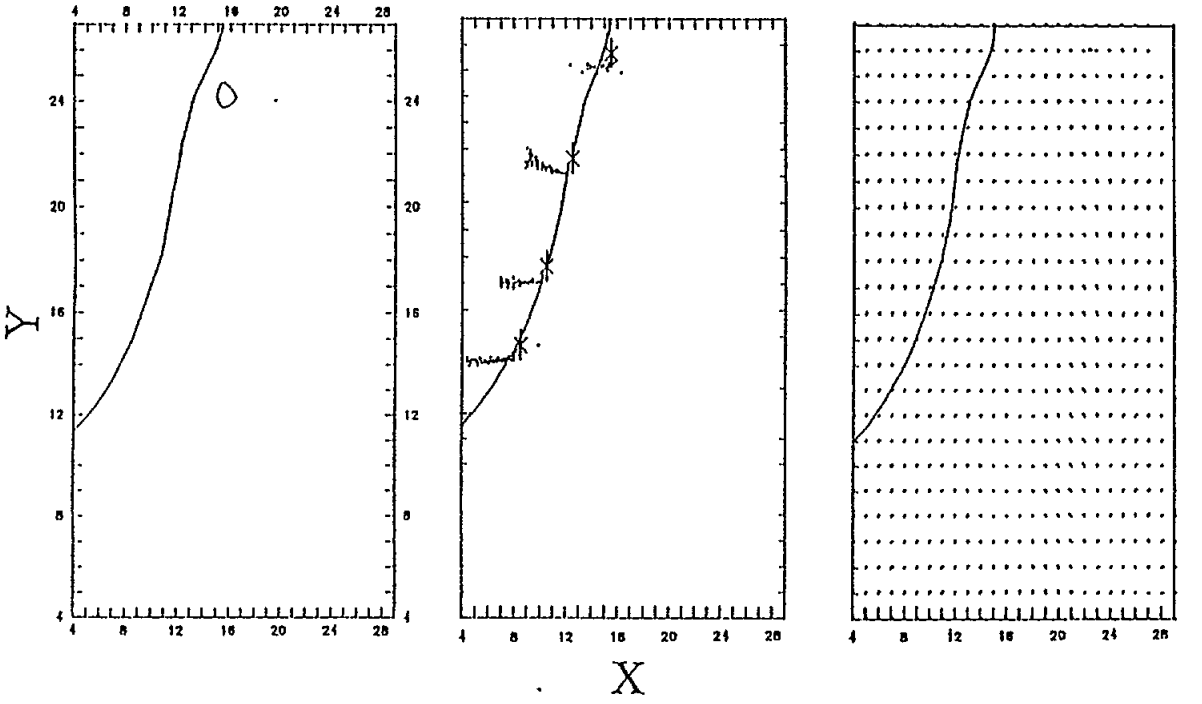

Fig.2(b) Local time = 06.00

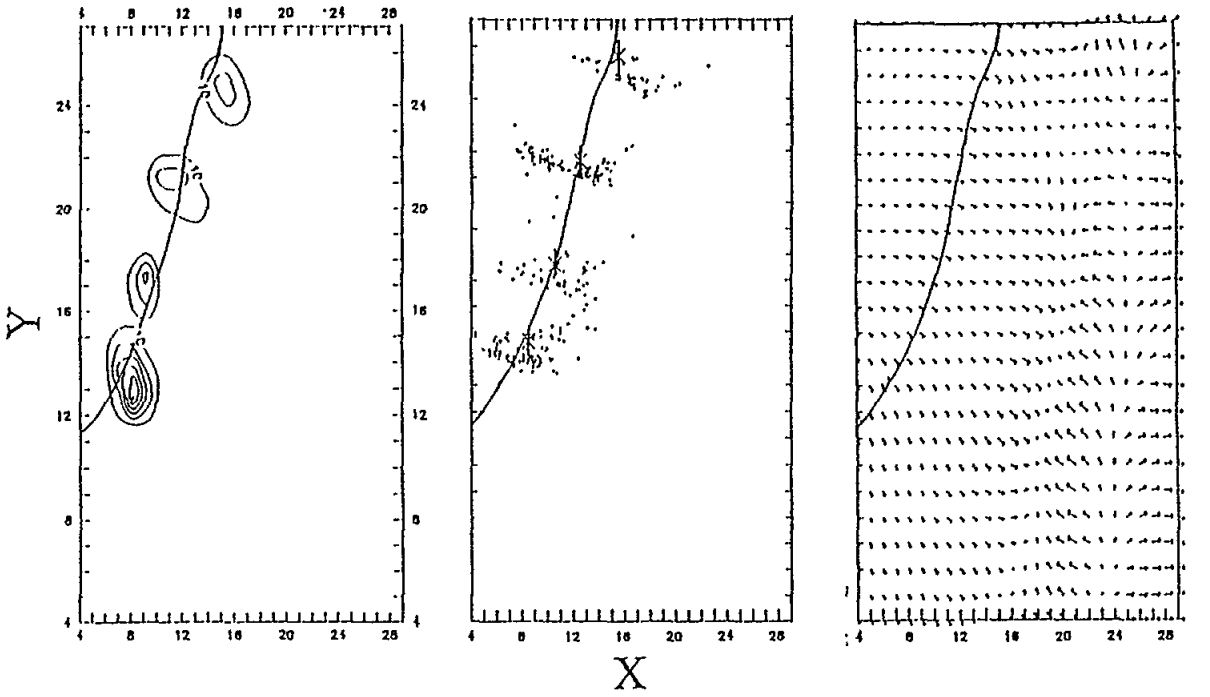

Fig.2(c) Local time = 10.00

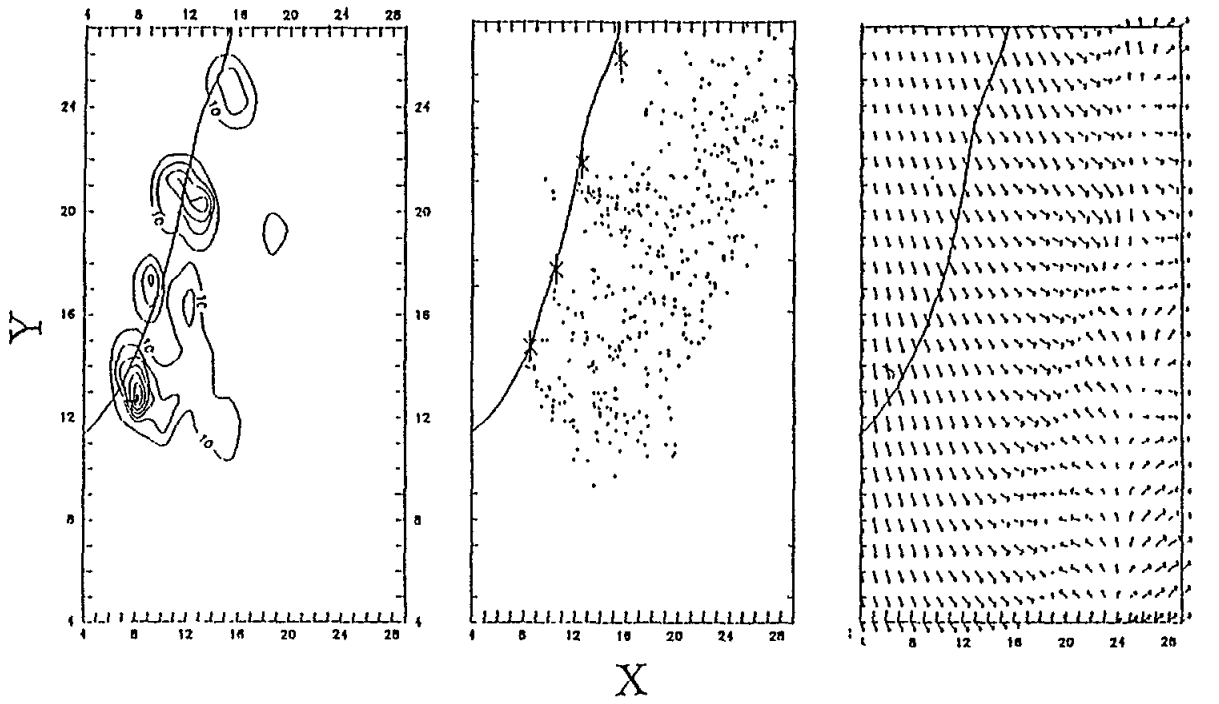

Fig.2(d) Local time = 14.00

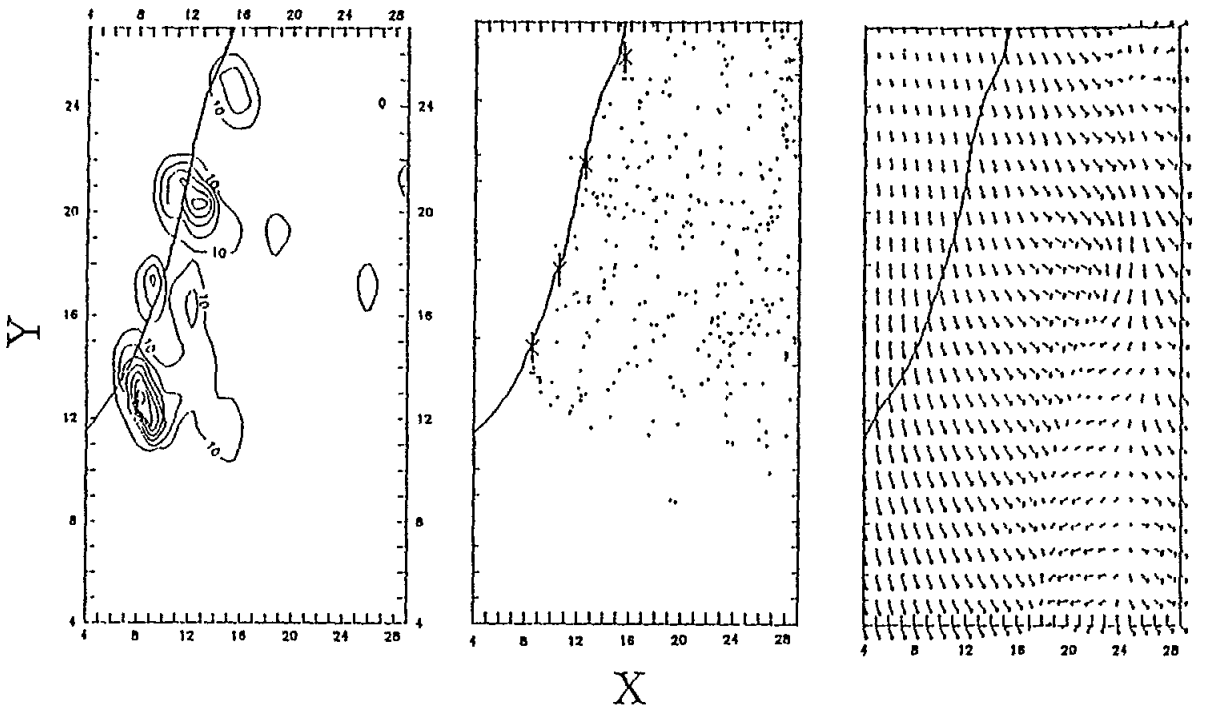

Fig.2(e) Local time = 18.00

3.2 Winter day simulation

At 02.00 LT, the 10 metre height winds are northerly over the sea, while over the land they are northwesterly along the coast in the Haifa area and northeasterly along the coast south of Haifa. Wind speeds are higher over the sea. Pollutants emitted during this time move to the south, thus they are carried inland in the northern part of the simulated domain, and along the coast south of the Haifa area. Pollutants do not reach the ground at this time.

At 06.00 LT, northeasterly winds are blowing over the sea. Over the land they are northwesterly in the Haifa area and southeasterly to the south of Haifa. The wind speeds increase, and pollutants are also being spread in the lateral direction. In the northern part of Israel, in the vicinity of Haifa and Hadera, pollutants reach the ground. It is interesting to notice that pollutants from the Haifa sources are being transported inland, while those originating at the Hadera power plants are moving toward the sea.

At 10.00 LT. easterly winds prevail over the sea. In the Haifa area the winds are northerly, and south of the Haifa area they are southeasterly. Pollutants reach ground level only in the vicinity of Haifa and Hadera. Pollutants originating at the Haifa sources move inland while those from the Hadera and Tel-Aviv areas are moving towards the sea.

At 14.00 LT, winds in the Haifa and Hadera areas are northwesterly, in the Tel-Aviv area they are westerly and in the Ashdod area they are northwesterly. Wind velocities have

increased during the past two hours reaching a maximal value of about 4 ms^{-1}. Pollutants are spread along the entire coastal area of Israel, both over land and over sea, at all heights.

At 18.00 LT, winds become more northerly at about the same speeds as earlier. Unlike the summer day, the wind directions during the winter day vary appreciably with height. Thus the initial direction of the pollution depends on the height of release.

The effect of recirculation of pollutants is pronounced during the summer day. Pollutants emitted during the night are initially transported towards the sea. With the onset of the seabreeze, these pollutants are recirculated inland. At about 12 am the air over the sea is almost clean of air pollutants.

In the winter, mesoscale phenomena (sea and land breezes and mountain and valley winds) are no longer dominant. Wind patterns are mainly dictated by the large scale flow and, therefore, no clear diurnal pattern is found. Very often the meteorological situation causes pollutants to remain over the sea area the whole day long.

Concentrations are higher when calculations are made for upper levels in the atmosphere, reaching a maximum at the height between the stack height and stack effective height, and then there is a decrease in concentrations.

Calculations of the photochemical model show a sulphate formation of about 3 $\mu g/m^3$ for every 1 ppm sulphur dioxide emitted after 3 hours dispersion during daytime on the summer day. On the winter day, calculated sulphate concentrations are 2-2.5 $\mu g/m^3$ for every 1 ppm SO_2 emitted.

It is important to note that the above calculated concentrations are for the plume zone. Concentrations near the ground will depend on the type of the plume dispersion. In the looping type of dispersion, where the plume touches the ground, sulphate concentrations near the ground can be high. For other plume dispersion types, where the smaller part of the plume reaches the ground, concentrations would be lower.

Figs.3(a), (b), (c), (d) and (e) show the wind and pollutant fields in the simulated area for different hours during a winter day. The left drawing depicts isoplates of SO_2, the centre a horizontal view of particles' location (particles were released starting at 01.00 LT), and the right the horizontal wind vector at a height of 50m (a one horizontal grid distance in the x direction (equal to 5 km) represents a wind speed of 10 ms^{-1}).

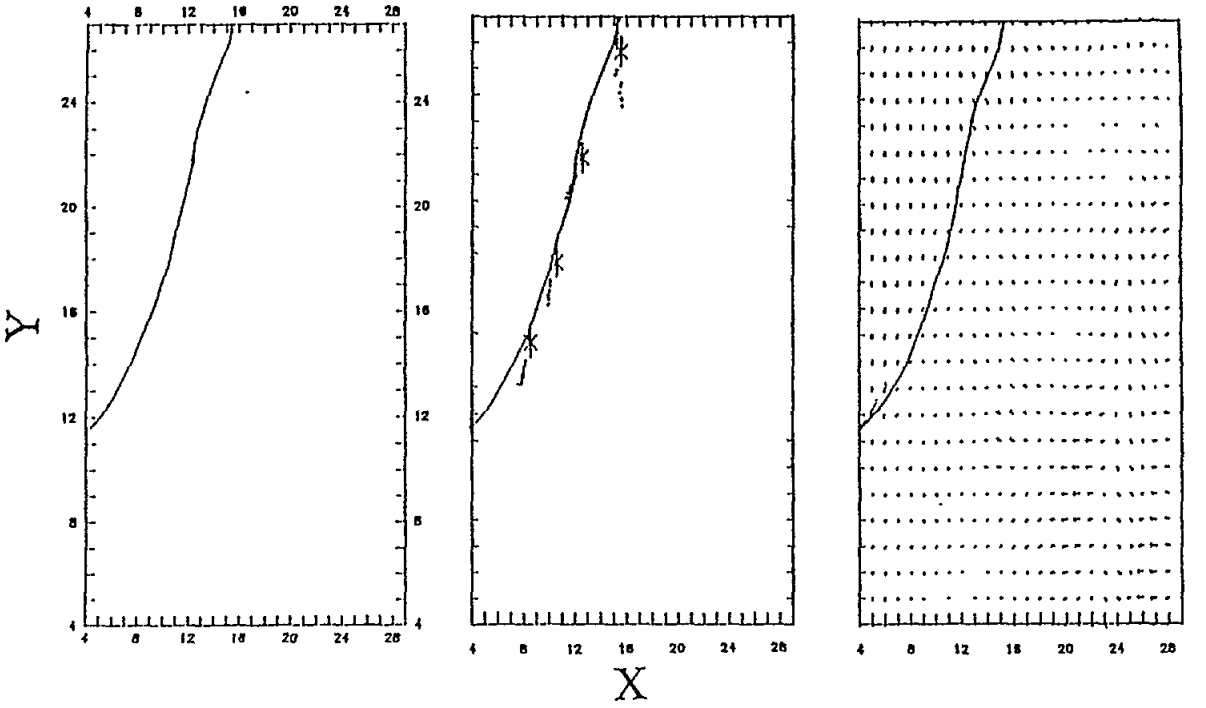

Fig.3(a) Local time = 02.00

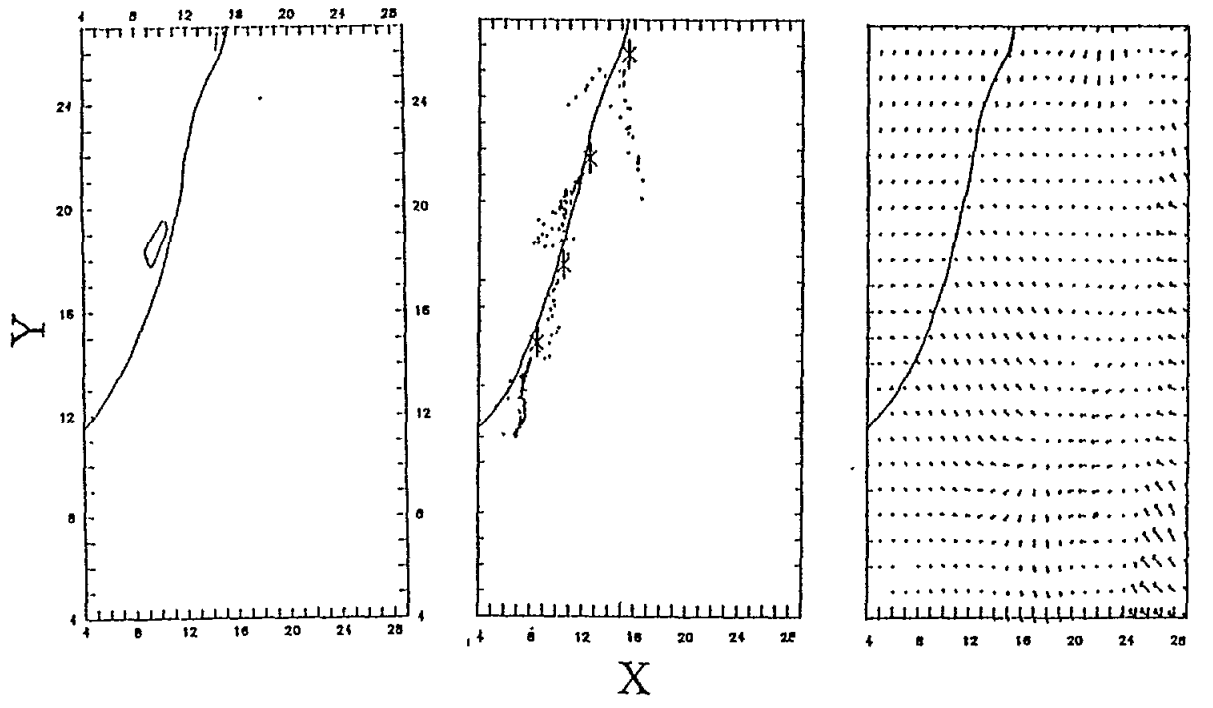

Fig.3(b) Local time = 06.00

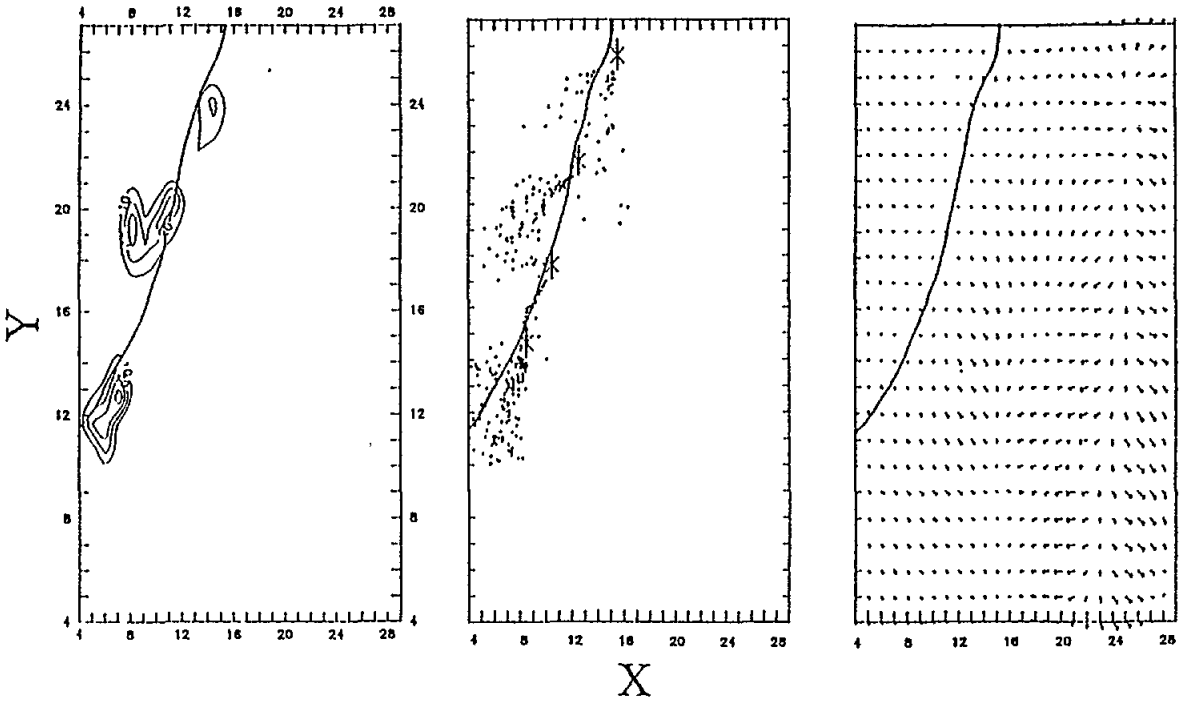

Fig.3(c) Local time = 10.00

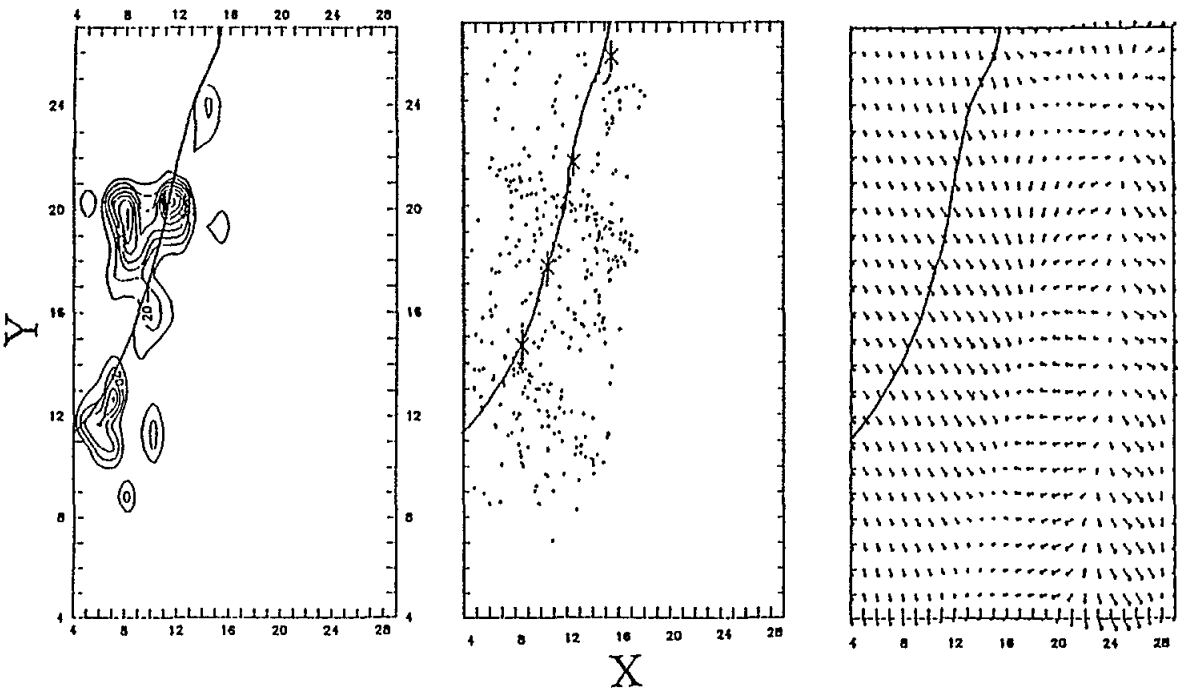

Fig.3(d) Local time = 14.00

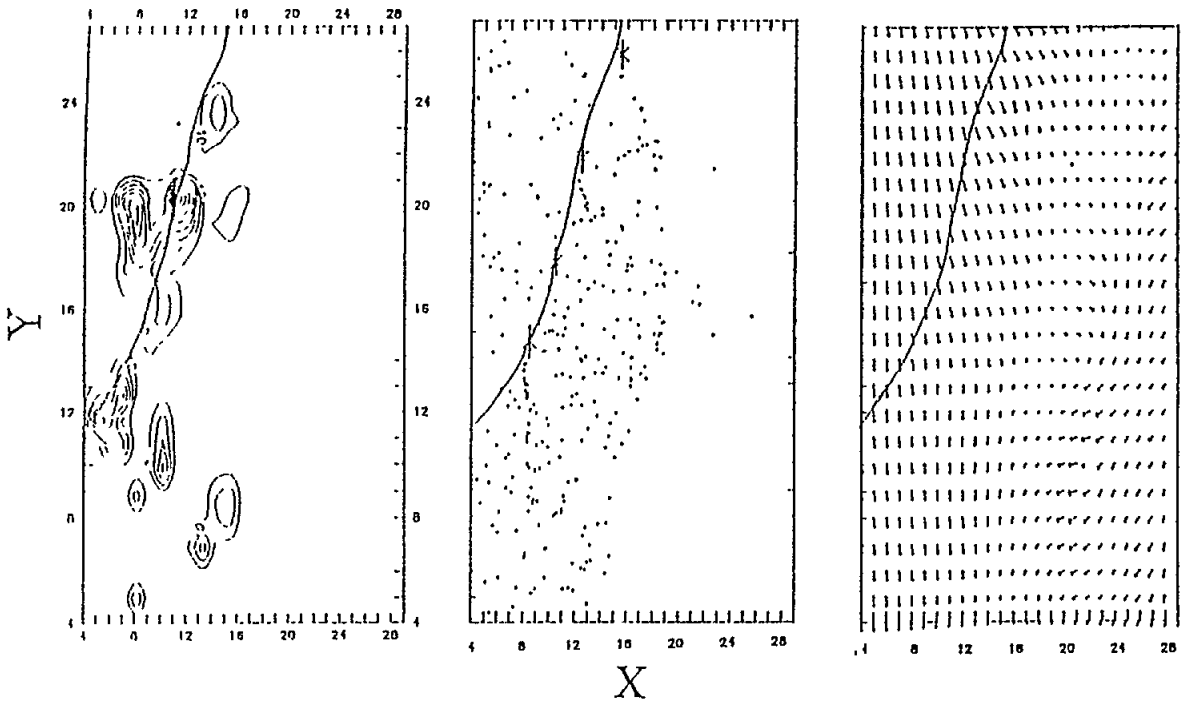

Fig.3(e) Local time = 18.00

DISPERSION OF SO_2 RELEASED FROM A LARGE INDUSTRIAL INSTALLATION LOCATED NEAR THE NORTH COAST OF THE EASTERN CORINTHIAN GULF IN GREECE

By

G. KALLOS

University of Athens
Department of Applied Physics
Ippocratous 13, 10680 Athens, Greece

A B S T R A C T

In this presentation, some results from a numerical investigation of the mesoscale circulations and pollution transport in the coastal area of the Eastern Corinthian Gulf in Greece are given. The source of the released air pollutants is an aluminium plant which will be operated at a distance of about 1 km from the northern coastline of the Corinthian Gulf. The released SO_2 is estimated up to 1.6 tn/hour, from eight stacks with heights ranging from 30 to 50 m above ground level in a position having a mean evaluation of 130 m above sea level.

The topography around the plant is very complex (high mountains, small valleys, complicated coastline). Over this terrain, local circulations like sea/land breezes, drainage flows, etc., are developing on a regular basis. The interaction between these local circulations with the synoptic flow is a phenomenon which cannot be easily described. Consequently, the dispersion of the released air pollutants is also very complex and cannot be described with conventional methods. For this reason, a two-stage procedure was employed. In the first stage, the 3-D version of the Colorado State University Mesoscale Model (CSUMM) was used to predict the meteorological fields over the examined area. In the second stage, a Lagrangian Particle Dispersion Model (LPDM) was used. In this way, it was possible to estimate the near-ground concentrations of SO_2 for different hours and for different atmospheric conditions.

MODELLING THE FLOW FIELDS OVER COASTAL AREAS : IMPLICATIONS TO AIR POLLUTION

By

G. KALLOS

University of Athens
Department of Applied Physics
Ippocratous 13, 10680 Athens, Greece

A B S T R A C T

In order to accurately evaluate environmental impacts from point or area sources of air pollutants, it is necessary to have a detailed description of some crucial atmospheric parameters. Such atmospheric parameters are the Planetary Boundary Layer (PBL) depth and the 3-D wind fields. This is especially true in coastal areas, where land-water distribution, variations in elevation, landscape, etc., are responsible for the development of a variety of phenomena. Such phenomena are sea-land breezes, convergence zones, development of thermal internal boundary layers, upslope-downslope circulations, etc. These phenomena show significant temporal and spatial variations and make the dispersion processes very complicated. The interactions between the circulations of different scales are considered as equally important. All these complicated processes are highly non-linear and cannot be described even with a dense observational network or a simple modelling approach. Therefore, there is a need for the use of mesoscale atmospheric models, capable of accurately representing most of the physical processes taking place in such cases and, consequently, accurately representing the variations in PBL depth and wind fields. If these models are combined with the appropriate dispersion diffusion and/or photochemical models, it is possible to investigate several environmental impacts caused from the point or area sources of air pollutants. This methodology is becoming more attractive during the last few years because of the significant advance in computer performance.

In this presentation, some results from model simulations over Athens and the Saronic Gulf in Greece are presented. The atmospheric model used for these simulations is the Regional Atmospheric Modelling System (RAMS) from Colorado State University. In order to accurately simulate the flow fields over this area, the nesting capabilities of this model were used. This was necessary in order to describe the interaction between regional and mesoscale circulations. Three domains (one inside the other) were used; the first covers a significant portion of the northeastern Mediterranean (16 km grid resolution), the second covers a large portion of southeastern Greece (4 km grid resolution) and the third the province of Attiki and most of the Saronic Gulf. In this way, significant details of the flow fields over the area were accurately described. These details could not be described with simpler modelling approaches.

PUBLICATIONS OF THE MAP TECHNICAL REPORTS SERIES

1. UNEP/IOC/WMO: Baseline studies and monitoring of oil and petroleum hydrocarbons in marine waters (MED POL I). MAP Technical Reports Series No. 1. UNEP, Athens, 1986 (96 pages) (parts in English, French or Spanish only).

2. UNEP/FAO: Baseline studies and monitoring of metals, particularly mercury and cadmium, in marine organisms (MED POL II). MAP Technical Reports Series No. 2. UNEP, Athens, 1986 (220 pages) (parts in English, French or Spanish only).

3. UNEP/FAO: Baseline studies and monitoring of DDT, PCBs and other chlorinated hydrocarbons in marine organisms (MED POL III). MAP Technical Reports Series No. 3. UNEP, Athens, 1986 (128 pages) (parts in English, French or Spanish only).

4. UNEP/FAO: Research on the effects of pollutants on marine organisms and theirpopulations (MED POL IV). MAP Technical Reports Series No. 4. UNEP, Athens, 1986 (118 pages) (parts in English, French or Spanish only).

5. UNEP/FAO: Research on the effects of pollutants on marine communities andecosystems (MED POL V). MAP Technical Reports Series No. 5. UNEP, Athens, 1986 (146 pages) (parts in English or French only).

6. UNEP/IOC: Problems of coastal transport of pollutants (MED POL VI). MAP TechnicalReports Series No. 6. UNEP, Athens, 1986 (100 pages) (English only).

7. UNEP/WHO: Coastal water quality control (MED POL VII). MAP Technical Reports Series No. 7. UNEP, Athens, 1986 (426 pages) (parts in English or French only).

8. UNEP/IAEA/IOC: Biogeochemical studies of selected pollutants in the open waters of the Mediterranean (MED POL VIII). MAP Technical Reports Series No. 8. UNEP, Athens, 1986 (42 pages) (parts in English or French only).

8. UNEP: Biogeochemical studies of selected pollutants in the open waters of the Medi-
Add. terranean MED POL VIII). Addendum, Greek Oceanographic Cruise 1980. MAP Technical Reports Series No. 8, Addendum. UNEP, Athens, 1986 (66 pages) (English only).

9. UNEP: Co-ordinated Mediterranean pollution monitoring and research programme (MED POL - PHASE I). Final report, 1975-1980. MAP Technical Reports Series No. 9. UNEP, Athens, 1986 (276 pages) (English only).

10. UNEP: Research on the toxicity, persistence, bioaccumulation, carcinogenicity and mutagenicity of selected substances (Activity G). Final reports on projects dealing with toxicity (1983-85). MAP Technical Reports Series No. 10. UNEP, Athens, 1987 (118 pages) (English only).

11. UNEP: Rehabilitation and reconstruction of Mediterranean historic settlements. Documents produced in the first stage of the Priority Action (1984-1985). MAP Technical Reports Series No. 11. UNEP, Priority Actions Programme, Regional Activity Centre, Split, 1986 (158 pages) (parts in English or French only).

12. UNEP: Water resources development of small Mediterranean islands and isolated coastal areas. Documents produced in the first stage of the Priority Action (1984-1985). MAP Technical Reports Series No. 12. UNEP, Priority Actions Programme, Regional Activity Centre, Split, 1987 (162 pages) (parts in English or French only).

13. UNEP: Specific topics related to water resources development of large Mediterranean islands. Documents produced in the second phase of the Priority Action (1985-1986). MAP Technical Reports Series No. 13. UNEP, Priority Actions Programme, Regional Activity Centre, Split, 1987 (162 pages) (parts in English or French only).

14. UNEP: Experience of Mediterranean historic towns in the integrated process of rehabilitation of urban and architectural heritage. Documents produced in the second phase of the Priority Action (1986). MAP Technical Reports Series No. 14. UNEP, Priority Actions Programme, Regional Activity Centre, Split, 1987 (500 pages) (parts in English or French only).

15. UNEP: Environmental aspects of aquaculture development in the Mediterranean region. Documents produced in the period 1985-1987. MAP Technical Reports Series No. 15. UNEP, Priority Actions Programme, Regional Activity Centre, Split, 1987 (101 pages) (English only).

16. UNEP: Promotion of soil protection as an essential component of environmental protection in Mediterranean coastal zones. Selected documents (1985-1987). MAP Technical Reports Series No. 16. UNEP, Priority Actions Programme, Regional Activity Centre, Split, 1987 (424 pages) (parts in English or French only).

17. UNEP: Seismic risk reduction in the Mediterranean region. Selected studies and documents (1985-1987). MAP Technical Reports Series No. 17. UNEP, Priority Actions Programme, Regional Activity Centre, Split, 1987 (247 pages) (parts in English or French only).

18. UNEP/FAO/WHO: Assessment of the state of pollution of the Mediterranean Sea by mercury and mercury compounds. MAP Technical Reports Series No. 18. UNEP, Athens, 1987 (354 pages) (English and French).

19. UNEP/IOC: Assessment of the state of pollution of the Mediterranean Sea by petroleum hydrocarbons. MAP Technical Reports Series No. 19. UNEP, Athens, 1988 (130 pages) (English and French).

20. UNEP/WHO: Epidemiological studies related to environmental quality criteria for bathing waters, shellfish-growing waters and edible marine organisms (Activity D). Final report on project on relationship between microbial quality of coastal seawater and health effects (1983-86). MAP Technical Reports Series No. 20. UNEP, Athens, 1988 (156 pages) (English only).

21. UNEP/UNESCO/FAO: Eutrophication in the Mediterranean Sea: Receiving capacity and monitoring of long-term effects. MAP Technical Reports Series No. 21. UNEP, Athens, 1988 (200 pages) (parts in English or French only).

22. UNEP/FAO: Study of ecosystem modifications in areas influenced by pollutants (Activity I). MAP Technical Reports Series No. 22. UNEP, Athens, 1988 (146 pages) (parts in English or French only).

23. UNEP: National monitoring programme of Yugoslavia, Report for 1983-1986. MAP Technical Reports Series No. 23. UNEP, Athens, 1988 (223 pages) (English only).

24. UNEP/FAO: Toxicity, persistence and bioaccumulation of selected substances to marine organisms (Activity G). MAP Technical Reports Series No. 24. UNEP, Athens, 1988 (122 pages) (parts in English or French only).

25. UNEP: The Mediterranean Action Plan in a functional perspective: A quest for law and policy. MAP Technical Reports Series No. 25. UNEP, Athens, 1988 (105 pages) (English only).

26. UNEP/IUCN: Directory of marine and coastal protected areas in the Mediterranean Region. Part I - Sites of biological and ecological value. MAP Technical Reports Series No. 26. UNEP, Athens, 1989 (196 pages) (English only).

27. UNEP: Implications of expected climate changes in the Mediterranean Region: An overview. MAP Technical Reports Series No. 27. UNEP, Athens, 1989 (52 pages) (English only).

28. UNEP: State of the Mediterranean marine environment. MAP Technical Reports Series No. 28. UNEP, Athens, 1989 (225 pages) (English only).

29. UNEP: Bibliography on effects of climatic change and related topics. MAP Technical Reports Series No. 29. UNEP, Athens, 1989 (143 pages) (English only).

30. UNEP: Meteorological and climatological data from surface and upper measurements for the assessment of atmospheric transport and deposition of pollutants in the Mediterranean Basin: A review. MAP Technical Reports Series No. 30. UNEP, Athens, 1989 (137 pages) (English only).

31. UNEP/WMO: Airborne pollution of the Mediterranean Sea. Report and proceedings of a WMO/UNEP Workshop. MAP Technical Reports Series No. 31. UNEP, Athens, 1989 (247 pages) (parts in English or French only).

32. UNEP/FAO: Biogeochemical cycles of specific pollutants (Activity K). MAP Technical Reports Series No. 32. UNEP, Athens, 1989 (139 pages) (parts in English or French only).

33. UNEP/FAO/WHO/IAEA: Assessment of organotin compounds as marine pollutants in the Mediterranean. MAP Technical Reports Series No. 33. UNEP, Athens, 1989 (185 pages) (English and French).

34. UNEP/FAO/WHO: Assessment of the state of pollution of the Mediterranean Sea by cadmium and cadmium compounds. MAP Technical Reports Series No. 34. UNEP, Athens, 1989 (175 pages) (English and French).

35. UNEP: Bibliography on marine pollution by organotin compounds. MAP Technical Reports Series No. 35. UNEP, Athens, 1989 (92 pages) (English only).

36. UNEP/IUCN: Directory of marine and coastal protected areas in the Mediterranean region. Part I - Sites of biological and ecological value. MAP Technical Reports Series No. 36. UNEP, Athens, 1990 (198 pages) (French only).

37. UNEP/FAO: Final reports on research projects dealing with eutrophication and plankton blooms (Activity H). MAP Technical Reports Series No. 37. UNEP, Athens, 1990 (74 pages) (parts in English or French only).

38. UNEP: Common measures adopted by the Contracting Parties to the Convention for the Protection of the Mediterranean Sea against pollution. MAP Technical Reports Series No. 38. UNEP, Athens, 1990 (100 pages) (English, French, Spanish and Arabic).

39. UNEP/FAO/WHO/IAEA: Assessment of the state of pollution of the Mediterranean Sea by organohalogen compounds. MAP Technical Reports Series No. 39. UNEP, Athens, 1990 (224 pages) (English and French).

40. UNEP/FAO: Final reports on research projects (Activities H,I and J). MAP Technical Reports Series No. 40. UNEP, Athens, 1990 (125 pages) (English and French).

41. UNEP: Wastewater reuse for irrigation in the Mediterranean region. MAP Technical Reports Series No. 41. UNEP, Priority Actions Programme, Regional Activity Centre, Split, 1990 (330 pages) (English and French).

42. UNEP/IUCN: Report on the status of Mediterranean marine turtles. MAP Technical Reports Series No. 42. UNEP, Athens, 1990 (204 pages) (English and French).

43. UNEP/IUCN/GIS Posidonia: Red Book "Gérard Vuignier", marine plants, populations and landscapes threatened in the Mediterranean. MAP Technical Reports Series No. 43. UNEP, Athens, 1990 (250 pages) (French only).

44. UNEP: Bibliography on aquatic pollution by organophosphorus compounds. MAP Technical Reports Series No. 44. UNEP, Athens, 1990 (98 pages) (English only).

45. UNEP/IAEA: Transport of pollutants by sedimentation: Collected papers from the first Mediterranean Workshop (Villefranche-sur-Mer, France, 10-12 December 1987). MAP Technical Reports Series No. 45. UNEP, Athens, 1990 (302 pages) (English only).

46. UNEP/WHO: Epidemiological studies related to environmental quality criteria for bathing waters, shellfish-growing waters and edible marine organisms (Activity D). Final report on project on relationship between microbial quality of coastal seawater and rotarus-induced gastroenterities among bathers (1986-88). MAP Technical Reports Series No.46, UNEP, Athens, 1991 (64 pages) (English only).

47. UNEP: Jellyfish blooms in the Mediterranean. Proceedings of the II workshop on jellyfish in the Mediterranean Sea. MAP Technical Reports Series No.47. UNEP, Athens, 1991 (320 pages) (parts in English or French only).

48. UNEP/FAO: Final reports on research projects (Activity G). MAP Technical Reports Series No. 48. UNEP, Athens, 1991 (126 pages) (parts in English or French only).

49. UNEP/WHO: Biogeochemical cycles of specific pollutants. Survival of pathogens. Final reports on research projects (Activity K). MAP Technical Reports Series No. 49. UNEP, Athens, 1991 (71 pages) (parts in English or French only).

50. UNEP: Bibliography on marine litter. MAP Technical Reports Series No. 50. UNEP, Athens, 1991 (62 pages) (English only).

51. UNEP/FAO: Final reports on research projects dealing with mercury, toxicity and analytical techniques. MAP Technical Reports Series No. 51. UNEP, Athens, 1991 (166 pages) (parts in English or French only).

52. UNEP/FAO: Final reports on research projects dealing with bioaccumulation and toxicity of chemical pollutants. MAP Technical Reports Series No. 52. UNEP, Athens, 1991 (86 pages) (parts in English or French only).

53. UNEP/WHO: Epidemiological studies related to environmental quality criteria for bathing waters, shellfish-growing waters and edible marine organisms (Activity D). Final report on epidemiological study on bathers from selected beaches in Malaga, Spain (1988-1989). MAP Technical Reports Series No. 53. UNEP, Athens, 1991 (127 pages) (English only).

54. UNEP/WHO: Development and testing of sampling and analytical techniques for monitoring of marine pollutants (Activity A): Final reports on selected microbiological projects. MAP Technical Reports Series No. 54. UNEP, Athens, 1991 (83 pages) (English only).

55. UNEP/WHO: Biogeochemical cycles of specific pollutants (Activity K): Final report on project on survival of pathogenic organisms in seawater. MAP Technical Reports Series No. 55. UNEP, Athens, 1991 (95 pages) (English only).

56. UNEP/IOC/FAO: Assessment of the state of pollution of the Mediterranean Sea by persistent synthetic materials which may float, sink or remain in suspension. MAP Technical Reports Series No. 56. UNEP, Athens, 1991 (113 pages) (English and French).

57. UNEP/WHO: Research on the toxicity, persistence, bioaccumulation, carcinogenicity and mutagenicity of selected substances (Activity G): Final reports on projects dealing with carcinogenicity and mutagenicity. MAP Technical Reports Series No. 57. UNEP, Athens, 1991 (59 pages) (English only).

58. UNEP/FAO/WHO/IAEA: Assessment of the state of pollution of the Mediterranean Sea by organophosphorus compounds. MAP Technical Reports Series No. 58. UNEP, Athens, 1991 (122 pages) (English and French).

59. UNEP/FAO/IAEA: Proceedings of the FAO/UNEP/IAEA Consultation Meeting on the Accumulation and Transformation of Chemical contaminants by Biotic and Abiotic Processes in the Marine Environment (La Spezia, Italy, 24-28 September 1990), edited by G.P. Gabrielides. MAP Technical Reports Series No. 59. UNEP, Athens, 1991 (392 pages) (English only).

60. UNEP/WHO: Development and testing of sampling and analytical techniques for monitoring of marine pollutants (Activity A): Final reports on selected microbiological projects (1987-1990). MAP Technical Reports Series No. 60. UNEP, Athens, 1991 (76 pages) (parts in English or French only).

61. UNEP: Integrated Planning and Management of the Mediterranean Coastal Zones. Documents produced in the first and second stage of the Priority Action (1985-1986). MAP Technical Reports Series No. 61. UNEP, Priority Actions Programme, Regional Activity Centre, Split, 1991 (437 pages) (parts in English or French only).

62. UNEP/IAEA: Assessment of the State of Pollution of the Mediterranean Sea by Radioactive Substances. MAP Technical Reports Series No. 62, UNEP, Athens, 1992 (133 pages) (English and French).

63. UNEP/WHO: Biogeochimical cycles of specific pollutants (Activity K) - Survival of Pathogens - Final reports on Research Projects (1989-1991). MAP Technical Reports Series No. 63, UNEP, Athens, 1992 (86 pages) (French only).

PUBLICATIONS "MAP TECHNICAL REPORTS SERIES"

1. PNUE/COI/OMM: Etudes de base et surveillance continue du pétrole et des hydrocarbures contenus dans les eaux de la mer (MED POL I). MAP Technical Reports Series No. 1. UNEP, Athens, 1986 (96 pages) (parties en anglais, français ou espagnol seulement).

2. PNUE/FAO: Etudes de base et surveillance continue des métaux, notamment du mercure et du cadmium, dans les organismes marins (MED POL II). MAP Technical Reports Series No. 2. UNEP, Athens, 1986 (220 pages) (parties en anglais, français ou espagnol seulement).

3. PNUE/FAO: Etudes de base et surveillance continue du DDT, des PCB et des autres hydrocarbures chlorés contenus dans les organismes marins (MED POL III). MAP Technical Reports Series No. 3. UNEP, Athens, 1986 (128 pages) (parties en anglais, français ou espagnol seulement).

4. PNUE/FAO: Recherche sur les effets des polluants sur les organismes marins et leurs peuplements (MED POL IV). MAP Technical Reports Series No. 4. UNEP, Athens, 1986 (118 pages) (parties en anglais, français ou espagnol seulement).

5. PNUE/FAO: Recherche sur les effets des polluants sur les communautés et écosystèmes marins (MED POL V). MAP Technical Reports Series No. 5. UNEP, Athens, 1986 (146 pages) (parties en anglais ou français seulement).

6. PNUE/COI: Problèmes du transfert des polluants le long des côtes (MED POL VI). MAP Technical Reports Series No. 6. UNEP, Athens, 1986 (100 pages) (anglais seulement).

7. PNUE/OMS: Contrôle de la qualité des eaux côtières (MED POL VII). MAP Technical Reports Series No. 7. UNEP, Athens, 1986 (426 pages) (parties en anglais ou français seulement).

8. PNUE/AIEA/COI: Etudes biogéochimiques de certains polluants au large de la Méditerranée (MED POL VIII). MAP Technical Reports Series No. 8. UNEP, Athens, 1986 (42 pages) (parties en anglais ou français seulement).

8. PNUE: Etudes biogéochimiques de certains polluants au large de la Méditerranée
Add. (MED POL VIII). Addendum, Croisière Océanographique de la Grèce 1980. MAP Technical Reports Series No. 8, Addendum. UNEP, Athens, 1986 (66 pages) (anglais seulement).

9. PNUE: Programme coordonné de surveillance continue et de recherche en matière de pollution dans la Méditerranée (MED POL -PHASE I). Rapport final, 1975-1980. MAP Technical Reports Series No. 9. UNEP, Athens, 1986 (276 pages) (anglais seulement).

10. PNUE: Recherches sur la toxicité, la persistance, la bioaccumulation, la cancérogénicité et la mutagénicité de certaines substances (Activité G). Rapports finaux sur les projets ayant trait à la toxicité (1983-85). MAP Technical Reports Series No. 10. UNEP, Athens, 1987 (118 pages) (anglais seulement).

11. PNUE: Réhabilitation et reconstruction des établissements historiques méditerranéens. Textes rédigés au cours de la première phase de l'action prioritaire (1984-1985). MAP Technical Reports Series No. 11. UNEP, Priority Actions Programme, Regional Activity Centre, Split, 1986 (158 pages) (parties en anglais ou français seulement).

12. PNUE: Développement des ressources en eau des petites îles et des zones côtières isolées méditerranéennes. Textes rédigés au cours de la première phase de l'action prioritaire (1984-1985). MAP Technical Reports Series No. 12. UNEP, Priority Actions Programme, Regional Activity Centre, Split, 1987 (162 pages) (parties en anglais ou français seulement).

13. PNUE: Thèmes spécifiques concernant le développement des ressources en eau des grandes îles méditerranéennes. Textes rédigés au cours de la deuxième phase de l'action prioritaire (1985-1986). MAP Technical Reports Series No. 13. UNEP, Priority Actions Programme, Regional Activity Centre, Split, 1987 (162 pages) (parties en anglais ou français seulement).

14. PNUE: L'expérience des villes historiques de la Méditerranée dans le processus intégré de réhabilitation du patrimoine urbain et architectural. Documents établis lors de la seconde phase de l'Action prioritaire (1986). MAP Technical Reports Series No. 14. UNEP, Priority Actions Programme, Regional Activity Centre, Split, 1987 (500 pages) (parties en anglais ou français seulement).

15. PNUE: Aspects environnementaux du développement de l'aquaculture dans la région méditerranéenne. Documents établis pendant la période 1985-1987. MAP Technical Reports Series No. 15. UNEP, Priority Actions Programme, Regional Activity Centre, Split, 1987 (101 pages) (anglais seulement).

16. PNUE: Promotion de la protection des sols comme élément essentiel de la protection de l'environnement dans les zones côtières méditerranéennes. Documents sélectionnés (1985-1987). MAP Technical Reports Series No. 16. UNEP, Priority Actions Programme, Regional Activity Centre, Split, 1987 (424 pages) (parties en anglais ou français seulement).

17. PNUE: Réduction des risques sismiques dans la région méditerranéenne. Documents et études sélectionnés (1985-1987). MAP Technical Reports Series No. 17. UNEP, Priority Actions Programme, Regional Activity Centre, Split, 1987 (247 pages) (parties en anglais ou français seulement).

18. PNUE/FAO/OMS: Evaluation de l'état de la pollution de la mer Méditerranée par le mercure et les composés mercuriels. MAP Technical Reports Series No. 18. UNEP, Athens, 1987 (354 pages) (anglais et français).

19. PNUE/COI: Evaluation de l'état de la pollution de la mer Méditerranée par les hydrocarbures de pétrole. MAP Technical Reports Series No. 19. UNEP, Athens, 1988 (130 pages) (anglais et français).

20. PNUE/OMS: Etudes épidémiologiques relatives aux critères de la qualité de l'environnement pour les eaux servant à la baignade, à la culture de coquillages et à l'élevage d'autres organismes marins comestibles (Activité D). Rapport final sur le projet sur la relation entre la qualité microbienne des eaux marines côtières et

les effets sur la santé (1983-86). MAP Technical Reports Series No. 20. UNEP, Athens, 1988 (156 pages) (anglais seulement).

21. PNUE/UNESCO/FAO: Eutrophisation dans la mer Méditerranée: capacité réceptrice et surveillance continue des effets à long terme. MAP Technical Reports Series No. 21. UNEP, Athens, 1988 (200 pages) (parties en anglais ou français seulement).

22. PNUE/FAO: Etude des modifications de l'écosystème dans les zones soumises à l'influence des polluants (Activité I). MAP Technical Reports Series No. 22. UNEP, Athens, 1988 (146 pages) (parties en anglais ou français seulement).

23. PNUE: Programme national de surveillance continue pour la Yougoslavie, Rapport pour 1983-1986. MAP Technical Reports Series No. 23. UNEP, Athens, 1988 (223 pages) (anglais seulement).

24. PNUE/FAO: Toxicité, persistance et bioaccumulation de certaines substances vis-à-vis des organismes marins (Activité G). MAP Technical Reports Series No. 24. UNEP, Athens, 1988 (122 pages) (parties en anglais ou français seulement).

25. PNUE: Le Plan d'action pour la Méditerranée, perspective fonctionnelle; une recherche juridique et politique. MAP Technical Reports Series No. 25. UNEP, Athens, 1988 (105 pages) (anglais seulement).

26. PNUE/UICN: Répertoire des aires marines et côtières protégées de la Méditerranée. Première partie - Sites d'importance biologique et écologique. MAP Technical Reports Series No. 26. UNEP, Athens, 1989 (196 pages) (anglais seulement).

27. PNUE: Implications des modifications climatiques prévues dans la région méditerranéenne: une vue d'ensemble. MAP Technical Reports Series No. 27. UNEP, Athens, 1989 (52 pages) (anglais seulement).

28. PNUE: Etat du milieu marin en Méditerranée. MAP Technical Reports Series No. 28. UNEP, Athens, 1989 (225 pages) (anglais seulement).

29. PNUE: Bibliographie sur les effets des modifications climatiques et sujets connexes. MAP Technical Reports Series No. 29. UNEP, Athens, 1989 (143 pages) (anglais seulement).

30. PNUE: Données météorologiques et climatologiques provenant de mesures effectuées dans l'air en surface et en altitude en vue de l'évaluation du transfert et du dépôt atmosphériques des polluants dans le bassin méditerranéen: un compte rendu. MAP Technical Reports Series No. 30. UNEP, Athens, 1989 (137 pages) (anglais seulement).

31. PNUE/OMM: Pollution par voie atmosphérique de la mer Méditerranée. Rapport et actes des Journées d'étude OMM/PNUE. MAP Technical Reports Series No. 31. UNEP, Athens, 1989 (247 pages) (parties en anglais ou français seulement).

32. PNUE/FAO: Cycles biogéochimiques de polluants spécifiques (Activité K). MAP Technical Reports Series No. 32. UNEP, Athens, 1989 (139 pages) (parties en anglais ou français seulement).

33. PNUE/FAO/OMS/AIEA: Evaluation des composés organostanniques en tant que polluants du milieu marin en Méditerranée. MAP Technical Reports Series No. 33. UNEP, Athens, 1989 (185 pages) (anglais et français).

34. PNUE/FAO/OMS: Evaluation de l'état de la pollution de la mer Méditerranée par le cadmium et les composés de cadmium. MAP Technical Reports Seri es No. 34. UNEP, Athens, 1989 (175 pages) (anglais et français).

35. PNUE: Bibliographie sur la pollution marine par les composés organostanniques. MAP Technical Reports Series No. 35. UNEP, Athens, 1989 (92 pages) (anglais seulement).

36. PNUE/UICN: Répertoire des aires marines et côtières protégées de la Méditerranée. Première partie - Sites d'importance biologique et écologique. MAP Technical Reports Series No. 36. UNEP, Athens, 1990 (198 pages) (français seulement).

37. PNUE/FAO: Rapports finaux sur les projets de recherche consacrés à l'eutrophisation et aux efflorescences de plancton (Activité H). MAP Technical Reports Series No. 37. UNEP, Athens, 1990 (74 pages) (parties en anglais ou français seulement).

38. PNUE: Mesures communes adoptées par les Parties Contractantes à la Convention pour la protection de la mer Méditerranée contre la pollution. MAP Technical Reports Series No. 38. UNEP, Athens, 1990 (100 pages) (anglains, français, espagnol et arabe).

39. PNUE/FAO/OMS/AIEA: Evaluation de l'état de la pollution par les composés organohalogénés. MAP Technical Reports Series No. 39. UNEP, Athens, 1990 (224 pages) (anglais et français).

40. PNUE/FAO: Rapports finaux sur les projets de recherche (Activités H, I et J). MAP Technical Reports Series No. 40. UNEP, Athens, 1990 (125 pages) (anglais et français).

41. PNUE: Réutilisation agricole des eaux usées dans la région méditerranéenne. MAP Technical Reports Series No. 41. UNEP, Priority Actions Programme, Regional Activity Centre, Split, 1990 (330 pages) (anglais et français).

42. PNUE/UICN: Rapport sur le statut des tortues marines de Méditerranée. MAP Technical Reports Series No. 42. UNEP, Athens, 1990 (204 pages) (anglais et français).

43. PNUE/UICN/GIS Posidonie: Livre rouge "Gérard Vuignier" des végétaux, peuplements et paysages marins menacés de Méditerranée. MAP Technical Reports Series No. 43. UNEP, Athens, 1990 (250 pages) (français seulement).

44. PNUE: Bibliographie sur la pollution aquatique par les composés organophosphorés. MAP Technical Reports Series No. 44. UNEP, Athens, 1990 (98 pages) (anglais seulement).

45. PNUE/AIEA: Transfert des polluants par sédimentation: Recueil des communications présentées aux premières journées d'études méditerranéennes (Villefranche-sur- Mer, France, 10-12 décembre 1987). MAP Technical Reports Series No. 45. UNEP, Athens, 1990 (302 pages) (anglais seulement).

46. PNUE/OMS: Etudes épidémiologiques relatives aux critères de la qualité de l'environnement pour les eaux servant à la baignade, à la culture de coquillages et à l'élevage d'autres organismes marins comestibles (Activité D). Rapport final sur le projet sur la relation entre la qualité microbienne des eaux marines côtières et la gastroentérite provoquée par le rotavirus entre les baigneurs (1986-88). MAP Technical Reports Series No.46. UNEP, Athens, 1991 (64 pages) (anglais seulement).

47. PNUE: Les proliférations de méduses en Méditerannée. Actes des IIèmes journées d'étude sur les méduses en mer Méditerranée. MAP Technical Reports Series No.47. UNEP, Athens, 1991 (320 pages) (parties en anglais ou français seulement).

48. PNUE/FAO: Rapports finaux sur les projets de recherche (Activité G). MAP Technical Reports Series No. 48. UNEP, Athens, 1991 (126 pages) (parties en anglais ou français seulement).

49. PNUE/OMS: Cycles biogéochimiques de polluants spécifiques. Survie des Pathogènes. Rapports finaux sur les projets de recherche (activité K). MAP Technical Reports Series No. 49. UNEP, Athens, 1991 (71 pages) (parties en anglais ou français seulement).

50. PNUE: Bibliographie sur les déchets marins. MAP Technical Reports Series No. 50. UNEP, Athens, 1991 (62 pages) (anglais seulement).

51. PNUE/FAO: Rapports finaux sur les projets de recherche traitant du mercure, de la toxicité et des techniques analytiques. MAP Technical Reports Series No. 51. UNEP, Athens, 1991 (166 pages) (parties en anglais ou français seulement).

52. PNUE/FAO: Rapports finaux sur les projets de recherche traitant de la bioaccumulation et de la toxicité des polluants chimiques. MAP Technical Reports Series No. 52. UNEP, Athens, 1991 (86 pages) (parties en anglais ou français seulement).

53. PNUE/OMS: Etudes épidémiologiques relatives aux critères de la qualité de l'environnement pour les eaux servant à la baignade, à la culture de coquillages et à l'élevage d'autres organismes marins comestibles (Activité D). Rapport final sur l'étude épidémiologique menée parmi les baigneurs de certaines plages à Malaga, Espagne (1988-1989). MAP Technical Reports Series No. 53. UNEP, Athens, 1991 (127 pages) (anglais seulement).

54. PNUE/OMS: Mise au point et essai des techniques d'échantillonnage et d'analyse pour la surveillance continue des polluants marins (Activité A): Rapports finaux sur certains projets de nature microbiologique. MAP Technical Reports Series No. 54. UNEP, Athens, 1991 (83 pages) (anglais seulement).

55. PNUE/OMS: Cycles biogéochimiques de polluants spécifiques (Activité K): Rapport final sur le projet sur la survie des microorganismes pathogènes dans l'eau de mer. MAP Technical Reports Series No. 55. UNEP, Athens, 1991 (95 pages) (anglais seulement).

56. PNUE/COI/FAO: Evaluation de l'état de la pollution de la mer Méditerranée par les matières synthétiques persistantes qui peuvent flotter, couler ou rester en suspension. MAP Technical Reports Series No. 56. UNEP, Athens, 1991 (113 pages) (anglais et français).

57. PNUE/OMS: Recherches sur la toxicité, la persistance, la bioaccumulation, la cancérogénicité et la mutagénicité de certaines substances (Activité G). Rapports finaux sur les projets ayant trait à la cancérogénicité et la mutagénicité. MAP Technical Reports Series No. 57. UNEP, Athens, 1991 (59 pages) (anglais seulement).

58. PNUE/FAO/OMS/AIEA: Evaluation de l'état de la pollution de la mer Méditerranée par les composés organophosphorés. MAP Technical Reports Series No. 58. UNEP, Athens, 1991 (122 pages) (anglais et français).

59. PNUE/FAO/AIEA: Actes de la réunion consultative FAO/PNUE/AIEA sur l'accumulation et la transformation des contaminants chimiques par les processus biotiques et abiotiques dans le milieu marin (La Spezia, Italie, 24-28 septembre 1990), publié sous la direction de G.P. Gabrielides. MAP Technical Reports Series No. 59. UNEP, Athens, 1991 (392 pages) (anglais seulement).

60. PNUE/OMS: Mise au point et essai des techniques d'échantillonnage et d'analyse pour la surveillance continue des polluants marins (Activité A): Rapports finaux sur certains projets de nature microbiologique (1987-1990). MAP Technical Reports Series No. 60. UNEP, Athens, 1991 (76 pages) (parties en anglais ou français seulement).

61. PNUE: Planification intégrée et gestion des zones côtières méditerranéennes. Textes rédigés au cours de la première et de la deuxième phase de l'action prioritaire (1985-1986). MAP Technical Reports Series No. 61. UNEP, Priority Actions Programme, Regional Activity Centre, Split, 1991 (437 pages) (parties en anglais ou français seulement).

62. PNUE/AIEA: Evaluation de l'état de la pollution de la mer Méditerranée par les substances radioactives. MAP Technical Reports Series No. 62, UNEP, Athens, 1992 (133 pages) (anglais et français).

63. PNUE/OMS: Cycles biogéochimiques de polluants spécifiques (Activité K) - Survie des pathogènes - Rapports finaux sur les projets de recherche (1989-1991). MAP Technical Reports Series No. 63, UNEP, Athens, 1992 (86 pages) (français seulement).

Issued and printed by:

Mediterranean Action Plan
United Nations Environment Programme

Additional copies of this and other publications issued by
the Mediterranean Action Plan of UNEP can be obtained from:

Co-ordinating Unit for the Mediterranean Action Plan
United Nations Environment Programme
Leoforos Vassileos Konstantinou, 48
P.O.Box 18019
11610 Athens
GREECE

Publié et imprimé par:

Plan d'action pour la Méditerranée
Programme des Nations Unies pour l'Environnement

Des exemplaires de ce document ainsi que d'autres
publication de Plan d'action pour la Méditerranée
de PNUE peuvent être obtenus de:

Unité de coordination du Plan d'action pour la Méditerranée
Programme des Nations Unies pour l'Environnement
Leoforos Vassileos Konstantinou, 48
B.P. 18019
11610 Athènes
GRECE